The biology of kidney malformations

by

Paul Julian Douglas Winyard

A thesis submitted to the University of London in

fulfillment of the requirement for the degree of

Doctor of Philosophy

May, 1998

Developmental Biology and Nephrourology Units,

Institute of Child Health, 30 Guilford Street,

London, WC1N 1EH.

ProQuest Number: U106229

ProQuest

ProQuest U106229

To my family at home

and my extended family at work.

Abstract

Kidney malformations, such as dysplastic kidneys, are the commonest cause of chronic renal failure in infants and young children. It has been suggested, based on anatomical descriptions, that failure of ureteric bud branching and mesenchymal induction leads to dysplasia, yet little is known about the underlying molecular mechanisms. In this thesis, therefore, I have examined several aspects of the cell biology of human dysplastic kidneys, and compared them with normal developing and mature kidneys.

In normal developing kidneys, proliferation was prominent in the nephrogenic cortex whilst apoptosis was predominantly detected in early nephron precursors and in the medulla. The transcription factor PAX-2 was expressed in actively proliferating cells in both ureteric bud ampullae and condensing mesenchyme. In contrast, the transcription factor WT-1 and survival factor BCL-2 were solely detected in the condensing mesenchyme and developing nephrons, whilst the cell adhesion molecule galectin-3 was restricted to the ureteric bud lineage. In the mature kidney PAX-2 and BCL-2 were downregulated, whilst WT-1 expression persisted in podocytes and galectin-3 was detected in α-intercalated cells of collecting ducts.

In dysplastic kidneys, proliferation was prominent in dysplastic tubules and cysts, and PAX-2, BCL-2 and galectin-3 were persistently expressed in these epithelia. Therefore, continuous proliferation signals in combination with ectopic survival factors may explain cyst formation in these 'immature' dysplastic epithelia. In contrast, apoptosis was prominent in cells in the surrounding loosely arranged 'mesenchymal' tissue. These cells expressed WT-1, but did not

express PAX-2 and BCL-2 and these factors may therefore be essential for precursor survival and proliferation during nephron formation.

In addition, in preliminary experiments, cells were cultured from dysplastic kidneys and transduced with a simian virus 40 (SV40) large T antigen construct. In future, culture and characterisation of these potentially immortal cells may provide a novel method to investigate the functional biology of kidney malformations.

Acknowledgements

Abbreviations

ABC	avidin-biotin peroxidase complex
ADPKD	autosomal dominant polycystic kidney disease
ARPKD	autosomal recessive polycystic kidney disease
BCL	B-cell leukaemia / lymphoma gene
BMP	bone morphogenetic protein
bp	base-pair
BSA	bovine serum albumin
cM	centimorgan
DAB	diaminobenzidine tetrahydrochloride
DNA	deoxyribonucleic acid
EDTA	ethylene-diamine tetra-acetic acid
EGF	epidermal growth factor
EGR	early growth response gene
Et Br	ethidium bromide
FGF	fibroblast growth factor
FITC	fluoroscein isothiocyanate
GDNF	glial cell-line derived neurotrophic factor
H and E	hematoxylin and eosin
HGF	hepatocyte growth factor / scatter factor
HOX	homeobox containing gene
IGF	insulin-like growth factor
KAL	X-linked Kallmann's syndrome gene
kb	kilobase
kD	kilodalton
L	litre
LB	Lennox broth
M	Molar *i.e.* concentration in moles per litre
µg	microgram
µl	microlitre

MDCK	Madin Darby canine kidney
ml	millilitre
mg	milligram
mRNA	messenger RNA
PAX	paired box containing genes
PBS	phosphate buffered saline
PCR	polymerase chain reaction
PDGF	platelet-derived growth factor
PI	propidium iodide
RNA	ribonucleic acid
RNase	ribonuclease
rpm	revolutions per minute
RT-PCR	reverse transcription polymerase chain reaction
SDS	sodium lauryl sulphate
SSC	sodium chloride / sodium citrate buffer
TAE	tris acetate EDTA electrophoresis buffer
TE	tris EDTA
TEMED	N, N, N', N' tetramethylethylenediamine
TGF	transforming growth factor
TRITC	tetramethylrhodamine isothiocyanate
UTP	uridine triphosphate
TNF	tumour necrosis factor
UV	ultra violet
VEGF	vascular endothelial growth factor
WT	Wilms' tumour associated gene
xg	times gravity

Contents

Published articles are enclosed in the pocket attached to the back cover of this thesis.

List of figures

List of tables

Chapter 1. Introduction

Aim of this thesis

The aim of this thesis is to investigate the biology of human renal malformations with particular emphasis on renal dysplasia, the commonest cause of chronic renal failure in infants. In order to achieve this aim, the current understanding of the anatomy and molecular biology of nephrogenesis is described in this introductory chapter whilst experimental details and results are described later.

Hypotheses

Much of the data on normal and abnormal nephrogenesis has been derived from animal experiments. In many cases, it is uncertain whether the same principles apply to, or molecules are involved in, human renal development. The following hypotheses are therefore tested in this thesis:

1) Many of the genes expressed in animal nephrogenesis will also be expressed in, and hence be of potential importance in, human renal development.

2) Dysplasia is associated with aberrant expression of genes which are expressed in normal development.

3) Aberrant gene expression is likely to result in deregulation of basic processes such as proliferation and apoptosis, which are tightly controlled during normal development.

Overview

A wide variety of molecules and processes are examined in this thesis in order to test these hypotheses. Firstly, the extent of proliferation and apoptosis is defined in normal human nephrogenesis and in human dysplastic kidneys. Secondly, the expression patterns of potentially important molecules such as the transcription factors PAX-2 and WT-1, the survival factor BCL-2 and the cell adhesion molecule galectin-3 are described. This is the first time that proliferation, apoptosis and the expression patterns of these genes have been described in dysplastic kidneys, and for some molecules it is also the first detailed description of protein distribution in the normal human kidney. Finally, cell lines are generated from dysplastic kidneys, which potentially provides a novel method for investigation of functional abnormalities in human dysplasia.

General aspects

Mammalian kidneys perform a number of functions which are essential for normal post-natal life including excretion of nitrogenous waste products, homeostasis of water and electrolytes and production of hormones. The complex development of the kidney reflects these diverse functions and this process is conventionally called "nephrogenesis", although this term more correctly refers to differentiation of the nephron tubules alone.

The anatomy of normal human nephrogenesis has been described in detail by a number of authors (Kampmeier, 1926; Torrey, 1954; Potter, 1972) and similar descriptive accounts have documented the pathological changes found in developmental abnormalities such as renal dysplasia (Risdon, 1971; Potter, 1972; Woolf and Winyard, 1998). In addition, malformation syndromes such as the branchio-oto-renal, renal-coloboma and Kallmann's syndromes have implicated genetic mutations in a limited number of human renal malformations. There is still, however, very little known about the cell biology of most human malformations.

In the mouse, by contrast, there is a much greater understanding of the molecular basis of nephrogenesis because large quantities of embryonic and fetal material are available, and it is possible to use experimental strategies such as kidney organ culture and transgenic technology to define the roles, and importance, of specific genes (Bard and Woolf, 1992; Lechner and Dressler, 1997).

Anatomy of normal nephrogenesis

There are three pairs of 'kidneys' in the mammalian embryo: the pronephros, mesonephros and metanephros. These arise sequentially from intermediate mesoderm on the dorsal body wall (Larsen, 1993). This is shown in Figure 1. The pronephros and mesonephros degenerate during mammalian fetal life whilst the metanephros develops into the adult kidney. In contrast, the pronephros is the functioning kidney in the adult hagfish and some amphibians whereas the mesonephros is the excretory organ in adult lampreys, some fishes and amphibians.

The pronephros

It is possible to detect the first evidence of the pronephros at the ten somite stage on day 22 after fertilisation in humans, which is morphologically equivalent to embryonic day 9 in mice. At this stage, it comprises a small group of nephrotomes with segmental condensations, grooves and vesicles between the second and sixth somites. The nephrotomes are nonfunctional and most likely represent vestiges of the pronephric kidney of lower vertebrates. The pronephric duct develops from the intermediate mesoderm lateral to the notochord (Gilbert, 1991) from around the level of the ninth somite. The duct elongates caudally and reaches the cloacal wall on day 26. It is renamed as the mesonephric, or Wolffian duct, as mesonephric tubules develop. The nephrotomes and pronephric part of the duct involute and cannot be identified by day 24 or 25 after fertilisation (Gilbert, 1991).

A) 24 days B) 26 days C) 33 days

Pronephros

Mesonephric duct

Intermediate mesoderm

Mesonephros

Ureteric bud

Metanephros
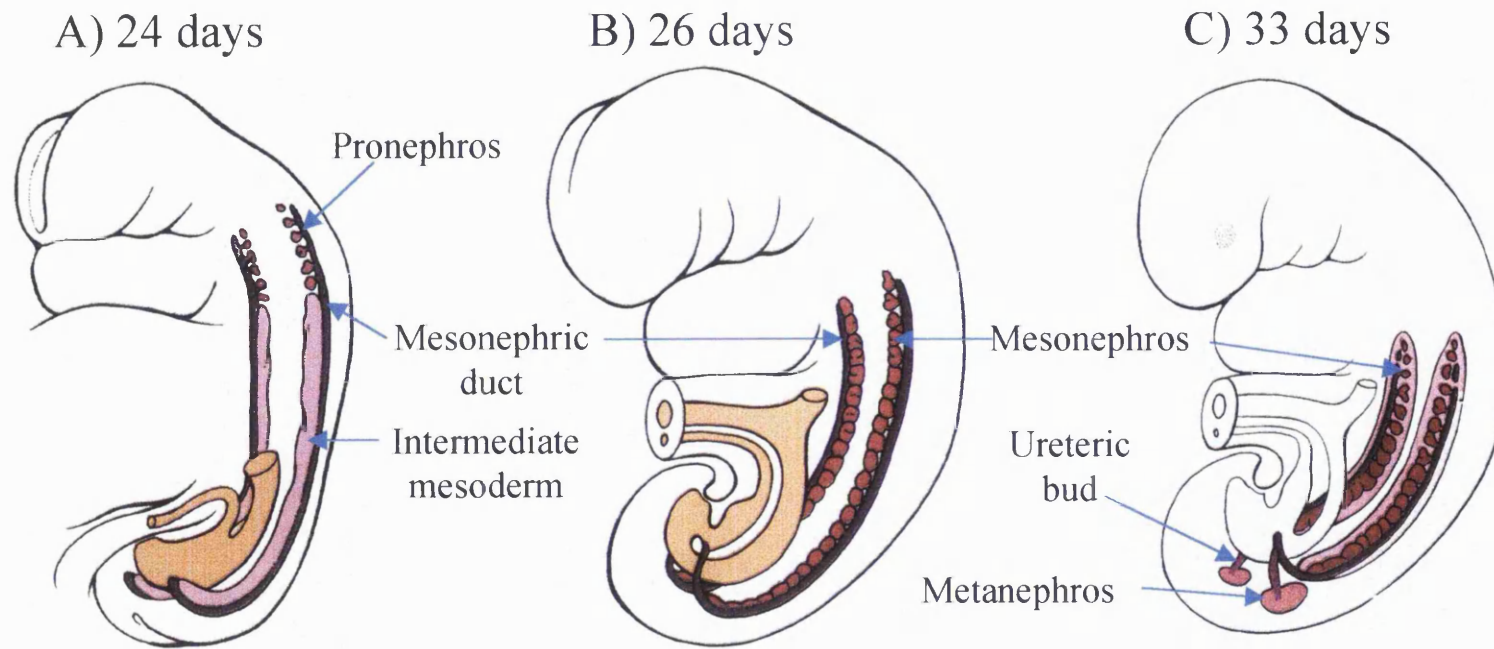
Figure 1. Early development of the human urinary system. A) The mesonephric ducts appear adjacent to pronephric tubules and grow caudally. B) Pronephric tubules regress and mesonephric glomeruli and tubules are formed. C) The ureteric bud branches from the caudal mesonephric duct and enters the metanephric mesenchyme. Adapted from Larsen, 1993.

The mesonephros

In humans, the long sausage-shaped mesonephros develops from around 24 days of gestation and consists of the mesonephric duct and adjacent mesonephric tubules. The mesonephric duct begins as a solid rod of cells which canalises in a caudocranial direction after fusion with the cloaca. Mesonephric tubules develop from intermediate mesoderm medial to the duct by 'mesenchymal to epithelial' transformation, a process which is subsequently reiterated during nephron formation in metanephric development. In humans, a total of around 40 mesonephric tubules are produced (several per somite), but the cranial tubules regress at the same time as caudal ones are forming so that there are never more than 30 pairs at any time (Larsen, 1993).

Each human mesonephric tubule consists of a medial cup-shaped sac encasing a knot of capillaries, respectively analagous to the Bowman's capsule and glomerulus of the mature kidney, and a lateral portion in continuity with the mesonephric duct. Other segments of the tubule resemble mature proximal and distal tubules histologically but there is no loop of Henle. The nephrons are reported to produce small quantities of urine between weeks 6 and 10 (Moore, 1988) which drain via the mesonephric duct. In contrast, the mouse mesonephros does not contain well-differentiated glomeruli (Sainio *et al.*, 1997).

The body of the mesonephros involutes completely by mid gestation in humans, although part of the duct is retained as the vas deferens (Moore, 1988). This involution has been shown to occur by apoptosis, or programmed cell death in the chick (Wride *et al.*, 1994) and the mouse (Camp and Martin, 1996). Apoptosis in the human metanephros is described in detail later in this thesis.

The metanephros

The adult human kidney develops from the metanephros which consists of two cell types at its inception: the epithelial cells of the ureteric bud, and the mesenchyme cells of the metanephric mesenchyme. A series of reciprocal interactions between these tissues cause the ureteric bud to branch sequentially to form the ureter, renal pelvis, calyces and collecting tubules whilst the mesenchyme undergoes an epithelial conversion to form the nephrons from glomerulus to distal tubule. This process is depicted graphically in Figures 2 and 3. In addition, a third cell type, the interstitial cells are also thought to be derived from the mesenchyme.

Recent evidence suggests, however, that renal cell lineages may be more plastic than described above. Qiao and colleagues (1995) genetically tagged ureteric bud and mesenchyme cells with a LacZ expressing retrovirus and showed that mesenchyme cells contribute to a minor extent to the collecting system, and ureteric bud cells contribute to the nephrons. There are, however, some methodological questions over such experiments since they depend on the initial isolation of an absolutely pure cell population.
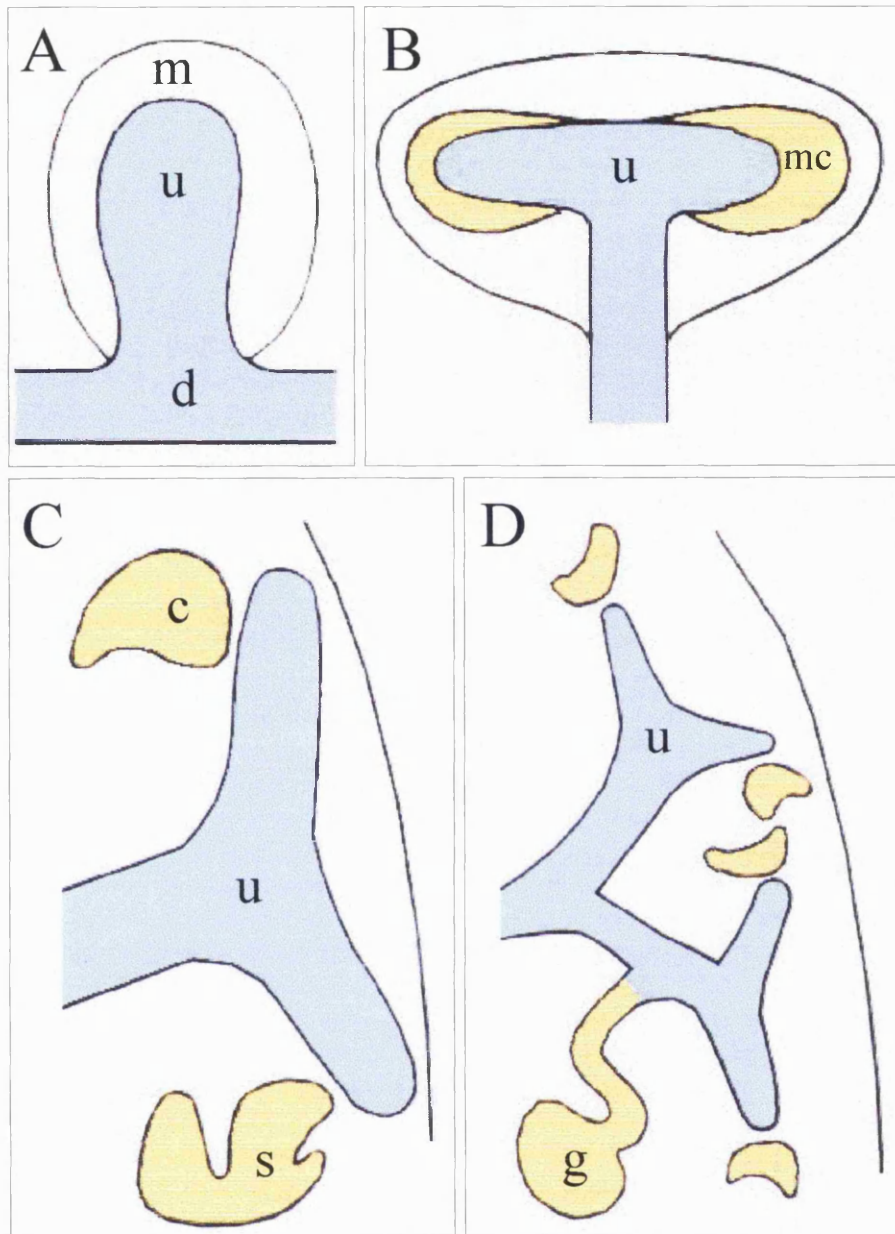
Figure 2. Early branching of the ureteric bud and nephron formation.
A) In the fifth week the ureteric bud grows into metanephric mesenchyme from
the mesonephric duct. B) In week 6 the bud has branched once and mesenchyme
condenses around the ampullae. C) Comma and S-shaped nephron precursors
have formed by the 8th week. D) The first glomeruli have formed by the 9th
week, and further branching of the ureteric bud and mesenchymal condensation
continues in the nephrogenic cortex. Adapted from Woolf et al., 1995.
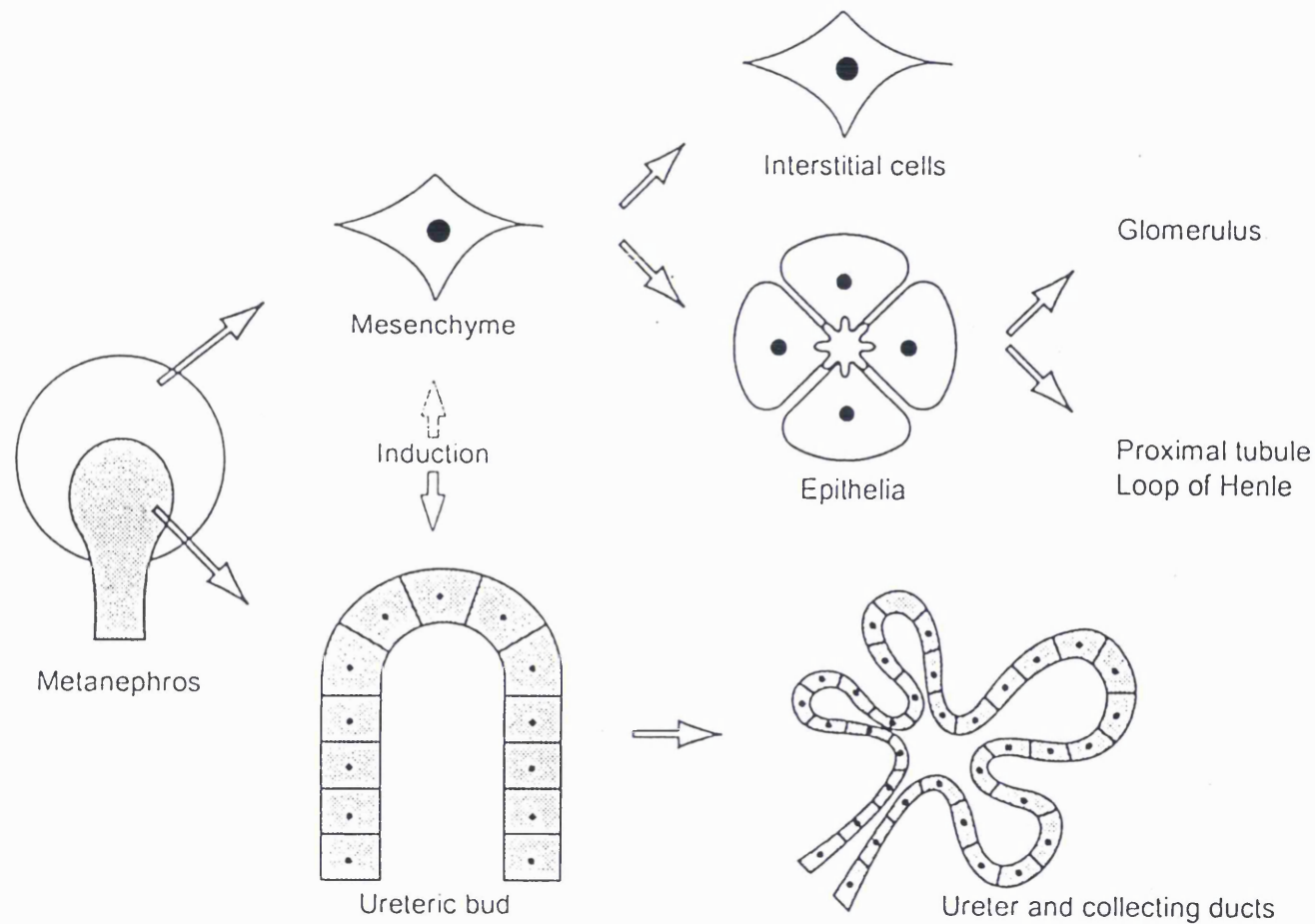
Figure 3. Cell lineages in nephrogenesis. Mutual induction between the ureteric bud (shaded) and the mesenchyme (white) in the metanephros causes serial branching of the bud to form the ureter and collecting ducts and differentiation of the mesenchyme into polarised epithelial and interstitial / stromal cells. Adapted from Woolf (1997).

Timing of nephrogenic events

In humans, metanephric kidney development begins at day 28 after fertilisation when the ureteric bud sprouts from the distal part of the mesonephric duct (Larsen, 1993). By day 32 the tip (ampulla) of the bud penetrates a portion of sacral intermediate mesenchyme called the metanephric blastema, and this condenses around the growing ampulla. The first glomeruli form by 8 - 9 weeks and nephrogenesis continues in the cortex of the fetal kidney until 34 to 36 weeks (Potter, 1972). Nephrons elongate and continue to differentiate postnatally but no new nephrons are formed. In mice, the ureteric bud enters the metanephric mesenchyme by embryonic day 11.5, the first glomeruli form by embryonic day 14 and nephrogenesis continues for 14 days after birth. The timing of nephrogenesis in humans / mice is shown in Table 1.

Structure		Human	Mouse
Pronephros	appears	22 days	9 days
	regresses	25 days	10 days
Mesonephros	appears	24 days	10 days
	regresses	16 weeks	14 days
Metanephros		32 days	11.5 days
Renal pelvis		33 days	12.5 days
Collecting tubules / nephrons		44 days	13 days
Glomeruli		9 weeks	14 days
Nephrogenesis ceases		34 – 36 weeks	14 days after birth
Length of gestation		40 weeks	20 days

Table 1. Timing of nephrogenic events.

This table summarises the time of first appearance of renal structures during human and murine nephrogenesis, unless otherwise stated.

Differentiation of the ureteric bud and its derivatives

Branching of the ureteric bud

As the ureteric bud grows into the metanephric blastema it becomes invested with condensed mesenchyme and the ampullary tip begins to divide. This process of growth and branching occurs repeatedly during nephrogenesis, particularly in the outer or nephrogenic cortex where new nephric units are formed until 34 - 36 weeks of human gestation (Potter, 1972). It leads to an arborialised (tree-like) collecting duct system connected to nephrons which develop concurrently from mesenchymal condensates adjacent to the ampullary tips (see below).

There is great inter-species variation in the number of nephrons which reflects the number of branches of the ureteric bud required to both induce these nephrons and form the collecting ducts to drain urine from them. It has been estimated that it requires 9 to 10 branching generations in mice to obtain 10 to 20,000 nephrons and a further 10 generations to give rise to one million nephrons in each human kidney (Ekblom, 1994).

Branching of the human collecting duct system has been described in detail by Potter (1972) and is subdivided into 4 stages:
1) In the first stage, there is dichotomous branching with each ampullary tip associated with a developing nephron. The first branch is symmetrical but subsequent dichotomous branches are asymmetrical because the space available between adjacent branches get smaller (Fig. 4).

31
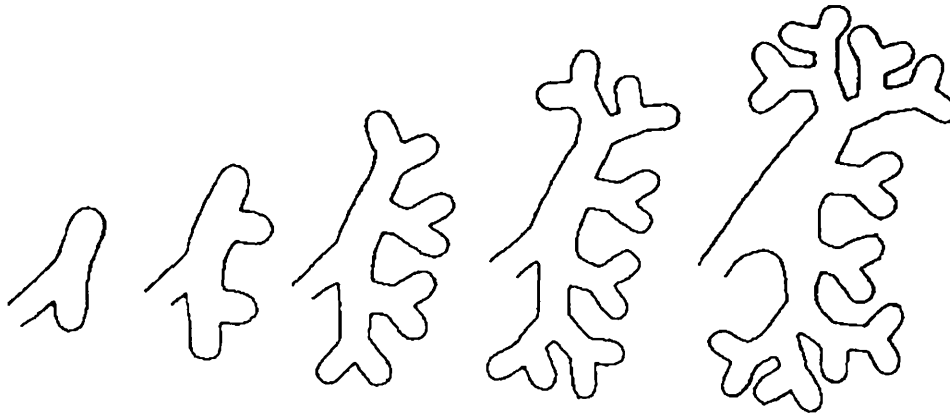
Figure 4. Branching of the ureteric bud. Schematic representation of the branching of the ureteric bud showing repeated formation of two branches from each ampulla. Note that the branching soon becomes asymmetric as the space around each branch becomes occupied. Modified from Potter, 1972.

2)   In the second period of development, arcades of nephrons are formed which connect to the same ampulla. Newer nephrons become attached to the ampulla more proximally whilst the older nephrons shift their attachment to the connecting piece of the younger nephron. One arcade may have up to seven attached nephric units in humans. This process also occurs in other mammals but there are fewer nephrons per arcade.

3)   In the third period, the tips of the collecting ducts extend past the attachment point of the arcade and stop branching. Instead new terminal nephrons are induced sequentially by the growing tip of the bud and become attached individually to the collecting duct, mainly in the nephrogenic cortex.

4)   Finally, the terminal inducing ampullae disappear and new nephron formation ceases at around 34 - 36 weeks. Further growth of the kidney occurs by lengthening of the proximal tubules, loops of Henle and collecting ducts.

Formation of the renal pelvis and calyces

The mature collecting ducts drain into minor calyces which in turn connect to the major calyces of the renal pelvis before the ureter. These intervening structures are formed by the coalescence of many of the early branches of the ureteric bud. This concept of remodeling has been recognised for many years as can be seen from Figure 5 which is adapted from an article by Kampmeier in 1926. He described 'vestigial' and 'provisional' zones in the human medulla in which nephrons initially developed but subsequently degenerated.

The exact number of generations of branches which are remodeled is unknown although Potter estimated that the first 3 - 5 generations form the pelvis and the next 3 - 5 give rise to the minor calyces and papillae (Fig. 6). Nephrons which were initially attached to these early branches were described by Potter to either transfer to a later branch or degenerate during development.
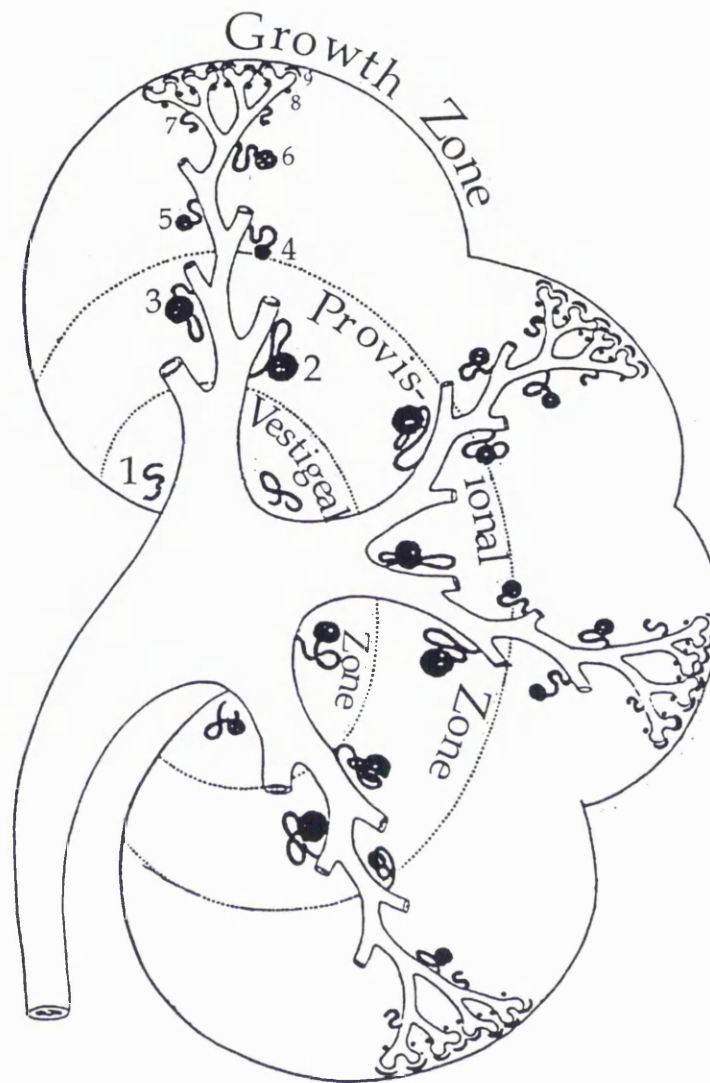
Figure 5. Diagram illustrating the 'fate of the different generations of uriniferous tubules' (Kampmeier, 1926). Successive generations of nephrons are labeled 1 to 9. Kampmeier reported that the first generation of human tubules were vestiges from the beginning, whilst the second and third generations were perfectly formed but transitory. He also suggested that the fourth to ninth generations were permanent, and gave rise to the definitive nephrons. Hence the zones containing these different generations were termed vestigeal, provisional and growth zones. Modified from Kampmeier, 1926.
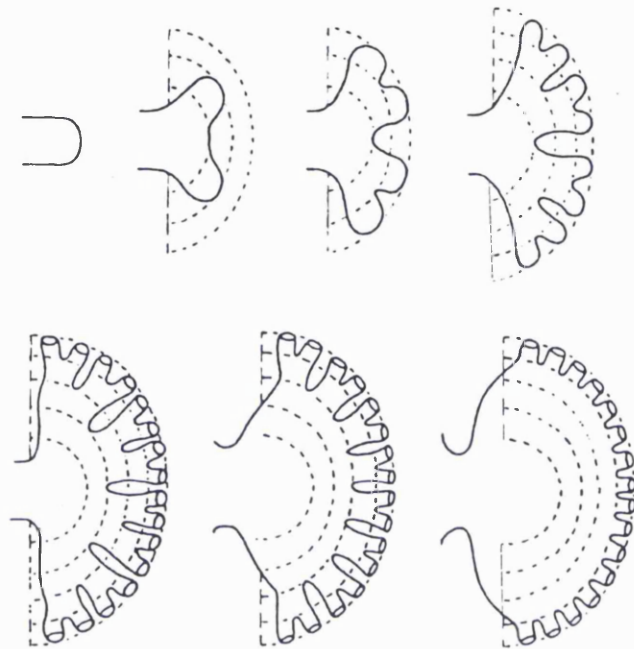
Figure 6. Coalescence of ureteric bud branches. Potter reported that coalescence of the first 4 - 5 polar and 2 - 3 interpolar branches of the ureteric bud branches led to the formation of the renal pelvis and collecting system. The next 3 - 5 generations of branches formed the minor calyces. Nephrons which were originally attached to these branches were reported to either regress, or move their attachment to later generations. Modified from Potter, 1972.

Further differentiation of the collecting ducts

Mature collecting ducts contain three functionally distinct cell types (Fejes-Toth and Naray-Fejes-Toth, 1991). Principal cells have few organelles whereas the α and β-intercalated cells contain a high density of mitochondria. Principal cells reabsorb Na^+ via apical amiloride-sensitive Na^+ channels driven by the basolateral Na^+-K^+ ATPase, and they secrete K^+ via apical Ba^{++}-sensitive K^+ channels. They also contain water channels which are responsive to antidiuretic hormone (ADH). The α-intercalated cells have an apical $H^+ATPase$ and secrete protons whilst the β cells reabsorb protons and secrete HCO_3^-. A modified version of the red cell Cl^--HCO_3^- exchanger, known as band 3, is expressed on the basal surface of α-intercalated cells (Wainwright *et al.*, 1989). Antibodies against band 3 are used to identify α-intercalated cells later in this thesis.

In mice, collecting duct cells demonstrate phenotypic plasticity since β-intercalated cells can give rise to both α-intercalated and principal cells *in vitro*, although principal cells do not give rise to intercalated phenotypes (Fejes-Toth and Naray-Fejes-Toth, 1992). It is therefore possible that the intercalated cells may be progenitor cells in the ureteric bud branches, although this has not yet been demonstrated either *in vivo*, or in human cells.

Differentiation of the mesenchyme and its derivatives

Each nephron develops from mesenchyme adjacent to an ampullary tip of the ureteric bud. The mesenchyme is initially loosely arranged but the cells destined to become nephrons condense around the bud tips and undergo mesenchyme to epithelial transformation to form an epithelial renal vesicle. This elongates to form a comma shape which folds back on itself to become an S-shaped body. This epithelial tubule continues to elongate and differentiate to give rise to the proximal convoluted tubule, the descending and ascending limbs of the loop of Henle and the distal convoluted tubule. The distal end fuses with the collecting ducts to form a continuous functional unit. Further differentiation of the nephron is outlined below.

Glomerulus

The proximal end of the S-shaped tubule invaginates into a cup shape and forms Bowman's capsule, which encases a tuft of capillaries to form the glomerulus. The mature glomerulus consists of four main cell types:

1) Visceral epithelia (podocytes) have foot processes which are in intimate contact with the glomerular basement membrane. These cells are essential for protein size restriction in the ultrafiltrate of urine.

2) Parietal epithelia of Bowman's capsule.

3) Mesangial cells embedded in extracellular matrix. These cells have multiple roles including physical support for glomerular capillary loops and modulation of both matrix production and degradation.

4) Endothelial cells lining the capillaries. These were thought to arise from direct ingrowth of vessels from the dorsal aorta in a process called angiogenesis. Recent data, however, suggests that some of the cells may develop *in situ* by vasculogenesis (Woolf and Loughna, 1998).

Proximal tubule

The proximal tubule continues directly after the glomerulus and derives from the middle part of the S-shaped body. It consists of a proximal convoluted portion, the pars convoluta, which is a continuation of the parietal epithelium of Bowman's capsule, and a straight portion, the pars recta. The epithelial cells have a characteristic appearance with a well-developed brush border to increase the surface area for reabsorption and numerous mitochondria and lysosomes which reflect their high metabolic rate. The main role of the proximal convoluted tubule is to reabsorb minerals, ions (Na^+, HCO_3^-, Cl^-, K^+, Ca^{++}, PO_4^{3-}) water and organic solutes such as glucose and amino acids. Approximately two thirds of the ultrafiltrate is reabsorbed in the proximal tubule.

Loop of Henle

The loop of Henle is composed of the straight portion of the proximal tubule (pars recta), the thin limb segments, and the straight portion of the distal tubule (thick ascending limb). The loops extend deep into the medulla and are essential for generating an osmolar gradient which permits the reabsorption of water by the collecting ducts. Elongation and maturation of the loops occurs postnataly.

Distal segments

The distal tubules consist of the thick ascending limb of the loop of Henle which is involved in active ion transport (particularly Cl^-) and the distal convoluted tubule. This includes the specialised macula densa portion which senses the amount of sodium delivered to the distal tubule and modulates renin secretion via the juxtaglomerular apparatus.

Connecting tubule

The distal tubule is attached to the collecting duct by the connecting tubule which has been thought to be derived from the renal mesenchyme. This hypothesis has, however been challenged by Howie and colleagues (1993) who suggested that the connecting tubule is derived from the ureteric bud. This was based on blood group antigen, Tamm-Horsfall protein and cytokeratin staining which are similar in the connecting piece and collecting ducts. The retroviral tagging experiments described above (Qiao *et al.*, 1995), however, showed that cells from the mouse ureteric bud may contribute to proximal structures which were previously thought to be derived from the mesenchyme and conversely the mesenchyme may contribute to more distal structures. It is therefore possible that the connecting tubule may be derived from both lineages.

Chapter 2. Molecular biology of nephrogenesis

The molecular control of nephrogenesis is complex and most of the available data comes from animal studies whereas this thesis concentrates on human nephrogenesis. It is, however, pertinent to review the wider literature on the biology of nephrogenesis because 'functional' animal studies provide a valuable insight into the potential roles of specific genes which may be relevant to human studies. Much of the descriptive information is available on the internet via the kidney development database on the world wide web which was set up by Dr Jonathon Bard and Dr Jamie Davies and can be accessed at http://mbisg2.sbc.man.ac.uk/kidbase/kidhome.html.

The following sections describe the methods available to study nephrogenesis, the basic mechanisms and molecules involved in nephrogenesis, with particular emphasis on apoptosis and proliferation, and the specific molecules which are examined in this thesis.

The nomenclature used to describe human and animal genes in this thesis is as follows: human gene abbreviations will be described in capital letters (i.e. PAX-2), animal gene abbreviations will be described in small letters (i.e. pax-2) and capitals will be used if both human and animal genes are mentioned together. In addition, capitals will be used if there is any ambiguity in interpretation, for example if a human, or non-specified, protein is used in a mouse organ culture experiment.

Methods for studying nephrogenesis

There are two complementary ways in which nephrogenesis has been investigated: descriptive studies define the temporal and spatial expression of mRNA and protein whilst functional studies establish the role of specific genes using *in vivo* and *in vitro* methodologies.

Descriptive studies

Most of the information on human renal development has been derived from descriptive studies since it is difficult to obtain sufficient material for repeated functional studies and there are ethical limits on human experiments. In their simplest form, descriptive studies document the gross anatomy and developmental stage of the normal kidney and renal malformations. They also describe patterns of gene expression by defining the distribution of mRNA by *in situ* hybridisation and protein by immunohistochemistry. This may be at a specific timepoint, or at a series of different times / stages. These experiments may identify candidate genes which potentially play an essential role in nephrogenesis, by virtue of their temporal and spatial expression patterns, although animal functional studies are often required to confirm this role.

Functional Studies - *in vitro*

Organ culture

The metanephros can be grown for several days in organ culture following dissection of the mouse fetus. During this time it will develop in a morphologically normal manner with serial branching of the ureteric bud and new nephron formation, although the rate of development is slower than normal and the glomeruli are avascular. Grobstein used this technique nearly 50 years ago to demonstrate that the mesenchyme and ureteric bud fail to develop when cultured separately, although some nephrons do form when mesenchyme is co-cultured with spinal cord (Grobstein, 1955). This was an important experiment since it proved that interactions between the bud and mesenchyme are essential for normal development and that other tissues have the potential to induce normal development. Several growth factors have now been identified which are involved in the

41

mutual induction between bud and mesenchyme (Woolf and Cale, 1997).

It is possible to manipulate cultured metanephroi by adding exogenous substances to the culture medium. Examples are growth factors, blocking antibodies to growth factors or cell adhesion molecules, and antisense oligonucleotides which block expression of specific genes (Rogers *et al.*, 1992 and 1993; Rothenpieler and Dressler, 1993). Individual cells have also been labeled using retroviral mediated gene transfer to follow their subsequent fate using *in vitro* lineage analysis (Herzlinger *et al.*, 1992; Qiao *et al.*, 1995).

One limitation of the organ culture technique is that the cultured metanephros appears to be much more sensitive to perturbed development than the normal kidney. Therefore, some genes appear to be essential in organ culture but transgenic knockouts are normal. Several explanations have been proposed for this phenomenon. For example, it may be because organ culture is a stressful situation which pushes the metanephros beyond normal limits, or there may be circulating or maternal factors which compensate for the deficient factor and rescue the phenotype *in vivo* (Letterio *et al.*, 1994). In addition, homologous molecules may be upregulated over a longer period and hence may be able to compensate *in vivo*.

Cell lines

Cell lines can be generated from the developing kidney. These can be characterised on the basis of their morphology, membrane constituents, intracellular proteins, synthesis and release of specific products such as growth factors, and extracellular matrix proteins cells (Burrow and Wilson, 1993; Karp *et al.*, 1994; Woolf *et al.*, 1995). In this way it is possible to isolate homogeneous populations of cells which have a defined lineage, and these are the ideal populations to

assess the response of specific cell types to exogenous factors (as above). Biochemical pathways can also be investigated such as ligand binding, receptor kinetics and intercellular signaling pathways.

There are also limitations to the isolation of cell lines. Firstly, both mouse and human cells will only divide for a few generations and then become senescent. This can be circumvented by generating conditionally immortal lines (Jat *et al.*, 1991) but it is essential that this process does not alter the phenotype of the cells. Secondly, it must be appreciated that cells may also change their phenotype depending on the culture conditions, as Fejes-Toth and Naray-Fejes-Toth described with collecting duct cells (1992). And thirdly, cell culture tends to favour rapidly dividing cells which may not be representative of the endogenous kidney cell population.

Functional studies - *in vivo*

Nephrogenesis can be perturbed *in vivo* in animals using a number of approaches including treatment with teratogens, and physical and genetic manipulation.

Teratogens

Animals can be exposed to high levels of teratogens in an effort to generate an abnormal phenotype (Brown, 1997). Examples of proven renal teratogens in animals are alcohol which causes hydronephrosis (Gage and Sulik, 1991) and retinoic acid which causes renal agenesis in mice when it is given at one day before the metanephros is formed (Tse *et al.*, 1997). Humans are unlikely to be exposed to such high levels, but even low doses may be important in the pathogenesis of multifactorial disease.

Physical obstruction

Obstruction of the nephric duct, ureter and bladder has been performed in animals, with variable results. Surgical interruption of the mesonephric duct in the chick prevents the conversion of intermediate mesoderm into mesonephric tubules and subsequent formation of the metanephros (Berman and Maizels, 1982). Complete obstruction of the fetal sheep ureter in midgestation generates hydronephrosis and renal dysplasia whereas subcortical cysts are produced by obstruction later in pregnancy (Beck, 1971; Attar *et al.*, 1998). The marsupial opossum is accessible for ureteric obstruction as it enters the pouch and some aspects of dysplasia are generated by obstruction at that point (Steinhardt *et al.*, 1988).

Transgenic technology

The expression of metanephric molecules can be altered by genetic engineering of animals, usually mice. Techniques available include: i) microinjection of recombinant DNA into the pronuclei of fertilized eggs, ii) retroviral infection of preimplantation embryos, iii) reconstitution of early embryos with genetically engineered embryonal stem (ES) cells. Using these techniques, genes can be overexpressed by introducing the coding sequence of a gene linked to a strong promoter.

Genes can also be ablated in embryonic stem cells by homologous recombination in which the gene of interest is replaced by a homologous but non-functional fragment of DNA. The cells are then injected into the blastocyst where they are randomly incorporated into a variety of lineages. If the engineered cells contribute to the germ line, then animals with heterozygous and homozygous mutations can be generated by further breeding (Merlino *et al.*, 1991). Many such transgenic 'knock out' mice have abnormal renal development, often in conjunction with other malformations, as summarised in Table 2.

Gene	Phenotype	Author	
bf-2	Renal hypoplasia, large mesenchymal condensates	Hatini *et al.*, 1996	T
emx-2	Absent kidneys, ureters, gonads and genital tracts	Miyamoto *et al.*, 1997	T
hoxa-11 / hoxd-11**	Renal dysplasia or hypoplasia, and absence of radius and ulna	Davis *et al.*, 1995	T
lim-1	Renal agenesis, absent gonads and head structures	Shawlot and Behringer, 1995	T
pax-2	Renal agenesis and eye defects. Heterozygotes have renal hypoplasia	Torres *et al.*, 1995; Keller *et al.*, 1994	T
shh	Kidney defect of unspecified type	Chiang *et al.*, 1996	T
wt-1	Renal agenesis and abnormalities in respiratory system, heart and gonads	Kreidberg *et al.*, 1993	T
bmp-7	Renal dysplasia, eye and skeletal defects	Dudley *et al.*, 1995; Luo *et al.*, 1995	G
ret	Renal agenesis or dysplasia, and defects in the enteric nervous system	Schuchardt *et al.*, 1994	G
egfr	Cystic dilation of the collecting ducts. Defects in hair follicles, skin, tongue, gastrointestinal tract and brain	Threadgill *et al.* 1995	G
gdnf (ret ligand)	Renal agenesis	Sanchez *et al.*, 1996; Pichel *et al.*, 1996; Moore *et al.*, 1996	G
pdgf-β	Absent mesangial cells and heart defects	Leveen *et al.*, 1994	G
pdgf-rβ	Absent mesangial cells and heart defects	Soriano, 1994	G
rar-α and β **	Renal agenesis, or hypoplasia. Respiratory tract, gasrtrointestinal, heart, thymus, diaphragm and genito-urinary abnormalities	Mendelsohn *et al.*, 1994	G
bcl-2	Cystic kidneys and hypoplasia	Veis *et al.*, 1993	S
p57-kip2	Dysplasia and Beckwith-Wiedemann like syndrome	Zhang *et al.*, 1997	S
alpha-8 integrin	Failure of ureteric bud growth and nephron epithelialisation	Muller *et al.*, 1997	M
wnt-4	Renal dysplasia (?)	Stark *et al.*, 1994	M
Id (formin)	Renal agenesis and limb defects	Chan *et al.*, 1995; Maas *et al.*, 1994	O

Table 2. Transgenic null-mutant mice with kidney malformations.

This table summarises the abnormalities in null-mutant mice with kidney malformations. The classes of molecules involved include: 'T' - transcription factor, 'G' - growth factor or growth factor receptor, 'S' - survival factor, 'M' - matrix or adhesion factor, 'O' - other. Some of the phenotypes, indicated by '**', were generated by ablation of two different but homologous genes.

45

Basic mechanisms of development

Organogenesis involves a balance between key events at a cellular level including proliferation, death, differentiation and morphogenesis. It has been postulated that kidney malformations, cystic diseases and tumours are likely to result from disruption of this balance (Bard and Woolf, 1992) and many of these processes are examined later in this thesis.

Cell proliferation

The adult mammalian kidney develops from less than a thousand cells at its inception to many millions in the mature organ and it is self evident that this process requires extensive cell proliferation. The most actively proliferating areas of the metanephros, in the mouse, are the tips of the ureteric bud branches and the adjacent mesenchymal cells in the nephrogenic cortex (Hanai *et al.*, 1993). This is also demonstrated in the developing human kidney in the chapter on cell proliferation later in this thesis.

Stem cells are also thought to reside in the undifferentiated renal mesenchyme and it is postulated that these divide to generate a copy of themselves and another cell which differentiates into either nephron epithelia or interstitial cells (Burrow and Wilson, 1993). These cells are potentially important in the context of renal malformations since, if they are still present, it may be possible to stimulate elements of normal nephron formation if the appropriate inductive signals can be defined. True stem cells are not considered to be present in the mature adult kidney, although some cells can dedifferentiate after insults such as acute tubular necrosis to regenerate some parts of the nephron (Kawaida *et al.*, 1994).

Proliferating cell nuclear antigen

Proliferation in tissue sections can be assessed using a number of markers which are expressed in proliferating cells. Staining with Proliferating cell nuclear antigen (PCNA) was used in this thesis. PCNA, or 'cyclin', is a nuclear protein which was originally identified by immunofluorescence in proliferating cells (Reviewed by Baserga *et al.*, 1991). It is the auxiliary co-factor of DNA polymerase delta I and it is essential for DNA replication in the S phase of the cell cycle, along with roles in DNA repair (Jonsson and Hubscher, 1997).

The human PCNA gene is located on chromosome 20p12 and two pseudogenes have also been identified on Xpter-q13 and 6pter-p12. The gene codes for a protein of 261 amino acids which has been highly conserved during evolution since there is 70% and 98% homology with *drosophila* and rat pcna respectively.

PCNA has a number of functions in DNA proliferation. The toroidal shaped protein is thought to encircle DNA and its main function appears to be to tether the polymerase catalytic unit to the DNA template for rapid and processive DNA synthesis. It may also interact with proteins involved in cell-cycle progression which are not a part of the DNA polymerase apparatus. Some of these interactions may have a direct effect on DNA synthesis while the roles of several other interactions are not fully understood (Kelman, 1997).

The expression of pcna during different phases of the cell cycle has been analysed by flow cytometry in the mouse (Kurki *et al.*, 1986). Pcna is not expressed in significant amounts in G0 - G1, but it is dramatically upregulated in cells in late G1 and S-phase. Levels fall in G2 - M cells although they are still elevated relative to G0 - G1 cells.

47

The intranuclear distribution of PCNA has also been described in cultured human cell lines (Celis and Celis, 1985). Early in S phase, PCNA is found throughout the nucleoplasm with the exception of the nucleoli, but it then redistributes initially into a punctate pattern with foci of staining throughout the nucleus and later into the nucleoli when DNA synthesis is at or near its maximum. Intensity of PCNA staining then falls and reverts to the punctate pattern as S-phase finishes.

A number of studies have compared the use of PCNA staining with other measures of proliferation including the incorporation of bromodeoxyuridine and staining with Ki-67, another nuclear marker of proliferation. In general, there is good correlation between the different techniques although PCNA staining may slightly overestimate the amount of proliferation since the protein has been reported to persist in the cell for a variable time after S-phase (Howie *et al.*, 1995; Larsson *et al.*, 1996). PCNA staining has also been used to generate an estimate of proliferative activity in normal and cystic renal epithelia (Nadasdy *et al.*, 1994 and 1995).

Cell death

Kampmeier (1926) reported 'vestigial' and 'provisional' zones in the human metanephros in which the first three generations of nephrons are destined to die before birth (Fig. 5). Potter (1972) also suggested that early nephrons may die unless they moved their attachments to later branches of the ureteric bud (Fig. 6). It is only recently, however, that the extent and mechanism of cell death has been investigated. Indeed, Coles and colleagues (1993) estimated that as many as 50% of the cells which are born in the developing rat kidney will die by a process known as apoptosis, or programmed cell death.

Apoptosis

The term apoptosis, which means 'leaves falling from a tree' in greek, was derived by Kerr, Wyllie and Curry (1972) to describe death in a variety of normal and pathological contexts which was accompanied by specific cellular morphological changes. Apoptosis is often used interchangeably with 'programmed cell death' and these terms have been used to mean both the pre-programming of cells to die at a certain stage of development and the actual apoptotic program in which there is a defined sequence of histological and biochemical events. These concepts are described in more detail below.

Morphology of apoptosis

Morphological changes occur in the following sequence during apoptosis: i) decrease in cell size, ii) change in cell shape (rounding up), iii) condensation and fragmentation of the nuclear chromatin, iv) budding off of 'apoptotic bodies' consisting of plasma membrane-bound vesicles containing fragments of condensed chromatin and intact cellular organelles and v) phagocytosis and clearance of apoptotic cells and debris by neighbouring cells and macrophages. Apoptotic cell death does not lead to an inflammatory response and is relatively rapid. Both of these factors make it difficult to detect the true extent of apoptosis over time from analysis at one time point.

The alternative cell death pathway is necrosis, but this process is morphologically distinct (Wyllie *et al.*, 1980). In necrosis, cells swell, the plasma membrane breaks down and cytosolic contents leak into the surrounding tissue where they generate an inflammatory reaction.

Biochemical changes during apoptosis

The central biochemical event in apoptosis, in eukaryotic cells, is the cleavage of nuclear DNA into nucleosome sized fragments of 180 - 200 base pairs. This phenomenon is induced by a cascade of molecular events involving a number of membrane receptors and cytoplasmic proteins (Schwartz and Osborne, 1993) which are described below.

The apoptotic cell death program

For many years apoptotic cell death was thought to be a biochemically active process which involved transcription of specific genes and production of new proteins, since inhibitors of RNA and protein synthesis appeared to block apoptosis (Vaux and Weissman, 1993). This argument is flawed, however, since cells in which the nucleus has been removed (cytoplasts) cannot generate new mRNA yet they can still be induced to go through the cytoplasmic changes of apoptosis (Jacobsen *et al.*, 1996). In addition, cytoplasts derived from cells expressing high levels of the B-cell leukaemia / lymphoma gene (bcl-2), which will be described later, are resistant to apoptosis (Jacobsen *et al.*, 1996).

These data suggest that apoptotic effector proteins are constitutively expressed in cells and has led Raff and colleagues to propose that all cells are programmed to commit suicide unless they continuously receive survival signals from neighbouring cells (Raff *et al.*, 1993; Jacobsen *et al.*, 1997). The classical example which supports this theory occurs during normal neuronal development: up to 50% of the neurons which are produced will die and it appears that this apoptotic death occurs because the neurons compete for neurotrophic survival factors secreted by the target cells they innervate (Raff *et al.*, 1993).

Apoptosis is a dynamic process consisting of several steps including cellular signals which induce apoptosis, cellular machinery which carries out the apoptotic death program and clearance of apoptotic cells. These processes are described below and have been extensively reviewed in a special edition of the journal *Cell* (Vol 8, February 7, 1997).

A number of signals / signalling pathways have been identified which activate apoptosis. One of the best characterised is the Fas-based pathway (reviewed by Cohen, 1997). Fas is a member of the tumour necrosis factor (TNF) receptor family and activation of Fas by its ligand, Fas-L, leads to apoptosis. This has been implicated in development of the immune system, in cytotoxic T-cell mediated killing and in malignant transformation (Cohen, 1997). TNF can also induce apoptosis via the TNF receptor, TNFR-1, and members of the transforming growth factor-β (TGF-β) family have also been implicated in cell death signalling. Treatment with glucocorticoids, inhibitors of nucleotide metabolism or DNA damaging drugs also induces apoptosis in some cells. Some growth factors can not only control proliferation and differentiation but can also enhance apoptosis (Oberhammer *et al.*, 1993) or act as survival factors (Collins *et al.*, 1994).

The basic intracellular effector mechanisms which lead to apoptosis are highly conserved across evolution and studies in the nematode *Caenorhabditis elegans* have defined many of the genes required for cell death. This worm generates 1089 cells during development and 131 of these cells die by apoptosis. Three genes were identified as being of crucial importance: on the one hand, ced-3, and ced-4 are absolutely required for cell death and on the other hand, ced-9 prevents cell death. Mammalian homologues have now been identified (Vaux, 1993) with similar functions.

Ced-3 encodes a cysteine protease which is similar to the human enzyme interleukin-1β converting enzyme (ICE) and a number of other related proteases have recently been identified (Alnemri *et al.*, 1996). Members of this family of proteases are now known as caspases and these are thought to be central effectors within the apoptotic pathway; caspase-8, for example, is activated during Fas mediated apoptosis.

Ced-9 has similar anti-apoptotic effects to BCL-2 and programmed cell death can be prevented in *Caenorhabditis elegans* by expressing human BCL-2 (Vaux, 1993). The function of the BCL-2 gene is discussed elsewhere in this chapter, but it is of note that the BCL-2 protein is located in the mitochondrial membrane and opening of mitochondrial permeability-transition pores, or megachannels, has been implicated in apoptosis (Zamzami *et al.*, 1996).

Apoptotic cells are rapidly cleared (Wyllie, 1980) and two mechanisms have been postulated for this process: phagocytosis by neighbouring cells or by macrophages. An inflammatory response is rarely seen in areas of apoptosis during development and this, coupled with the histological finding of apoptotic bodies within normal cells, led to the hypothesis that apoptotic cells are solely cleared by neighbouring cells during normal development. This hypothesis has, however, been challenged, at least in the kidney, by workers in our laboratory who have demonstrated that macrophages are present in areas of apoptosis from the earliest stages of metanephric development (Personal communication – Dr Catherine Cale). It is therefore likely that both neighbouring cells and macrophages are involved in clearing apoptotic cells during normal development. Similarly, Savill and colleagues (1992) have demonstrated that glomerular mesangial cells and macrophages ingest apoptotic cells during glomerulonephritis.

Apoptosis in renal development

Apoptosis was first described systematically in the developing rat kidney by Coles *et al.* (1993), although earlier authors have commented on cell death during remodeling of the early branches of the ureteric bud (Kampmeier, 1926; Potter, 1972). In the rat kidney, programmed cell death was notable in the nephrogenic region and medullary papillae. Up to 3% of the cells showed changes consistent with apoptosis in these areas at any one time point. The authors extrapolated these figures, based on the predicted time course over which apoptotic cells could be detected, to speculate that cell death may be as frequent in the kidney as in neuronal development i.e. 50% of cells born in the kidney may die by apoptosis. Interestingly, treatment of one day old rats with epidermal growth factor (EGF) reduced renal cell death in the kidneys, which are still developing at that stage. This finding is consistent with the possibility that the cells normally die during development because they lack sufficient survival factors.

Apoptosis has also been demonstrated in metanephric organ culture (Koseki *et al.*, 1992). In these experiments, apoptosis was prominent in mesenchyme adjacent to the 'induced' mesenchyme which was undergoing mesenchyme to epithelial conversion. These changes could be prevented by treatment with actinomycin-D or cycloheximide or by co-incubation of the mesenchyme with a heterologous inducer such as embryonic spinal cord. Once again, EGF reduced the extent of apoptosis but the mesenchyme did not differentiate in response to this growth factor. This suggests that the conversion of mesenchyme to epithelium is at least a two step process involving rescue of the mesenchyme from apoptosis and induction of differentiation. More recently, Perantoni *et al.* (1995) showed that fibroblast growth factor 2 (FGF-2) can also rescue the mesenchyme from apoptosis. Conversely, tumour necrosis factor α

53

(TNF-α) treatment increases the amount of apoptosis in mouse organ culture (Cale *et al.*, 1998)

Differentiation

The process by which cells acquire a specialised phenotype is known as differentiation. A classic example occurs in the renal mesenchyme where some cells undergo epithelial differentiation to form nephrons while others differentiate into stromal cells, or interstitial fibroblasts. Terminal differentiation occurs at a later stage. For example, cells within a nephron precursor will form the glomerular parietal and visceral epithelia as well as the cells which comprise the proximal tubule and loop of Henle. The term 'lineage' describes the series of phenotypes as a precursor differentiates into a mature cell.

Morphogenesis

The processes outlined above occur in individual cells whereas 'morphogenesis' describes the developmental process by which groups of cells acquire complex three-dimensional shapes. Examples include the formation of nephron tubules from renal mesenchymal cells, serial branching of the ureteric bud to form the collecting duct system and capillary formation by angiogenesis and vasculogenesis.

Molecules expressed during nephrogenesis

Several classes of molecules are expressed during nephrogenesis, including transcription factors, growth factors, survival factors and the adhesion molecules. These categories are not mutually exclusive since certain molecules fall into two categories, an example being EGF, or its embryonic form - transforming growth factor α (TGF-α), which appears to act as both a survival factor for renal mesenchyme (see above) and a growth and differentiation factor.

Molecules from several major groups are examined in this thesis including transcription factors (PAX-2 and WT-1), survival factors (BCL-2) and cell / matrix adhesion molecules (galectin-3). These are described in detail in the appropriate section below, whilst other important molecules in these classes are briefly mentioned in order to provide a balanced overview. Molecules which do not fall into specific categories are discussed at the end of this section.

Transcription factors

Transcription factors regulate the expression of other genes, acting as 'master regulators' to set up basic embryonic pattern formation. They contain DNA binding domains which recognise specific sequences and hence modulate the transcription of mRNA from the target gene. The specific genetic targets of many of the transcription factors are, however, currently unknown. The transcription factors examined in this thesis are PAX-2 and WT-1, whilst other important factors are bf-2 (Hatini *et al.*, 1996), hoxa-11 and hoxd-11 (Davis *et al.*, 1995), lim-1 (Shawlot and Behringer, 1995), n-myc (Stanton *et al.*, 1992) and sox-9 (Bell *et al.*, 1997)

PAX genes – general aspects

PAX genes are transcription factors containing a paired-box DNA binding domain which are found in a number of organisms including *drosophila*, zebrafish, frog, turtle, chick, mouse and human (Gruss *et al.*, 1992). In organisms such as drosophila, pax homologues control embryonic patterning (Gruss *et al.*, 1992) and cell specification (Halder *et al.*, 1995), while a zebrafish pax gene has been implicated in retinal development (Hyatt *et al.*, 1996). In the mouse, pax genes regulate development of the brain, eye, lymphoid system, musculature, neural crest, thymus and vertebrae (Max *et al.*, 1995; Keller *et al.*, 1994; Matsuo *et al.*, 1993; Goulding *et al.*, 1991; Wallin *et al.*, 1996). In addition, transgenic overexpression of pax genes causes cell transformation in cell cuture and the mouse, and may contribute to tumour formation (Maulbecker and Gruss, 1993).

Nine PAX genes have been described in humans and some of these genes encode a homeobox domain and an octapeptide region in addition to the conserved paired box domain (Table 3; Stapleton *et al.*, 1993).

Gene	Chr	Structure	Expression pattern	Loss of function	Gain of function
PAX-1	20p		vertebral column, thymus	Mouse: undulated	?
PAX-2	10q		neural tube, kidney, optic cup, auditory vesicle	Human: renal-coloboma syndrome Mouse: *Krd*	Human: possible role in Wilms' tumour Mouse: abnormal kidneys
PAX-3	2q		neural crest, neural epithelium	Human: Waardenberg's syndrome Mouse: *splotch*	Human: possible role in rhabdomyosarcoma
PAX-4	7		possible pseudogene	?	?
PAX-5	9p		neural tube, B cells, kidney	Mouse: B-cell & brain abnormalities	Human: possible role in astrocytoma
PAX-6	11p		neural tube, optic cup	Human: aniridia Mouse: *small eye*	Mouse: abnormal ciliary body and lens
PAX-7	1p		neural tube, muscle	?	?
PAX-8	2q		neural tube, kidney	?	Human: possible role in Wilms' tumour
PAX-9	14q		vertebral column, nervous system, sclerotome	?	?

Table 3. Overview of PAX genes. This table shows the basic structure of the protein, and chromosome location (Chr), of human PAX genes including the ■ Paired box domain, □ Octapeptide domain and ■ Homeobox domain. The expression pattern, and results of loss of function or gain of function in mice and humans are also shown. '?' indicates that the phenotype is unknown.

The majority of the PAX genes are expressed in the developing nervous system, with the exception of PAX-1 which is only expressed in mesoderm derivatives. Mutations of PAX-2, 3 and 6 have been implicated in human syndromes. PAX-2 is described in detail below. PAX-3 mutations cause Waardenberg's syndrome type 1 and 2 (Tassabehji *et al.*, 1993; Read *et al.*, 1995) which is an autosomal dominant condition consisting of pigmentary disturbance and facial abnormalities (broad nasal bridge and lateral displacement of the inner corners of the eye) with occasional deafness and mental retardation. These abnormalities correlate well with sites of expression of pax-3 expressing neural crest cells in the mouse. The naturally-occurring *Splotch* mutant mouse is caused by pax-3 mutations and homozygous *splotch* mutants have additional abnormalities of the neural tube and limb muscles, which correspond with pax-3 expression in the dermomyotome and limb buds. Rearrangements of PAX-3 have also been reported in human soft tissue tumors (Barr *et al.*, 1993).

PAX-6 mutations cause aniridia in humans (Hanson *et al.*, 1993), characterised by partial or complete absence of the iris, whereas homozygous mutations in the mouse homolog, *small eye,* lack both nasal structures and eyes (Hill *et al.*, 1991). This suggests that gene dosage may be important for pax genes, at least in eye and face development, since the phenotype of mouse mutants is more severe when both alleles are mutated. This has been partially confirmed in *drosophila* where targeted overexpression of the eyeless (ey) gene, which is homologous to human PAX-6, caused ectopic eyes to develop (Halder *et al.*, 1995). Moreover, further evidence that gene dosage is important is that transgenic expression of human PAX-6 rescues eye development in the *small eye* mouse mutant but further eye abnormalities are seen if it is overexpressed (Schedl *et al.*, 1996).

PAX-2, 5 and 8 are structurally similar genes with a truncated homeodomain and a conserved octapeptide region. Only PAX-2 and PAX-8 are expressed in the kidney. Pax-5 (BSAP) is transiently expressed in the mesencephalon and spinal cord in mouse embryos but expression then shifts to the fetal liver where it correlates with the onset of B lymphopoiesis (Adams *et al.*, 1992). Expression persists in mature B lymphocytes and is also seen in the testis of the adult mouse. This expression pattern implicates pax-5 in B-cell differentiation and spermatogenesis as well as in neural development. Pax-8 is expressed in the developing mesonephric tubules and then in the condensing mesenchyme of the murine metanephros (Plachov *et al.*, 1990). It is not expressed in either the mesonephric duct or the ureteric bud and it is downregulated in maturing nephron epithelia (Poleev *et al.*, 1992). Other sites of pax-8 expression during development include the spinal cord and thyroid gland (Plachov *et al.*, 1990). A complete list of the regulatory targets for PAX-8 is unknown, although the protein has been shown to both bind and activate the promoter for the neural cell adhesion molecule (NCAM; Holst *et al.*, 1994). Expression of NCAM is downregulated, however, as nephrons develop from the condensed mesenchyme (Klein *et al.*, 1988a) and it is therefore unlikely that PAX-8 is the only controlling factor for this adhesion molecule.

PAX-2

In early development of the mouse kidney, pax-2 mRNA is expressed in the mesonephric duct, the tips of the ureteric bud and the condensing mesenchyme (Dressler *et al.*, 1990). This pattern is repeated in the outer cortex throughout nephrogenesis. Expression of the protein persists in nephron precursors such as the comma and S-shaped bodies but then decreases as these epithelia mature (Dressler *et al.*, 1992). In contrast, there is little expression in ureteric bud derivatives aside from low levels in the collecting ducts.

Detailed distribution of the PAX-2 protein had not been reported in either normal or dysplastic human nephrogenesis prior to the work described in this thesis.

Two murine pax-2 transcripts, generated by alternative RNA splicing, can be detected in the developing mouse kidney. The different RNA isoforms are around 4.2 kb and 4.7 kb in size, encoding proteins of 392 and 415 amino acids respectively (Dressler *et al.*, 1990). It is unknown whether the two isoforms have different functions, although the smaller protein is more abundant during development (Dressler *et al.*, 1990). In humans, the two RNA isoforms are around 4.2 and 4.5kb (Eccles *et al.*, 1992).

A series of experiments in mice and mutation analysis in humans have highlighted the importance of PAX-2 in renal development.

Mice with homozygous null mutations for pax-2 have aberrant mesonephroi, which do not contain tubules, and the metanephroi fail to form because the ureteric buds are absent (Torres *et al.*, 1995). In organ culture, addition of antisense pax-2 DNA-oligonucleotides leads to repression of pax-2 protein (Rothenpieler and Dressler, 1993) which causes inhibition of mesenchymal condensation and blocks the transition of mesenchyme to epithelium. Interestingly, the mesonephric tubules are also formed by mesenchyme to epithelium conversion which implicates pax-2 as an essential molecule in this process (Torres *et al.*, 1995).

Heterozygous mutations of pax-2 alone causes hypoplastic kidneys with reduced branching of the ureteric bud, reduced numbers of nephrons and cortical thinning (Torres *et al.*, 1995). The heterozygous phenotype is much more variable in *Krd* mice which were generated fortuitously when a 7cM fragment of chromosome 19 (which includes the pax-2 locus) was deleted by the random insertion of an unrelated

transgene (Keller *et al.*, 1994). The *Krd* heterozygotes had around a 25% incidence of gross renal abnormalities including renal agenesis, cysts and dilated ureters. At a microscopic level, cortical thinning, reduced numbers of nephrons and medullary cysts were observed. Eye defects were also seen in these heterozygotes with retinal thinning, caused by malformations of the cellular layers, and abnormal electroretinograms. The severity of the lesions varied in different strains of mice which suggests that other modifying genes, determined by the genetic background, may affect the mutant phenotype.

Transgenic overexpression of pax-2 in mice also causes kidney abnormalities as Dressler and colleagues described (1993). In this experiment, a human CMV promoter was fused to complementary DNA encoding the more abundant 392 amino acid pax-2 isoform and injected into zygotes. Fetal transgenic mice had ectopic pax-2 expression, particularly in the visceral glomerular epithelium which is destined to become the podocytes and the glomerular capillary loop endothelium was poorly fenestrated with reduced numbers of podocyte foot processes. The glomeruli appeared atrophic, but the glomerular basement membrane was normal. Other features were multifocal microcystic tubule dilatation, proteinuria and renal failure. This phenotype was thought to be similar to the Finnish-type human congenital nephrotic syndrome but the PAX-2 locus has subsequently been excluded (Kestila *et al.*, 1994).

PAX-2 mutations have recently been described in humans in the 'renal-coloboma' syndrome consisting of optic nerve colobomas, renal anomalies and vesicoureteral reflux (Sanyanusin *et al.*, 1995). The original report described a New Zealand family in which the father had bilateral optic nerve colobomas and mild renal dysfunction (proteinuria and plasma creatinine of around 1.7 mg / dl), whilst 3 of 5 sons had colobomas and more severe renal dysfunction. Other members of the

family were clinically normal and analysis of the affected patients revealed a mutation in PAX-2. This was a single nucleotide deletion in exon five, within the conserved octapeptide sequence and the mutation arose *de novo* in the father. The phenotype of these patients was initially thought to be analogous to heterozygous *Krd* mice but a new mouse frameshift mutation (Pax-2(1Neu)) has subsequently been described (Favor *et al.*, 1996) which is identical to this human mutation. Heterozygous mutant mice also have defects in the kidney, optic nerve, and retinal layer of the eye. Homozygous mutant embryos have severe developmental abnormalities of the optic nerve, kidney, ventral regions of the inner ear and brain (cerebellum and the posterior mesencephalon).

Further human patients have now been reported with PAX-2 mutations with additional abnormalities such as microcephaly, mental retardation and high-frequency hearing loss. Several patients had mutations in exon 2 (Schimmenti *et al.*, 1997) but there was remarkable variability in the their clinical presentation, even in a mother and son with an identical mutation. Homozygous PAX-2 mutations have not been described in humans although kindreds have been reported with kidney and Mullerian agenesis which superficially resemble the (female) mouse null-mutants (Torres *et al.*, 1995; Battin *et al.*, 1993).

The experiments described above suggest that both the number of copies of this transcription factor and the timing of its expression are essential for normal renal development. The defects in homozygous mutants are easily understood since these animals completely lack the pax-2 protein. In the heterozygous mutants it is likely that haploinsufficiency, a partial lack of functional protein, leads to the aberrant phenotype. Ectopic, persistent expression of pax-2 in the mouse appears to prevent epithelial maturation, particularly in the glomeruli, and causes cyst development.

Levels of PAX-2 may also be regulated by other genes. In a recent article (Liu *et al.*, 1997) it was shown that expression of pax-2 can be modulated in cultured rabbit proximal tubule cells by a number of molecules: egf increased pax-2 levels and both retinoic acid and tgf-β1 decreased levels. Interestingly, tgf-β1 did not affect the rate of transcription of pax-2 but it decreased the stability of the mRNA.

Persistent expression of PAX genes is seen in some human tumors, including Wilms' tumour of the kidney: PAX-2 (Eccles *et al.*, 1992; Dressler *et al.*, 1992) and PAX-8 (Poleev *et al.*, 1992). This suggests that the normal mechanism for down-regulation or switching off these genes is defective. The Wilms' tumour 1 (WT-1) gene is mutated in a minority of Wilms' tumours and loss of heterozygosity has been also reported. There is now increasing evidence, summarised below, that WT-1 and PAX-2 / 8 expression is closely related during both development and oncogenesis.

During development of the kidney the temporal relationship between pax-2 and wt-1 expression has been described by Ryan and colleagues (1995). The sequence of expression is: i) wt-1 at low levels in the uninduced mesenchyme, ii) high levels of pax-2 at the tips of the ureteric bud and in the condensing mesenchyme, iii) high levels of wt-1 and pax-2 in the mesenchyme and iv) persistent expression of wt-1 in the developing nephron as pax-2 levels decline. In addition Ryan showed, by DNase I footprinting analysis, that there are three high affinity wt-1 binding sites in the 5' untranslated sequence of the pax-2 mRNA. Moreover, in transient co-transfection experiments, wt-1 represses transcription of a CAT reporter gene fused to a fragment of the pax-2 gene including these potential regulatory sequences.

These experiments suggest that pax-2 is a target gene for wt-1, at least in the mouse, and upregulation of wt-1 may lead to repression of pax-2 during nephrogenesis.

PAX genes may also be involved in the regulation of WT-1. In a recent report (McConnel et al., 1997) the human PAX-2 protein was found to bind to two sites in the WT-1 promoter sequence. Co-transfection experiments with PAX-2 showed up to a 35 fold increased expression of a reporter gene fused to the PAX-2 bindings sites on the WT-1 gene. Similarly, PAX-8 may positively regulate WT-1 expression since several isoforms of mouse pax-8 have been shown to bind to a wt-1 promoter and stimulate promoter activity (Dehbi and Pelletier, 1996). This data suggests that both PAX-2 and PAX-8 may activate WT-1 expression during development. Overexpression of these three transcription factors has been described in both endogenous Wilms' tumours (Dressler et al., 1992; Eccles et al., 1992) and in heterotransplant Wilms' tumours in nude mice (Tagge et al., 1994). The data outlined above suggests that increased levels of the PAX genes may activate WT-1 expression and the mutated WT-1 protein may not be able to down regulate the PAX genes, thus forming a positive feedback loop. It is, however, unclear which is the primary event in tumour formation.

Other examples implicating over expression of these PAX genes in tumours are: I) high levels of PAX-2 expression in actively proliferating renal clear cell carcinoma lines and the decline in rates of proliferation when these cells are treated with specific PAX-2 antisense oligonucleotides (Gnarra and Dressler, 1995), ii) transformation of NIH3T3 fibroblasts when PAX genes are overexpressed in them and the tumours which result from injection of these cells into nude mice (Maulbecker and Gruss, 1993) and iii) downregulation of human p53, a tumour suppresser gene, by PAX-2, 5 and 8 with the theoretical

consideration that overexpression of these genes might block p53 tumour suppression (Stuart *et al.*, 1995).

The oncogenic potential of the PAX genes is dependent on the DNA-binding function of the paired domain (Maulbecker and Gruss, 1993). Theoretically, mutations of the paired domain would change DNA binding capabilities which may be important in the regulation of oncogenesis. To date, however, mutations of PAX-2 and PAX-8 have not been described in human tumours.

WT-1

Wilms' tumour of the kidney is one of the commonest solid tumours in childhood with an estimated incidence of 1 in 10,000 (Pritchard-Jones and Hawkins, 1997). Most tumours are sporadic but a family predisposition is occasionally seen (2 - 5% of cases). Children may also have associated urogenital abnormalities, especially in the Denys-Drash and WAGR syndromes, described below.

The possibility that Wilms' tumours may be caused by mutations of a tumour suppresser gene was first suspected when a group of patients were found to have a constitutional deletion of chromsomal bands on 11p. The first Wilms' tumour gene, WT-1, was then cloned on 11p13 (Gessler *et al.*, 1990), but this is only mutated in a minority of tumours and it is likely that there are at least two other Wilms' tumour genes, one at 11p15 (WT-2), another at 17q12 and possibly others which are unmapped (Pritchard-Jones and Hawkins, 1997). This discussion deals exclusively with WT-1 and the results presented later represent the first description of WT-1 protein distribution in human dysplastic kidneys.

The WT-1 gene encodes a transcription factor protein containing four zinc-finger motifs which are important for DNA binding. Several studies have documented expression of both WT-1 mRNA and protein during general mammalian development (Pritchard-Jones *et al.*, 1990; Armstrong *et al.*, 1993) and specifically in the urogenital system and Wilms' tumours (Pelletier *et al.*, 1991; Grubb *et al.*, 1994). Major, non-renal, expression sites of WT-1 include the brain, spleen, genital ridge, fetal gonad and mesothelium. During early human nephrogenesis, WT-1 mRNA is expressed in the mesonephric glomeruli and at low levels in condensing metanephric mesenchyme (Pritchard-Jones *et al.*, 1990). As the comma and S-shaped bodies develop, the levels of WT-1 increase and become restricted to the visceral glomerular epithelia. Expression is restricted to podocytes in the adult kidney. Using confocal laser scanning microscopy, it is also possible to demonstrate that the WT-1 protein is restricted to the nucleus during development (Mundlos *et al.*, 1993). Increased expression of WT-1 has also been reported in Wilms' tumours (Pritchard-Jones *et al.*, 1990).

The expression pattern described above correlates well with the abnormalities detected in humans with two conditions associated with mutations of WT-1: the Denys-Drash and Wilms' tumour, aniridia, genitourinary (WAGR) syndromes. The Denys-Drash syndrome consists of genitourinary abnormalities, including ambiguous genitalia in 46 XY males, nephrotic syndrome with mesangial sclerosis leading to renal failure and a predisposition to Wilms' tumour (Little and Wells, 1997). Point mutations of WT-1 have been described in Denys-Drash syndrome, and interestingly these seem to predominantly affect the DNA binding zinc finger domains: Pelletier and colleagues (1991) described 10 cases, 9 of which had mutations in exon 9 (zinc finger III) and 1 in exon 8 (zinc finger II).

66

The WAGR syndrome consists of Wilms' tumour, aniridia, genitourinary abnormalities including gonadoblastoma and mental retardation. Much larger deletions have been reported in this syndrome including the PAX-6 locus which explains the aniridia (Jordan *et al.*, 1996).

In both of these syndromes, loss of only one WT-1 allele leads to these abnormalities, yet the patients still have one normal WT-1 allele. Several hypotheses have been proposed to explain this apparent dominant effect (Junien and Henry, 1994). Firstly, the aberrant protein may compromise binding of wild-type WT-1 to its normal target, resulting in a dominant-negative effect. Secondly, the mutations may confer the ability to recognise new, incorrect, binding sequences which may exacerbate the lack of binding to normal targets by either activating or repressing new genes. And thirdly, it has been reported that there is loss of heterozygosity in some tumours which may lead to transcription of only the mutant allele. A similar effect could be produced by imprinting, although this has not been demonstrated conclusively for WT-1.

In transgenic mice, by contrast, heterozygotes which have only one normal copy of wt-1 are said to be completely normal with no predilection to Wilms' tumours (Kreidberg *et al.*, 1993). Homozygous mutants die before birth at around embryonic day 14 or 15, probably because of defects in mesothelial derived components in the heart and lungs, and kidneys are absent. Closer examination of kidney development shows that mesonephric tubules are formed normally, although in smaller numbers, but the ureteric bud fails to branch from the Wolffian duct and the intermediate mesoderm which would normally give rise to the nephrons dies by apoptosis (Kreidberg *et al.*, 1993). There was also no pax-2 expression in the mesenchyme, and explants of mutant blastema did not form nephrons following heterologous culture with spinal cord. This data suggests that WT-1 is

absolutely required for survival and early differentiation of the metanephric blastema.

The human WT-1 gene consists of 10 exons and the protein contains 4 zinc finger domains towards the carboxy-terminus. Four different isoforms of the protein are produced by alternative splicing of the mRNA at two sites: exon 5 containing 17 amino acids may be included or excluded, and the three amino acids lysine, threonine and serine (KTS) may also be included or excluded. The four isoforms can therefore be referred to as -/-, -/+, +/- and +/+. The commonest form encodes the largest protein which includes both extra domains (i.e. +/+) and the ratio of the mRNA for the isoforms is said to be consistent throughout development and within different tissues (Charlieu *et al.*, 1995). This does not automatically mean that the levels of protein are the same, however (Haber *et al.*, 1991).

There are several lines of evidence which support the role of WT-1 as a transcription factor, mostly as a transcriptional repressor. Firstly, WT-1 binds to guanine-rich sequences with moderately high affinity (Rauscher *et al.*, 1990). Secondly, binding to such guanine-rich sequences linked to reporter genes leads to decreased expression of the reporter (Madden *et al.*, 1991). Finally, the repression domain can be transferred from WT-1 to other proteins such as the early growth response 1 (EGR-1) gene and this converts them from transcriptional activators to repressors. Several endogenous targets have been proposed for regulation by WT-1 including the insulin-like growth factor 2 gene (IGF-2) and PAX-2, as above. In addition, WT-1 is a powerful repressor of its own gene, and it binds to multiple sites in its own promoter (Rupprecht *et al.*, 1994).

The precise role of the four splice isoforms is unknown but it has been reported that the +KTS form binds to a more limited range of DNA

sequences than the -KTS form. There is circumstantial evidence that this is important because the -KTS and +KTS forms are preserved in all vertebrate whereas the 17 amino acid insert of exon 5 is only found in mammals (Kent *et al.*, 1995). There is also direct evidence that the ratio of +KTS to -KTS forms is important because Frasier syndrome, characterised by focal glomerular sclerosis, delayed kidney failure and complete gonadal dysgenesis has recently been shown to be caused by specific intronic point mutations of WT-1 which reduce the proportion of the +KTS isoform (Barbaux *et al.*, 1997; Klamt *et al.*, 1998).

Sub cellular localisation experiments may explain the importance of the two -KTS and +KTS isoforms. Charlieu aand colleagues (1995) used a number of techniques, including immunoprecipitation, confocal microscopy and cell culture, to demonstrate that the +KTS form associates with small nuclear ribonucleoproteins (snRNP) in spliceosomes whereas the -KTS form is found in conjunction with the transcriptional apparatus. They postulated that WT-1 may therefore also be involved in RNA splicing as well as transcriptional repression.

HOX genes

Vertebrate hox genes encode homeodomain transcription factors which specify positional information along the anterior posterior axis. Individual null mutations of these genes do not have kidney abnormalities but double knockouts generated by interbreeding of hoxa-11 and hoxd-11 mutants often have renal agenesis or hypoplasia (Davis *et al.*, 1995). Hoxa-11 mRNA is normally expressed in metanephric mesenchyme (Hsieh-Le *et al.*, 1995).

MYC genes

C-myc RNA is expressed in uninduced mesenchyme and in very early epithelial structures in the mouse. Its expression is downregulated as the kidney matures and its expression pattern appears to correlate with areas of cellular proliferation during nephrogenesis (Schmid *et al.*, 1989). N-myc is upregulated during the mesenchymal-epithelial conversion, where it appears to be a marker of induction, and expression is confined to the condensates, comma and S-shaped bodies (Mugrauer and Ekblom, 1991). Homozygous null-mutant mice for n-myc have mesonephroi which are hypoplastic, with increased apoptotic cells and the embryos die at around embryonic day 11.5 (Stanton *et al.*, 1992). L-myc is restricted to the ureter of the mature kidney and it is not expressed by proliferating or embryonic cells (Mugrauer and Ekblom, 1991).

BF-2

BF-2 is one of the few genes which have been implicated in formation of interstitial cells from the mesenchyme lineage. It is a member of the winged helix family of transcription factors which are related to the *drosophila* fork head gene (Lai *et al.*, 1993). In mice, bf-2 is expressed in the cells immediately surrounding condensed mesenchyme cells, which express pax-2. Mice with null mutations have rudimentary, fused kidneys and die soon after birth (Hatini *et al.*, 1996). Interestingly, the mesenchyme condenses in the null mutant mice but does not develop any further and neither comma nor S-shaped bodies are formed. The ureteric bud also fails to branch normally and ret is widely distributed in the bud epithelium, rather than confined to the bud tips. It seems likely, therefore, that bf-2 modulates expression of a factor, or factors, from the 'uninduced' cells which is essential for ureteric bud growth and maturation of pretubular aggregates. This factor has not yet been identified.

Survival / proliferation factors

Survival and proliferation are key cellular events and a number of genes have been identified in renal development which are linked to these processes. Distribution of the B-cell lymphoma/leukaemia protein (BCL-2) in the normal, and dysplastic, developing human kidney is described for the first time in this thesis.

BCL-2

The BCL-2 gene was originally discovered in human follicular B-cell lymphomas with a translocation between chromosomes 14 and 18. It is now known to be part of a large family of genes which are involved in the control of apoptotic cell death (Knudson and Korsmeyer, 1997). The function of many of these genes has been preserved throughout evolution (see *Apoptosis* section of this thesis). BCL-2 and some members of the gene family such as BCL-X_L, Mcl-1 and A-1 repress apoptosis whereas others including BAX, BCL-X_S, BAD and BAK promote apoptosis. The balance between these processes is modulated by homo- and heterodimerisation between the different related genes and several articles within the last year have discussed this issue in detail (Kroemer, 1997; Knudson and Korsmeyer, 1997).

The BCL-2 protein consists of a carboxy-terminal transmembrane domain and four domains, eponymously called BCL-2 homology or BH domains, which are found in various amounts in other family members. BCL-2 protein is located in a number of sub-cellular sites including the outer mitochondrial membrane, nuclear membrane and endoplasmic reticulum. There is some evidence from targeting experiments in Madin Darby canine kidney (MDCK) cells, a line which is derived from dog collecting ducts, that mitochondria are the main site at which the anti-apoptosis effects of bcl-2 are mediated (Zhu *et al.*, 1996). It is not the only site of action, however, since bcl-2 deletion mutants which

71

either lack the membrane insertion domain (Hockenbery *et al.*, 1993), or specifically target it to the endoplasmic reticulum (Zhu *et al.*, 1996), conserve part of their anti-apoptotic function.

Bcl-2 is expressed in a wide variety of murine tissues during development but then becomes restricted to limited sites in the adult mouse. In early development, bcl-2 protein is expressed in tissues derived from all three germ layers (Novack and Korsmeyer, 1994), but it is then downregulated and restricted to specific areas such as the developing nervous system (Merry *et al.*, 1994), immunological tissues (Merino *et al.*, 1994) and diverse epithelia (Novack and Korsmeyer, 1994). Expression patterns of BCL-2 protein are similar in human fetal tissues (LeBrun *et al.*, 1993).

In the developing mouse central nervous system bcl-2 protein is detected in ventricular neuroepithelial cells and postmitotic cells of the cortical plate, cerebellum, hippocampus and spinal cord (Merry *et al.*, 1994). Postnatally, bcl-2 levels decline in central nervous system as the mice grow older, although it can still be detected in the granule cells of the cerebellum and dentate gyrus of the hippocampus. In contrast, in the peripheral nervous system, neurons and supporting cells of sympathetic and sensory ganglia retain substantial bcl-2 protein throughout life. There is a tremendous degree of 'plasticity' in the development of the nervous system since many more neurons are born than are required in the adult. Excess neurons, which do not establish the correct connections, are eliminated by apoptosis and it is likely that bcl-2 plays an important role in regulating neuronal survival cells, as discussed earlier (Raff *et al.*, 1993; Jacobsen *et al.*, 1997).

During maturation of lymphocyte lineages, in the mouse, bcl-2 protein is highly expressed in CD43+ B cell precursors (pro-B cells) and mature B cells but downregulated in pre-B and immature B cells

(Merino *et al.*, 1994). These cells are also eliminated by apoptosis, and experimental susceptibility to apoptosis following dexamethasone treatment correlates with the levels of Bcl-2 protein.

Bcl-2 is expressed in a number of epithelia in the mouse including the developing lung and intestinal epithelium (Merritt *et al.*, 1995). Expression of bcl-2 is confined to rapidly proliferating areas in the crypts and lower villi rather the tips of the villi, where cells have been reported to die by apoptosis (Gavrelli *et al.*, 1992).

In the murine kidney, bcl-2 protein is upregulated in the mesenchyme as it condenses around the ureteric bud tips (Novack and Korsmeyer, 1994). Expression persists in this lineage in the glomeruli and tubules during development of the nephrons but it is then downregulated and undetectable in the mature kidney. A similar pattern is seen in the developing human kidney (LeBrun *et al.*, 1993). Other sites of murine bcl-2 expression include the developing limb where Bcl-2 is expressed in the digital zones, but not in the interdigital zones of cell death, and in hair follicles.

Bcl-2 is so widely expressed during mouse development that one might have predicted that transgenic mice which lack bcl-2 would die *in utero*. This is not, however, the case since homozygous null mutants survive until birth and only later develop growth retardation with a reduced lifespan ranging from 2 to 10 weeks (Veis *et al.*, 1993). Very few abnormalities were described in the null mutants, but significant defects were detected in haematopoiesis, hair and kidney development. Haematopoiesis is initially normal but the thymus and spleen later undergo massive apoptosis and involute. Thymocytes from mutant mice are also more susceptible to apoptosis induced by irradiation or dexamethasone. The first coat of hair is normal but the second coat appears later than normal and the hair is hypopigmented.

The original report stated that kidneys in bcl-2 null mutant mice displayed pronounced histological abnormalities including cystic dilation of proximal and distal tubular segments associated with hyperproliferation of both the epithelia and interstitium (Veis *et al.*, 1993). Cysts were found in animals as young as 10 days and there was no relationship between age and the size of cysts. These abnormalities lead to a progressive rise in creatinine and renal failure is thought to contribute to their early death. Further reports analysed nephrogenesis in greater detail in the knockout mice and showed that there are much more fundamental abnormalities in metanephric development (Sorensen *et al.*, 1995 and 1996). At embryonic day 12, kidneys from homozygous null mutant mice are the same size as heterozygous, wild type kidneys. At birth, however, they are much smaller and hypoplastic with fewer nephrons and smaller nephrogenic zones (Sorenson *et al.*, 1995).

These abnormalities are accentuated in cultured metanephroi. 'Fulminant' apoptosis occurs in the homozygous mutant kidneys and this is the likely mechanism for these differences in renal development. Postnatally, cysts develop in all segments of the tubules including the proximal tubule, distal tubule / medullary thick ascending limb of Henle's loop, and collecting duct (Sorenson *et al.*, 1996). Cystogenesis is accompanied by increased proliferation in the cortex and medulla, as assessed by incorporation of 5-bromo-2'-deoxyuridine, and apoptosis of cells within cysts and in the renal interstitium. It therefore appears that the primary deregulation of cell survival in the bcl-2 null mutant mice leads to a secondary upregulation of proliferation in the kidney.

P53

Mutations of p53 lead to tumours in humans and it is therefore thought to act as a tumour suppressor gene. The p53 mRNA is normally expressed in comma and S-shaped bodies in the mouse (Schmid *et al.*, 1991) but homozygous deletion of P53 has no affect on murine renal development (Donehower *et al.*, 1995). In contrast, overexpression of p53 leads to smaller kidneys with fewer nephrons which is thought to be caused by incomplete mesenchymal differentiation (Godley *et al.*, 1996).

P57-KIP2

Cyclin-dependent kinases are essential for regulation of the cell cycle and proliferation. Cyclin kinase inhibitors such as p57-KIP2 block proliferation by binding to the kinases in G1 / S phase. The p57-kip2 gene is expressed in podocytes in glomeruli and stromal cells between the renal tubules during renal development and null mutants have fewer renal tubules and small inner medullary pyramids (Zhang *et al.*, 1997). Poorly formed medullary pyramids are also seen in human Beckwith-Wiedemann syndrome which is caused by loss of the imprinted, expressed maternal allele on chromosome 11p15.5. This site is close to the p57-KIP2 gene and heterozygous mutations have been reported in some Beckwith-Wiedemann patients. The mechanism for aberrant development in the null mutant mice has not been reported but it seems logical that cell proliferation will be more prominent in null mutants and this may perturb apoptotic remodeling of the medulla.

Growth factors / growth factor receptors

Growth factors and their cell surface receptors play an important role in nephrogenesis. There are three modes of action: paracrine factors are secreted by one cell and act on neighbouring cells, autocrine factors act on the producing cell and juxtacrine factors become inserted into the plasma membrane of the cell which produced it and interact with receptors on adjoining cells. The growth factors bind to specific cell surface receptors, mainly receptor tyrosine kinases. Binding of the ligand cause the receptors to dimerise and they are then autophosphorylated and transduce growth signals into the cell. These signals may stimulate many different processes including cell division, cell survival, apoptosis, differentiation or morphogenesis. Several important growth factors / growth factor receptors are discussed below.

HGF / MET

Hepatocyte Growth factor (HGF), was initially identified as the main mitogenic component for hepatocytes in serum from rats and humans with hepatic failure (Nakamura *et al.*, 1984; Gohda *et al.*, 1988). Scatter factor (SF) was concurrently identified as a factor released by human embryo fibroblasts which caused scattering of Madin Darby canine kidney (MDCK) cells in monolayer culture (Stoker *et al.*, 1985). It was subsequently shown that these two factors were identical (Gherardi *et al.*, 1989) and the abbreviation HGF will be used in this thesis. HGF is the ligand for C-MET, a receptor tyrosine kinase (Bottaro *et al.*, 1991).

Activation of the HGF / MET system has a number of biological actions including mitogenesis (Nakamura *et al.*, 1984), motogenesis or scattering of cells (Stoker *et al.*, 1985) and morphogenesis (Montesano *et al.*, 1991). This latter property is especially interesting in the context of renal development since exogenous HGF causes branching morphogenesis of MDCK cells in culture, and no other factors have been reported to have this effect.

During murine nephrogenesis, hgf mRNA is expressed in the renal mesenchyme, particularly in the cortex as the kidney matures (Sonnenberg *et al.*, 1993). Met is mainly localised to the developing epithelial tubular structures, although expression has also been detected in mesenchymal cells (Woolf *et al.*, 1995). Hgf is required for growth and branching in metanephric organ culture since blocking experiments perturb nephrogenesis (Santos *et al.*, 1994; Woolf *et al.*, 1995). Overexpression of hgf leads to renal failure in transgenic mice, although details of renal histopathology were not reported (Takayama *et al.*, 1996). Mice with homozygous hgf or met null mutations die at embryonic day 13 to 14 with placental, liver and muscle pathologies but early nephrogenesis is surprisingly normal (Schmidt *et al.*, 1995).

HGF and MET mRNA has been detected in a number of developing organs in humans (Wang *et al.*, 1994). Our group has also demonstrated HGF and MET mRNA and protein in early human nephrogenesis (Kolatsi-Joannou *et al.*, 1997). In that study, MET was shown, by immunohistochemistry, to be strongly expressed in ureteric bud branches and at a lower level in early nephron precursors. Interestingly, co-expression of MET and HGF protein was also detected in the epithelia and cysts of dysplastic kidneys (see later) which may implicate this system in the pathogenesis of these renal malformations (Kolatsi-Joannou *et al.*, 1997).

GDNF / RET

Glial cell line-derived neurotrophic factor (GDNF) has recently been discovered to be the ligand for the receptor tyrosine kinase RET (Vega *et al.*, 1996). This combination of growth factor and receptor are essential for nephrogenesis since homozygous null mutations of either factor in mice leads to renal agenesis or severe dysplasia (Schuchardt *et al.*, 1994; Moore *et al.*, 1996; Pichel *et al.*, 1996; Sanchez *et al.*, 1996). Heterozygous gdnf mutants also display defective ureteric bud branching suggesting that the levels of gdnf are critical for this process. In normal murine development ret mRNA is expressed in the mesonephric duct and branching tips of the ureteric bud in the metanephros and gdnf is expressed in the adjacent mesenchyme (Towers *et al.*, 1998). Organ culture experiments demonstrated that isolated mesenchyme from ret null mutants was able to induce normal branching of wild type ureteric bud, whereas mutant bud did not respond to wild type mesenchyme. Exogenously added gdnf causes a significant increase in ureteric bud branching and extra buds may also form (Towers *et al.*, 1998).

Binding of GDNF to the RET receptor requires an additional adapter molecule, GDNF receptor α (GDNFR-α). This molecule is also found in the epithelium of the ureteric bud coincident with ret and adjacent to sites of gdnf expression (Towers *et al.*, 1998). Interestingly, the ret null mutant mice also have aberrant development of the enteric nervous system which is similar to Hirschsprung's disease in humans but abnormal renal development has only rarely been reported in this condition (Santos *et al.*, 1988).

EGF / EGF receptor

Epidermal growth factor (EGF) and its embryonic homologue transforming growth factor-α (TGF-α) both bind to the epidermal growth factor receptor (EGF-R). Rogers and colleagues (1992) showed that E13 rat metanephroi produced tgf-α and nephrogenesis could be perturbed by using blocking antibodies against tgf-α. EGF is a potent inhibitor of cell death within the developing kidney *in vivo* (Coles *et al.*, 1993). It also rescues isolated renal mesencyme from apoptosis *in vitro* (Koseki *et al.*, 1992). Interestingly, mice with null mutations of egf-r have different renal phenotypes which are dependant on the specific genetic background of the animal (Threadgill *et al.*, 1995), since only one strain develops collecting duct cysts.

Cell adhesion molecules

Adhesion molecules mediate two forms of attachment, namely cell-cell and cell-matrix adhesion. Examples of cell-cell adhesion proteins are the calcium independent neural cell adhesion molecule (NCAM) (Bellairs *et al.*, 1995; Klein *et al.*, 1988a) and calcium dependent E-cadherin (also known as uvomorulin; Vestweber and Kemler, 1985). Molecules involved in cell-matrix adhesion include the collagens, fibronectin (Bellairs *et al.*, 1995), galectin-3 (Bao and Hughes, 1995), KAL (Duke *et al.*, 1995; Soussi-Yanicostas *et al.* 1996), laminins (Klein *et al.*, 1988b), nidogen (Ekblom *et al.*, 1994), tenascin (Aufderheide *et al.*, 1987) and integrin cell surface receptors (Kreidberg *et al.*, 1996; Muller *et al.*, 1997). Adhesion molecules may also have additonal roles since some molecules, particularly proteoglycans such as syndecan (Vainio *et al.*, 1989) and heparan sulphate, are able to sequester growth factors (such as FGFs) and modulate binding between growth factors and their cell-surface receptors. A general review is given below, followed by a detailed description of galectin-3, which is examined in this thesis.

General aspects

Uninduced metanephrogenic mesenchyme expresses collagen I, III and fibronectin in the mouse (Ekblom, 1981; Ekblom *et al.*, 1981). The cell surface NCAM is expressed by the uninduced mesenchyme and, after induction, NCAM expression decreases as the nephron matures (Klein *et al.*, 1988a; Lackie *et al.*, 1990). The proteoglycan syndecan acts as a receptor for interstitial matrix molecules and it is a marker for early induction of the mesenchyme-epithelial transition (Vainio *et al.*, 1989). Following induction, as the mesenchymal cells begin their transition to polarised epithelia they lose the interstitial collagens and fibronectin and begin to express uvomorulin, collagen type IV and laminin A chain (Vestweber and Kemler, 1985; Ekblom, 1981; Ekblom *et al.*, 1981). Laminin is a large multidomain cruciform basement membrane glycoprotein, which consists of A, B1 and B2 polypeptide chains. Uninduced metanephric mesenchyme expresses the B1 and B2 chains whilst laminin A is expressed at the onset of epithelial polarisation.

In mouse metanephric organ culture, antibodies to fragments E3 and E8 of the laminin A chain perturb tubule formation by preventing the conversion of mesenchymal cells to polarized epithelial cells (Klein *et al.*, 1988b). The E3 fragment of laminin binds the dystroglycan complex and antibodies which interfere with this binding inhibit the conversion of mesenchyme to epithelia (Durbeej *et al.*, 1995). The basement membrane glycoprotein known as either nidogen or entactin is produced by mesenchymal cells and binds to domain III on the laminin B2 chain. This laminin B2 / nidogen binding is critical for the production of epithelial basement membranes of epithelial structures formed during early nephrogenesis (Ekblom *et al.*, 1994).

Integrins are expressed on the cell surface as hetero-dimers, composed of alpha and beta-chains. Different combinations of alpha and beta-

chains confer ligand specificity on the integrins. An example is alpha 8 beta 1 integrin which binds to fibronectin, vimentin and tenascin (Muller et al., 1997). Integrins are widely expressed in the developing kidney and they are essential for normal tubulogenesis: targeted null mutation of the alpha 3 or alpha 8 subunit, which perturb expression of alpha 3 beta 1 and alpha 8 beta1 integrins respectively, disrupts growth and branching of the ureteric bud (Kreidberg et al., 1996; Muller et al., 1997). Antibodies to the alpha 6 subunit, which is a cell-surface receptor for the E8 fragment of laminin, also perturb tubule formation in metanephric organ culture (Sorokin et al., 1990). Aberrant expression of integrins have also recently been implicated in cystic kidney diseases: Daikha-Dahmane (1997) and colleagues described markedly increased expression of the alpha 1 subunit in polycystic kidney disease (PKD) along with irregular expression of alpha 2, alpha 3 and alpha 6 in PKD and cystic controls.

Mesenchymal cells which do not become epithelial continue to express interstitial collagens and fibronectin in the mouse but also express the mesenchymal matrix molecule tenascin (Aufderheide et al., 1987). Uninduced mesenchyme does not express tenascin until adjacent cells are induced. Proteoglycans, such as heparin and chondroitin sulphate are important in the formation of basement membranes (Lelongt et al., 1988; Davies et al., 1995). Proteoglycans can bind and store certain growth factors thus modulating their activity. Heparan sulphate can bind fibroblast growth factors, in doing so it prevents their degradation and facilitates the interaction of the growth factor with its cell surface receptor (Kiefer et al., 1990). The cell surface proteoglycan syndecan binds basic FGF (Elenius et al., 1992), and TGF-β can bind to beta-glycan whereas the extracellular matrix molecule decorin binds and neutralises the activity of this growth factor (Ruoslahti and Yamaguchi, 1991).

Galectin-3

Lectins are naturally occurring proteins which bind specific configurations of carbohdrate residues of glycoproteins (Sharon and Lis, 1989). Galectins comprise a family of Ca^{2+}-independent water soluble β-galactoside binding lectins (Barondes et al., 1993) and galectin-3 (formerly known as Mac-2) is a 30 - 42 kD molecule found in a variety of mammalian species (Hughes et al., 1994). The study of galectin-3 in normal and dysplastic human nephrogenesis comprises a major part of this thesis.

The human galectin-3 protein consists of an amino-terminal half containing a repetitive domain sequence rich in proline, glycine and tyrosine (Herrmann et al., 1993) which is sensitive to collagenases and elastases, in contrast to the carboxy-terminal half containing the carbohydrate recognition domain. The latter binds molecules with poly-N-acetyllactosamine side chains and ABH blood group determinants (Sato et al., 1992).

Galectin-3 protein has been identified, in many species, within cells in nuclear and cytoplasmic distributions (Hughes et al., 1994). It is also a secreted molecule which can either adhere to the cell surface (Sato et al., 1994) or appear in conditioned medium of galectin-3 expressing cell lines (Sato et al., 1993). The latter observations are interesting in view of the apparent absence of a secretory signal in the galectin-3 protein suggesting the use of a novel secretory pathway which is independent of the endoplasmic reticulum and Golgi apparatus (Sato et al., 1993).

Galectin-3 is expressed by preimplantation mouse embryos (Weitlauf et al., 1992), and by notocord, skeleton and skin later in development (Fowlis et al., 1995). The galectin-3 protein has also been reported to

be expressed during the late nephrogenic period in hamsters (Foddy *et al.*, 1990) but the detailed renal expression patterns were not defined.

In the adult mammal, galectin-3 expression has been described in a variety of epithelia *in vivo* including the colon and it can be detected on the surface of thioglycollate-elicited inflammatory macrophages (Hughes, 1994). The distribution of galectin-3 in many different types of cells together with varied subcellular localisation of the protein suggests many different roles for this molecule. In the nucleus galectin-3 associates with ribonucleoproteins and here it may play a role in pre-mRNA splicing (Dagher *et al.*, 1995; Wang *et al.*, 1995). Interestingly, loss of nuclear galectin-3 staining has been reported in colonic neoplasia (Lotz *et al.*, 1993) and this correlates with neoplastic progression. Other reports linking this molecule to cell proliferation include the upregulation of galectin-3 in stimulated 3T3 fibroblast cells prior to S-phase (Moutsatsos *et al.*, 1987; Agrwal *et al.*, 1989), and in lymphocytes transformed with human T-cell Leukaemia Virus I (Hsu *et al.*, 1996). Similarly, *in vivo*, levels of galectin-3 are increased in a variety of tumors (Schoepnner *et al.*, 1995; Xu *et al.*, 1995) and correlate with the metastatic potential of certain tumour cell lines (Raz *et al.*, 1990). Furthermore, galectin-3 may also have a role in preventing programmed cell death since overexpression of galectin-3 in T-cells makes them resistant to apoptosis (Yang *et al.*, 1996): of note, galectin-3 has some homology with BCL-2, a survival factor associated with nuclear and mitochondrial membranes (Yang *et al.*, 1996). Finally, secreted galectin-3 may mediate cell-matrix interactions since it is able to bind embryonic glycoforms of laminin and fibronectin which have polylactosamine side chains (Sato *et al.*, 1992), and galectin-3 has been shown to modulate laminin / integrin interactions hence mediating cell attachment and spreading *in vitro* (Sato *et al.*, 1992).

In cell culture, galectin-3 protein is synthesised by MDCK cells, epithelial cells with characteristics of kidney collecting ducts (Bao and Hughes, 1995). MDCK cells form three dimensional cysts when cultured in collagen type I gels and cyst size can be modulated by perturbing galectin-3 expression: blocking antibodies increase cyst growth and exogenous galectin-3 slows cyst growth (Bao and Hughes, 1995). This could be viewed as an *in vitro* model of cystogenesis and it is intriguing that galectin-3 can modulate cyst growth in this situation.

In view of these findings which implicate galectin-3 in a number of processes which may be important in both normal and cystic renal development, the precise distribution of galectin-3 is determined in this thesis.

KAL

The KAL gene is mutated in X-linked Kallmann's syndrome and affected patients have aberrations of renal and olfactory bulb development. Up to 40% of patients have renal agenesis (Kirk *et al.*, 1994). The predicted protein has homologies with NCAM and fibronectin. When the gene was transfected into mammalian cells in culture, an N-glycosylated protein was synthesised and a secreted form localised on the cell surface (Soussi-Yanicostas *et al.* 1996), possibly binding to heparan-sulphate proteoglycans. Our group has shown, using a combination of *in situ* hybridisation and RT-PCR, that KAL mRNA is expressed in the nephrogenic cortex of the early human kidney (Duke *et al.*, 1995) and it may be that interactions between KAL and other matrix molecules are essential for normal metanephric development.

Other molecules

Many functionally important metanephric molecules do not fall into the categories described above. These include: cyclo-oxygenase2 (cox-2) an enzyme involved in synthesis of prostaglandins (Morham *et al.*, 1995); formins, molecules of uncertain function without which the embryonic kidneys fail to form (Maas *et al.*, 1994); mpv-17, a peroxisomal protein implicated in the integrity of the glomerular filtration barrier; retinoic-acid receptors (RAR), which are important in morphogenesis (Mendelsohn *et al.*, 1994); and the wnt genes including wnt-1, 4 and 11 (Herzlinger *et al.*, 1994; Stark *et al.*, 1994).

Carbohydrate expression and lectin binding

Expression of different cell surface carbohydrate residues occurs in different parts of the nephron. Lectins are proteins, or glycoproteins, which bind to carbohydrate residues, and lectin binding patterns can therefore be used to identify specific nephron segments. Several lectins have been well characterised in mature kidneys including: *Tetragonolobus lotus purpurea* – proximal tubules, *Arachis hypogaea* - collecting ducts, *Dolichos biflorus* – ureteric bud and its derivatives and *Ulex europaeus* – endothelia (Holthofer, 1981 and 1984; Verani *et al.*, 1989). Some authors have also reported that *Ulex europaeus* labels collecting ducts as well as endothelia (Howie and Johnson, 1992).

Lectin staining has, however, not been as well characterised in the developing kidney and, confusingly, the mature distal segment marker *Arachis hypogaea* has been described in developing proximal tubules at 10 and 13 weeks of gestation (Hanioka *et al.*, 1990). Similarly, there have only been limited reports of lectins in dysplastic kidneys (Matsell *et al.*, 1996), and lectin binding is therefore examined in developing normal and dysplastic kidneys later in this thesis.

Chapter 3.

Abnormal human nephrogenesis

Renal malformations are the commonest cause of chronic renal failure in children (Warady *et al.*, 1997). They consist of a wide spectrum of developmental abnormalities, yet little is known about their pathogenesis.

The range of renal malformations includes agenesis, hypoplasia and dysplasia (Bialestock, 1964; Bernstein, 1971; Risdon, 1971; Potter, 1972; Woolf and Winyard, 1998). In the most extreme case, renal agenesis, the kidney is absent and the adjoining ureter is also often missing. In renal dysplasia the kidney contains abnormally developed structures (see below) and may be very small, or aplastic, or it may contain cysts in the multicystic dysplastic kidney. In renal hypoplasia the kidneys are small and contain fewer nephrons than normal. Some hypoplastic kidneys contain grossly enlarged nephrons in the condition of oligomeganephronia. All of these conditions may be associated with malformations of the urinary tract such as malformed ureters, duplications, obstruction and vesicoureteric reflux.

Incidence of human renal malformations

In humans, the combined incidence of all forms of renal or urinary tract malformation is reported to be as high as 10% (Woolf, 1995). The incidence of severe kidney malformations is much lower although there is a great variability in quoted incidence between different publications. Bilateral renal agenesis has a reported incidence of 1 to 3 in 10,000 births compared to 1 in 10,000 for bilateral renal dysplasia. Both of these conditions may present as neonates, if there is no functioning renal tissue, with the Potter sequence of oligohydramnios, face and limb deformities and lung hypoplasia. The reported incidence of

86

unilateral agenesis varies from 1 to 30 per 10,000 births and unilateral multicystic dysplastic kidneys occur at 1 in 10,000.

There are a number of reasons for the variability in reported incidence of these malformations. Firstly, unilateral disease may be clinically silent if the contralateral kidney is able to compensate functionally and the incidence may be underestimated. This ascertainment error may be eliminated in future studies since malformations are increasingly being detected on routine antenatal ultrasound scan which should eventually generate more reliable incidence figures. Historical data on unilateral disease, however, is still based on postmortem findings or on selected populations which had renal imaging for other reasons. Secondly, if there is severe bilateral disease then the fetuses may be terminated or die soon after birth and these cases will not be included in surveys of older children or adults. And finally, dysplasia is a histological diagnosis (see below) which can only be inferred from radiological studies since tissue samples are rarely obtained from abnormal kidneys during life.

A further confounding issue is that the phenotype may change over time in at least two circumstances: i) dysplastic kidneys may involute and disappear completely giving rise to an aplastic phenotype (Dungan et al., 1990; Rickwood et al., 1992; Mesrobian et al., 1993; Al-Khaldi et al., 1994) which biases the ratio of aplasia to dysplasia in studies of adult patients (see below), and ii) there is an increased incidence of pyelonephritis in dysplastic kidneys (Bialestock, 1964) which may cause scarring and lead to glomerulosclerosis which masks the initial pathology.

Pathology of dysplasia

In its strictest sense, renal dysplasia is a histological diagnosis characterised by the presence of primitive ducts which are lined by relatively tall, often ciliated, columnar epithelium and surrounded by fibromuscular collars with additional nests of metaplastic tissue, classically cartilage (Bernstein, 1971). Commonly, however, the term dysplasia is used to refer to kidneys, or areas of renal tissue, in which there are elements resembling fetal structures or containing poorly differentiated epithelium i.e. metaplastic cells surrounding poorly branched ureteric bud derivatives (Risdon, 1971). A number of authors have described specific histological abnormalities in dysplastic kidneys and often attempted to provide a mechanistic explanation for these abnormalities. Several of these reports are summarised below.

Bialestock (1964) divided renal malformations into three groups depending on associated vesicoureteric reflux or obstruction. The groups were: type 1 – kidneys subjected to reflux in which obstruction was excluded, type 2 – kidneys subjected to the effects of both reflux and obstruction, and type 3 - kidneys subjected to obstruction without reflux. All of the type 2 kidneys were severely abnormal with hypoplastic and dysplastic areas whereas the degree of abnormality was reduced in types 1 and 3. She concluded that "the metanephric malformations occur *ab initio*, but hydrodynamic effects of reflux and obstruction might disturb further the differentiation of the sensitive developing parenchymal structures".

Osathanondh and Potter performed a series of microdissection studies on normal and cystic dysplastic kidneys which were reported in the *Archives of Pathology* (1964) and summarised in Potter's book *Normal and abnormal development of the kidney* (1972). In dysplastic kidneys, they described decreased branching of the ampullary portion of the collecting ducts derived from the ureteric bud which led to failure of nephron formation and the development of cysts (Fig. 7). They suggested that an extrinsic agent was responsible for this failure of development, but it is not clear how this led to the pathological changes.

Figure 7. Development of a multicystic dysplastic kidney. Potter described diminished branching of the ureteric bud with terminal cystic dilatation of the enlarged branches, and an increased quantity of surrounding connective tissue. Modified from Potter, 1972.

Risdon (1971) reviewed 76 cases of renal dysplasia and the associated urinary tract abnormalities. He suggested that "renal dysplasia is the abnormal, disorganised development of renal parenchyma due to anomalous differentiation of metanephric tissue" and described three types of dysplasia: group 1 was gross cystic dysplasia involving the whole kidney with absence of the renal pelvis or ureter, group 2 was segmental dysplasia in conjunction with anatomical or functional abnormalities in the ureter and group 3 was segmental dysplasia, often in conjunction with obstruction of the lower urinary tract. Pyelonephritis was a common finding in groups 2 and 3. He also reported that the contralateral kidney was hydronephrotic in three cases.

Bernstein has published extensively on the subject of renal dysplasia and hypoplasia. He described renal dysplasia as "the abnormal development of nephronic and ductal structures resulting in total or partial renal malformation (1971)". He theorised that this resulted from "faulty metanephric differentiation resulting from extrinsic influences". One of the major influences was said to be "back-pressure on the developing kidney" which produced both cortical and medullary dysplasia. This may be especially relevant in multicystic dysplastic kidneys which are often connected to a completely obstructed or atretic ureter.

Several studies have also demonstrated that up to 50% of kidneys contralateral to dysplastic kidneys are either structurally abnormal or affected by vesicoureteric reflux (Greene et al., 1971; Atiyeh et al., 1993). An example of this is renal aplasia on one side and dysplasia on the other, which has been reported in some individuals. In addition, families have been described where different members have aplasia, dysplasia or other urinary tract abnormalities such as vesico-ureteric reflux, duplications and horseshoe kidneys (McPherson et al., 1987).

Moreover, since the kidney phenotype may change (see *Natural history of dysplastic kidneys* below) it may be appropriate to consider a spectrum of renal malformations including aplasia and dysplasia and this has been termed renal "adysplasia".

Cysts in dysplastic kidneys

Cysts, of variable size, are often seen in dysplastic kidneys but very little has been written about the molecular pathogenesis of these cysts. It is self evident that there must be epithelial cell proliferation to generate cysts but this has not been quantified in dysplastic kidneys and much of the experimental work has been hampered by the lack of a good animal model of renal dysplasia.

Two recent articles have, however, described aberrant growth factor / receptor expression in dysplastic kidneys. Our group showed that dysplastic epithelia express MET and its ligand, HGF, is located in both the epithelia and surrounding cells (Kolatsi-Joannou *et al.*, 1997). Similarly, Matsell and colleagues (1997) described aberrant expression of IGF2 and IGF2-binding protein in cyst epithelia. Aberrant expression of growth factors may therefore be important in dysplastic cyst formation.

Cysts in polycystic kidney disease

A number of aberrations of cell biology have been implicated in cyst formation in both human and animal polycystic kidney diseases. These include increased cell proliferation (Grantham, 1992; Nadasdy *et al.*, 1995), altered polarity (Avner *et al.*, 1992, Woo *et al.*, 1994) with increased fluid secretion into cysts (Grantham, 1992), abnormal matrix deposition (Wilson *et al.*, 1992) and increased apoptosis in autosomal dominant polycystic kidney diseases (ADPKD; Woo, 1995).

The gene which is mutated in the majority of ADPKD patients, PKD-1, has been cloned and its gene product, polycystin 1, is believed to be involved in cell-matrix interactions (European polycystic kidney disease consortium, 1994). The gene for autosomal recessive polycystic kidney disease (ARPKD) has not been cloned, although the locus has been defined on 6p21 (Zerres et al., 1994).

Some of the aberrations in cell biology correlate with aberrant protein expression within polycystic epithelia. For example, C-MYC is reportedly upregulated in ADPKD (Lanoix et al., 1996) and cpk/cpk mice (Harding et al., 1992), and overexpression of c-myc in mice causes renal cysts (Trudel et al., 1991). In cell culture, overexpression of c-myc causes either proliferation or apoptosis depending on the concentrations of growth factors (Harrington et al., 1994) and both of these have been reported in polycystic kidneys. In addition, mice with null mutations of bcl-2 have fulminant metanephric apoptosis and develop cystic kidneys (Veis et al., 1993; Sorenson et al., 1995). Imbalance of growth factors such as EGF (Gattone et al., 1990) and HGF (Horie et al., 1994) have also been reported in polycystic disease.

At present it is uncertain whether similar mechanisms may lead to cyst formation in dysplastic kidneys. The extent of apoptosis and galectin-3 expression had not been defined in ARPKD prior to this thesis, and I have therefore examined these aspects of polycystic cell biology and compared them to dysplastic and normal samples.

Natural history of dysplastic kidneys

There is a small risk that dysplastic kidneys may become malignant or cause hypertension and, for this reason, it has been advocated that dysplastic kidneys should be surgically removed (Webb *et al.*, 1997). There is increasing evidence from serial ultrasound scans, however, that dysplastic kidneys become smaller with time and may involute completely (Dungan *et al.*, 1990; Mesrobian *et al.*, 1993; Al-Khaldi *et al.*, 1994). Many centres, therefore, manage dysplastic kidneys expectantly with regular renal ultrasound and blood pressure measurements. Surgery is reserved for the rare cases of multicystic dysplastic kidneys which become so large that they cause mechanical obstruction or patients with refractory urinary tract infections and pyelonephritis.
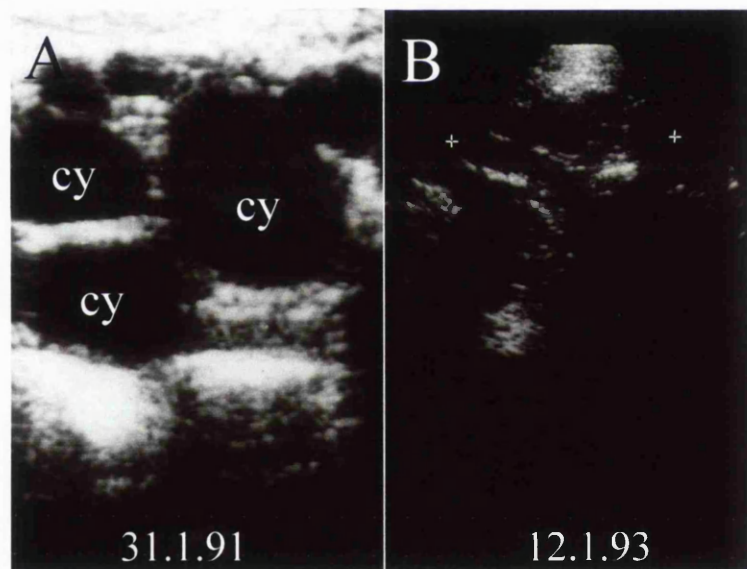
Figure 8. Involution of a multicystic dysplastic kidney.

A) Ultrasound scan from 1991 showing 3 large cysts (cy) in a multicystic dysplastic kidney. Note that the kidney also contains echogenic dysplastic tissue between the cysts. B) Scan from two years later showing a much smaller kidney (upper and lower limits marked by + signs) with decrease in size of both the cysts and dysplastic tissue.

Causes of dysplasia

The majority of cases of human renal malformations appear to be sporadic without a detectable cause for the disruption of the normal program of nephrogenesis. In a limited number of patients, however, the aetiology has been defined and falls into one of three categories: teratogens, physical obstruction of the urinary tract and genetic causes.

Teratogens

A number of teratogenic factors have been identified which perturb human kidney development. High blood glucose levels during pregnancy are associated with a number of defects including renal malformations, and drugs such as angiotensin converting enzyme and thalidomide cause aberrant kidney development (Novak and Robinson, 1994; Barr and Cohen, 1991).

Low levels of exposure to teratogens may also be important but these are difficult to detect unless they are specifically sought from the history. For example a recent study showed that Vitamin A can be teratogenic at a daily dosage of higher than 10,000 IU; this included a relatively weak association with urogenital defects (Rothman *et al.*, 1995).

Physical obstruction

There is a strong association between human renal malformations and obstruction to the urinary tract in a significant minority of girls and approximately half of boys (Bernstein *et al.*, 1997). This is particularly striking in multicystic dysplastic kidneys with atretic ureters and boys with posterior urethral valves in which there is bladder outlet obstruction, often in conjunction with tortuous dilated ureters. Obstruction at other sites such as the pelviureteric and vesicoureteric junction may also associated with aberrant renal development.

94

Kidneys associated with obstruction in early gestation are usually dysplastic whereas obstruction in the last third of gestation is associated with hydronephrosis and subcortical cysts.

It is possible to surgically decompress the obstruction of the lower urinary tract by inserting a vesico-amniotic shunt. Small-scale studies of this procedure have not, however, shown a consistent improvement in renal function (Elder *et al.*, 1987; Freedman *et al.*, 1996) and large scale controlled trials have not yet been reported. Two theoretical reasons may explain this lack of improvement with shunting. Firstly, the obstruction is often not detected until late in pregnancy and the fetus may then be monitored for several weeks (amniotic fluid volume, urine quality) before the shunting procedure. Irreparable renal damage may have already occurred by this time during development. And secondly, it may be that the same pathological event which caused the obstruction has also perturbed renal development and the kidneys are abnormal from the start.

Animal experiments give conflicting support for the role of obstruction in the genesis of dysplasia. Obstruction of the ureters in the chick at the earliest stages, before nephrons are formed, causes hydronephrosis but not dysplasia (Berman and Maizels, 1982). In the opossum, surgical obstruction of the developing animal in the marsupial pouch gives some features of dysplasia (Steinhardt *et al.*, 1988) and treatment with IGF-1 is reported to reduce the degree of dysplasia (Steinhardt *et al.*, 1995). In the fetal sheep dysplasia is generated by early obstruction, whereas sub cortical cysts and hydronephrosis occurs in later gestation (Beck, 1971).

Our group has also recently examined the effects of ureteric obstruction in the fetal sheep (Attar *et al.*, 1998) and the results of these experiments will be reviewed in the *Discussion* later in this thesis.

Obstruction and apoptosis

There have been a number of reports which suggest that there is increased apoptosis in kidneys connected to an obstructed ureter in the neonatal rat (Kennedy *et al.*, 1994; Chevalier *et al.*, 1996; Truong *et al.*, 1996). There is also decreased expression of clusterin, a protein which potentially protects against apoptosis, in neonatal compared to adult rats (Chevalier *et al.*, 1996). Increased clusterin expression has however been reported in a number of human cystic diseases, including dysplasia (Dvergsten *et al.*, 1994). This data suggests that the developing and mature kidney respond differently to obstruction and it has been postulated that excess apoptosis prevents normal growth and development in the former. Interestingly, EGF reduces the extent of apoptosis in rat ureteric obstruction (Kennedy *et al.*, 1997). The relevance of these findings to human ureteric obstruction is not clear.

Genetic causes

Most patients with kidney malformations do not have a family history of renal disease although this does not rule out *de novo* mutations. There is strong evidence from animal studies, however, that mutations in genes which are expressed during nephrogenesis cause renal malformations. The family studies and the association between renal malformations and genetic syndromes described below do however implicate genetic mutations in the pathogenesis of some human renal malformations (Woolf and Winyard, 1998).

Family studies

There have been a number of reports describing families with several affected siblings or affected relatives in two or more generations, suggesting a transmissible genetic defect. Twelve such families were described by Cain and colleagues (1974), including one case of 2 siblings in which the first had bilateral renal agenesis while the second had agenesis with contralateral dysplasia. In a large study with index cases of bilateral agenesis / severe dysplasia it was shown that 9% of relatives had asymptomatic renal malformations, most often unilateral agenesis (Roodhooft et al., 1984). Many of the reported cases of agenesis and severe dysplasia are suggestive of autosomal dominant inheritance as McPherson and colleagues (1987) described in 7 families. Autosomal recessive and X-linked inheritance of renal malformations have also been described but the genes which are involved have not been defined.

Vesicoureteric reflux is often detected in patients with renal malformations and segregation analysis of primary vesicoureteric reflux patients by Chapman and colleagues (1985) suggested that a single major locus was the most important causal factor in this condition. More recent studies from the same group in New Zealand identified a sub group of reflux patients with optic nerve colobomas and PAX-2 mutations (Sanyanusin et al., 1995).

Syndromes with renal malformations

Many chromosomal abnormalities, including complete trisomies, 4p-syndrome, partial trisomy 22 and dup (10p)/del (10q) cause syndromal malformations with renal defects of varying severity. In the majority of renal malformations associated with syndromes, however, there are no macroscopic cytogenetic aberrations although a proportion are inherited in recognised Mendelian patterns. Attempts have been made to define the mutations causing these syndromes using both linkage and candidate gene strategies. This technique has defined the disease locus or the specific genetic in several syndromes and a list of these syndromes is listed in table 4. Several of these syndromes are discussed briefly below, but a more comprehensive listing can be found in McKusick's *Mendelian Inheritance in Man* (1992) and other references (Woolf and Winyard, 1998).

Table 4. Human renal malformation syndromes with a genetic basis

Non-syndromic

Renal aplasia and dysplasia (adysplasia)

Primary vesicoureteric reflux

Associated with syndromes

Apert syndrome (FGFR-2 mutation)

Bardet Biedl syndrome

Branchio-oto-renal syndrome (EYA-1 mutation)

Campomelic dysplasia (SOX-9 mutation)

Di George syndrome

Fanconi anaemia (FAA mutation)

Kallmann's Syndrome (KAL mutation)

Meckel syndrome

Renal-coloboma syndrome (PAX-2 mutation)

Simpson-Golabi-Behmel syndrome (GPC-3 mutation)

Smith-Lemli-Opitz syndrome (defect in cholesterol biosynthesis)

Zellweger syndrome (peroxisomal protein mutation)

This table shows non-syndromic and syndromic causes of human renal malformations in which a genetic basis has been reported in some cases. The genetic defects, where known, are shown in brackets.

Apert syndrome (FGFR-2)

Apert syndrome consists primarily of craniosynostosis (premature closure of cranial sutures) with syndactyly (fused digits) of the hands and feet. This is associated with variable renal abnormalities in 10-20% of patients including cysts, hydonephrosis and duplication of the renal pelvis. It is transmitted as an autosomal dominant malformation disorder and mis-sense mutations in the extracellular domain of fibroblast growth factor receptor 2 (FGFR-2) have recently been identified in individuals with this syndrome (Wilkie *et al.*, 1996). Mutations of the paternal allele on chromosome 10 may also arise de novo. The FGFR-2 gene encodes two alternative splice variants: BEK which is expressed by the renal mesenchyme and binds to FGF-2 and KGFR, an epithelial-associated receptor expressed by the ureteric bud which binds to FGF-7, or keratinocyte growth factor (Woolf and Cale, 1997).

FGF-2 is likely to be involved in paracrine signaling between the ureteric bud and renal mesenchyme because it is expressed by the ureteric bud and exogenous FGF-2 can induce the first steps of nephron formation in cultures of isolated murine renal mesenchyme (Perantoni *et al.*, 1995). The role of FGF-7 is not so clear but preliminary experiments have shown that addition of FGF-7 to metanephric organ culture disrupts development of ureteric bud branches and the renal pelvis (Qiao *et al.*, 1996) and transgenic overexpression leads to renal cyst formation (Nguyen *et al.*, 1996).

The mutations in Apert syndrome may affect signal transduction by both KGFR and BEK isoforms so it is not surprising that renal and ureteric malformations are present in Apert syndrome. The fact that not all these patients have renal defects, however, suggests that other genes or environmental factors can modify the kidney phenotype.

Bardet-Biedl syndrome

Bardet-Biedl syndrome is characterised by retinal degeneration, polydactyly, obesity, mental retardation, hypogenitalism, cystic renal dysplasia and short stature. It is an autosomal recessive disorder with at least four identified gene loci: BBS-1 on 11q13, BBS-2 on 16q21, BBS-3 on 3p12 and BBS-4 on 15q22 (Beales *et al.*, 1997)

Up to 50% of patients have cystic dysplastic kidneys (Elbedour *et al.*, 1994) and these occasionally present antenatally or soon after birth with renal failure (Gershoni-Baruch *et al.*, 1992). They may be incorrectly diagnosed as the Meckel syndrome (see later) although Bardet-Biedl patients have a characteristic electroretinogram and rarely have structural brain abnormalities.

Branchio-oto-renal syndrome (EYA-1)

The Branchio-oto-renal syndrome is an autosomal dominant disorder of high penetrance and variable expression (Heimler and Lieber, 1986). Significant renal disorders occur in two thirds of affected individuals, often varying within the same family from renal aplasia and dysplasia to abnormalities of the renal pelvis and ureters. Branchial defects consist of preauricular pits, cervical fistulas or cysts, and ear defects include structural defects of the outer, middle or inner ear, and sensorineural, conductive or mixed deafness.

This gene has recently been cloned on chromosome 8q13.3 (Abdelhak *et al.*, 1997) and although the exact function of the gene is not known it appears to be homologous to the *Drosophila* eyes absent gene. Two similar human genes (EYA-2 and EYA-3) have also been cloned and the authors suggested that this is a novel new gene family. In mice, the gene is expressed in the mesenchyme adjacent to the branching ureteric bud tip, as well as in the developing ear (Abdelhak *et al.*, 1997).

Campomelic dysplasia (SOX-9)

Campomelic dysplasia is a devastating syndrome which consists of short-limbed dwarfism, cleft palate, absent olfactory bulbs, dilated cerebral ventricles, patent ductus arteriosus, ventricular septal defect, renal and genital anomalies (Houston *et al.*, 1983). Affected patients ususally die soon after birth. The renal defects include hypoplasia, cysts (rare), hydronephrosis and hydroureter.

Mutations of the SOX-9 gene (17q) leading to haploinsufficiency have recently been described in Campomelic dysplasia. SOX-9 encodes a putative transcription factor which is structurally related to the testis determining factor gene called SRY. The gene is expressed in many tissues during mouse and chick development including the skeletal system, testis and metanephric collecting ducts (Kent *et al.*, 1996). The protein has been shown to bind to specific sequences in the first intron of one form of collagen, COL-2A1, in humans and expression of this collagen in fetal cartilage is directly regulated by sox-9 *in vivo* in the mouse (Bell *et al.*, 1997). This may explain the skeletal abnormalities seen in campomelic dysplasia but collagen types 1 and 4 predominate in the developing kidneys and interactions with these genes have not been reported.

Di George syndrome

The Di George syndrome is part of the spectrum of phenotypes associated with deletions around chromosome 22q11.2 (Glover, 1995). Microdeletions within this region cause cardiac defects, abnormal facies, thymic hypoplasia, cleft palate and hypocalcaemia and the acronym CATCH 22 has been given to this group of disorders. Over half of the patients with these mutations have a broad spectrum of kidney abnormalities and these may be detected on antenatal ultrasound scan (Goodship *et al.*, 1997).

Fanconi anaemia (FAA)

Fanconi anaemia is associated with progressive bone marrow failure, a predisposition to acute myeloid leukaemia and variable renal malformations including agenesis, collecting system duplication, ectopia and horseshoe kidney. The syndrome is transmitted by autosomal recessive inheritance but it is genetically heterogeneous with at least 5 complementation groups, called A-E. The gene for the commonest form, FAA has recently been cloned (Foe *et al.*, 1996; The Fanconi anaemia / Breast cancer consortium, 1996) on chromosome 16q24. The predicted gene product contains a putative nuclear localisation signal and it is expressed in the kidney.

Kallmann's syndrome (KAL)

X-linked Kallmann syndrome consists of olfactory bulb agenesis with anosmia and infertility due to a failure of migration of olfactory and gonadotropin-releasing hormone synthesising neurons from the olfactory placode into the brain. This has been discussed earlier in the thesis in the section *Cell adhesion molecules*.

Meckel syndrome

Meckel syndrome is a combination of abnormal sloping forehead, posterior encephalocele, polydactyly and cystic dysplasia of the kidneys (Fraser and Lutwyn, 1981). Hepatic malformations such as arrested development of the intrahepatic biliary system at the stage of biliary cylinders with varying degrees of reactive bile duct proliferation, bile duct dilatation, portal fibrosis, and portal fibrous vascular obliteration have also been described. The condition is usually fatal in the perinatal period. The syndrome is inherited in an autosomal recessive manner and maps to 17q21-q24 although the gene has not been identified (Paavola *et al.*, 1995).

Renal-coloboma syndrome (PAX-2)

The recently described Renal-coloboma syndrome consists of renal hypoplasia, proteinuria, vesico-ureteric reflux and optic nerve colobomas (Sanyanusin *et al.*, 1995). It is caused by mutations of the transcription factor PAX-2 described earlier, and the distribution of the PAX-2 protein in dysplastic and normal kidneys is determined in this thesis.

Simpson-Golabi-Behmel syndrome (GPC-3)

The Simpson-Golabi-Behmel syndrome is an X-linked disorder characterised by overgrowth leading to very tall affected males, visceral and skeletal abnormalities. Renal malformations include nephromegaly, renal cysts, hydonephrosis, double renal pelvis, dysplasia and Wilms' tumour (Hughes-Benzie *et al.*, 1992). Mutations of the GPC-3 gene (Xq26) have recently been reported in this syndrome (Pilia *et al.*, 1996). The gene product is a putative extracellular proteoglycan, called glypican-3, which is expressed in the fetal kidney and other mesoderm derived tissues.

Smith-Lemli-Opitz syndrome

The Smith-Lemli-Opitz syndrome comprises mental retardation, hypotonia, micrognathia, cleft palate, polydactyly and genital malformations, including ambiguous genitalia in males. Renal malformations such as hydronephrosis, duplication and cystic dysplasia are also common, occurring in 57% of a large series of patients (Joseph *et al.*, 1987). The syndrome is caused by a defect in cholesterol biosynthesis with deficiency of 7-dehydrocholesterol reductase and the gene has been mapped to 7q32.1.

Interestingly, cholesterol attaches to the N-terminal domain of hedgehog proteins during autoprocessing and the C-terminal domain acts as an intramolecular cholesterol transferase (Porter *et al.*, 1996). The Hedgehog gene was first discovered in *drosophila* where it plays a crucial role in embryonic patterning, but homologues have been found in a number of species including man. Sonic hedgehog is expressed in the human fetal kidney (Marigo *et al.*, 1995) and it may be that the perturbed cholesterol biosynthesis in Smith-Lemli-Opitz syndrome leads to defective modification of this, or other similar, genes.

Zellweger syndrome

Zellweger syndrome is a multisystem disorder characterised by prenatal growth failure, characteristic facies, limb abnormalities with stippled chondral calcification on X-ray, congenital heart defects, genital malformations and cystic kidneys. The syndrome can be diagnosed by elevated long chain fatty acids in plasma, fibroblasts and amniocytes and affected infants often die soon after birth. It is caused by mutations in several different genes involved in peroxisome biogenesis (Braverman *et al.*, 1995) including peroxin-2 (PEX-2, chromosome 8), peroxin-5 (PEX-5, chromosome 12), peroxin-6 (PEX-6, chromosome 6) and there is probably a further Zellweger syndrome locus on 7q11. Inheritance is autosomal recessive and the mechanism of renal cyst formation is unknown.

Human renal malformations - conclusion

There are several conclusions which can be drawn from the range of human renal malformations described above. Firstly, in spite of the variety of mutations in different nephrogenesis genes there is only a limited spectrum of malformations. This suggests that there are only a limited number of ways in which the developing metanephros can respond. Secondly, the same genetic defect can give rise to different phenotypes e.g. a patient with dysplasia and contralateral aplasia, or families with adysplasia. This suggests that other genes may overlap in functional terms and be able to compensate to some extent or other local events such as obstruction may be superimposed in generating the final phenotype. This adds an extra level of complexity to the search for genetic causes of human renal malformations. Finally, there are now a large number of genes which have been shown to be essential for mouse nephrogenesis and it seems likely that mutations of some of the human homologues of these, such as RET and WT-1, may eventually be found to be involved.

Chapter 4. Experimental strategy

The aim of this thesis was to investigate the biology of human renal malformations with particular emphasis on renal dysplasia. Two central themes helped to define my experimental strategy. Firstly, the anatomical descriptions of dysplastic kidneys, outlined above, suggests that dysplasia represents a failure of normal development. It was therefore logical to compare dysplastic kidneys with normal developing and mature kidneys. Secondly, much of the data on normal and abnormal nephrogenesis has been derived from animal experiments. In many cases, however, it is uncertain whether the same principles apply to, or molecules are involved in, human renal development. I therefore used the data from animal experiments as a guide to select the processes and molecules which I examined in this thesis.

The first part of the study involved the collection of appropriate human samples. This initially involved a written request asking for permission to use human material to the relevant hospital Ethics Committees. Then, specific consent was obtained, where applicable, from the parents of affected children. After these steps, it was possible to obtain specimens of fresh fetal material and archived antenatal and postnatal normal, dysplastic and polycystic kidneys. Fresh postnatal samples of dysplastic and normal tissue adjacent to Wilms' tumours were also collected directly from the operating theatre.

The next part of the thesis involved the experimental analysis of normal, dysplastic and, in some experiments, polycystic kidneys. I planned to investigate:

1) The origin of the different cell types in dysplastic kidneys by comparing intermediate filament expression and lectin binding patterns in dysplastic kidneys with normal developing and mature kidneys.

2) Basic biological processes such as proliferation and apoptosis. These processes are tightly controlled during normal development but the growth of cysts in some dysplastic kidneys and the involution of others suggested that proliferation and apoptosis may be deregulated in renal dysplasia.

3) Expression of PAX-2, WT-1, BCL-2 and galectin-3. These genes had been implicated in normal and abnormal development in animals but not previously investigated in human dysplastic kidneys.

In the final part of the study I planned to determine whether it is feasible to culture cells from dysplastic kidneys and, if possible, transduce them with a potentialy immortalising construct. This may provide a novel method for the investigation of functional abnormalities in human dysplasia in the future.

Chapter 5. Materials

General reagents

The majority of the reagents used in this thesis were supplied by BDH Ltd (Poole, Dorset, UK). Sigma Chemicals Company (Poole, Dorset, UK) also supplied Trizma base, bovine serum albumin (BSA), ethidium bromide, coomassie blue, β-mercaptoethanol, sodium dodecyl lauryl sulphate, bromphenol blue, sodium orthovanadate, phenylmethylsulphonyl fluoride, aprotinin, ampicillin, methicillin, paraformaldehyde, phenol, TEMED, Ponceau S, glutaraldehyde and proteinase K.

Other companies supplied the following: Histoclear (National Diagnostics, Atlanta, Georgia, USA), Phosphate buffered saline (PBS; Gibco BRL, Paisley, UK), Citifluor™ (Chemical Labs, University of Kent, Canterbury, Kent, UK), ABC kit (Dako, High Wycombe, Bucks, UK), Apoptag™ kit (Oncor, Gaithersburg, Maryland, USA), Enhanced chemiluminescence reagents (ECL; Amersham International, Little Chalfont, Bucks., UK), RNase A and proteinase K (Boehringer-Mannheim, Mannheim, Germany).

Tissue culture equipment

Cell culture media and supplements were supplied by Gibco BRL (Paisley, UK). Tissue culture plastics were supplied by Philip Harris (London, UK) and Nunc (Naperville, Illinois, USA) Millicell filters were obtained from Millipore Corporation (Bedford, Massachusetts, USA).

Human tissues

Ethical approval

Human tissues were collected from a variety of sources during this thesis. Ethical approval for the collection and use of this material was obtained in each case from the appropriate Ethical committee.

The embryonic and fetal tissues were obtained from terminations at the Elizabeth Garrett Anderson Hospital, University College London (UCL), London. Separate consent to use embryonic and fetal material for medical research was obtained from the mothers, by the hospital staff, prior to termination. Collection and further use of these samples was approved by the Joint UCL / University College Hospital (UCH) Committee on the Ethics of Human Research and supervised by Professor Peter Thorogood at the Institute of Child Health. Regular collections have now been established and the material is stored in the Medical Research Council (MRC) funded human embryo bank at Institute of Child Health (ICH).

Later antenatal samples were obtained from Dr Virginia Sams, Senior Lecturer and Honorary Consultant Pathologist in the Pathology Department at University College London Medical School (UCLMS). Use of this material was also approved by the Joint UCL / UCH Committee on the Ethics of Human Research.

Postnatal samples were obtained from Professor Anthony Risdon in the Pathology Department at The Hospital for Sick Children, Great Ormond Street, London. Approval for the use of these specimens was obtained directly from Mr Mike Elliot, chairman of the Hospital for Sick Children / Institute of Child Health Ethics Committee. He felt that formal ethical approval was not required for this material since excess,

or redundant, tissues were used which had no effect on the patient and would otherwise have been discarded.

Classification of samples

All of the kidney samples used in this thesis were reviewed by a trained pathologist, usually Dr Virginia Sams or Professor Anthony Risdon. Gross morphology and routine histopathology were examined before the specimens were classified as normal, dysplastic or polycystic.

Dysplastic samples all had classical histological criteria of this disorder including dysplastic tubules, 'undifferentiated mesenchymal' tissue and metaplastic cartilage. Many of them also had cysts of a variable size. Polycystic samples, used in the apoptosis and galectin-3 expression studies, were also classified according to the site of origin of the cysts, liver histology and family history. Further details of these samples are given in the tables below.

Early preterm samples (before 12 weeks of gestation)

Normal human fetuses were collected from first trimester chemically induced (RU486) terminations of pregnancy. The fetus was collected immediately after delivery, transported on ice in Leibovitz 15 (L-15) medium and then staged according to standard criteria described by Larsen (1993). Ten samples were obtained between 5 and 11 weeks of gestation.

The samples were either fixed intact in ice cold 4% paraformaldehyde in phosphate buffered saline (PBS – pH 7.0) overnight at 4^0C and processed for histology as below, or the organs were dissected, separated and used for protein isolation. All samples were processed within two hours of collection.

Later preterm samples (after 12 weeks of gestation)

The normal samples in the later preterm group comprised both spontaneous miscarriages and phenotypically normal kidneys from abortions performed for severe abnormalities in other organ systems which would have compromised the survival of the fetus or infant. The other abnormalities were also examined and classified by a trained pathologist. Dysplastic and polycystic kidneys were collected under similar conditions. In these three groups the parents were given time to mourn the loss of the child. Then the fetus was stored at 4^0C until autopsy when organs were fixed in 10% formalin. All specimens were processed using routine laboratory procedures within 24 hours. Details of the specimens are given in Table 5.

Table 5. Later preterm samples (after 12 weeks of gestation)

Gestational age (weeks)	Sex	Renal histology	Termination / spontaneous abortions	Other abnormalities
17	M	Dysplasia	T	None
19	M	Dysplasia	T	Hydrocephalus
19	M	Dysplasia	T	Urethral obstruction
19	F	Dysplasia	T	None
20	M	Dysplasia	T	Hypoplastic lungs
22	M	Dysplasia	T	Urethral obstruction, atrial septal defect
22	M	Dysplasia	T	None
24	F	Dysplasia	T	Hypoplastic lungs
32	F	Dysplasia	S	Hypoplastic lungs
34	M	Dysplasia	S	Hypoplastic lungs
17	M	Normal	T	Neural tube defect
19	F	Normal	T	Trisomy 21
20	M	Normal	S	Thalassemia trait
20	F	Normal	S	None
22	M	Normal	T	Anorectal abnormality
25	M	Normal	S	Hyaline membrane disease
25	F	Normal	S	Hyaline membrane disease

Gestational age (weeks)	Sex	Renal histology	Termination / spontaneous abortions	Other abnormalities
27	M	Normal	S	Septicaemia
28	F	Normal	S	Growth retardation
32	F	Normal	S	Maternal pre-eclampsia
32	M	Normal	S	Pneumothorax, liver tear
20	M	ARPKD	T	None
34	F	ARPKD	S	None
35	F	ARPKD	S	Liver fibrosis
35	M	ARPKD	S	Liver fibrosis

Table 5. Later preterm samples (after 12 weeks of gestation).
This table shows the patient details of kidneys obtained after 12 weeks of gestation including their sex, gestational age, associated abnormalities in other organ systems and the indications for termination of pregnancy. There is no significant difference in age and sex distribution between the normal and dysplastic samples. Karyotypes were normal, as assessed by the regional cytogenetics centre, in all cases assessed apart from the single case of Trisomy 21. Two of the dysplastic samples were associated with urethral obstruction. All dysplastic organs contained cysts. The ARPKD samples had classical features of this disease with multiple small cysts arising from distal segments and liver fibrosis in two of the patients.

Samples from infancy and childhood

The postnatal dysplastic and normal samples were harvested surgically by Mr Patrick Duffy, Mr Phillip Ransley and Mr Pierre Mouriquand (Consultant Urologists) and their surgical teams at The Hospital for Sick Children, Great Ormond Street. This approach controls for any potential changes in tissue morphology which may be induced by either general anaesthesia or surgery. Normal samples consisted of the kidney tissue adjacent to, but unaffected by, Wilms' tumours. None of the children had received chemotherapy prior to nephrectomy and none of them had mutations in the WT-1 gene (personal communication - Dr. Richard Grundy, Department of Haematology and Oncology, Hospital for Sick Children, Great Ormond Street, London). A further, histologically normal, control group comprised kidneys from infants and children who died from Sudden Infant Death Syndrome (SIDS) without any pathological cause being found. These samples were obtained at post mortem.

Surgical specimens were placed on ice, examined by a pathologist and fixed in 10% formalin for histology. Fragments of two dysplastic samples were snap frozen in liquid nitrogen for DNA extraction and fixed in 3% glutaraldehyde in 0.1 M sodium cacodylate and 5 mM NaCl (pH 7.4) for electron microscopy (see *DNA laddering*, and *Electron microscopy* sections later in this thesis). Details of these samples are shown in Table 6.

Table 6. Samples from infancy and childhood

Age (months)	Sex	Renal histology	Additional pathology	Obstruction
4	F	Dysplasia	Obstructed ureterocoele	Yes
4	M	Dysplasia	Vesicoureteric junction obstruction	Yes
5	F	Dysplasia	None	No
6	M	Dysplasia	Nonobstructed megaureter	No
8	F	Dysplasia	Duplex with dysplastic obstructed upper pole	Yes
8	M	Dysplasia	Contralateral hydronephrosis	No
9	F	Dysplasia	Contralateral vesicoureteric reflux	No
9	F	Dysplasia	None	No
14	F	Dysplasia	None	No
15	M	Dysplasia	Ipsilateral reflux	No
19	M	Dysplasia	None	No
24	M	Dysplasia	None	No
3	F	Normal	SIDS	No
3	F	Normal	SIDS	No
3	F	Normal	SIDS	No
4	F	Normal	SIDS	No
4	F	Normal	SIDS	No

Age (months)	Sex	Renal histology	Additional pathology	Obstruction
5	F	Normal	SIDS	No
5	M	Normal	SIDS	No
6	M	Normal	SIDS	No
7	M	Normal	SIDS	No
14	F	Normal	SIDS	No
5	F	Normal	Wilms' tumor	No
8	M	Normal	Wilms' tumor	No
28	M	Normal	Wilms' tumor	No
30	M	Normal	Wilms' tumor	No
38	M	Normal	Wilms' tumor	No
72	F	Normal	Wilms' tumor	No
10	F	ARPKD	Creatinine 98 μmol / l	No
11	M	ADPKD		No
48	M	ARPKD	Creatinine 322 μmol / l	No
72	M	ARPKD		No

Table 6. Samples from infancy and childhood. This table shows the patient details of kidneys obtained from infants and children including their age, sex and associated pathology. Three of the polycystic kidney samples were archival material from open surgical biopsies and one, with an elevated creatinine of 322 μmol / l, was from a recipient nephrectomy at the time of renal transplant. One sample contained cysts from all segments of the nephron and was diagnosed as ADPKD. The parents of this child, who were in their early twenties, had normal renal ultrasound scans.

Microscopy

Light and fluorescent microscopy was performed on a Zeiss Axiophot microscope (Carl Zeiss, Oberkochen, Germany) using lenses of 4x, 10x, 20x, 40x and 63x (oil immersion) magnification. Specimens were photographed on Fuji Super G 100 colour negative or Kodak Ektachrome 64 colour positive film.

Dark field microscopy was examined on an Olympus BH-2 microscope (Olympus, Tokyo, Japan) using lenses of 4x, 10x, 20x, and 40x magnification. Ilford FP-4 film was used for black and white images.

Confocal fluorescent microscopy used a Leica Aristoplan microscope and computer confocal laser scanning system (Aristoplan-Leica, Heidleberg, Germany) with oil immersion lenses of 4x, 10x, 25x, 40x, 63x and 100x and sofware interpolation of intermediate magnifications. Images were saved as tagged image format (TIF) files and imported, for labeling, into Adobe Photoshop (Version 3; Adobe Systems Europe, Edinburgh, UK) or Microsoft Powerpoint (Version 4; Microsoft Corporation, Seattle, USA)

Ultrathin sections for electron microscopy were prepared by Mr Brian Young in the Electron microscopy department, Institute of Neurology, Queen's Square, London. They were then examined on a Joel 100 CX transmission electron microscope.

Gel electrophoresis and blotting

Agarose (Gibco BRL, Paisley, UK). Protogel (National Diagnostics, Atlanta, Georgia, USA). X-ray film: Kodak X-OMAT AR. 3MM chromatography paper (Whatmann Ltd., Maidstone, Kent, UK). Hybond-C Extra (Amersham International, Little Chalfont, Bucks., UK).

Molecular size markers

Rainbow markers (Amersham International, Little Chalfont, Bucks., UK). 123 and 1 Kb ladder (Gibco BRL, Paisley, UK).

Electrophoresis and Western blotting equipment

Horizontal gel electrophoresis tanks (Life technologies supplied by Gibco BRL, Paisley, UK); Mini-Protein apparatus, Trans-blot SD semi-dry transfer cell (BIO-RAD supplied by Gibco BRL, Paisley, UK).

Antibodies

The primary antibodies used during this thesis were raised against the following molecules:

Alpha-smooth muscle actin (A-2547; Sigma, Poole, Dorset, UK): mouse monoclonal (IgG2a) antibody raised against a synthetic decapeptide at the amino terminal of human α-smooth muscle actin.

Band 3: mouse monoclonal antibodies were supplied by Professor David Anstee at the International Blood Group Research Laboratory, Bristol. The band 3 protein is found in red cells and a truncated protein is located on the basal surface of the hydrogen secreting α-intercalated cells in the distal nephron (Wagner *et al.*, 1987; Tanner, 1996). I used 2 antibodies (BRIC 154 and BRIC 155) which were raised against the membrane domain of the human erythrocyte anion transport protein. These have been shown to react with presumptive α-intercalated cells in the kidney (Wainwright *et al.*, 1989).

BCL-2 (M887; Dako, High Wycombe, Bucks, UK): mouse monoclonal (IgG1) antibody raised against a synthetic peptide comprising amino acids 41-54 of human BCL-2. This reacts specifically with the 25kD protein on immunoblotting (Pezzella *et al.*, 1990).

119

Galectin-3: rabbit polyclonal antibody (plus pre-immune serum) was supplied by Dr Colin Hughes, National Institute for Medical Research, Mill Hill, London. The antibody was raised against the amino terminus of hamster galectin-3 protein, detects a single band on immuno-blot (Foddy *et al.*, 1990) and cross-reacts with canine galectin-3 (Bao and Hughes, 1995). It had not been validated on human tissue prior to this work.

Ki-67 (M0722; Dako, High Wycombe, Bucks, UK): mouse monoclonal (IgG1) raised human Ki-67 which reacts with cells at several stages of the cell cycle including late G1, S, M and G2 phases, but not in the G0 stage.

Large T antigen: mouse monoclonal antibody was supplied by Dr Parmjit Jat, Ludwig Institute, UCL. It has been shown to detect the 53 kD large T antigen on Western blotting (Harlow *et al.*, 1981) and immunohistochemistry (Woolf *et al.*, 1995).

'Pan cytokeratin' (C-1801; Sigma, Poole, Dorset, UK): mouse monoclonal (IgG1) antibody raised against a cytokeratin preparation from human epidermis. The antibody recognises members of the type II neutral-to-basic subfamily on immunoblotting, including the 58kD cytokeratin 5, 56 kD cytokeratin 6 and the 52 kD cytokeratin 8 (Moll and Franke, 1982).

PAX-2: rabbit polyclonal antibody was supplied by Dr Greg Dressler, Howard Hughes Institute, Ann Arbor, Michigan. This antibody was raised against amino acids 188 - 385 in the carboxyterminal domain of PAX-2 (Dressler *et al.*, 1992): this sequence does not include the highly conserved amino-terminal paired domain (Dressler *et al.*, 1990). Using cells transfected with PAX-2, 5 and 8 there is only significant reactivity to the former protein and, using deletion mutants of PAX-2, this antibody recognises major epitopes between amino acids 270 - 338 (Phelps and Dressler, 1996). On western blot of mouse metanephros the antibody recognises a single major doublet of 46 - 48 kD (Dressler *et al.*, 1990).

PCNA (Ab-1; Oncogene Science, Cambridge, Massachussetts, USA): mouse monoclonal antibody (IgG2) to the human DNA-polymerase delta associated protein which is expressed at high levels during S phase (Bravo *et al.*, 1987). This gene is highly conserved across different species (Suzuka *et al.*, 1989) and our group have recently shown that this antibody detects a single band in the developing sheep kidney (Attar *et al.*, 1998).

Vimentin (1 112 457; Boehringer Mannheim, Mannheim, Germany): mouse monoclonal (IgG2a) antibody which recognises the 58 kD human protein as well as numerous other species. This protein is found in fibroblasts, endothelial cells, lymphoid cells and melanocytes.

Von Willebrand factor (F-3520; Sigma, Poole, Dorset, UK): rabbit IgG fraction of antibody raised against purified human von Willebrand factor. Reacts specifically with the cytoplasm of human endothelial cells, platelets and megakaryocytes (Sigma data sheet).

WT-1 (C-19; Santa Cruz, Santa Cruz, California, USA): rabbit polyclonal IgG fraction raised against an 18 amino acid peptide mapping to the carboxyterminus of human WT-1 which is conserved in all 4 isoforms of the protein. This antibody has been found by both the manufacturer and other groups to specifically recognise the WT-1 transcription / splicing factor protein on western blot (Larsson *et al.*, 1995).

Secondary biotinylated antibodies which combined anti mouse / anti rabbit IgG was derived from the ABC kit (DAKO, High Wycombe, Bucks, UK). Fluorescent FITC and TRITC conjugated antibodies against rabbit and mouse IgG, and rhodamine conjugated anti-digoxigenin were from Boehringer Mannheim (Mannheim, Germany).

Lectins

FITC and TRITC conjugated lectins were obtained from Sigma (Poole, Dorset, UK). Lectins are proteins or glycoproteins, often derived from natural sources such as plants, which bind to specific carbohydrate residues. The specificities of lectins used in this thesis were: *Arachis hypogaea* (peanut) – β-gal(1-3)galNAc, *Dolichos biflorus* – α-galNAc, *Tetragonolobus purpureas* (asparagus pea) – α-L-fuc and *Ulex europaeus* – $(glcNAc)_2$. In the kidney, lectins can be used to identify different parts of the mature nephron (Holthofer, 1981 and 1984; Verani *et al.*, 1989). Examples are: *Tetragonolobus lotus purpurea* – proximal tubules, *Arachis hypogaea* - collecting ducts, *Dolichos biflorus* – ureteric bud and its derivatives and *Ulex europaeus* – endothelia.

Chapter 6. Methods

Immunohistochemistry

Immunohistochemistry is a well established technique which allows detection of protein epitopes in a tissue section using an antibody which is specific for the protein of interest (Coons, 1955).

For conventional immunohistochemistry using tissue sections, the tissues are first fixed to preserve morphology, then dehydrated and embedded in a wax block. Thin sections of the block (3 - 6 μm) are cut on a microtome and transferred to a microscope slide. Next, the sections are rehydrated, pre-treated to increase penetration of the antibodies (optional), blocked to avoid non specific binding and the antibody is applied. The antibody is then detected using secondary antibodies or other amplifying secondary detection techniques (see ABC below). The distribution of the protein can be determined using fluorescent or light microscopy.

Immunocytochemistry on cultured cells is broadly similar, although these do not need to be embedded in wax.

Fixation, wax embedding and sectioning

Samples of kidney tissue were fixed for between 1 hour and 24 hours, depending on size, in freshly made 4% paraformaldehyde (2 grams paraformaldehyde, 50 ml 1x PBS dissolved at 65°C). The fixed samples were then washed twice with saline (0.83% NaCl in water) and dehydrated through 30%, 50%, 70%, 85%, 95% and 100% (twice) ethanol. Solutions were changed at 30 minute intervals and were kept at 4°C until the 85% stage.

Next the samples were immersed in Histoclear, twice, for 30 minutes each followed by a 1:1 Histoclear : wax mix at 60°C for 1 hour. The

wax was then changed 3 times, each for 30 minutes at 60°C. Samples were then transferred to and orientated in a mould, and the wax was allowed to set. Sections of between 3 - 6 μm in thickness were cut and floated in a water bath at 45°C until any creases disappeared. The sections were then picked up on glass slides pretreated with poly-L-lysine. Slides were dried at 37°C overnight and stored at 4°C.

Rehydration and pretreatment

Sections were dewaxed and rehydrated. The slides were placed in a rack and sequentially passed through Histoclear twice for 10 minutes each and a graded alcohol series of 100% twice, 95%, 85%, 70%, 50% and 30% for 5 minutes each.

The next step was to treat the sections to improve antibody penetration. This was achieved by microwaving the sections which causes antigen unmasking (Shi *et al.*, 1991), apart from a few preliminary WT-1 and BCL-2 experiments in which I used proteinase K. Slides were washed thoroughly in running tap water and then transferred into citric acid buffer (2.1 g Citric acid in 1 litre milliRo water, adjusted to pH 6.0). They were then microwaved at full power in a 700 W oven in a covered plastic container for several minutes. The microwaving time was optimised for the number and type of specimens, ranging between 6 minutes for small friable embryonic / cystic tissues and 20 minutes for larger numbers of samples. Slides were left to stand and cool for 20 minutes (occasionally speeded up by surrounding container with running water) before washing again in running tap water, followed by two short dips in milliRo water and PBS, twice, for 5 minutes. In the experiments using pretreatment with proteinase K the slides were washed twice in PBS for 5 minutes

each and then immersed in 0.2 g / l proteinase K in 50 mM Tris HCl pH 8.0, 5 mM EDTA pH 8.0, for 15 minutes. Slides were finally washed twice in PBS for 5 minutes.

Blocking steps

The next two steps were designed to eliminate non-specific signal by blocking endogenous peroxidase and non-specific binding. Slides were dipped in 3% hydrogen peroxide in PBS for 15 minutes (1 in 10 dilution of 30% solution) and then washed twice in milliRo water and once in PBS for 5 minutes. This step was omitted for fluorescent microscopy. Next they were immersed in 10% fetal calf serum in PBS for 30 minutes. At the same time, a humid slide chamber was prepared from a slide box with PBS-soaked tissues.

Primary antibody

In the next step, the primary antibody was applied. Excess blocking solution was carefully wiped off around the tissue and 50 to 100 μl of antibody, diluted in PBS : 1% BSA, was pipetted onto the sections. The optimal concentration of the antibody was determined on serial sections. A 1 in 50 dilution was used for all antibodies, apart from 1 in 200 for PAX-2. Each section was covered with a plastic coverslip to ensure even distribution of the antibody and the slides were placed in the humid chamber at 37^{0}C for one hour, or at 4^{0}C overnight. After incubation, the coverslips were removed and slides were washed three times in PBS.

Double staining with two primary antibodies, such as galectin-3 and band 3 (Fig. 45), was used in some experiments. In these experiments, it was essential that there was no cross reactivity between the primary antibodies and secondary detection systems. Hence, primary antibodies raised in different species were used,

and then detected using different flurophores. Antibodies were both applied at the same time and other procedures were unchanged.

Detection and mounting

Two detection systems were used: fluorescent secondary antibodies, or a commercial avidin-biotin conjugate (ABC) kit followed by diaminobenzidine (DAB) staining.

For fluorescent staining a secondary antibody was applied which had been pre-conjugated to a flurophore such as fluoroscein isothiocyanate (FITC) or tetramethylrhodamine isothiocyanate (TRITC). The second antibody was selected specifically to detect the primary. Thus, for example, the anti PAX-2 antibody was a rabbit polyclonal and this was detected using an anti rabbit immunoglobulin antibody, whereas the anti BCL-2 antibody was a mouse monoclonal so this was detected with anti mouse IgG.

Secondary fluorescent antibodies were applied to the tissue sections at 1 in 50 dilution, covered with a coverslip and incubated in the dark in the humid chamber for one hour at room temperature. Fluorescent double labeling with antibodies and lectins was also performed by adding fluorescently conjugated lectins at 1 in 50 dilution in PBS at the same time as the secondary antibody. The slides were then washed 3 times in PBS and mounted with glass coverslips in Citifluor™. The edges of these coverslips were sealed with nail varnish to prevent drying and the slides were stored in the dark at 4^0C until visualised.

The alternative detection method used an ABC kit. This system utilises an avidin-biotin-peroxidase system to amplify the signal. Avidin is a large glycoprotein found in egg white which has four high affinity

binding sites for biotin. A secondary biotinylated antibody (reagent C) is applied, followed by an avidin-peroxidase conjugate (reagents A and B) which binds to the biotin attached to the secondary antibody. Peroxidase activity is then detected by colorimetric changes in DAB.

Reagent C was applied at 1 in a 100 dilution in PBS to the sections and covered with plastic cover slips. At the same time a mixture containing reagents A and B, at 1 in 100 dilution in PBS, was prepared. After 20 minutes at room temperature in the humid chamber, the slides were washed three times in PBS and reagent A / B applied using the same technique for 20 minutes. The slides were then washed three times in PBS and immersed in 0.5 g / l DAB with 0.03% hydrogen peroxide. A brown precipitate is produced by the peroxidase in the A / B mixture and this reaction can be monitored by eye or microscopically. Therefore, the slides were allowed to develop for between 1 and 10 minutes depending on colour development and washed in running tap water. Slides were counterstained (see below), dehydrated through an ascending alcohol series to histoclear, and air-dried. They were then mounted with permount and glass coverslips.

Lectins

Fluorescently conjugated lectins were applied to sections at 1 in 50 dilution in PBS in a humid chamber at room temperature for 1 to 4 hours, or overnight at 4°C. They were then washed 3 times in PBS and mounted in Citifluor™. This technique was often used in combination with fluorescent antibody staining.

Negative controls

A number of controls were performed for the antibody staining. These consisted of:

1) Omission of the primary antibody and substitution with PBS. This allowed assessment of the background levels of peroxidase activity or autofluorescence.

2) Preincubation of the primary antibody with the appropriate antigen, where available, at ten fold excess (g for g)

3) Use of preimmune serum, where available, in place of the primary antibody.

General histological staining

Staining was performed to define the anatomy / histology of samples and conterstaining to help identify cells which expressed the epitope of interest. All staining was performed after dewaxing and rehydration of the samples as described above and regents were filtered prior to each use.

Haematoxylin and eosin

Haematoxylin and eosin (H&E) is a commonly used histological stain. Haematoxylin stains the nuclei dark purple and eosin stains the cytoplasm pink.

Rehydrated sections were dipped in 0.1% Harris' hematoxylin for 2 minutes and rinsed in running tap water for 5 minutes to 'blue' the sections. The slides were then dipped in 1% aqueous eosin for 1 minute, followed by running tap water for 5 minutes. They were then dehydrated and mounted as above, with an additional step of 70% alcohol: 1% hydrochloric acid to refine the eosin staining.

Methyl green

Methyl green stains nuclei in a blue / green colour which is an appropriate counter stain for DAB. The solution comprises 0.5% methyl green in 0.1 M sodium acetate pH 4.0.

Sections were immersed in methyl green solution for 10 minutes. Then they were washed three times in milliRo by dipping 10 times in the 1st and 2nd wash, then left for 30 seconds in the last wash. This wash procedure was repeated in three changes of butanol, followed by histoclear for 10 minutes. Specimens were then air dried and mounted as above.

Western blotting

The technique of Western blotting uses specific antibodies to identify proteins within tissue extracts (Sambrook *et al.*, 1989). Proteins are extracted from tissues, denatured and separated on sodium lauryl sulphate (SDS) - polyacrylamide gels. The proteins are then transferred to a nitrocellulose filter, the primary antibody is applied and adheres to the protein of interest. The protein is then shown as a band on the gel when the primary antibody is detected using an enzyme, or radioisotope, conjugated secondary antibody. The size of the detected protein can also be determined by comparison with molecular weight markers.

Protein extraction

The first stage in protein extraction is to collect the tissue and homogenise it in lysis buffer which breaks up the cells and allows solubilisation of the proteins. The initial procedures are performed on ice and the buffer contains proteinase inhibitors which prevent protein breakdown. After extraction the sample is spun to pellet solid debris and the supernatant contains the protein suspension.

Samples were collected and placed in lysis buffer (150 mM NaCl, 50 mM Tris pH8, 1% NP40, 0.5% DOC, 0.1% SDS) to which proteinase inhibitors had just been added (30 ml / l Aprotonin, 1 mM sodium orthovanadate, 0.1 g / l phenoxymethyl sulphoxide (PMSF)). Tissues

were homogenised by repeated syringing through needles of decreasing calibre and left to stand on ice for 15-30 minutes to allow the proteins to dissociate. The homogenate was next spun at 10,000 xg for 10 minutes at 4^{0}C and the supernatant containing the protein was removed. This was either used immediately or stored at -20^{0}C.

Polyacrylamide gels

The next step was to set up the apparatus and construct the SDS-polyacrylamide gels. Mini-Protean gel apparatus was used with two glass plates separated by 1 mm spacers. The resolving gel was mixed first and poured between the plate. Different concentrations were made depending on the size of the protein: 8% gels were used to resolve proteins in the range of 50 - 100 kD, and 12.5% for 14 - 66 kD. The gel contained milliRo water, a variable percetage of Protogel (37.5:1 acrylamide to bisacrylamide stabilized solution), 1.5 M Tris pH 8.8, 10% SDS, 10% fresh ammonium persulfate and 1% N,N,N',N' tetramethylethylenediamine (TEMED). TEMED catalyses free radical formation from ammonium persulfate which accelerates the polymerisation of acrylamide and bisacrylamide. After the resolving gel was poured it was covered with water saturated butan-1-ol which flattens the top surface of the gel and prevents oxygen diffusion into it which would inhibit polymerisation.

The gels were left at room temperature for 30 to 60 minutes to set. Then the overlaid water was poured off, and the upper surface of the gel was washed with milliRo and blotted dry with Whatman 3MM filter paper.

Next a stacking gel was poured on top of the resolving gel. This aligns the proteins in a very thin layer on the surface of the resolving gel which increases protein resolution. A 5% gel was used: each 2 ml mix comprised 1.4 ml deionised water, 0.33 ml Protogel, 0.25 ml 1.0 M Tris

pH 6.8, 0.02 ml 10% SDS, 0.02 ml 10% ammonium persulfate, and 2 μl TEMED. This was poured on top of the resolving gel until it reached the top of the smaller glass plate and a 10 well comb was inserted carefully to avoid bubbles. This was left to set for 30 minutes at room temperature and then immersed in tris-glycine buffer (diluted 5x stock: 25 mM Tris, 250 mM glycine pH 8.3, 0.1% SDS) in the running tanks. The Laemmli discontinuous buffer system was used (Laemmli et al., 1970) with part of the buffer between the gels and the rest in the running tank.

Loading and running samples

The protein homogenates were thawed and mixed with an equal volume of loading buffer (1 ml glycerol, 0.5 ml β-mercaptoethanol, 3 ml 10% SDS, 1.25 ml 1M Tris pH 6.7 and 0.001 g bromophenol blue). This was then heated to 95°C for 5 minutes and quenched on ice. This step reduces the proteins. Twenty μl of each suspension was carefully loaded into each well to prevent cross contamination. Protein marker solutions were also loaded in one or more lanes.

Gels were run at 40 volts until the bromophenol blue reached the interface with the resolving gel. Voltage was then increased to 70 volts until the bromophenol blue ran off the bottom of the gel.

Blotting

The glass plates were removed from the gel tank and the resolving gel was placed in transfer buffer (48 mM Tris, 39 mM glycine, 0.037% SDS, 20% methanol) for 10 minutes. One piece of nitrocellulose membrane and six pieces of Whatman 3MM filter paper were cut to the exact size of the gel and floated on transfer buffer at the same time.

Next the proteins were transferred from the gels to the nitrocellulose membrane with a semi-dry electroblotter. A sandwich of gels and filter

paper were placed on the anode in the following order: three pieces of filter paper, nitrocellulose membrane, resolving gel and three more pieces of filter paper. Air bubbles were rolled out with a 1 ml pipette. The lid which contained the cathode was then fitted and the proteins were blotted at 5 volts for 30 minutes.

Protein transfer was initially assessed by colour transfer of the marker proteins and further blotting was performed if these had not transferred completely. Further assessment used red Ponceau S solution which binds to proteins. The filter was marked by cutting off one corner to allow orientation of the proteins. It was then placed in a solution of Ponceau S for 5 minutes followed by several washes in milliRo water. As the stain washed out the proteins were visualised as pink bands.

Blocking, primary and secondary antibodies

The remaining steps are similar to immunohistochemistry since they involve blocking of non-specific binding, application of primary antibody and a conjugated secondary antibody / enzymatic detection system.

Membranes were incubated in blocking solution (5% non-fat milk in PBS with 0.1% Tween) overnight. All subsequent procedures, until the final washes, were done in this blocking solution since this reduced non specific background. The primary antibody was then applied at 1 in 500 dilution at 4^0C for one hour with gentle agitation. The membranes were washed thoroughly three times for 10 minutes with excess block.

Next, the primary antibodies were detected using horseradish peroxidase-conjugated secondary antibodies. Membranes were incubated with appropriate secondary antibodies diluted 1:2000 for 30 minutes at room temperature. They were then washed three times in a large volume of PBS.

Detection

The secondary antibody is conjugated with horse radish peroxidase which can be detected using colorimetric (DAB) or chemi-luminescent methods. The latter is more sensitive and was used in this thesis.

Excess PBS was drained off the membranes and enhanced chemiluminescence (ECL) reagent was applied for exactly 1 minute. This was, in turn, drained off and the membrane was wrapped in cling film. This was transferred to an X-Ray cassette and exposed to X-ray film under safelight conditions. Exposure times were varied depending on intensity of the signal. The size of the proteins which were detected was then assessed by reference to the size markers.

Controls

Positive controls were tissues which were known to express the protein, such as MDCK cells for galectin-3. Negative controls were preincubation of the primary antibody with a ten fold excess of the protein (g for g) and either omission of the primary antibody or substitution with preimmune serum. In several experiments the same filter was first used with preimmune serum to determine background staining and later probed with the primary antibody.

133

Techniques used to detect apoptosis

A number of techniques can be used to detect both the histological and biochemical changes in apoptosis. The 'gold standard' for morphological detection is electron microscopy since chromatin condensation can be clearly demonstrated. These changes can also be detected by light microscopy since the nuclei become small and irregular and these pyknotic nuclei stain intensely with both haematoxylin and propidium iodide. The latter can be clearly distinguished from necrotic cells using fluorescent microscopy (Coles *et al.*, 1993).

The small fragments generated by endonucleolytic cleavage of DNA during apoptosis can be detected in two ways. Firstly, DNA from apoptotic cells can be visualised as an arithmetic 'ladder' consisting of multiples of these fragments on electrophoresis (i.e. 180, 360, 540, 720 bp; Wyllie *et al.*, 1980). DNA laddering does not occur in necrosis although single-strand DNA breaks have been reported (Bortner *et al.*, 1995). This technique has the advantage that it integrates the amount of apoptosis in the whole sample. Secondly, by contrast, *in situ* end-labeling can determine the exact tissue distribution of apoptosis. In this technique, labeled nucleotides are tagged onto the free 3' ends generated by apoptotic DNA digestion and these are identified using a secondary antibody for conventional or fluorescent microscopy (Gavrelli *et al.*, 1992).

In rare cases, programmed cell death during development is not accompanied by these morphological or molecular events (Schwartz *et al.*, 1993) and DNA laddering is not always detected in cells dying by morphological criteria of apoptosis, since the DNA is sometimes cleaved into larger fragments (50 - 300 kb) (Bortner *et al.*, 1995).

Many of the techniques described in this section could be incorporated into other sections, but the detection of apoptosis is such an integral part of this thesis that they are described together rather than separately.

Propidium iodide staining

Propidium iodide is a fluorescent dye which intercalates with nucleic acids. Apoptotic cells can be identified in tissue sections by their small, fragmented (pyknotic) nuclei which stain brightly when they are visualised under fluorescence microscopy.

This technique was adapted from Coles and colleagues (1993) with minor modifications. Paraffin embedded sections were dewaxed and rehydrated to PBS as described above. Slides were then washed twice, for 5 minutes, in PBS and incubated in 0.004 g / l propidium iodide with 0.1 g / l RNase A in PBS at 37°C for 30 minutes. Slides were washed 3 times in PBS, mounted in Citifluor™ and examined using fluorescence microscopy. Nucleated red cells and mitotic cells also appear bright after propidium iodide labeling but these can generally be distinguished by their size and morphology.

In situ end-labeling

During apoptosis the nuclear DNA is digested by endonucleases leaving free 3' ends. These ends can be tagged with labeled nucleotides using the enzyme terminal deoxytransferase (TdT) and visualised on tissue sections using secondary detection systems. This technique was first described by Gavrelli and colleagues (1992) and this was modified by using an Apoptag™ kit with methyl green counterstaining. The principles of the end-labeling technique are shown in figure 9.

1) DNA digestion

Nucleosome-sized
DNA fragments

2) Add labeled nucleotide

Digoxigenin d-UTP tail

3) Bind antibody-enzyme
   conjugate

Peroxidase conjugate

4) Add secondary detection
   agent

Substrate staining
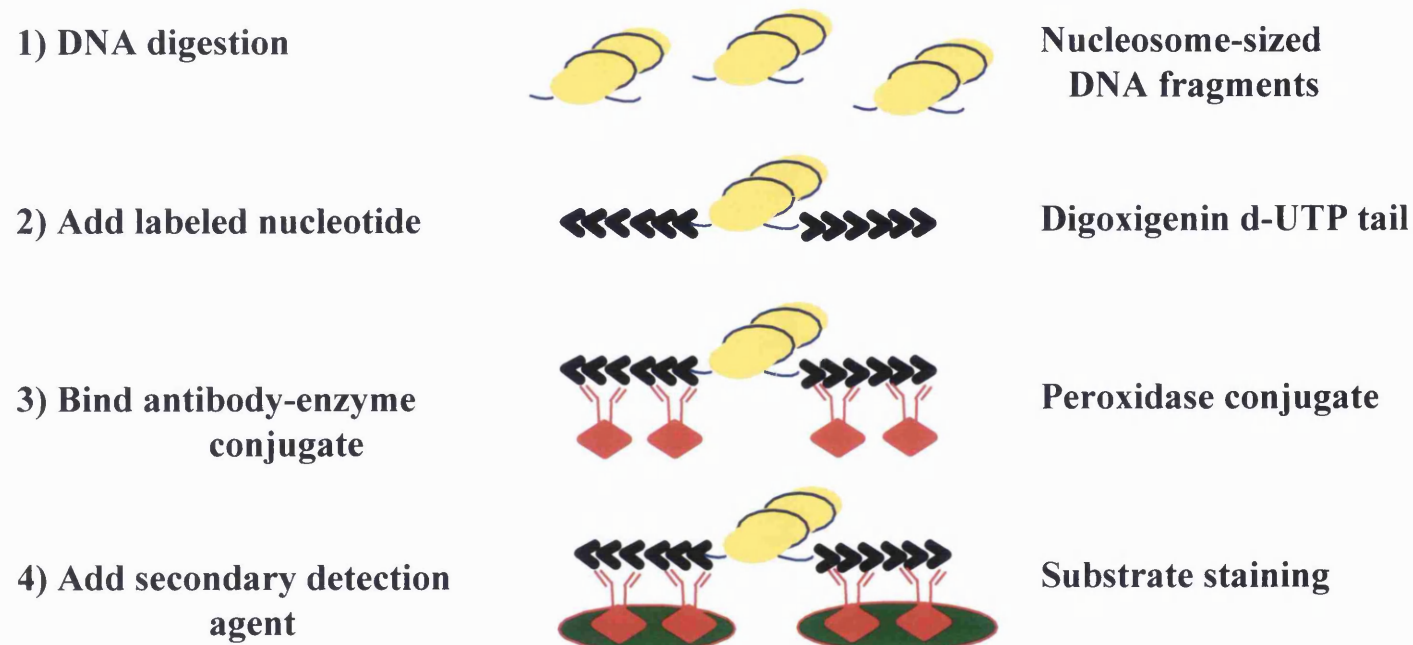
Figure 9. Principles of *in situ* end-labeling. 1) During apoptosis DNA is digested by endonucleases into nucleosome sized fragments which contain free 3 prime ends. 2) Labeled nucleotides are added to the free prime ends by the enzyme terminal deoxytransferase. In this illustration, digoxigenin d-UTP is shown, although radio-labeled or fluorescent tagged nucleotides may also be used. 3) Antibodies conjugated with peroxidase, or other reagents dependant on the secondary detection system, are added which specifically bind to the labeled nucleotides. 4) Secondary detection reagents, such as DAB, are added and stain the apoptotic cells.

Paraffin sections were rehydrated, pretreated to block endogenous peroxidase and immersed in proteinase K as described in *Immunohistochemistry* above. They were then washed four times in distilled water for 2 minutes and twice in PBS for 5 minutes. At the same time, an ice bath was prepared for the TdT solution, and both a humid slide chamber and a Coplin jar of stop / wash solution were prewarmed to 37°C. Excess liquid was removed from the slides by careful blotting around the sections and 100 μl of equilibration buffer was dropped onto the tissue for 15 seconds, followed by 100 μl of TdT working solution from the Apoptag™ kit. This contained TdT, digoxigenin conjugated UTP and reaction buffer. A plastic coverslip was then placed over the sections to ensure an even distribution of TdT solution and the slides were placed in the humid chamber at 37°C for one hour. The reaction was terminated by immersion in stop/wash buffer at 37°C for 30 minutes. Specimens were then washed in 3 changes of PBS for 5 minutes each, followed by 100 μl of anti digoxigenin antibody (diluted 1 in 50) conjugated to either rhodamine for fluorescent microscopy, or horse radish peroxidase which was detected using DAB on light microscopy (See *Immunohistochemistry* section).

Electron microscopy

Apoptotic cells have a characteristic appearance on electron microscopy with nuclear condensation around the periphery of the nucleus, cell shrinkage and budding off of both the nuclear and cell membranes.

Samples of dysplastic kidneys were fixed in 2% glutaraldehyde in 0.05 M cacodylate buffer, then in 1% Osmium tetroxide and finally embedded in epoxy resin. Ultrathin sections contrasted with uranyl acetate and lead citrate were examined with a Joel 100 CX transmission electron microscope. These experiments were

performed in conjunction with Mr Brian Young in the Electron Microscopy department at the Institute of Neurology, Queen's Square, London.

DNA electrophoresis

Endonucleases are activated during apoptosis which digest the DNA to produce nucleotide fragments which are multiples of 180 - 200 base pairs (i.e. 180, 360, 540, 720 bp). These can be visualised as a ladder (Wyllie, 1980) by agarose gel electrophoresis. This technique is used to separate DNA of different sizes which is then visualised under ultraviolet illumination (Sambrook *et al.*, 1989).

Fresh surgical specimens of dysplastic kidneys were thawed to room temperature (after storage at -70^0C), homogenised in a lysis buffer (10 mM Tris HCl (pH 8.0), 10 mM EDTA, 0.1% SDS, 0.1 g / l proteinase K) and incubated in the buffer overnight at 52^0C. DNA was then extracted using the phenol / chloroform technique which relies on the fact that DNA will separate into the aqueous phase. Equal volumes of phenol (equilibrated pH 8.0) and chloroform were added to the specimen and it was centrifuged at 5,000 xg. The aqueous layer was separated and the process repeated. DNA was then precipitated with an equal volume of ice cold 100% alcohol, washed in 70% ethanol and resuspended in TE buffer (0.1 M Tris-HCl, pH 8.0, 10 mM EDTA).

Next, an agarose gel was prepared for DNA electrophoresis. For this experiment, a 1.5% agarose gel was used, although variable concentrations can be used in order to separate different sizes of DNA. The agarose was was dissolved in TAE buffer (10x TAE: 0.4 M Tris-acetate, 0.01 M EDTA, pH 8.0) by microwaving, and 50 µl / l of ethidium bromide solution (stock 20 g / l) was added as it cooled. It was then poured into a gel frame and a comb was inserted to form the sample wells. Once set, it was transferred to Horizontal midi-gel apparatus and just covered with TAE buffer. Two µg of DNA was mixed with loading buffer (orange-G / glycerol or bromphenol blue / glycerol) and loaded into the wells. The gels were run at up to 100 volts and required approximately 45 minutes running time, according to the size of the DNA. Markers of specific size, such as the 123 and 1 kb ladder, were also run concurrently.

The next step was to visualise the DNA, and this step utiilises the fact that Ethidium bromide intercalates with nucleic acids and fluoresces under UV illumination. Therefore the gels were transferred to a light box, viewed under UV light and photographed.

Some samples were treated with 1 g / l of RNase A for 30 minutes before electrophoresis to ensure that there was no RNA contamination.

Quantification of apoptosis

Preliminary experiments with both propidium iodide and *in situ* end-labeled specimens showed that the number of apoptotic cells varied in different areas of the same section, although there was good correlation between the two techniques. Therefore, for each specimen, photographs were taken (at 20x magnification) of 10 random propidium iodide stained fields in order to integrate the quantity of apoptosis within the section. The number of pyknotic

nuclei was then counted by 3 'blinded' observers and these results were compared using a technique described by Bland and Altman (1986). They described a method by which different assessments of the same data can be compared by plotting the mean of the measurements (X-axis) against the difference between them (Y-axis). If the methods, or measurements, are in agreement then it should be possible to draw a horizontal straight line through the results. No observer bias was detected between the results using this technique. This data was then used to derive a pyknotic index for each specimen by taking the mean number of pyknotic nuclei per 10 fields.

This approach, however, failed to account for the fact that there are fewer cells per microscope field in the cystic areas. Therefore, the total number of cells was counted in a representative sample from each specimen and the quantity of apoptosis was then expressed as a percentage of the total number of nuclei. This is effectively the point prevalence of apoptosis in the samples at the time of collection.

Statistical analysis

The pyknotic indices and the percentage of apoptotic cells in each experimental group were not normally distributed. Therefore, the data was compared using the non-parametric Wilcoxon Rank Sum test. A probability value of < 0.05 was considered to be statistically significant.

Functional studies

It is very difficult to perform functional studies on human tissues, especially human fetal tissues since samples are scarce and there are ethical limitations on the research. One alternative is to isolate and culture cells from human dysplastic kidneys. These can then be characterised and their response to exogenous factors, which are known to be important in normal development, can be assessed. Unfortunately, however, normal human cells stop proliferating and their phenotype may change after a finite number of passages (Hayflick, 1965). This problem can be circumvented by conditional-immortalisation of the cells (O'Hare *et al.*, 1991; Bryan and Reddel, 1994).

In the final part of this thesis, therefore, cells derived from dysplastic kidneys were cultured and transduced with a temperature sensitive SV40 large T construct, as the first step to potential immortalisation of these cells. Preliminary characterisation of these cells has demonstrated both epithelial and mesenchymal phenotypes and these cells form the basis for a more extensive study in the future.

Culture of dysplastic cells

Pieces of 3 surgically removed dysplastic kidneys were obtained for cell culture. All of the specimens were from boys and lower urinary tract obstruction had been ruled out by a micturating cystogram. None of the specimens had detectable function on radioisotope imaging.

The first sample was from the upper pole of a duplex kidney removed at 20 months of age. Histology showed abnormal tubules with peritubular collarettes, and in addition there was a dense inflammatory infiltrate suggestive of chronic inflammation. The second sample was from a 6 month old child with an antenatal diagnosis of hydronephrosis and a postnatal (ultrasound) diagnosis of a multicystic dysplastic

kidney. Histology showed one large and numerous smaller cysts lined with a flattened epithelium surrounded by fibrous tissue containing scanty primitive tubules. The third sample was from a 7 month old child with an antenatal diagnosis of hydronephrosis which was confirmed postnatally. Histology showed multiple small cysts, primitive ducts, bars of cartilage and immature glomeruli.

After surgical removal the kidneys were transported on ice to the histopathology lab for inspection by the pathologist. A representative piece was then placed in culture medium (Dulbecco's Modified Eagle's Medium F-12 supplemented with 5% fetal calf serum, 1,000 U / l penicillin G, 0.001 g / l streptomycin and 0.025 g / l amphotericin) and immediately transferred to the laboratory. All subsequent procedures were performed in a tissue culture hood using aseptic techniques. The specimens were diced into numerous small pieces using two sterile blades. These were seeded onto a tissue culture dish containing just enough medium (as above) to cover the base of the dish. The cells were initially incubated in a standard incubator at 37^0C in a humidified 5% CO_2 / air atmosphere.

Culture plates were assessed daily to ensure that the cells were viable and the medium was not infected. Photographs were taken of these primary cultures to show cell numbers and gross phenotype. Cells were harvested and passaged when they were almost confluent by enzymatic dissociation (trypsin 1000 U / ml, 0.02% EDTA in Dulbecco's Modified Eagle's Medium) for 5 minutes at room temperature followed by centrifugation and resuspension in fresh medium. The first sample was characterised using vimentin and cytokeratin staining whilst two others were subsequently used for transduction experiments (see below). Aliquots of the primary cultures of cells used for transduction were stored in 10% DMSO / fetal calf serum in liquid nitrogen.

Transduction of dysplastic cells

Transduction of the dysplastic cells was performed by Dr Mike O'Hare at the Breast cancer Laboratory, Ludwig Institute for Cancer Research, UCL, London (O'Hare *et al.*, 1991). This is a level 3 containment laboratory which has been set up specifically for these procedures, and similar facilities were not available at the Institute of Child Health.

Principles of transduction and potential immortalisation

The first phase of the potential immortalisation of dysplastic cells involved transduction of the cells with the tsA58-U19 gene construct using an amphotropic replication defective retrovirus (see below). The tsA58-U19 construct contains two mutations. The first, U19, ablates sequence-specific DNA binding and prevents autonomous viral replication (Jat *et al.*, 1986). The second mutation, tsA58, renders the T antigen thermolabile at 39°C (Jat and Sharp, 1989). Hence, cells cultured at the-non permissive temperature of 39°C should have the same characteristics as the cells prior to transduction. In contrast, cells cultured at the permissive temperature of 33°C continue proliferating beyond the point at which normal cells undergo senescence. The cells can therefore be passaged multiple times at 33°C, to generate a large stock of cells, and then switched to a 39°C for specific experiments. For this reason, the cells are sometimes described as 'conditionally' immortal although this is not strictly accurate for human cells, as described below.

The effects of the SV40 large T antigen are different in humans and mice. The SV40 T antigen is sufficient for immortalisation in mice, but it only prolongs the number of potential divisions of human cells, a phase termed 'lifespan extension'. Some human cells may become immortalised, however, but they must first pass through a 'blast crisis'

stage in which most of the cells become senescent and die (O'Neill *et al.*, 1995).

The mechanism by which the SV40 T antigen prolongs lifespan in human cells is unknown but it may be mediated by complex formation between the large T antigen and the retinoblastoma and p53 proteins (Bryan and Reddel, 1994). These proteins normally act as growth / tumour suppresser molecules but complex formation prevents this function and allows the cells to proliferate. The mechanism underlying immortalisation is also unknown, although hybridisation analyses indicate that this is a gene inactivation event.

In order to transduce the cells with the tsA58-U19 construct, the construct must first be inserted into a shuttle vector and this must then be packaged in order to get into the cells. The vector used here was the pZipNeoSV(X)1 shuttle vector which also contains the neomycin resistance gene, allowing positive selection of infected cells (Cepko *et al.*, 1984). The amphotropic virus-producing line was generated by infecting PA317 packaging cells (Miller and Buttimore, 1986) with supernatant from an ecotropic packaging cell line (Stamps *et al.*, 1994).

Retroviral infection

Primary cultures of dysplastic cells, grown at 37⁰C, were transferred after one passage to the Ludwig Institute. They were then grown to around 50% confluency, washed with growth medium and then incubated with 5 ml of the viral supernatant diluted 1:2 (v/v) with medium for 2 - 4 hours. This process was repeated on three consecutive days at the semipermissive temperature of 36.5⁰C.

144

Selection for Neomycin resistance was performed around one week after infection. Cells were cultured in medium containing 0.5 g / l geneticin 418 (G418) and the surviving antibiotic resistant cells were passaged six more times before transfer back to our laboratory. Cells were grown in culture for several passages at the permissive temperature of 33⁰C without any gross change in phenotype and expressed the large T antigen (see *Results* section).

Western blot of cultured cells

Western blotting was performed on the cultured cells using the same principles as described earlier, although extraction of the protein is different.

Culture medium was removed from the petri dish and the cells were then washed for 5 minutes in PBS. The PBS was then removed, being careful to remove excess by tipping the dish and using blotting paper. One ml of ice-cold lysis buffer containing proteinase inhibitors (see earlier) was then applied to the cells and left on ice for 5 minutes. The cells were then scraped off the dish and disrupted by repeated aspiration through progressively smaller needles (i.e. 21 gauge, then 23, then 25). Samples were kept on ice during this procedure. Debris was pelleted by centrifugation at 3000 rpm at 4⁰C for 15 minutes and the supernatant was used for Western blotting.

MDCK cells

Madin Darby Canine Kidney cells are epithelial cells which have many of the characteristics of collecting ducts. These cells are commercially available and they were grown at 37°C in Dulbecco's Modified Eagle's medium, as described above. Cells were grown until near confluence and then harvested for protein.

Immunostaining of cells

Cells were grown in 4 well chamber slides for immunostaining. Media and culture conditions were as above. After a few days in culture, before the cells became confluent, the medium was removed and the chambers were washed twice with PBS. Cells were then fixed for 5 minutes by a number of techniques depending on the optimal conditions required for the primary antibody. These included 2% paraformaldehyde in PBS at room temperature, ice-cold methanol and ice cold acid / alcohol. Non specific binding was then blocked by incubation with 10% fetal calf serum in PBS. Cells were incubated at 4°C with primary antibodies which were detected with appropriate FITC-conjugated secondary antibodies as described in *Immunohistochemistry* earlier in this chapter.

Chapter 7. Results

Histology, intermediate filament and other staining, and lectin binding of normal and dysplastic kidneys

Histology

The ontogeny of normal and abnormal human kidney development is described in the *Introduction* section of this thesis and representative sections of the mesonephros, metanephros and dysplastic kidney specimens examined in this thesis are included below to illustrate normal and pathological nephrogenesis.

Normal kidneys

Mesonephros

(n = 6)

The mesonephros was detected posterior to the gonadal ridge in embryos from 38 days of gestation, the earliest stage examined (Fig. 10). It remained posterior to the gonad as it formed a distinct, elongated, sausage shaped organ in later development (shown in transverse section in Fig. 11). The mesonephros comprised the mesonephric duct and mesonephric tubules located medial to the duct (Fig. 10 and 11). Each tubule consisted of a large, vascularised mesonephric glomerulus, comprising a cup-shaped sac encasing a knot of capillaries and 'proximal' and 'distal' tubules, connected to the mesonephric duct (Fig. 11). The paramesonephric, or Mullerian, duct was located lateral to the mesonephric duct (Fig. 11).

Metanephros

(n = 17)

The metanephros was detected posterior to the mesonephros and gonads in early development (Figs. 12 and 13A). Initially, it comprised

147

of a central ureteric bud stalk, loose mesenchyme and a small number of

bud branches surrounded by condensed mesenchyme at the periphery

of the organ (Fig. 13B and C). Later in development, ureteric bud

branches and condensed mesenchyme were confined to the outer cortex

(Fig. 14) whilst developing nephrons and collecting ducts were detected

in deeper parts of the cortex, with more mature structures towards the

centre of the organ. Early nephron precursors such as comma and S-

shaped bodies were detected at eight weeks of gestation (Fig. 14C and

D) along with the first layer of glomeruli (Fig. 14A). Successive layers of

glomeruli were formed and further elongation and specialisation of the

remaining sections of the nephron lead to the formation of proximal

tubules and loops of Henle as the kidney developed (Fig. 14B). New

nephron formation, as assessed by the presence of ureteric bud

branches and condensed mesenchyme, appeared to continue in the

outer cortex until 36 weeks of gestation (data not shown).

Dysplastic kidneys

(Preterm n = 10; Postnatal n = 12)

Characteristic histological features of renal dysplasia, such as primitive

dysplastic tubules surrounded by whorls of close packed elongated cells,

were detected in all of the samples examined in this thesis (Figs. 15A

and B, and 16A and C). Cysts were also detected (Fig. 15C and D) in

the majority of the samples, although some kidneys contained multiple

small cysts whilst others had a few very large cysts. There was no

correlation detected between either the size, or the number, of cysts and

the presence of urinary tract obstruction.

Nests of dysplastic tubules (Fig. 16B), areas containing relatively normal

looking glomeruli (Fig. 16C) and metaplastic islands of cartilage (Fig.

16D) were occasionally seen in the dysplastic kidneys examined.

Intermediate filament and other staining, and lectin binding

Cells from different segments of the normal nephron can be distinguished by their specific intermediate filament proteins and surface glycoproteins. These markers were therefore used to determine whether it was possible to define the cell lineages in dysplastic kidneys by comparing them with normal kidneys from mid gestation and normal mature kidneys.

Normal kidneys

(Preterm n = 4; Postnatal n = 5)

Cytokeratin expression was detected in the collecting ducts, loops of Henle and Bowman's capsule of the glomerulus in mid gestation kidneys (Fig. 17A and B). In contrast, vimentin expression was limited to glomerular podocytes (Fig. 17C) in the developing and mature kidney. Alpha-smooth muscle actin was detected in vessel walls (Figs. 17D) and von Willebrand factor was expressed in vascular endothelia (not shown) in the normal kidney.

Mature proximal and distal tubules were distinguished, in the normal kidney, by lectin staining with *Tetragonolobus purpureas* (asparagus pea) agglutinin which labeled proximal tubules (Fig. 17E) and *Arachis hypogaea* (peanut) which identified distal segments (Fig. 17F). Staining was also performed with other lectins but often gave inadequate results. For example, *Dolichos biflorus* (horse gram) is reported to bind to the ureteric bud and its derivatives but I did not find consistent staining patterns with this lectin on the wax embedded sections used in this thesis. Similarly, *Ulex europaeus* (gorse) did not distinguish vascular endothelia as clearly as staining for the von Willebrand factor.

Dysplastic kidneys

(Preterm n = 5; Postnatal n = 6)

Both dysplastic tubules and dysplastic cyst epithelia expressed cytokeratin (Figs. 18A and 19A respectively). Dysplastic tubules were also positive for vimentin (Fig. 18B), although the cyst epithelia were vimentin negative (Fig. 19B). The cells surrounding both dysplastic tubules and cysts were positive for vimentin and α-smooth muscle actin (Figs. 18C and 19C). This latter observation is consistent with the histological description of fibromuscular collarettes surrounding dysplastic tubules. Neither undilated tubules nor cyst epithelia expressed α-smooth muscle actin.

Vascular endothelia in dysplastic kidneys were positive for von Willebrand factor (Fig. 18D) and *Ulex europaeus* bound to them (Fig. 19D) but the dysplastic epithelia and surrounding cells were negative. The majority of both tubules and cysts were positive for *Arachis hypogaea* agglutinin (Fig. 18F and 19F). Some tubules were positive for *Tetragonolobus purpureas* (Fig. 18E), but no cysts were positive for this agglutinin (Fig. 19E). None of the tubules or cysts were positive for both markers.

Summary of results of histology, intermediate filament and other staining, and lectin binding

Normal renal development involves intimate contact between ureteric bud and mesenchymal lineages. This causes the ureteric bud to branch serially and give rise to the collecting ducts and urothelium of the renal pelvis and ureter, while the renal mesenchyme undergoes epithelial conversion to form nephrons from glomerulus to loops of Henle.

	Cytokeratin	Vimentin	α-sma	Lotus	Arachis	Ulex
Normal kidneys (mid gestation and postnatal)						
Bowman's capsule	++	+/-	+/-	-	-	-
Podocytes	-	++	-	-	-	-
Proximal tubule	+/-	-	-	++	-	-
Loop of Henle	++	-	-	-	-	-
Immature collecting ducts	++	-	-	-	++	-
Mature collecting ducts	++	-	-	-	++	-
Blood vessels	-	-	++	-	-	++
Dysplastic kidneys (mid gestation and postnatal)						
Dysplastic tubules	++	++	-	+	++	-
Cyst epithelium	++	-	-	-	+	-
'Fibromuscular collarettes'	++	++	++	-	-	-
Loose cells	-	+	-	-	-	-
Blood vessels	-	-	-	-	-	++

Intermediate filament and other staining, and lectin binding.

This table summarises the staining for cytokeratin, vimentin, α-smooth muscle actin (α-sma) and lectin binding of *Tetragonolobus lotus purpurea* (Lotus), *Arachis hypogaea* (Arachis) and *Ulex europaeus* (Ulex) in mid gestation and postnatal samples of normal and dysplastic kidneys. '–' Indicates no staining, '+/-' indicates that less than 10% of cells were positive and '+' to '++' indicates increasing levels and / or intensity of staining.

Using haematoxylin and eosin staining, dysplastic kidneys contained tissues which superficially resembled those in the developing kidney: dysplastic tubules were similar to ureteric bud branches, adjacent close packed cells resembled condensed mesenchyme and more distant loosely arranged cells appeared analogous to uncondensed mesenchyme.

In the normal kidney, differentiated epithelia expressed cytokeratin whilst vimentin expression was restricted to glomerular podocytes. Alpha-smooth muscle actin was only found in vessel walls. *Tetragonolobus purpureas* and *Arachis hypogaea* bound to mature proximal and distal tubules respectively.

In dysplastic kidneys, undilated tubule epithelia were positive for both cytokeratin and vimentin, whereas cyst epithelia were positive for cytokeratin alone. Vimentin was also detected in the close packed cells around cysts and tubules, along with α-smooth muscle actin. Occasional tubule epithelia, but no cysts, bound *Tetragonolobus purpureas* but the majority of tubules and cysts were positive for *Arachis hypogaea*. Hence, there were significant differences in intermediate filament protein expression and lectin binding when dysplastic epithelia were compared to the ureteric bud, or the surrounding cells were compared to normal mesenchyme. These results are reviewed in the *Discussion*.
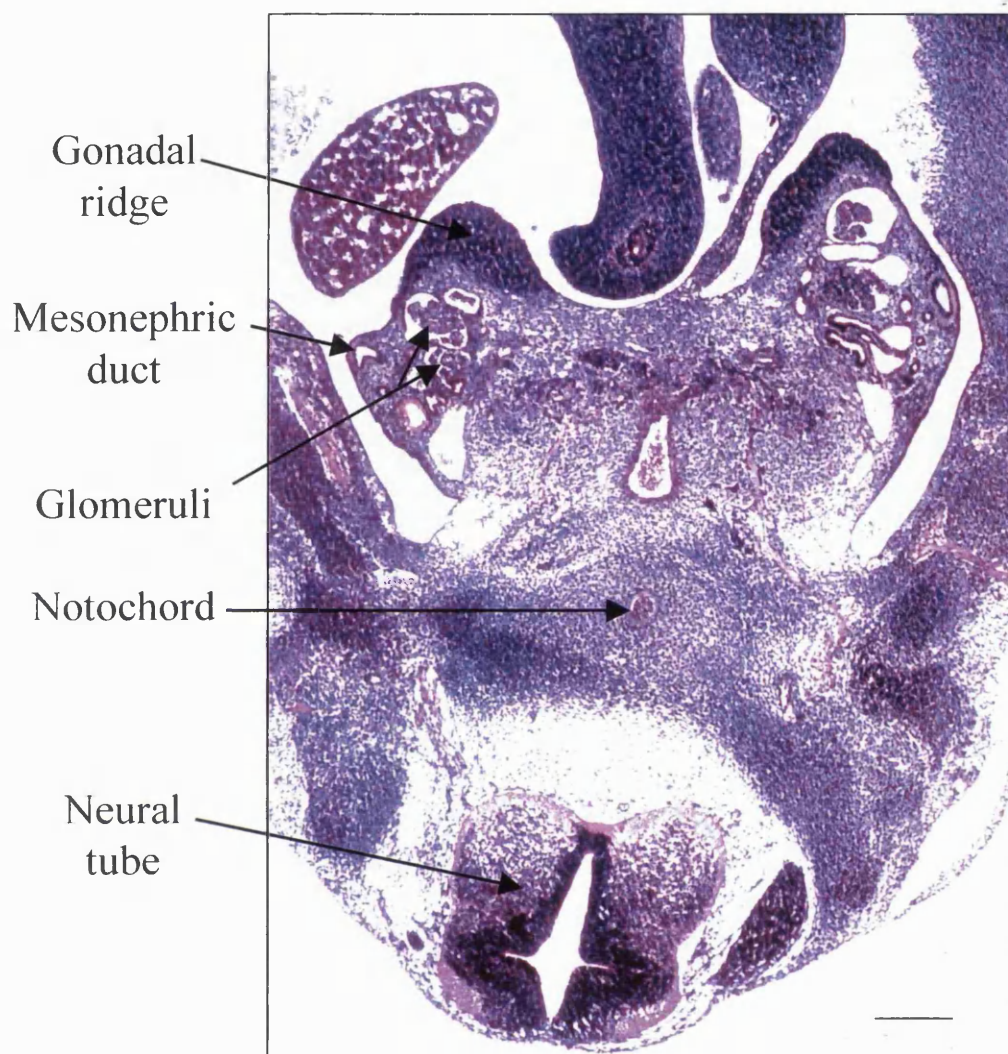
Figure 10. Mesonephros, low power view. Transverse section through the abdomen of a human embryo at 38 days of gestation stained with haematoxylin and eosin. Mesonephric tubules and relatively large glomeruli are seen in the mesonephros. At this stage the gonadal ridge is anterior to the mesonephros and the mesonephric duct is located laterally. Bar corresponds to 1 mm.
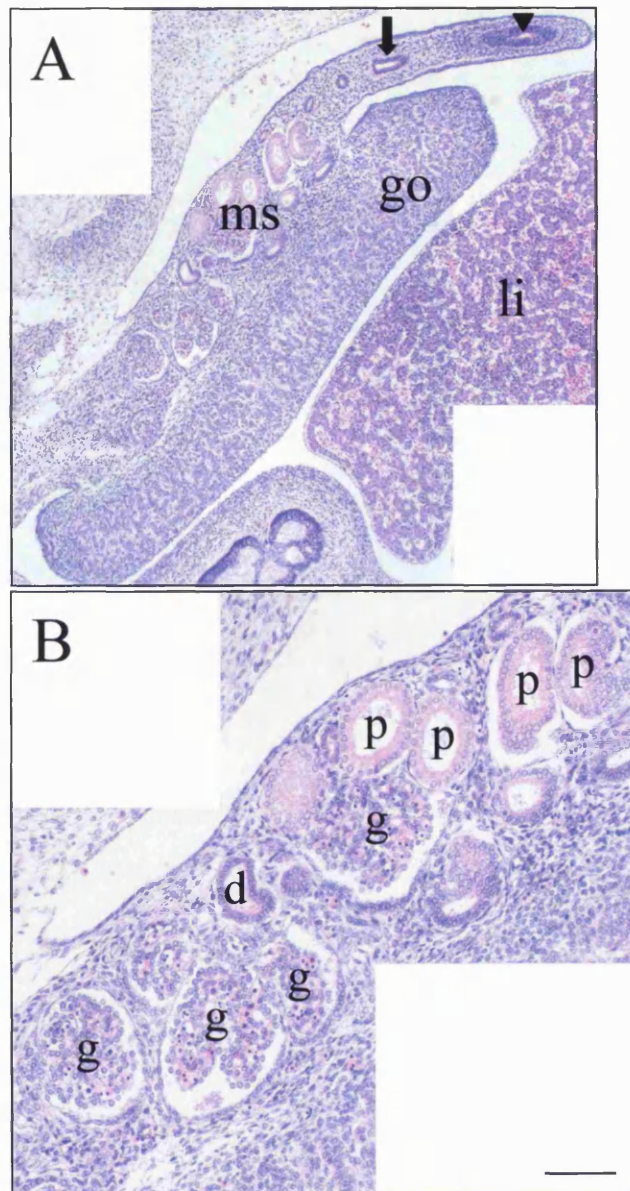
Figure 11. Mesonephros, high power view. Composite transverse sections through the abdomen of a human embryo at 42 days of gestation stained with haematoxylin and eosin. A) Mesonephros (ms) adjacent to the developing gonad (go) and liver (l). The mesonephric duct (arrow) and paramesonephric duct (arrowhead) are also seen. B) Higher power view shows mesonephric glomeruli (g) and tubules with proximal (p) and distal like (d) morphology. Bar corresponds to 500 μm in A) and 200μm in B).

Liver

Pancreas

Gonad

Mesonephros
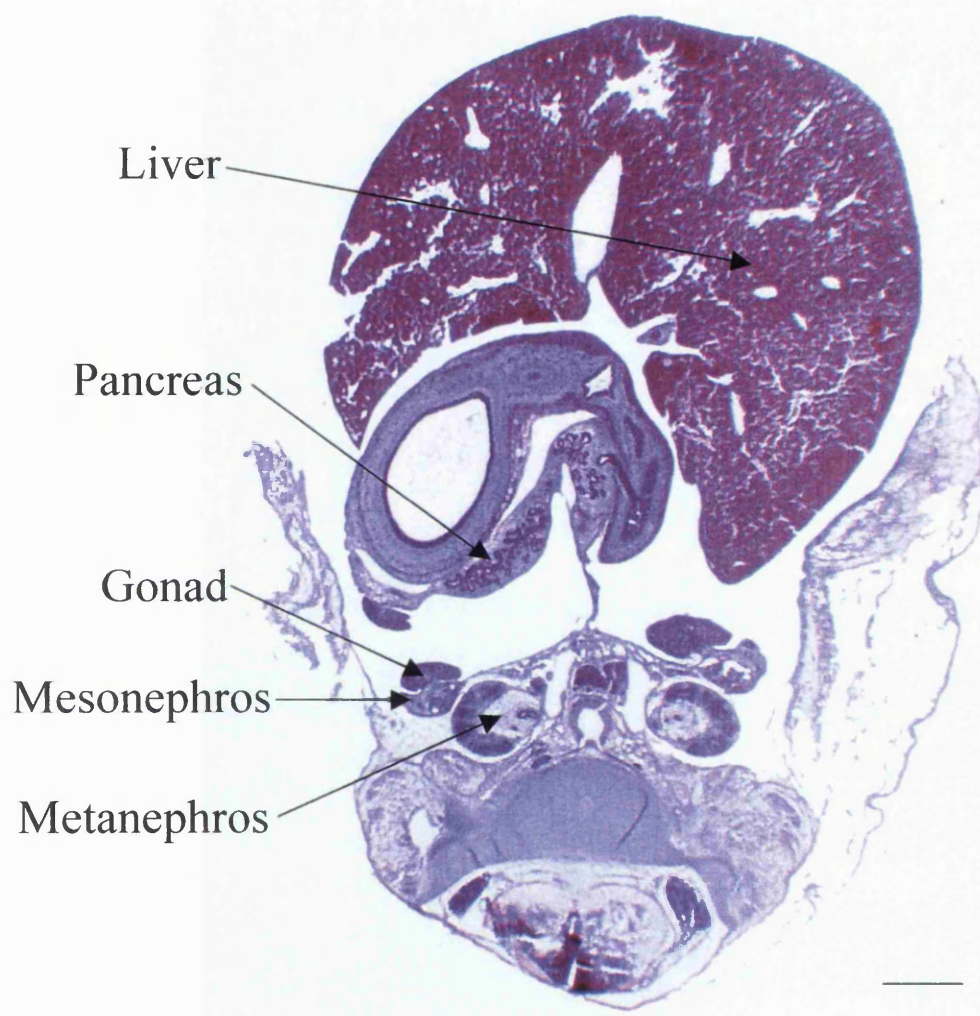
Metanephros

Figure 12. Metanephros, low power view. Transverse section through the abdomen of a human embryo at 42 days of gestation stained with haematoxylin and eosin. The metanephros is seen postero-medial to the mesonephros and gonad. Note the centrally located ureteric bud and peripheral branches surrounded by condensing mesenchyme. Bar corresponds to 500 μm.
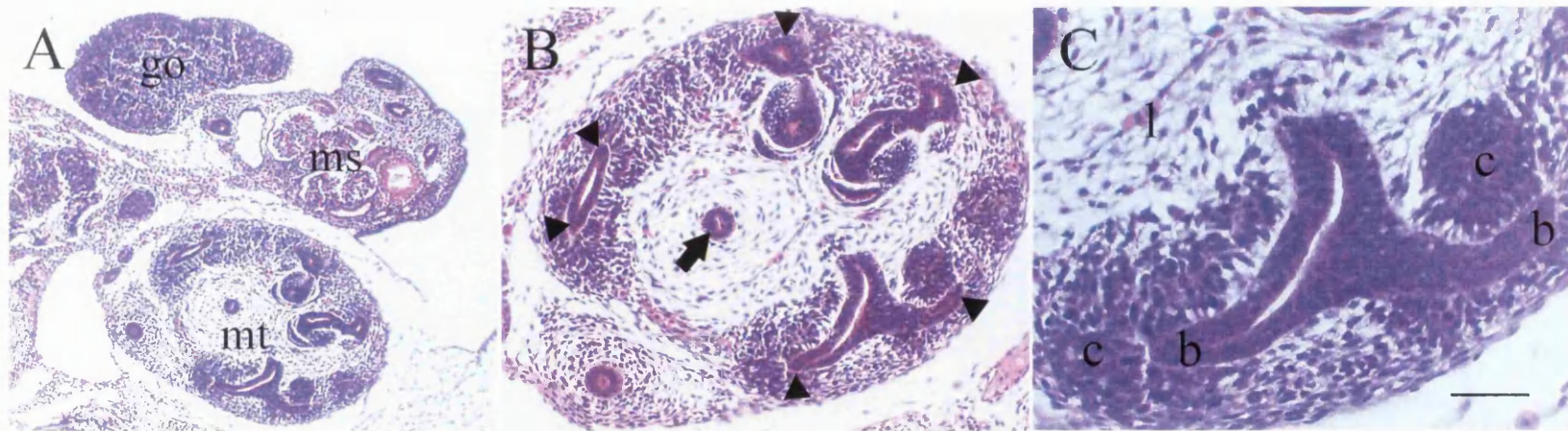
Figure 13. Metanephros, high power views. Haematoxylin and eosin stained sections from a human embryo at 42 days of gestation. A) The metanephros (mt) lies posterior to the mesonephros (ms) and gonad (go). B) Higher power view of the metanephros showing the central ureteric bud (arrow) and peripheral branches (arrowheads). C) Mesenchyme condenses (c) around the branching tips (b) of the ureteric bud. Loose mesenchyme (l) is also seen. Bar corresponds to 400 µm in A), 200 µm in B) and 80 µm in C).
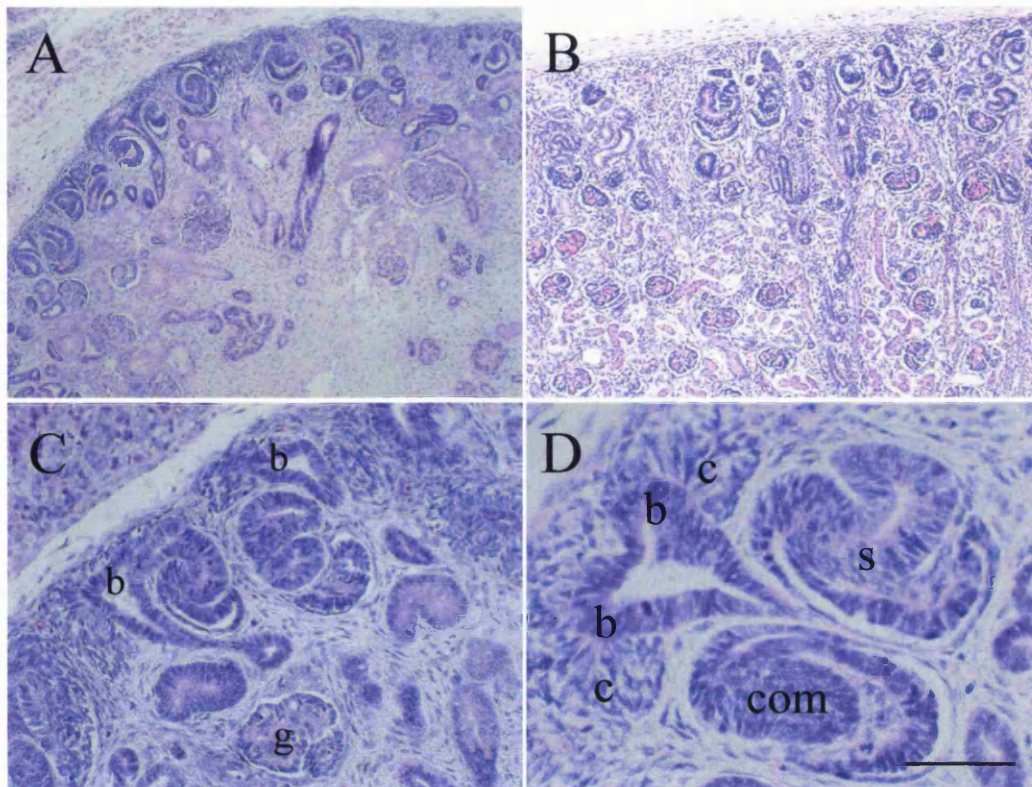
Figure 14. Fetal kidney. Haematoxylin and eosin stained sections of normal human fetal kidneys: A), C) and D) are from an 8 week, and B) is from a 20 week gestation fetus. A) and B) show the nephrogenic cortex with one layer and several layers of glomeruli respectively. C) and D) show higher power views of ureteric bud branches (b) surrounded by mesenchymal condensates (c). Early nephron precursors including comma (com) and S-shaped bodies (s) and an immature glomerulus (g) are also seen. Bar corresponds to 500 μm in A) and B), 200 μm in C) and 80 μm in D).
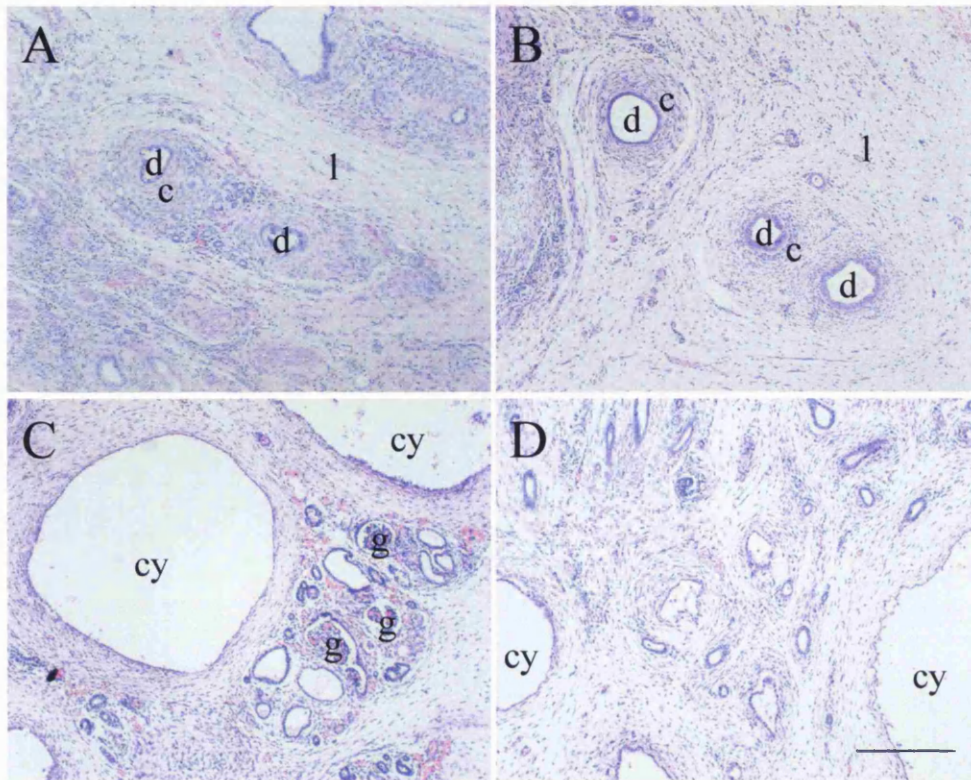
Figure 15. Dysplastic kidneys, low power view. Haematoxylin and eosin stained sections of dysplastic kidneys. A) is from a 15 month and B) is from a 22 month old child, whilst C) and D) are from a preterm infant of 34 weeks gestation. A) and B) show dysplastic tubules (d) surrounded by closely packed cells in the fibromuscular collarettes (c) and more distant loosely packed cells (l). C) and D) show cysts (cy) with occasional formed glomeruli (g) adjacent to them. Bar corresponds to 500 μm in all.
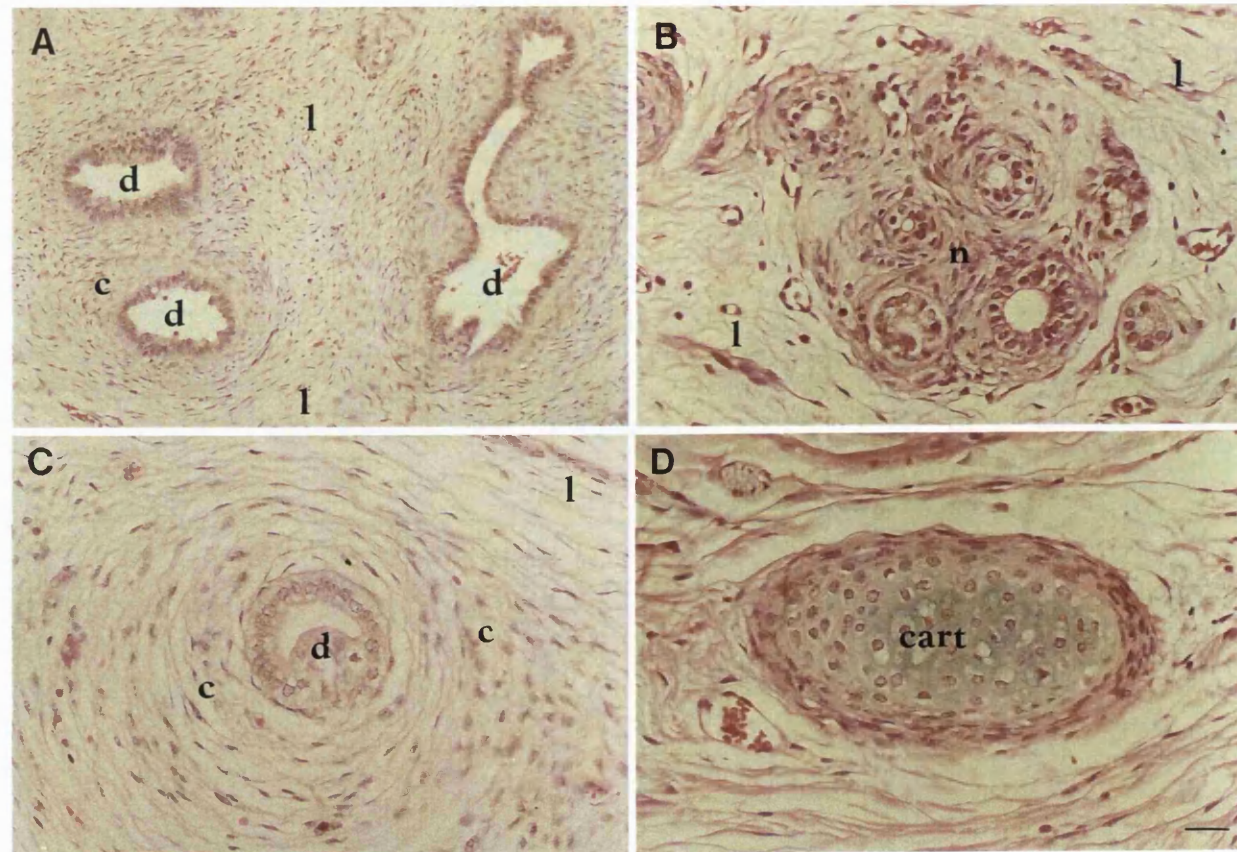
Figure 16. Dysplastic kidneys, high power view. Haematoxylin and eosin stained sections of postnatal dysplastic kidneys. A) Dysplastic tubules (d) surrounded by closely packed fibromuscular collarettes (c) and more distant loosely packed cells (l). Note the characteristic irregular outline of the largest tubule. B) A nest (n) of dysplastic tubules surrounded by loosely packed cells. C) Higher power of a dysplastic tubule. D) Metaplastic cartilage. Bar corresponds to 100 μm in A) and 50 μm in the other sections.
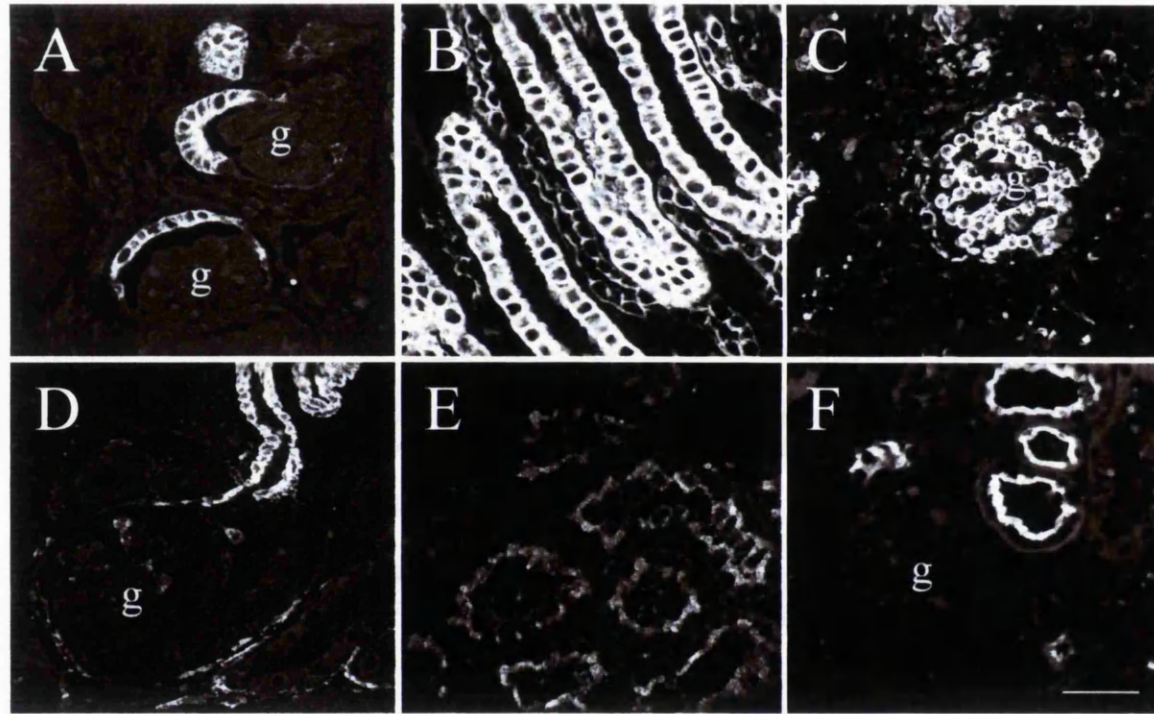
Figure 17. Intermediate filament and lectin staining of normal kidneys. Confocal laser scanning photomicrographs of sections of normal kidneys from mid gestation fetuses with fluorescently labeled antibodies against: A) and B) pan-cytokeratin, C) vimentin, D) *a*-smooth muscle actin. Lectins were: E) *Tetragonolobus purpureas* and F) *Arachis hypogaea*. A) and B) Cytokeratin positive cells are seen in Bowman's capsule of the glomeruli (g), collecting ducts and loops of Henle. C) Vimentin is restricted to glomerular podocytes. D) Alpha-smooth muscle actin is found in smooth muscle cells in vessel walls. E) *Tetragonolobus purpureas* labels proximal tubules. F) showsapical binding of *Arachis hypogaea*. Bar corresponds to 50 μm in all.
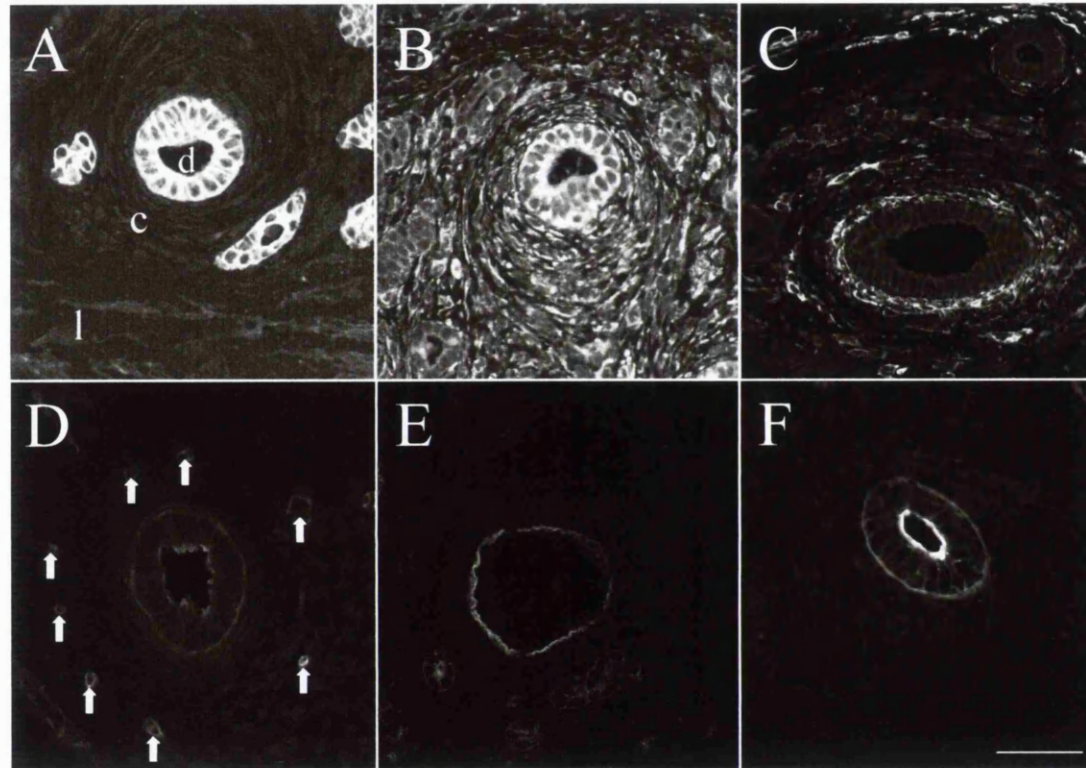
Figure 18. Intermediate filament and lectin staining of dysplastic tubules. Confocal laser scanning photomicrographs of sections of postnatal dysplastic kidneys with fluorescently labeled antibodies and lectins: A) pan-cytokeratin, B) vimentin and C) α-smooth muscle actin, D) *Ulex europaeus*, E) *Tetragonolobus purpureas* and F) *Arachis hypogaea*. Dysplastic tubules (d), collarettes (c) and loose mesenchyme like cells (l) are seen in each section. A) - C) show cytokeratin and vimentin positive tubule epithelia, whilst surrounding collarettes are positive for vimentin and α-smooth muscle actin. D) Tubules are negative but vessels (arrows) are positive for *Ulex europaeus*. E) and F) Occasional tubules are positive for *Tetragonolobus purpureas* but the majority bind *Arachis hypogaea*. Bar corresponds to 50 µm in all.
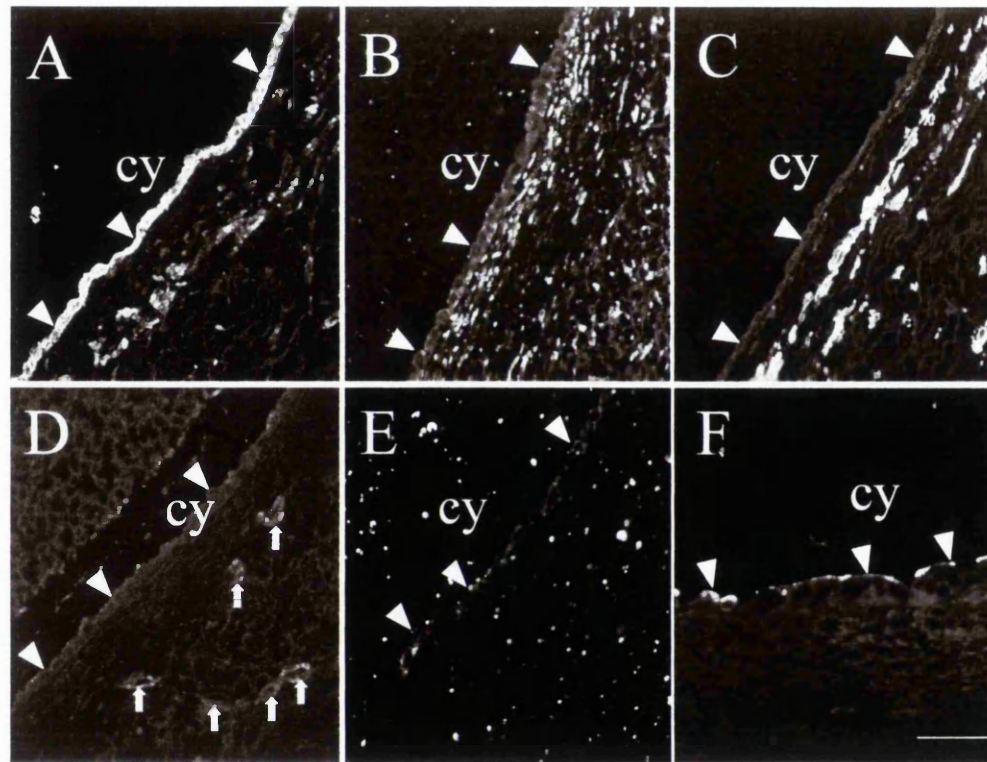
Figure 19. Intermediate filament and lectin staining of dysplastic cysts. Confocal laser scanning photomicrographs of postnatal dysplastic kidneys with fluorescently labeled antibodies against: A) pan-cytokeratin, B) vimentin, C) α-smooth muscle actin and D) von Willebrand factor. Lectins were: E) *Tetragonolobus purpureas* and F) *Arachis hypogaea*. Cyst (cy) epithelia - arrowheads. A) - C) Cyst epithelia are positive for cytokeratin but negative for vimentin whereas adjacent cells are positive for vimentin and α-smooth muscle actin. D) Capillaries are weakly positive for von Willebrand factor (arrows) but cyst epithelia are negative. E) and F) No cysts are detected which are positive for *Tetragonolobus purpureas* but the majority bind *Arachis hypogaea*. Bar corresponds to 50 μm in all.

Chapter 8. Results

Apoptosis and proliferation in normal and abnormal kidneys

Location of apoptosis

Normal kidneys

In the normal prenatal kidney, apoptotic cells were frequently detected in nephron precursors in the nephrogenic cortex, particularly in comma and S-shaped bodies (Figs. 20A and 21B). Mitotic figures were also seen in these structures (Fig. 20A) but these were readily identified by their characteristic morphology. Apoptotic cells were rarely seen in the undifferentiated mesenchyme or in more mature nephrons / tubule segments towards the centre of the kidney (Fig. 20B), although apoptosis was common in the interstitial cells in the medulla (not shown). By comparison, apoptosis was rarely detected in mature normal samples and was confined almost exclusively to the epithelial cells of proximal tubules (Fig. 21D). Apoptosis was not detected in either glomeruli or interstitial cells in the mature kidney (Figs. 20C and D, and 21D).

Dysplastic kidneys

In contrast to the normal samples, the pattern of apoptotic cell death was similar in both prenatal and postnatal dysplastic specimens. The levels of apoptosis, however, varied greatly between the different cell types. It was unusual to find apoptotic cells in the epithelia of dysplastic tubules or dysplastic cysts (Fig. 22A and D). Apoptosis was more common, but still rare, in the fibromuscular collarettes surrounding dysplastic tubules and cysts where occasional single apoptotic cells were seen (arrows in Fig. 22A and D). In contrast,

apoptosis was frequently detected in areas of undifferentiated tissue, which resemble renal mesenchyme, between the epithelial structures (Figs. 22B, C and E, and 23B and D). In these sites, groups containing several apoptotic cells were often observed. Apoptosis was never detected in metaplastic cartilage.

Polycystic kidneys

The polycystic kidney samples examined, most of which were ARPKD, contained large cysts and tubules of both normal and slightly dilated calibre (Fig. 24) . The histologically defined autosomal dominant specimen also contained cystic glomeruli (not shown). The tissue distribution of apoptosis within the kidney was similar in both pre and postnatal samples. Apoptosis was detected between cysts (Fig. 24B and E), in the interstitium (Fig. 24A) and in the epithelium of undilated tubules (not shown). Apoptotic nuclei were also seen within the epithelial lining of cysts (Figs. 24C and E), directly adjacent to areas of epithelial hypercellularity (Fig. 24C), and also in the ADPKD glomeruli with cystic dilatation of Bowmans' capsule (not shown). Interestingly, apoptotic cells were also noted around some undilated tubules in areas without cysts (Fig. 24A).

Electron microscopy

The 'gold standard' for diagnosing apoptosis is considered to be the demonstration of specific morphological changes such as cell shrinking, condensation of nuclear chromatin and formation of apoptotic bodies on electron microscopy. Two postnatal dysplastic kidney samples were examined and apoptosis was found in both of them. Condensed pyknotic nuclei were observed in, or adjacent to, cyst walls (Fig. 25A) and in the poorly differentiated mesenchyme (Fig. 25B). Cell shrinkage was also seen (Fig. 25A) and there was no

evidence of necrosis. Normal surrounding cells with normal nuclei were observed in both sites.

DNA laddering

DNA was extracted from 3 dysplastic samples and separated by agarose gel electrophoresis (Fig. 26). Laddering of the DNA was seen in two of the samples with up to five different bands detected (Fig. 26A and B). Only high molecular weight DNA, was detected in the other sample (Fig. 26C). As a control, to eliminate RNA contamination, the samples were treated with RNase prior to electrophoresis and an identical result was obtained (Fig. 26D to F).

Quantification of apoptosis

Apoptosis was detected in all of the samples examined using the propidium iodide technique and the level of apoptosis was quantified by counting the number of apoptotic cells per microscope field. The pyknotic index and percentage of pyknotic nuclei were derived for each specimen as described in the *Methods* chapter of this thesis. These results are shown in table 7 and graphically in Fig. 27.

Normal kidneys

The lowest number of apoptotic cells, as assessed by the pyknotic index, was seen in normal postnatal kidneys (n = 6), where the median (range) pyknotic index was 8.2 (2.7 - 15.0). Significantly more apoptosis was seen in the normal prenatal group (n = 6)(p < 0.05) which had a pyknotic index of 36.8 (15.3 - 70.8). These results were similar when the percentage of pyknotic cells were compared in the two groups: normal mature kidneys 0.05 (0.01 - 0.09), normal prenatal kidneys 0.16 (0.06 - 0.32) (p < 0.05).

Dysplastic kidneys

The pyknotic index of the prenatal specimens of dysplastic kidneys (n = 6) was 103.1 (52.8 - 205.0), significantly greater than the normal prenatal kidneys ($p < 0.01$). In the sections of postnatal dysplastic kidneys from infants and children (n = 4) a pyknotic index of 27.4 (24.0 - 38.8) was calculated. This was significantly lower than the prenatal dysplastic group ($p < 0.01$), but significantly higher than the normal postnatal kidney group ($p < 0.01$). The pyknotic percentage in dysplastic kidneys were prenatal 0.78 (0.40 - 1.56) and postnatal 0.24 (0.21 - 0.34). These results showed even greater differences between the normal and dysplastic kidneys since there were fewer cells in the cystic areas.

Polycystic kidneys

The pyknotic index of the samples of polycystic kidneys examined from the nephrogenic period (n = 4) was 55.5 (42.6 - 75.7). This was greater but not significantly different from the high levels of apoptosis seen in normal development. The value was still not significant when the pyknotic percentage was calculated (0.41 (0.31 - 0.55)) which probably reflects the low number of polycystic samples (Table 7). The postnatal polycystic patient group (n = 4) had a pyknotic index of 66.5 (46.5 - 143.1) and percentage of 0.55 (0.38 - 1.18), significantly higher than the normal postnatal group ($p < 0.02$).

The pyknotic index was higher in the two polycystic samples with elevated creatinine but did not appear to correlate with the plasma creatinine in the other specimens. Within these small groups there was no correlation between the gestational or chronological age of the specimens and pyknotic index.

Prenatal kidneys			Postnatal kidneys			
Age (weeks)	P. Index	P. %	Age (mths)	P. Index	P. %	Cr.
Normal kidneys						
17	46.9	0.21	5	2.7	0.01	60
19	15.3	0.07	8	15.0	0.09	65
20	43.0	0.20	28	6.0	0.04	35
20	26.6	0.12	30	3.5	0.02	48
21	12.9	0.06	38	10.4	0.06	34
22	70.8	0.32	72	12.8	0.08	38
Dysplastic kidneys						
17	61.8	0.47	8	30.9	0.27	50
19	97.1	0.74	15	24.0	0.21	33
20	109.2	0.83	16	38.8	0.34	32
22	110.0	0.83	60	23.6	0.21	38
24	205.0	1.56				
34	52.8	0.40				
Polycystic kidneys						
20	42.6	0.31	10	78.1	0.65	98
34	51.8	0.38	11*	55.0	0.45	14
35	75.7	0.55	48	143.1	1.18	322
35	59.3	0.44	72	46.5	0.38	50

Table 7. Quantification of apoptosis. This table shows the gestational age in weeks or postnatal age in months (mths), pyknotic index (P. Index) and percentage of pyknotic cells (P. %) for all samples in which the extent of apoptosis was assessed, plus the creatinine (Cr.), in $\mu M / l$ in postnatal samples. * Indicates the postnatal sample which appeared histologically to be ADPKD, although both parents had normal renal ultrasound scans in their early twenties.

Location of proliferation

Proliferation was assessed by immunohistochemical staining for the proliferating cell nuclear antigen (PCNA) which is strongly expressed in the nucleus in S phase (Kurki *et al.*, 1986). Unfortunately, I was unable to generate a quantitative proliferative index comparable with the pyknotic index since a spectrum of staining was obtained in the normal and dysplastic kidneys: ranging from densely staining nuclei to more diffuse, less intense staining throughout the cell. This finding was consistent with reports of lower levels of nuclear PCNA protein and subcellular distribution in the cytoplasm at other stages of the cell cycle. It was still possible, however to use PCNA staining to follow, and semiquantitate, the general patterns of proliferation.

Proliferation was further assessed by staining for Ki-67, a different marker of proliferation. I found that this antibody also generated a spectrum of staining intensity and localisation but it was also inconsistent, both between specimens and different sections of the same specimen. These results have not therefore been included in this thesis.

Normal kidneys

In the samples of normal prenatal kidneys, nuclei with PCNA immunoreactivity were scarce within the undifferentiated mesenchyme but the protein was highly expressed during the mesenchymal to epithelial transition and also in the ampullary tips of the branches of the ureteric bud (Fig. 28A and B). It was then rapidly downregulated in the deeper more mature areas. In postnatal normal kidneys PCNA positive cells were scarce (< 1% of total nuclei) although they were detected in all nephron segments (Fig. 28C and D).

Dysplastic kidneys

Similar results were seen for PCNA staining in both pre- and postnatal samples. The commonest site for PCNA expression was dysplastic epithelia although the extent of staining was highly variable. In some samples, virtually all of the epithelial nuclei in dysplastic tubules were positive for PCNA, whereas in others only 20 – 30% were positive (Fig. 28E). A similar range was seen in cystic epithelia (Fig. 28F). Rare nuclei were also positive for PCNA in the undifferentiated tissue around dysplastic tubules (Fig. 28E).

Summary of apoptosis and proliferation

Apoptosis was detected by propidium iodide staining or *in situ* end labeling in at least one histological section of all of the samples examined. It was rare in normal mature kidneys, but relatively common in normal prenatal kidneys, especially in early nephron precursors and the medulla. Apoptosis was more frequent in dysplastic kidneys than normal kidneys of a comparable age. Similarly, a high degree of renal cell death was seen in polycystic kidneys. The commonest site of apoptosis in dysplastic kidneys was in the loose poorly differentiated tissue, whilst it was rare in dysplastic epithelia. By contrast, apoptosis was found in cyst epithelia, between the cysts and even in the tissues around undilated tubules in polycystic kidneys.

Proliferation was detected at high levels in the actively branching tips of the ureteric bud, mesenchymal condensates and early nephron precursors. It was downregulated in the mature kidney. In dysplastic kidneys, a high level of proliferation was detected in the epithelia of both small undilated tubules and cysts. Proliferation, in contrast, was rare in cells around dysplastic epithelia. These results are summarised in Table 8.

	Apoptosis	Proliferation
Normal kidneys		
Undifferentiated mesenchyme	rare +	rare +
Mesenchymal condensates and vesicles	-	++
S-shaped bodies	+	++
Glomerular podocytes	-	rare +
Tips of ureteric bud (ampullae)	-	++
Immature collecting ducts	++	+
Mature collecting ducts	-	rare +
Dysplastic kidneys (pre and postnatal)		
Dysplastic tubules	rare +	++
Cyst epithelium	rare +	++
'Fibromuscular collarettes'	+	rare +
Loose cells	++	rare +
Polycystic kidneys (pre and postnatal)		
Cyst epithelium	++	na
Cells adjacent to cysts	+	na
Undilated tubules	+	na
Cells around tubules	+	na

Table 8. Apoptosis and proliferation. This table describes the extent of apoptosis and proliferation in various sites in normal, dysplastic and polycystic kidneys. '–' Indicates not detected, 'rare +' indicates that less than 10% of cells were affected and '+' to '++' indicates increasing levels of apoptotic or proliferating cells. Proliferation was not assessed in polycystic samples (na).
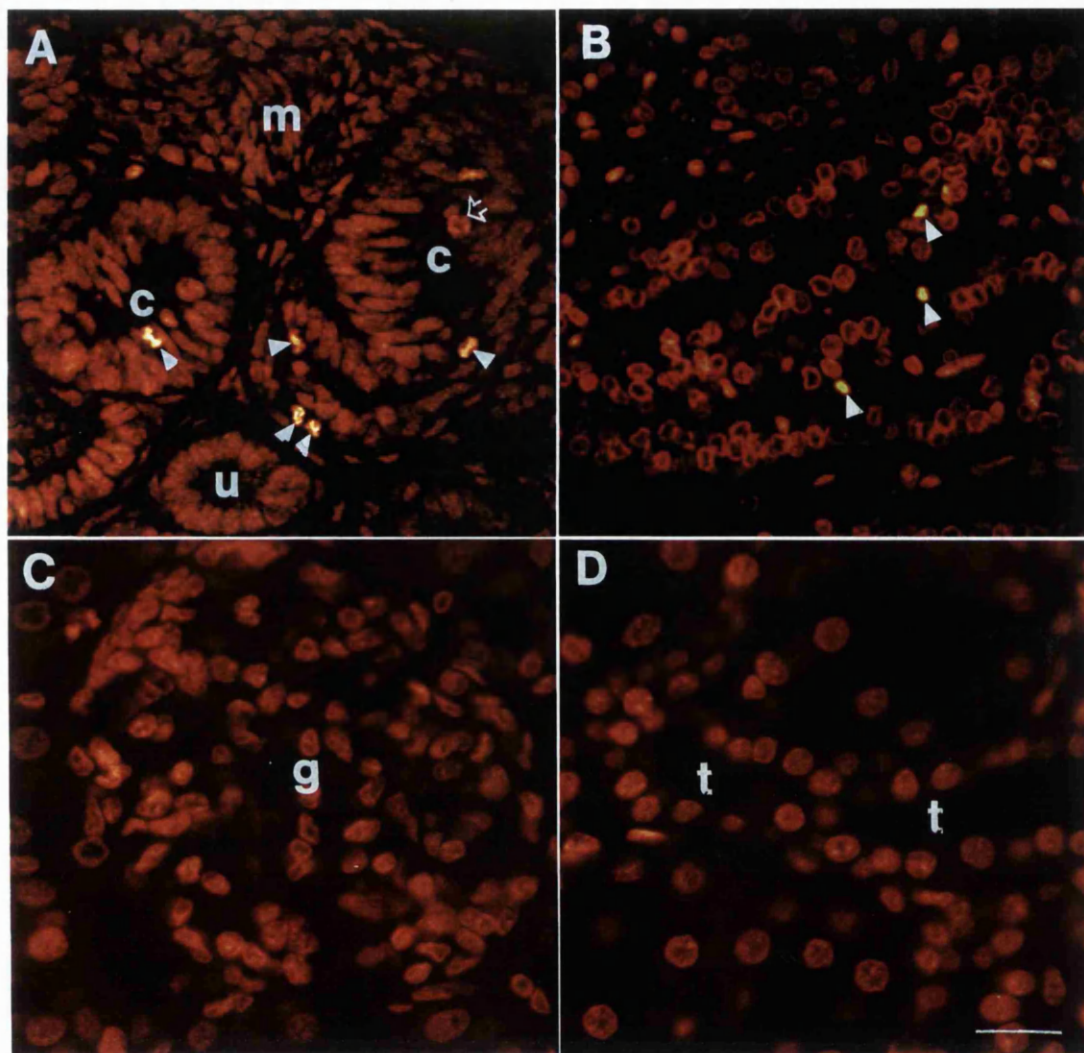
Figure 20. Location of apoptosis in propidium iodide stained sections of normal developing and mature kidneys. A) and B) are from a fetus of 20 weeks gestation and C) and D) are from a 2 year old child. A) Nephrogenic zone with ureteric bud (u), comma shapes (c) and condensed mesenchyme (m). Apoptotic nuclei are seen in comma shaped bodies (arrowheads) and a mitotic cell is also shown (open arrow). B) Medulla shows apoptosis in developing tubules (arrowheads). C) and D) Mature glomerulus (g) and proximal tubule (t) with no apoptotic cells visualised, although the nuclei in the glomerulus appear generally brighter. Bar corresponds to 30 μm in all.
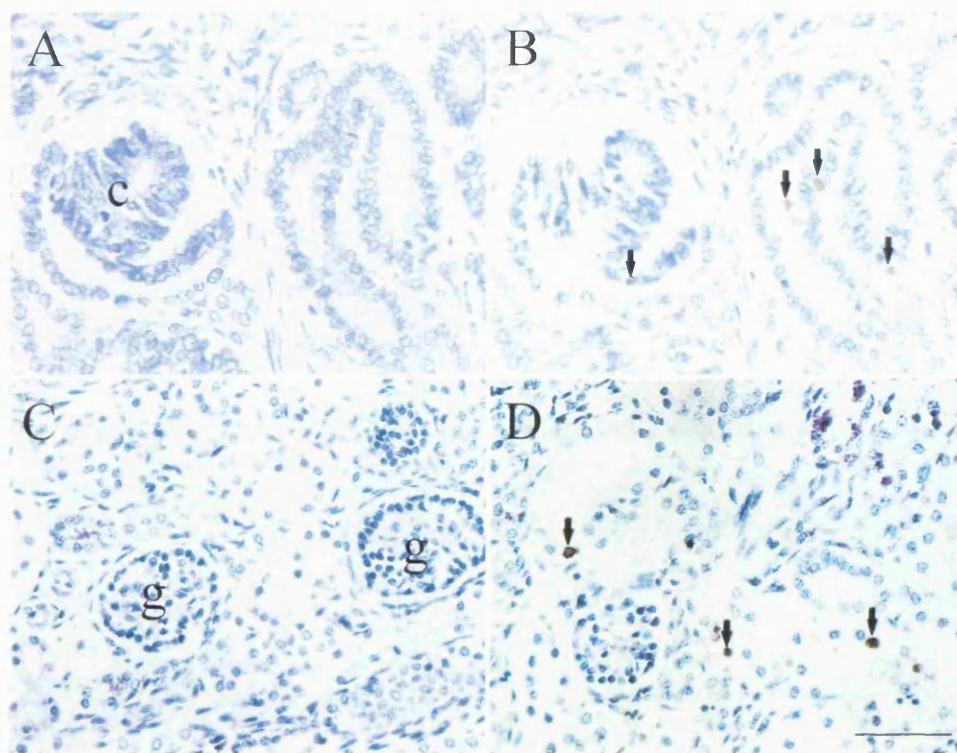
Figure 21. *In situ* **end-labeling of apoptotic cells in normal developing and mature kidneys.** Sections A) and B) are from a mid gestation fetus, and C) and D) are from a 2 year old child. A) and C) are control sections in which the terminal deoxytransferase enzyme was omitted. Note that labeled nuclei, which appear brown, are absent. B) and D) are adjoining sections which have been subjected to the complete end-labeling procedure using digoxigenin UTP as described in the *Methods*. All sections counterstained with methyl green after exposure to anti - digoxigenin peroxidase conjugate, detected by diamino-benzidine. A) and B) Nephrogenic zone containing comma shapes (c) and nephron precursors. Several apoptotic nuclei (arrows) are seen in the developing nephrons. C) and D) Mature cortex containing glomeruli (g) and tubules. Several apoptotic nuclei are seen in the tubular epithelial cells in this section, although this is unusual in mature kidneys. Bar corresponds to 30 μm in A) and B), and 50 μm in C) and D).

171
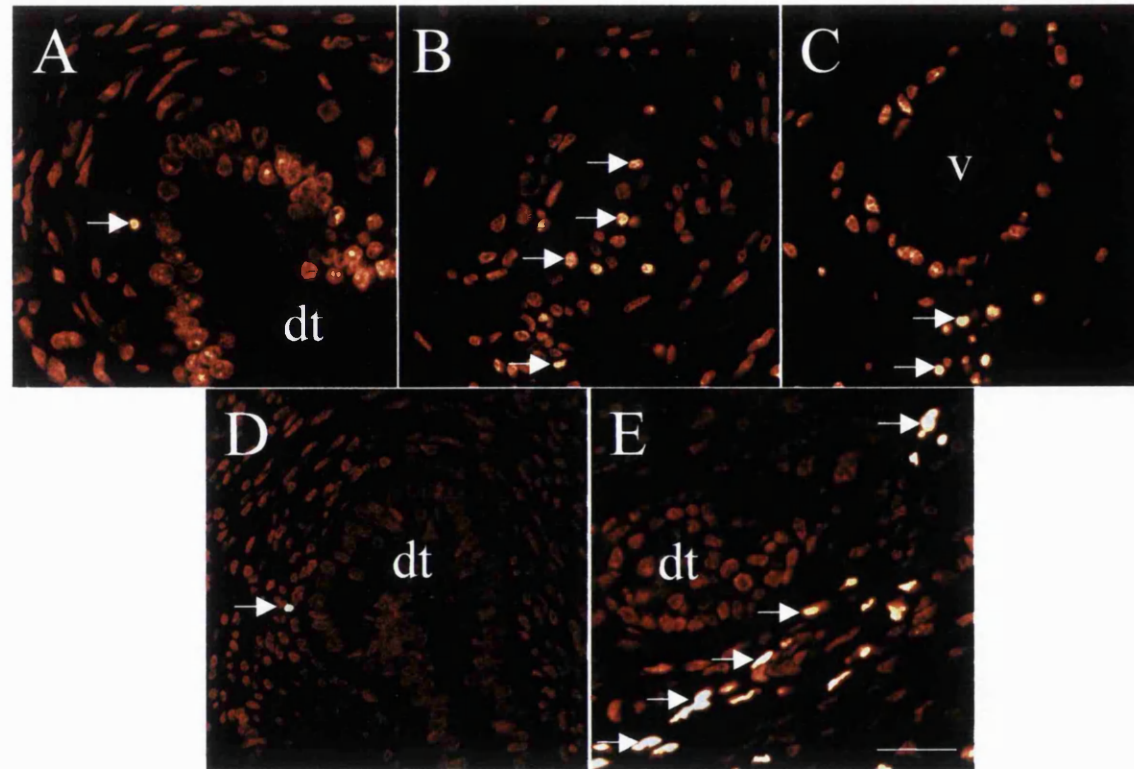
Figure 22. Apoptosis in dysplastic kidneys (1). Confocal laser scanning photomicrographs of postnatal dysplastic kidneys. A) to C) are stained with propidium iodide and D) to E) are *in situ* end-labeled sections using an anti digoxigenin antibody conjugated to FITC. Apoptotic cells are arrowed. A) and D) show a single apoptotic cell in the fibromuscular collarette around a dysplastic tubule (d). B), C) and E) show numerous apoptotic nuclei in the undifferentiated cells between cysts and around a vessel (v). Bar corresponds to 50 μm in D) and 30 μm in all other sections.
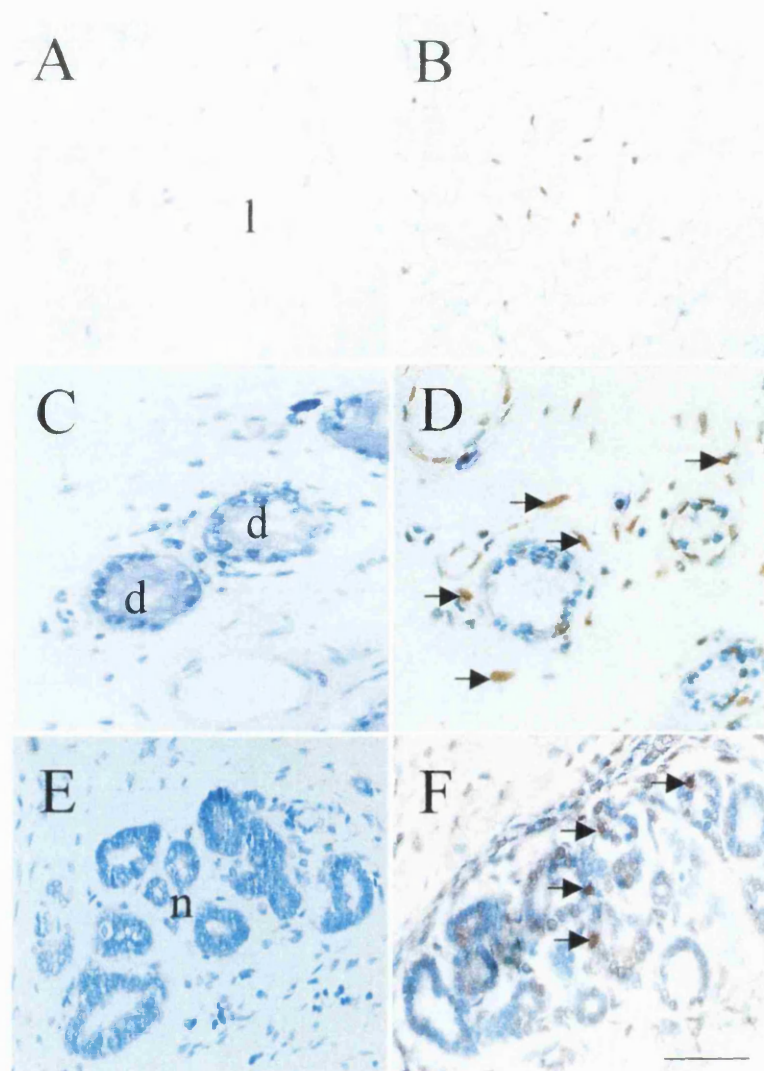
Figure 23. Apoptosis in dysplastic kidneys (2). Light photomicrographs of sections from postnatal dysplastic kidneys. A), C) and E) are control sections in which the terminal deoxytransferase enzyme was omitted, whilst B), D) and F) are similar sections which have been subjected to the complete end-labeling procedure. Positive nuclei appear brown. All sections are counterstained with methyl green. A) and B) show loose undifferentiated cells (l) which contain a large number of apoptotic nuclei. C) and D) show dysplastic tubules (d) with prominent apoptosis (arrows) in the surrounding cells. E) and F) show nests of dysplastic tubules (n) with rare apoptotic cells (arrows) in the tubule epithelia. Bar corresponds to 100 μm in A) and B), and 50 μm in the other sections.
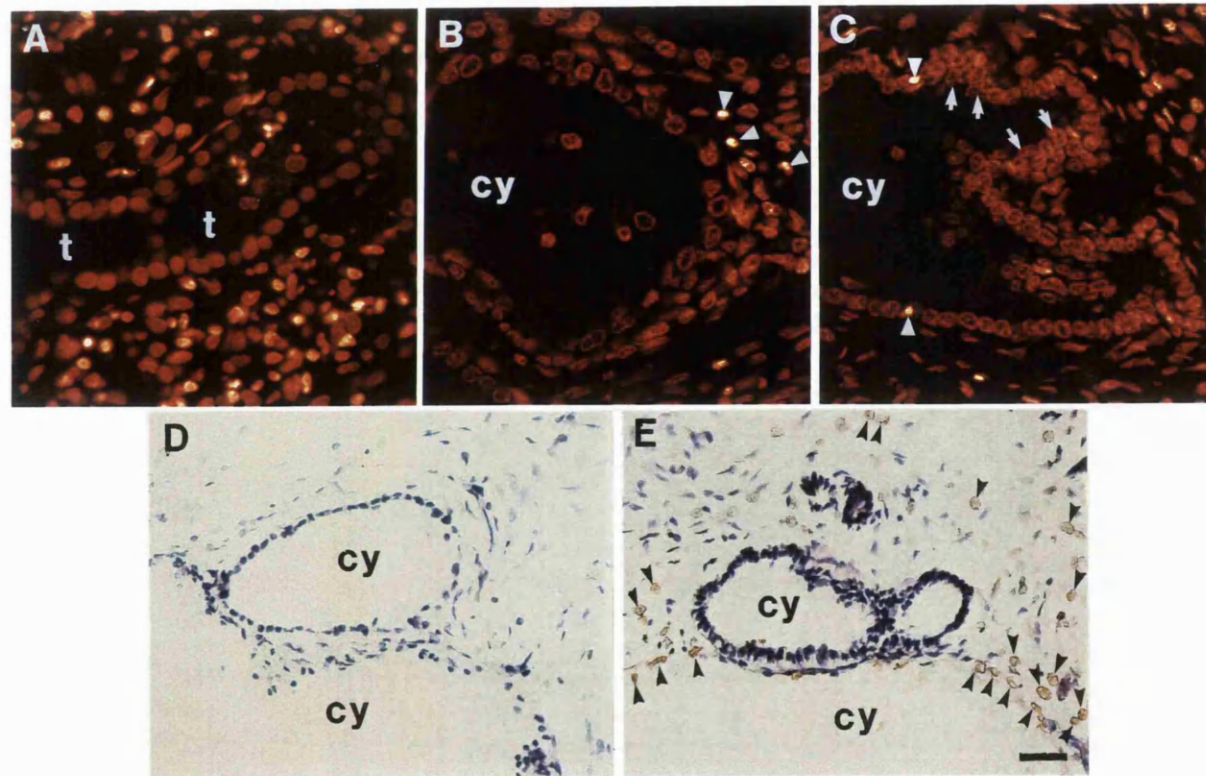
Figure 24. Apoptosis in polycystic kidney disease. A) to C) are propidium iodide labeled sections. D) and E) are control and *in situ* end-labeled sections, respectively, counterstained with methyl green. B) and C) are postnatal samples and C) is from an infant with ADPKD. The remaining sections are from a 34 week gestation fetus with ARPKD. A) and B) show apoptotic nuclei in the interstitial tissues around an undilated tubule (t) and a cyst (cy) respectively. Numerous apoptotic nuclei are shown in A) and are indicated by arrowheads in other panels. C) Apoptotic nuclei in the cyst epithelium close to a multilayered region suggestive of hyperproliferation (arrows). D) and E) Apoptotic nuclei are seen in the cyst epithelium and surrounding interstitial cells; the control section is negative. Bar corresponds to 30 μm in A) to C), and 50 μm in D) and E).
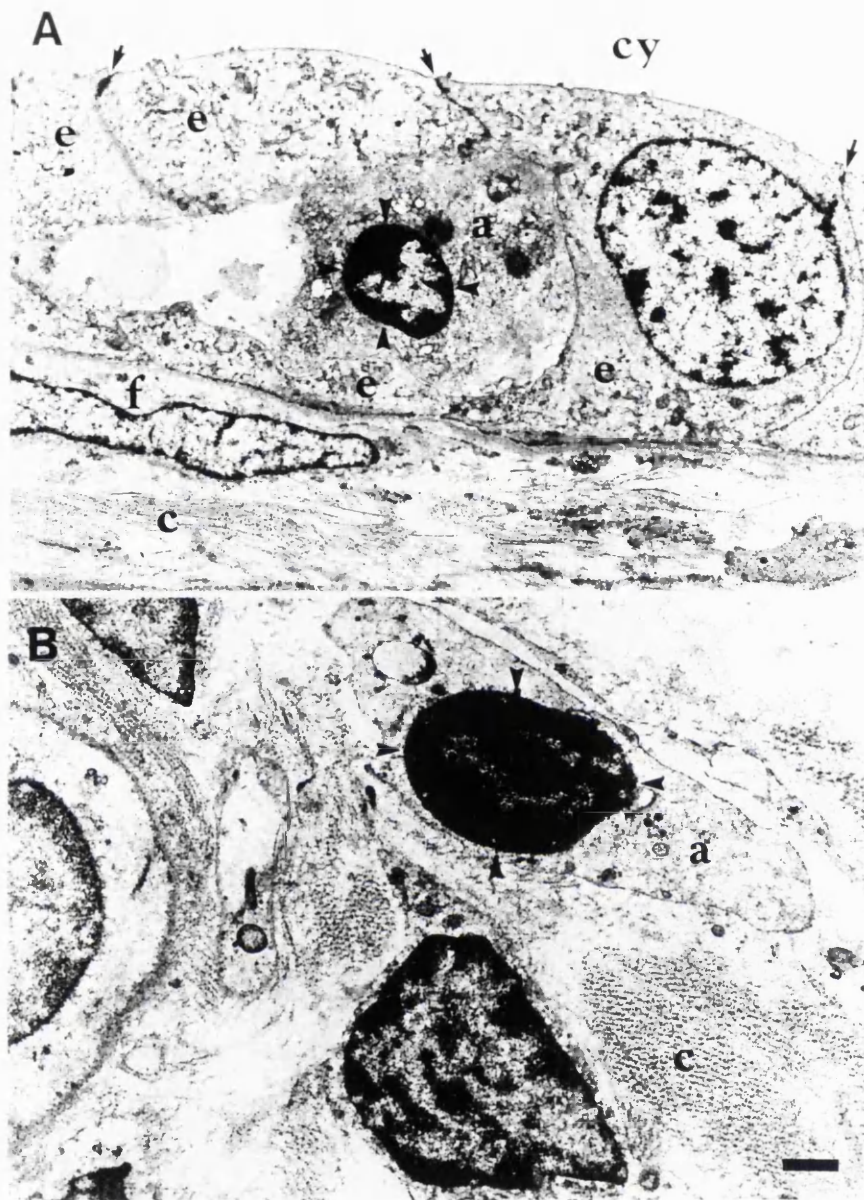
Figure 25. Electron microscopy of dysplastic kidneys. Both sections are from postnatal dysplastic kidneys. A) cyst (cy) showing an apoptotic cell (a) with a condensed pyknotic nucleus (arrowheads) surrounded by normal epithelial cells (e) which are separated by tight junctions (arrows). The apoptotic cell appears to be shrinking. Note also the fibroblast cell (f) and collagen fibres (c) below the epithelial layer. B) poorly differentiated mesenchyme showing both normal cells and one cell undergoing apoptosis with nuclear condensation. Bars are 1 μm.
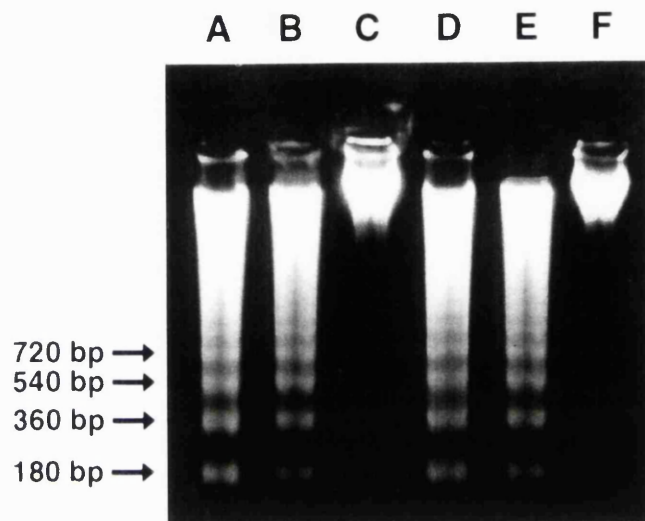
Figure 26. DNA laddering in dysplastic kidneys. DNA was extracted from fragments of three postnatal dysplastic kidneys and electrophoresed through a 1.5 % agarose gel as described in the *Methods*. Lanes A) and B) show DNA which has been digested by endonucleases during apoptosis to form a ladder consisting of several bands containing multiples of 180 base pairs (i.e. 180, 360, 540, 720 as indicated). DNA from the dysplastic kidney in lane C) does not have a detectable ladder by this technique. Lanes D) to F) are the same samples as A) to C) treated with RNAse A to rule out contaminating RNA.
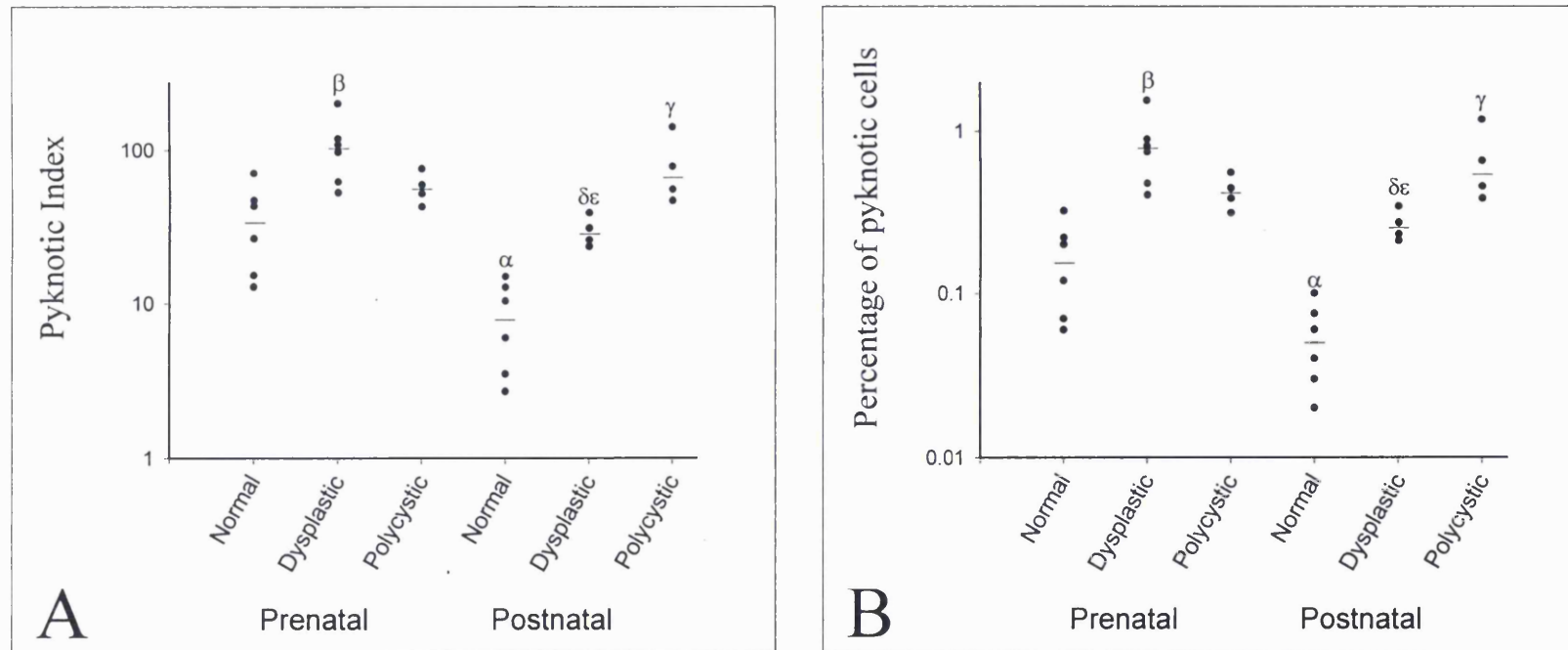
Figure 27. Quantification of apoptosis. Apoptosis was quantified in tissue sections using propidium iodide as described in the *Methods* section. A) shows the pyknotic index for individual patients which corresponds to the mean number of apoptotic cells per 10 microscope fields, whilst B) shows the percentage of pyknotic cells. The prenatal groups comprise normal, dysplastic and polycystic kidneys harvested before 36 weeks of gestation and the postnatal groups comprise normal, dysplastic and polycystic removed in infancy or childhood. The bar (-) indicates median of each group. Significant differences are: α – normal prenatal versus normal postnatal ($p < 0.05$), β – dysplastic prenatal versus normal prenatal ($p < 0.01$), γ – postnatal polycystic versus normal postnatal ($p < 0.02$), δ – dysplastic postnatal versus normal postnatal ($p < 0.01$) and ε – dysplastic prenatal versus dysplastic postnatal ($p < 0.01$).
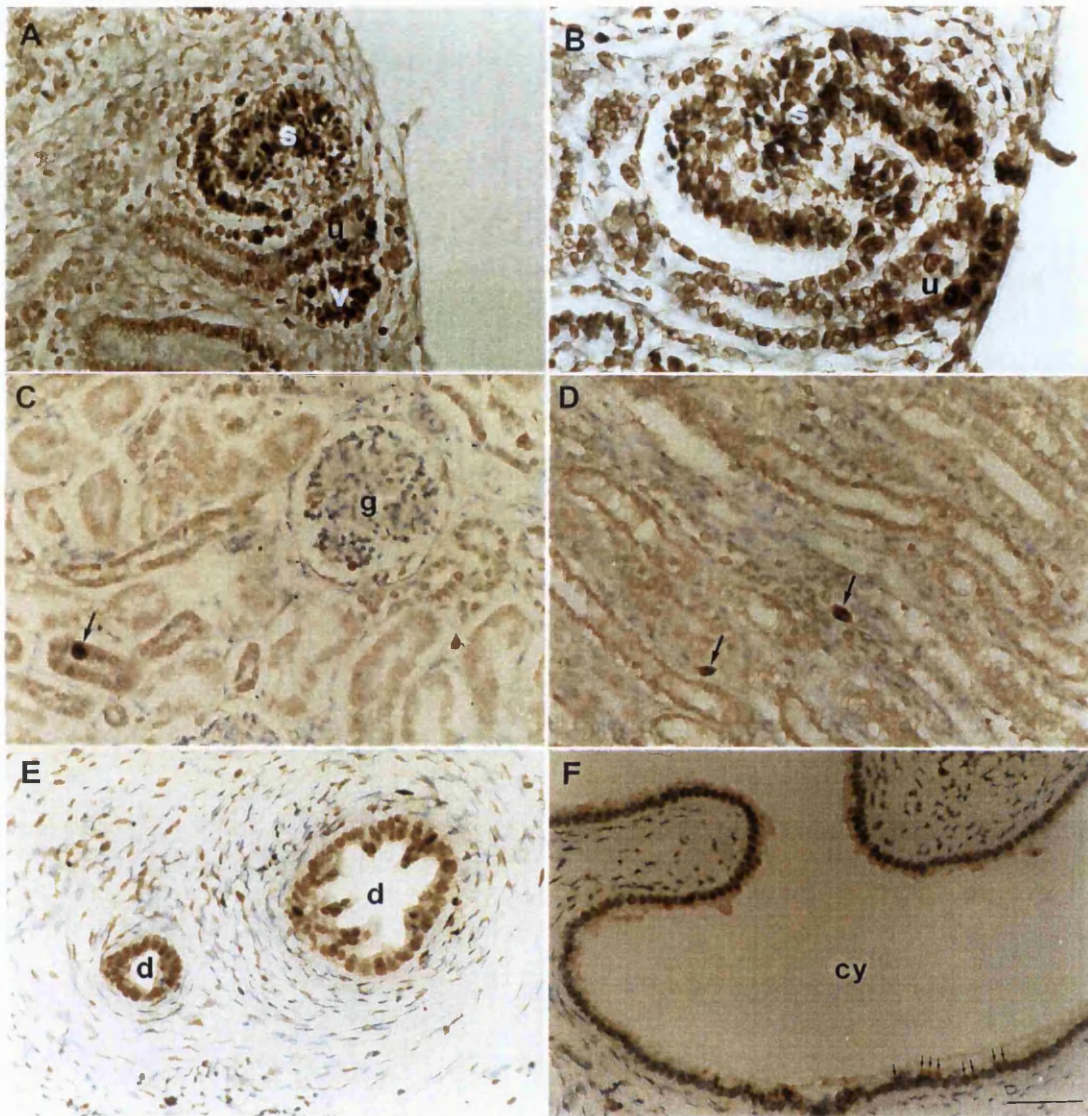
Figure 28. Proliferation in normal and dysplastic kidneys.

Light photomicrographs of PCNA immunohistochemistry counterstained with methyl green. A) and B) show active proliferation at the tips of the ureteric bud (u) and in early nephron precursors such as the renal vesicles (v) and S-shaped bodies (s) in the nephrogenic cortex of a mid gestation fetus. In contrast, very little proliferation is detected in either the uncondensed mesenchyme or deeper in the cortex. C) shows the cortex and D) the medulla of a mature postnatal kidney from a child aged six months. Proliferating cells (arrows) are not seen in glomeruli (g) and are rare in tubules and collecting ducts. E) shows dysplastic tubules (d) and F) a large cyst (cy) from a postnatal dysplastic kidney. Proliferation is common in these dysplastic epithelia (arrows in F), but rare in surrounding cells. Bar corresponds to 6 μm in (B) and 15 μm in the other sections.

Chapter 9. Results

PAX-2, WT-1, BCL-2 and galectin-3 distribution in normal and abnormal kidneys

PAX-2

Immunohistochemistry for the PAX-2 protein was performed using a rabbit polyclonal antibody which recognises major epitopes between amino acids 270 - 338 of the PAX-2 protein (Phelps and Dressler, 1996) as described in the *Materials* section of this thesis. The antibody specificity was tested by performing a Western blot on normal and dysplastic human tissues (Fig. 29) and one major isoform was detected of around 46 - 48 kD. This is consistent with the expected size of the human protein.

Normal kidneys

(Preterm n = 12; Postnatal n = 16)

PAX-2 was expressed in the developing human excretory system from the earliest stages examined. In the mesonephros, positive nuclear staining was detected in the mesonephric duct, distal tubules draining into it and the paramesonephric duct (Fig. 30A to D). Some proximal tubules also appeared positive but the site and intensity of staining were similar in negative control sections in which the primary antibody was omitted (not shown). This suggests that there was either inadequate quenching of endogenous peroxidase, or endogenous biotin within these tubules. The mesonephric glomeruli were negative.

In the early metanephros, nuclear PAX-2 protein was detected in the ureteric bud, which arises from the mesonephric duct, in the centre of the organ (Fig. 30E), and also in the peripheral bud tips (Fig. 30F). The majority of uninduced mesenchymal cells did not express PAX-2 (Fig. 30E) but the protein was markedly upregulated in the closely packed mesenchymal condensates adjacent to the bud tips. These cells are about to undergo mesenchyme to epithelial transition and pax-2 has previously been shown to be essential for this process during murine nephrogenesis (Rothenpieler and Dressler, 1993). A similar nuclear staining pattern was seen in later metanephric development in condensed mesenchyme and ureteric bud tip cells in the nephrogenic cortex throughout nephrogenesis (Figs. 31B and D and 32A). Occasional faint cytoplasmic staining was also detected in some sections (Figs. 32D, and 33A and B). This may be due to endogenous biotin within the tissues although the control sections were completely negative.

As the mesenchymal lineage differentiated, PAX-2 protein continued to be expressed in virtually all of the cells in the vesicles and comma-shaped bodies (Fig. 32A). At the next stage of nephron maturation, the S-shaped bodies, PAX-2 was detected in all elements apart from precursors of glomerular visceral epithelia (Fig. 32B). In the capillary loop stage of glomerulogenesis faint PAX-2 immunoreactivity was present in parietal epithelia and in adjoining proximal tubules (Fig. 32C and D). PAX-2 protein was not detected in mature glomeruli (Fig. 33A).

In the ureteric bud lineage, intense PAX-2 immunoreactivity was seen in branching ampullae, each of which was flanked by mesenchymal condensates (Figs. 31B and D, and 32A). Nuclei in fetal cortical and medullary collecting ducts showed weaker but consistent immunostaining (Fig. 32C, E and F).

Mature collecting duct cells generally did not have significant staining above control sections in which the anti-PAX-2 antibody had been omitted, although occasional (< 10%) nuclei had faint immunoreactivity (Fig. 33B).

Dysplastic kidneys

(Preterm n = 10; Postnatal n = 12)

The PAX-2 protein was strongly expressed in the epithelia of each dysplastic kidney examined (Fig. 33C and D). All nuclei of epithelia lining the dysplastic tubules stained intensely with the antiserum to PAX-2 and the flattened epithelial cells lining cysts were also positive (Fig. 33C and D). In contrast the poorly differentiated cells surrounding the tubules did not express PAX-2 (Fig. 33C and D). Strikingly, the same pattern of PAX-2 expression was seen in both prenatal and postnatal dysplastic kidneys which suggests that PAX-2 expression is not downregulated with time in these organs, in contrast to normal development. Metaplastic cartilage was negative for PAX-2.
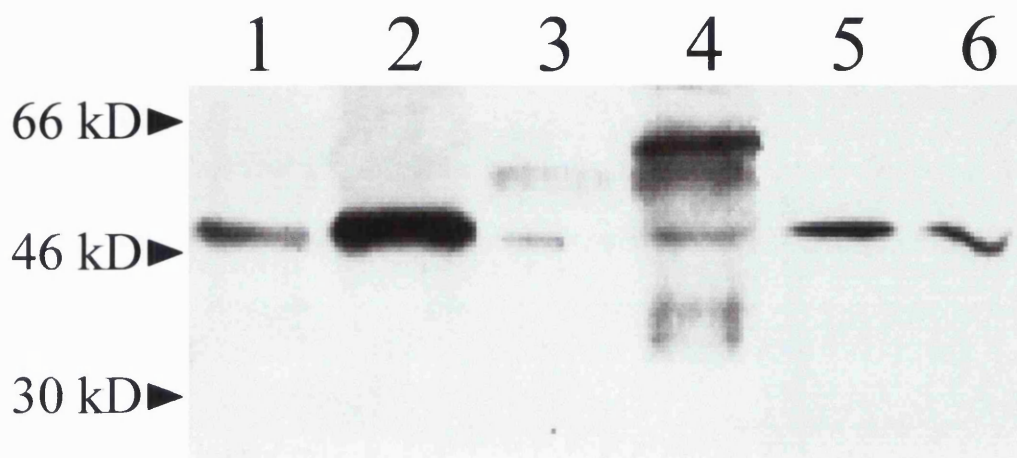
Figure 29. Western blot of PAX-2. All lanes were probed with the polyclonal anti-PAX-2 antibody used for immunohistochemistry (Figs. 30 to 33). Negative controls, in which the antibody was omitted, are completely clear. Sizes correspond to bands in rainbow marker lanes. A band of around 46 - 48 kD, corresponding to the expected size of the PAX-2 protein, is seen in all of the lanes. Lanes 1) and 2) contain extracts from postnatal dysplastic kidneys. Lanes 3) and 4) are from a Wilms' tumour: lane 3) is from a grossly normal part of the tissue and lane 4) from a fragment of tumour. Note that there is a much weaker PAX-2 signal in the normal sample and that there also appears to be a larger band in the tumour sample. Lanes 5) and 6) are positive control samples containing protein extracted from fetal kidneys from a mid gestation sheep fetus and an embryonic day 13 mouse respectively.
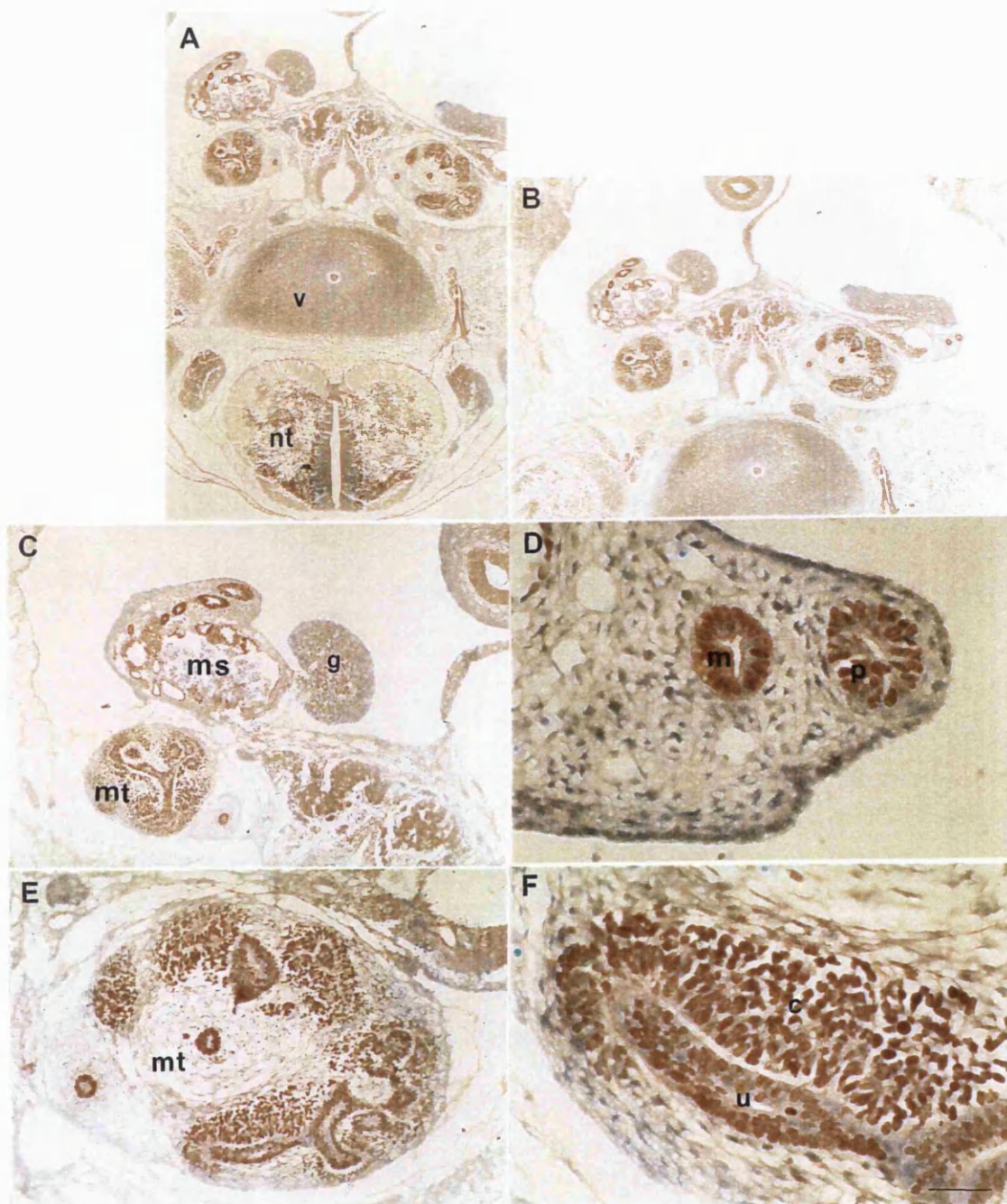
Figure 30. PAX-2 in early kidney development. Light photomicrographs of PAX-2 immunohistochemistry on sections of a 42 day gestation embryo counterstained with methyl green. A) and B) show the mesonephros and metanephros anterior to the vertebral body (v) and the neural tube (nt), which is PAX-2 positive. C) and D) show the mesonephros (ms) and metanephros (mt) with nuclear PAX-2 staining in cells in the mesonephric (m) and paramesonephric (p) ducts, but not in the gonad (g). E) and F) show the metanephros (mt); the ureteric bud (u) has branched several times. Strongly positive nuclear PAX-2 staining is detected in the ureteric bud and condensed mesenchyme (c). Uninduced mesenchyme is negative. Bar is 500 μm in A) and B), 200 μm in C), 80 μm in E) and 20 μm in D) and F).

183
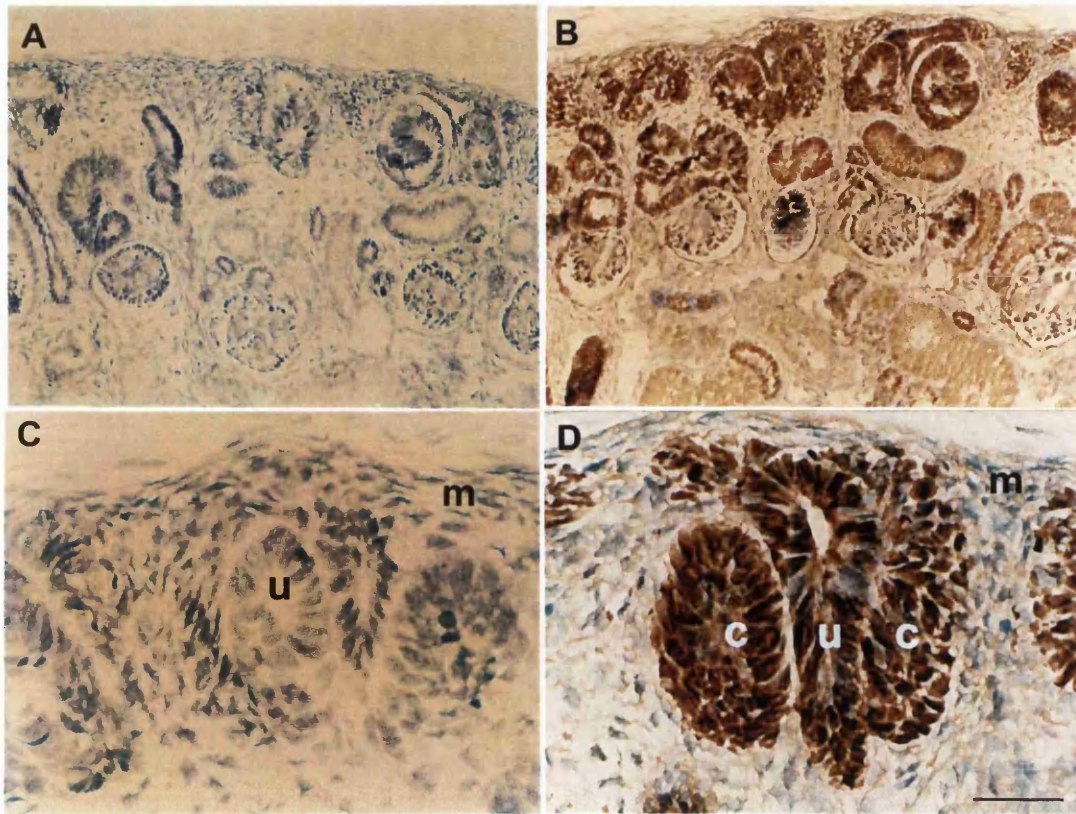
Figure 31. PAX-2 in the nephrogenic cortex.

Light photomicrographs of PAX-2 immunohistochemistry of a normal 10 week gestation human kidney counterstained with methyl green. A) and C) are the control sections in which the primary antibody was omitted, and these are completely negative. B) shows PAX-2 immunoreactivity in the nephrogenic zone with decreasing levels towards the maturing centre of the kidney. D) is a higher power view which shows that the PAX-2 protein is strongly expressed in the nuclei of the tips of the ureteric bud (u) and mesenchymal condensates (c), but it is not detected in uninduced mesenchyme (m). Bar corresponds to 80 μm in A) and B), and 20 μm in C) and D).
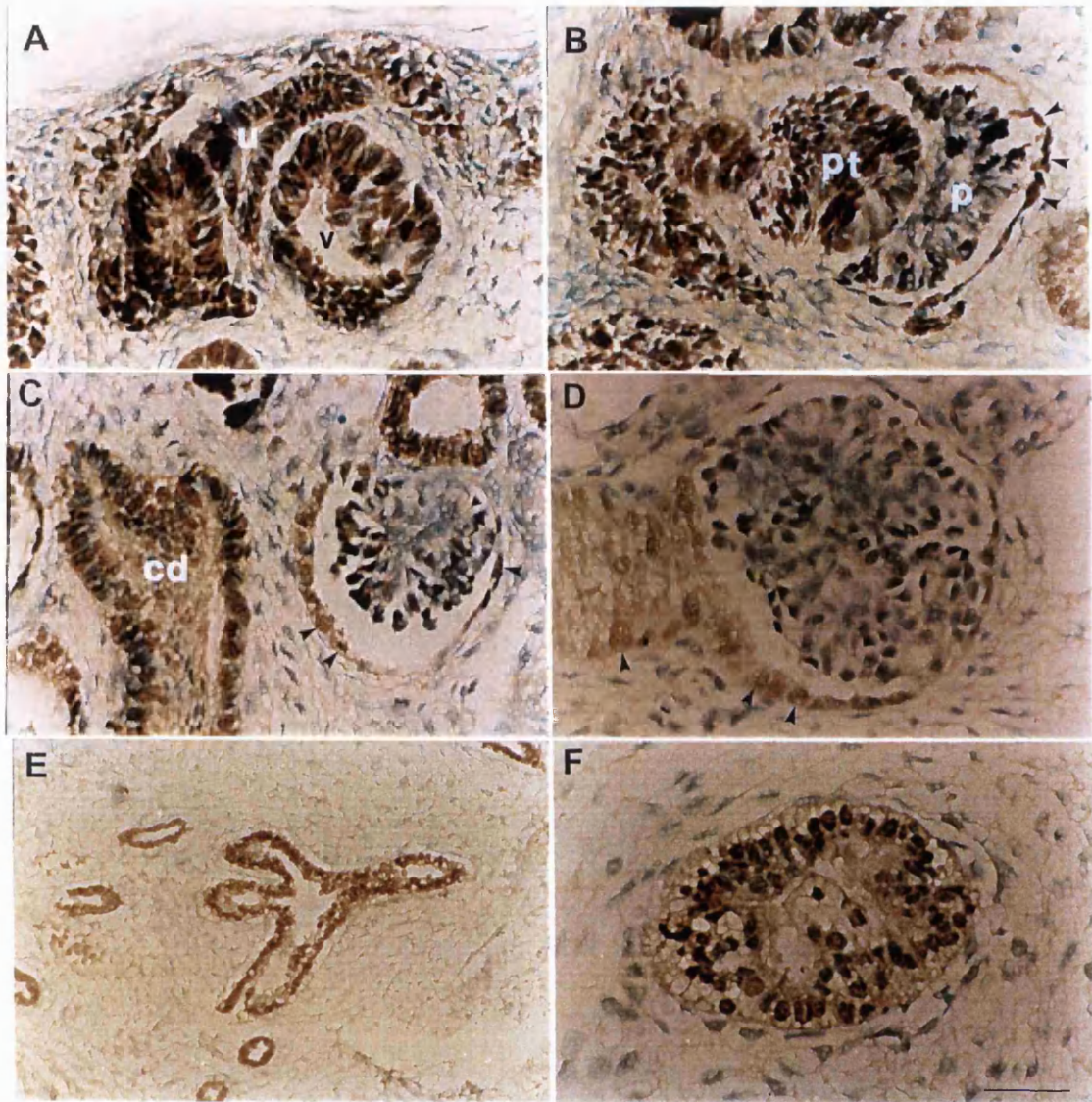
Figure 32. PAX-2 in the developing kidney. Light photomicrographs of PAX-2 immunohistochemistry of a normal 10 week gestation kidney counterstained with methyl green. Control sections are completely negative. A) Intense PAX-2 expression in a ureteric bud branch tip (u) and a vesicle (v) contrasts with negative staining of the undifferentiated mesenchyme. B) The developing proximal tubule (pt) and parietal glomerular epithelia are positive for PAX-2 but the protein is downregulated in maturing podocytes (p). C) On the left a maturing cortical collecting duct (cd) has less intense staining: on the right, a fetal glomerulus shows only faint PAX-2 staining in Bowman's capsule (arrows). D) A fetal glomerulus has faint PAX-2 staining in the epithelial cells of Bowman's capsule and the proximal tubule (arrows). E) and F) Medullary collecting ducts are positive for PAX-2. Bar corresponds to 30 μm in E) and 10 μm in all other sections.
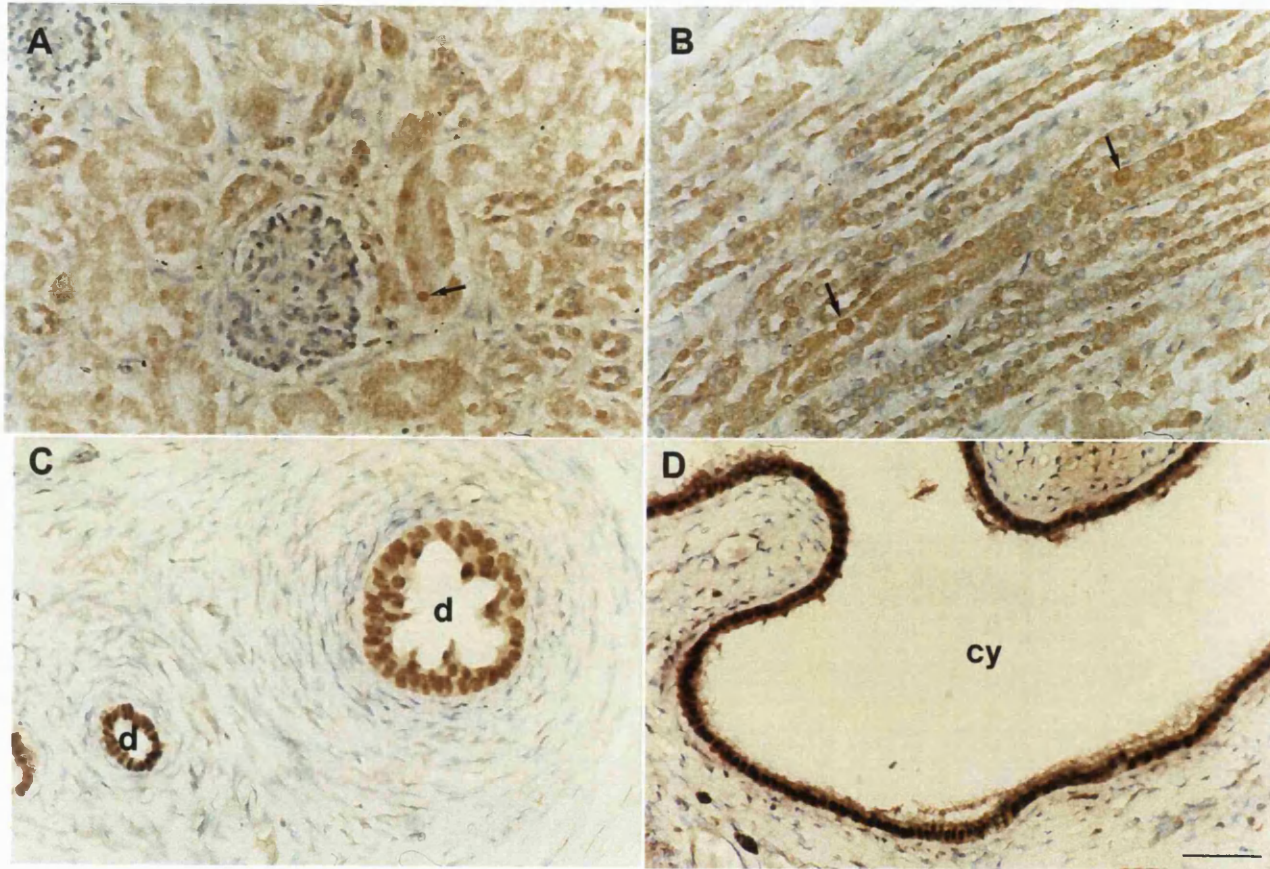
Figure 33. PAX-2 in normal adult kidneys and dysplastic kidneys. Light photomicrographs of PAX-2 immunohistochemistry counterstained with methyl green. A) and B) are sections from a normal kidney from a 6 month old child. PAX-2 is downregulated but rare nuclei are faintly positive (arrows) in tubules and collecting ducts. C) shows a dysplastic tubule (d) and D) a large cyst (cy) from a postnatal dysplastic kidney. The majority of the nuclei in the tubule express PAX-2 and the most intense immunostaining of any tissue examined is seen in the cyst epithelium. Surrounding undifferentiated cells are negative. Bar corresponds to 15 μm in all sections.

WT-1

Immunohistochemistry for WT-1 was performed using a commercially available antibody (Santa Cruz, C19) as described in the *Materials* section of this thesis. The specificity of this antibody was confirmed by Western blotting using normal and dysplastic tissues (Fig. 34). Two bands of approximately 46 – 48 kD were seen in most of the samples which was consistent with the predicted size and isoforms of this protein. Interestingly, a larger band was found in one of the samples from a dysplastic sample (Fig. 34 lane 3) which raises the possibility of abnormal glycosylation, differential splicing or a mutation.

Normal kidneys

(Preterm n = 12; Postnatal n = 16)

Faint WT-1 immunoreactivity was detected in the nuclei of mesenchymal condensates and vesicles in normal fetal kidneys (Figs. 35A and 38A). Very occasionally, positive cells were also detected in the loose mesenchyme, although the majority of mesenchymal cells were negative. The intensity of WT-1 staining increased in the proximal limbs of S-shaped bodies (Fig. 35A) with the highest levels in immature glomerular podocytes (Fig. 35A and B). This pattern persisted and glomerular podocytes were the only site of WT-1 expression in the mature kidney (data not shown). Nuclear WT-1 protein was not detected in the ureteric bud or its derivatives although weak immunoreactivity was sometimes observed in the cytoplasm of cells in the ureteric bud (Fig. 38A). The intensity of this staining was similar to control sections (not shown) and it may therefore reflect a failure to quench background levels of endogenous peroxidase or endogeous biotin within the tissues.

Dysplastic kidneys

(Preterm n = 10; Postnatal n = 12)

In dysplastic kidneys, WT-1 protein was detected in 10 - 80% of the cells in the fibromuscular collarettes and undifferentiated cells around malformed tubules (Figs. 35C and D, and 38C). The protein appeared to be localised in the nucleus and the intensity of staining was similar to that observed in the early stages of nephron formation but less than in glomerular podocytes (Fig. 35A and B). WT-1 immunoreactivity, above control levels, was not found in dysplastic epithelia.

BCL-2

Immunohistochemistry for BCL-2 was performed using a commercially available antibody (Dako, M887) as described in the *Materials* section of this thesis. The specificity of the antibody was determined by Western blotting (Fig. 36). A single band of around 30 kD was detected in all of the samples examined, which was not seen when the primary antibody was omitted.

Normal kidneys

(Preterm n = 12; Postnatal n = 16)

The BCL-2 protein, in common with PAX-2, was not expressed in uninduced renal mesenchyme but became upregulated as the mesenchyme condensed around ureteric bud tips (Fig. 37A to C). In contrast with PAX-2, however, it was rapidly down regulated in the comma and S-shaped bodies where it could only be detected in the epithelia of developing glomeruli. It was also detected in the descending loops of Henle (Fig. 37A). BCL-2 immunoreactivity was not seen in the ureteric bud or any of its derivatives at any stage of development (Fig. 37A to C). In the mature kidney, very little BCL-2 protein was detected although some cells in Bowman's capsule did have weak immunoreactivity (Fig. 37D). Positive immunostaining was never seen in the control sections.

Dysplastic kidneys

(Preterm n = 10; Postnatal n = 12)

BCL-2 protein was consistently detected in the epithelia of dysplastic kidneys. The majority of the cells in the dysplastic tubules (Figs. 37E and F, and 38D) and dysplastic cysts (Fig. 37F) were positive for BCL-2 immunoreactivity. This positivity was confined to the cytoplasm and cell membranes (Fig. 38D), although it was difficult to define the exact subcellular localisation on conventional light microscopy. BCL-2 expression was not downregulated postnatally in dysplastic tubules. Both the collarettes immediately surrounding the dysplastic tubules / cysts and the more distant poorly differentiated cells were negative for BCL-2 protein (Figs. 37E and F, and 38D). Metaplastic cartilage was negative for BCL-2. These results represent an ectopic expression pattern for BCL-2 since dysplastic tubules are reported to be derived from the ureteric bud (Potter, 1972), a lineage which does not normally express BCL-2.
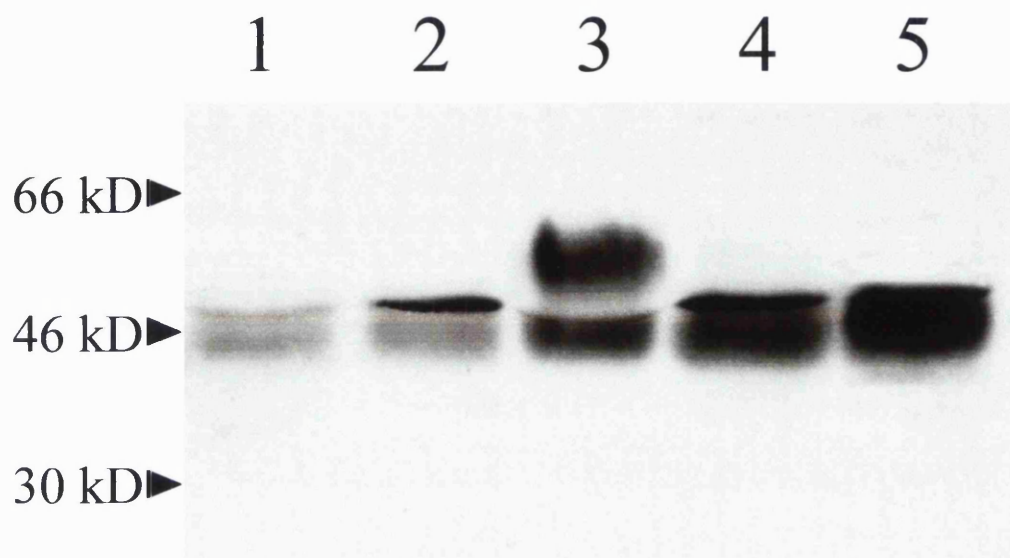
Figure 34. Western blot of WT-1. All lanes were probed with the rabbit polyclonal anti-WT-1 antibody used for immunohistochemistry (Figs. 35 and 38). Negative controls, in which the antibody was omitted, are completely clear. Sizes correspond to bands in rainbow marker lanes. Two bands of around 46 and 48 kD, are seen in the majority of the specimens which correspond to the expected size of the two most prevalent WT-1 isoforms. Lanes 1) to 3) contain extracts from postnatal dysplastic kidneys. An abnormal, larger band is seen in lane 3) which raises the possibility of either increased glycosylation, differential splicing or a mutation. Lanes 4) and 5) are from a Wilms' tumour: lane 4) is from a grossly normal part of the tissue and lane 5) from the tumour.
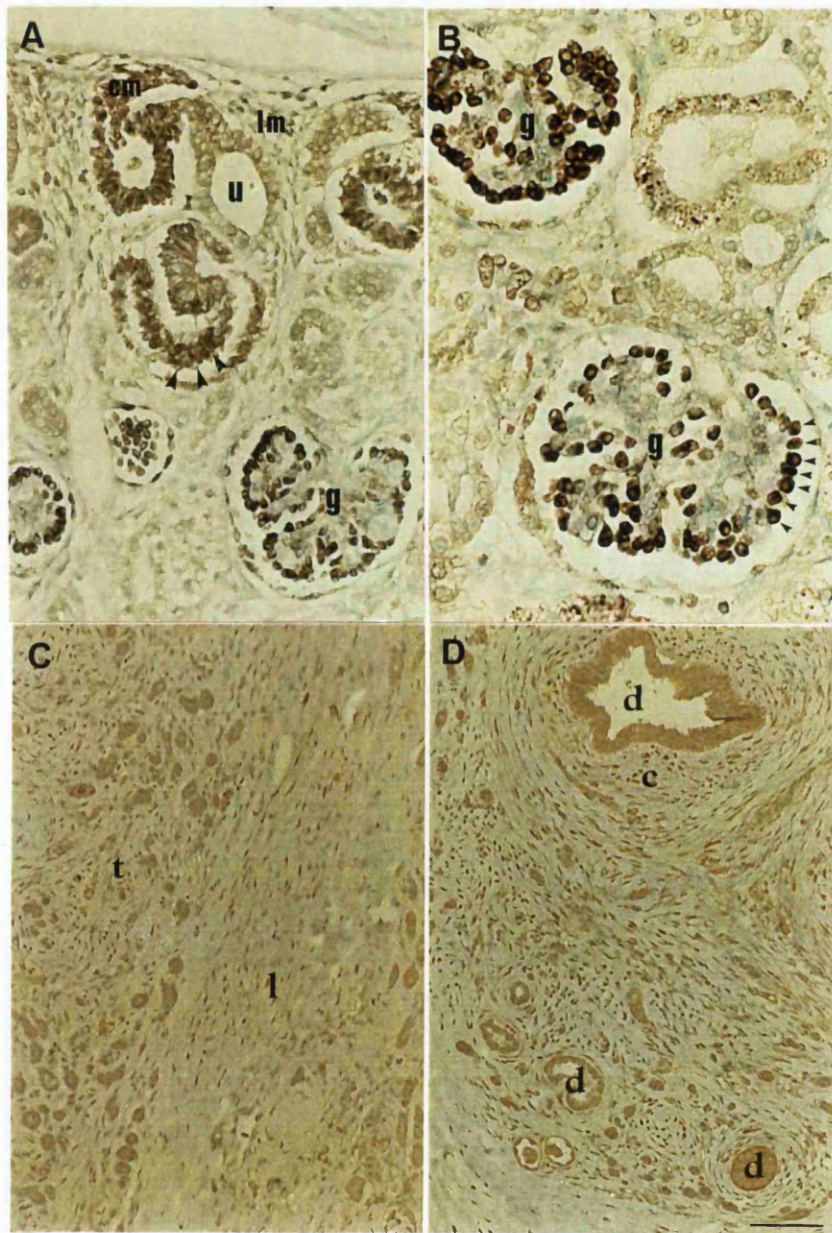
Figure 35. WT-1 in normal and dysplastic kidneys. Light photomicrographs of WT-1 immunohistochemistry counterstained with methyl green. A) and B) are sections of a normal fetal kidney whilst C) and D) are postnatal dysplastic kidneys. A) and B) illustrate the gradient of WT-1 immunoreactivity: cells in the condensates (cm) and vesicles are weakly positive for WT-1, expression increases in the proximal limb of the S-shaped body (arrowheads in A) and glomerular (g) podocytes have intense WT-1 staining (arrowheads in B). C) and D) Undilated dysplastic tubules (t) and mildly dilated dysplastic tubules and cysts (d) do not stain significantly with the WT-1 antibody, but WT-1 protein is detected in surrounding cells in the fibromuscular collarettes (c) and loosely arranged cells (l). Bar corresponds to 20 μm in A), 10 μm in B) and 50 μm in C) and D).

191
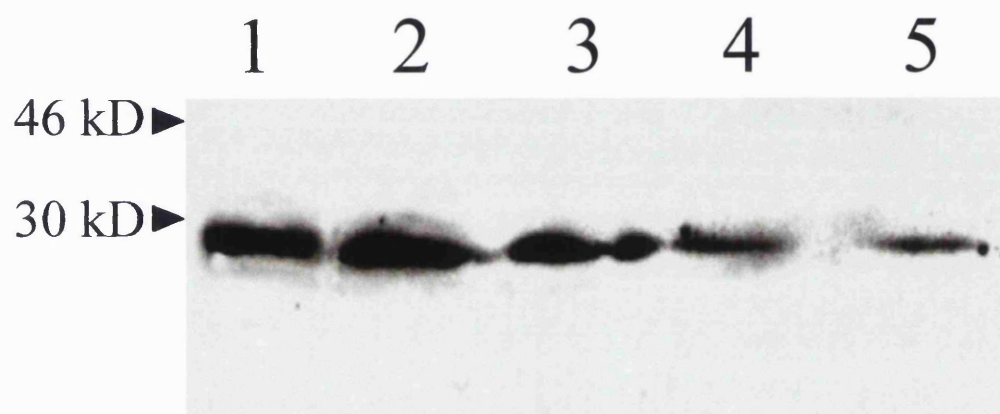
Figure 36. Western blot of BCL-2. All lanes were probed with the mouse monoclonal anti-BCL-2 antibody used for immunohistochemistry (Figs 37 and 38). Negative controls, in which the antibody was omitted, are completely clear. Sizes correspond to bands in rainbow marker lanes. A single band of 28 kD, corresponding to the expected size of the BCL-2 protein, is seen in all of the lanes. Lanes 1), 2) and 3) contain extracts from postnatal dysplastic kidneys. Lane 4) is from a fragment of grossly normal tissue adjacent to a Wilms' tumour and lane 5) is from the tumour. Levels of BCL-2 protein appear to be much higher in the dysplastic samples.
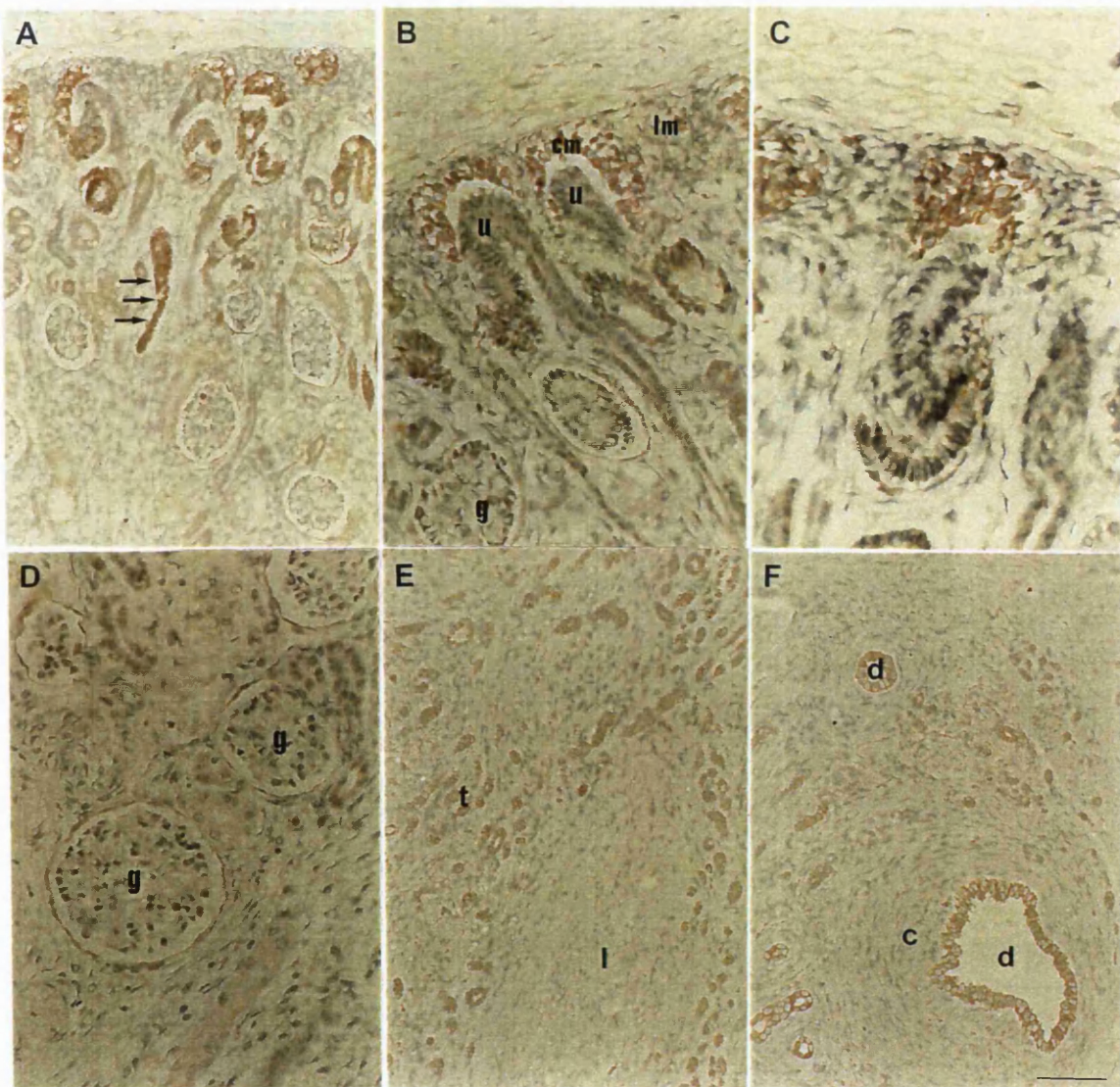
Figure 37. BCL-2 in normal and dysplastic kidneys. Light photomicrographs of BCL-2 immunohistochemistry counterstained with methyl green. A) to D) are from a normal 10 week gestation human kidney, whilst E) and F) are postnatal dysplastic kidney s. Control sections are completely negative. A) and B) show BCL-2 in the condensed mesenchyme (cm), but not in the loose mesenchyme (lm) or the ureteric bud (u). Note that the developing loops of Henle (arrows) are also positive. C) is a higher power view of the outer cortex showing that BCL-2 is downregulated in the S-shaped body of the developing nephron. D) shows faint BCL-2 staining in Bowman's capsule of the developing glomeruli. E) and F) show that dysplastic epithelia stain intensely for BCL-2, both in areas containing numerous small tubules (t) and in mildly dilated tubules / cysts (d). The fibromuscular collarettes (c) and loosely arranged cells (l) are negative. Bar corresponds to 50 μm in A), E) and F), 20 μm in B) and D), and 10 μm in C).

193
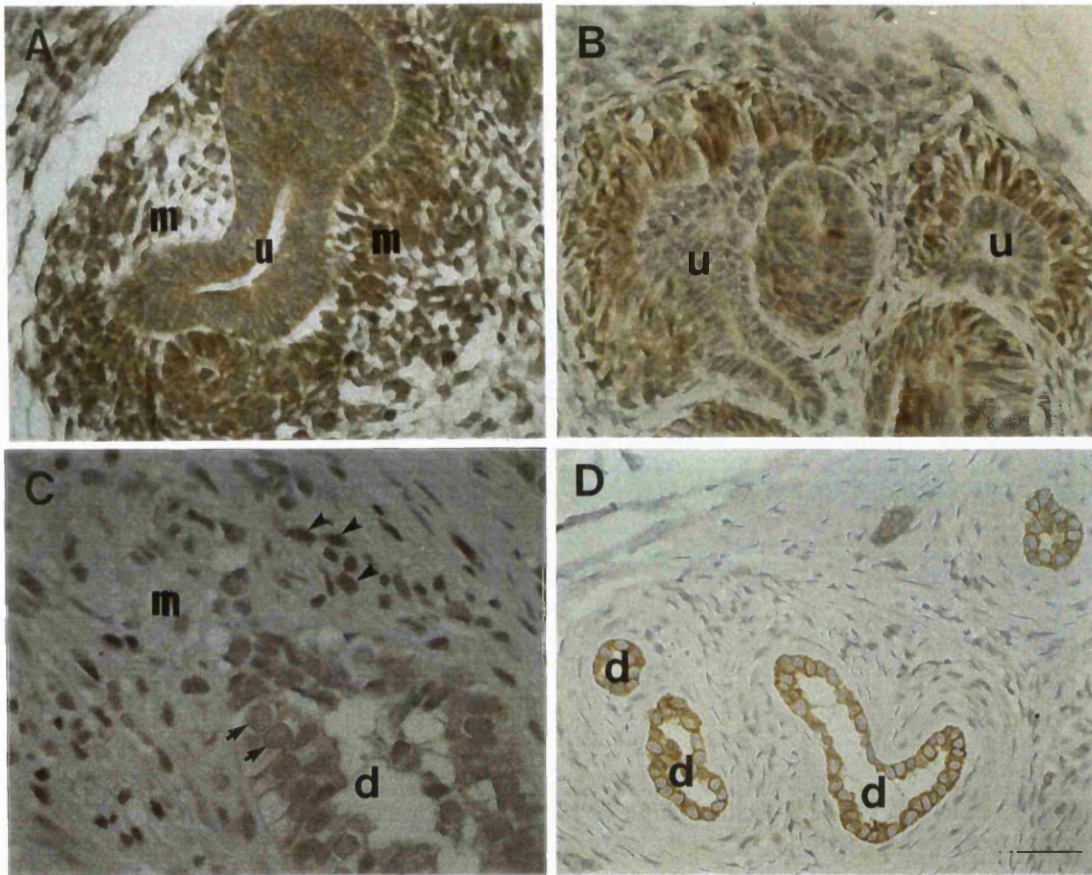
Figure 38. Comparison between WT-1 and BCL-2 in normal and dysplastic kidneys. Light photomicrographs of immunohistochemistry for WT-1 in A) and C) compared to BCL-2 in B) and D). All sections are counterstained with methyl green. A) and B) are sections of normal human fetal kidney and C) and D) are postnatal dysplastic kidneys. A) and B) demonstrate that both proteins are expressed in the condensing mesenchyme (m) around the ureteric bud (u). Note, however, that WT-1 staining is nuclear whereas BCL-2 appears cytoplasmic. C) shows that WT-1 is found in cells (arrowheads) in the mesenchyme-like areas (m) around dysplastic epithelia (d), but the epithelial cells are negative (arrows). D) In contrast BCL-2 is detected in virtually all of the epithelial cells, but none of the cells in mesenchyme-like areas. Bar corresponds to 20 μm in D and 10 μm in all other sections.

Galectin-3

Immunohistochemistry for galectin-3 was performed using the rabbit polyclonal antibody described in the *Materials* section of this thesis. The specificity of the antibody was confirmed by Western blotting. Human galectin-3 protein has a predicted size of 33 kD and a single band of this size was detected in a 10 week gestation normal human fetal kidney (Fig. 39 lane 1), cartilage from the same fetus (Fig. 39 lane 2) and in three postnatal dysplastic kidneys (Fig. 39 lanes 3 to 5). Canine galectin-3 is larger than the human protein and a 42 kD band was seen in protein extracted from MDCK cells. No signal was detected when the primary antibody was omitted or the samples were pre-incubated with excess galectin-3.

Normal kidneys

(Preterm n = 12; Postnatal n = 16)

Galectin-3 was expressed in both the mesonephros and the metanephros from day 42 of gestation, the earliest stage examined. In the mesonephros the protein was detected in the mesonephric duct and in distal mesonephric tubules (Figs. 40B, and 41B and C). In these cells, immunostaining appeared to be predominantly in the apical domain (Figs. 40B and 41C), probably in the plasma membrane. The paramesonephric duct was devoid of staining (Fig. 41C), which contrasts with the positive nuclear staining for PAX-2 in both of these ducts (Fig. 30D). Patchy cytoplasmic staining for galectin-3 was seen in the proximal mesonephric tubules using a peroxidase conjugated detection system (ABC and DAB) (Fig. 41C) but this result was not corroborated using immunofluorescence (Fig. 40A), which suggests that it may reflect unquenched background peroxidase activity or endogenous biotin in these tubules. Mesonephric glomeruli were negative using both techniques.

In the seven week metanephros galectin-3 immunoreactivity was detected in the stalk of the ureteric bud, again appearing to be confined to the apical plasma membrane (arrowheads in Fig. 41F). At this stage the bud had branched 3-4 times and mesenchymal condensates were detected around the branch tips (Fig. 41E). A very low level of galectin-3 immunoreactivity was seen in these condensates (Fig. 41D and F).

At later stages of nephrogenesis, and in the mature kidney, galectin-3 protein was restricted exclusively to the ureteric bud lineage. Three distribution patterns were seen during development, often co-existing in the same section (Fig. 43) which may reflect different stages of maturity. Firstly, in the nephrogenic cortex, there was a predominantly apical distribution in the branching tips of the ureteric bud (Fig. 42B and C) which reiterated the apical galectin-3 pattern detected in the mesonephric duct and ureteric bud in earlier embryos. Secondly, in the sub-cortical region, galectin-3 was expressed in more mature collecting duct structures (Fig. 43A to C): some cells in segments fused with primitive nephrons had a predominantly apical distribution (open arrows in Fig. 43A), whilst in others, galectin-3 immunoreactivity was noted inside the epithelial cells (arrows in Fig. 43A and C). Thirdly, the most intense signal for galectin-3 was found in medullary and papillary collecting ducts where staining appeared to be cytoplasmic as well as in the apical, lateral and basal plasma membranes (Fig. 44D to F). No significant background staining was seen in samples in which the primary antibody had been either omitted (Fig. 42A) or preabsorbed with excess galectin-3 (Fig. 44A to C).

In adult kidneys, galectin-3 expression was principally detected in the cytoplasm of a subset of cells in the cortex and medulla, with lower levels in the nucleus as assessed by serial confocal laser scans at 0.50 μm

intervals (arrowed cells in Figs. 45A and D, and 46B and D). These cells were restricted to the collecting ducts since the tubules co-stained with *Arachis hypogaea* agglutinin, a marker of the distal nephron (Fig. 45A to C) (Holthofer *et al.*, 1981). Interestingly, cells which were positive for galectin-3 (Fig. 45A) were negative for this lectin (Fig. 45B). *Arachis hypogaea* labels β-intercalated cells in rabbit collecting ducts (Fejes-Toth and Naray-Fejes-Toth, 1991) but it has not been characterised in detail in the human. In contrast, band 3, a transmembrane protein, has been well characterised in humans and a truncated protein is expressed on the basal surface of the hydrogen secreting α-intercalated cells (Wagner *et al.*, 1987). Further double labeling of sections co-localised galectin-3 and band 3 to the same cells which are therefore likely to be α-intercalated cells. The galectin-3 protein was also expressed in the renal pelvis and ureter, which are ureteric bud derivatives (not shown).

Dysplastic kidneys

(Preterm n = 10; Postnatal n = 12)

High levels of galectin-3 protein were detected in the epithelia of dysplastic kidneys: positive immunostaining was detected in a large proportion of dysplastic tubules and over 95% of dysplastic cysts (Fig. 47) in both preterm and postnatal specimens. Similar patterns were seen in obstructed and non obstructed systems. In the positive tubules and cysts, every epithelial cell expresses galectin-3 and the protein was located on the apical surface (Fig. 47B, C and E). Galectin-3 immunoreactivity was also detected in the nuclei of chondrocytes in areas of metaplastic cartilage (Fig. 47D). In one postnatal sample, part of the organ contained areas of tubules which looked relatively normal (Fig. 47F): an immature apical pattern was seen in some undilated tubules in these areas.

Polycystic kidneys

(Preterm n = 4; Postnatal n = 4)

Cystic epithelia were also universally positive for galectin-3 in both the preterm and postnatal polycystic samples examined (Fig. 48). In contrast to the dysplastic samples, however, the galectin-3 protein was located in the cytoplasm of the epithelial cells in the majority of the cysts (Fig. 48C and D). A small subpopulation, representing less than 10% of cysts, also had a predominantly apical location (Fig. 48E and F). It was not possible to demonstrate convincing nuclear staining in any of these samples using serial scanning confocal laser microscopy.
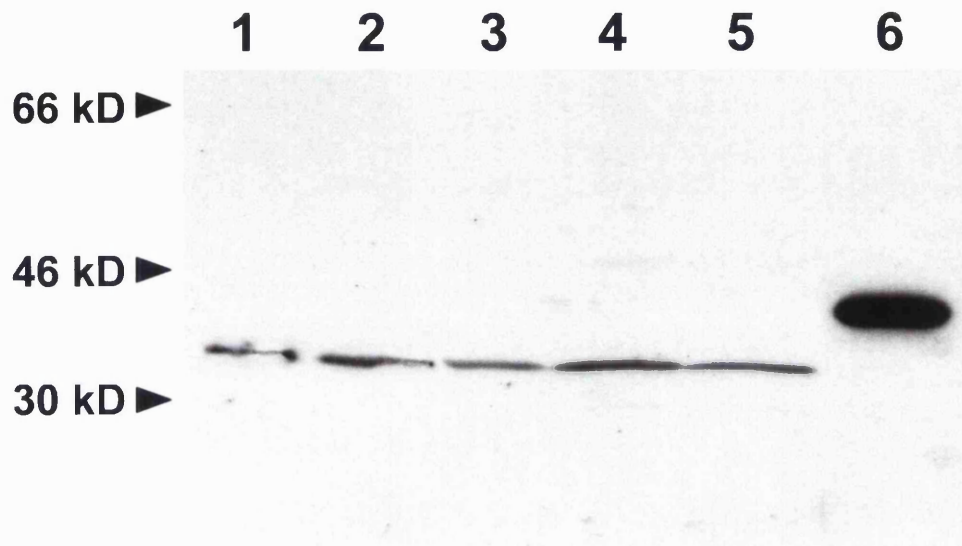
Figure 39. Western blot of galectin-3. All lanes were probed with the rabbit polyclonal galectin-3 antibody used in immunohistochemistry (Figs. 40 to 48). Lane 1) contains protein from a 10 week gestation fetal metanephros. Lane 2) is from the lower limb of the same fetus. Lanes 3) to 5) are postnatal dysplastic kidneys and lane 6) is MDCK cells. The predicted size of human galectin-3 is 33 kD and a band of this size is detected in all of the human tissues, whilst a larger band corresponding to the larger canine protein, is seen in the MDCK cells. Preincubation of the antibody with galectin-3 protein specifically blocked these bands and no signal was detected when the primary antibody was omitted.
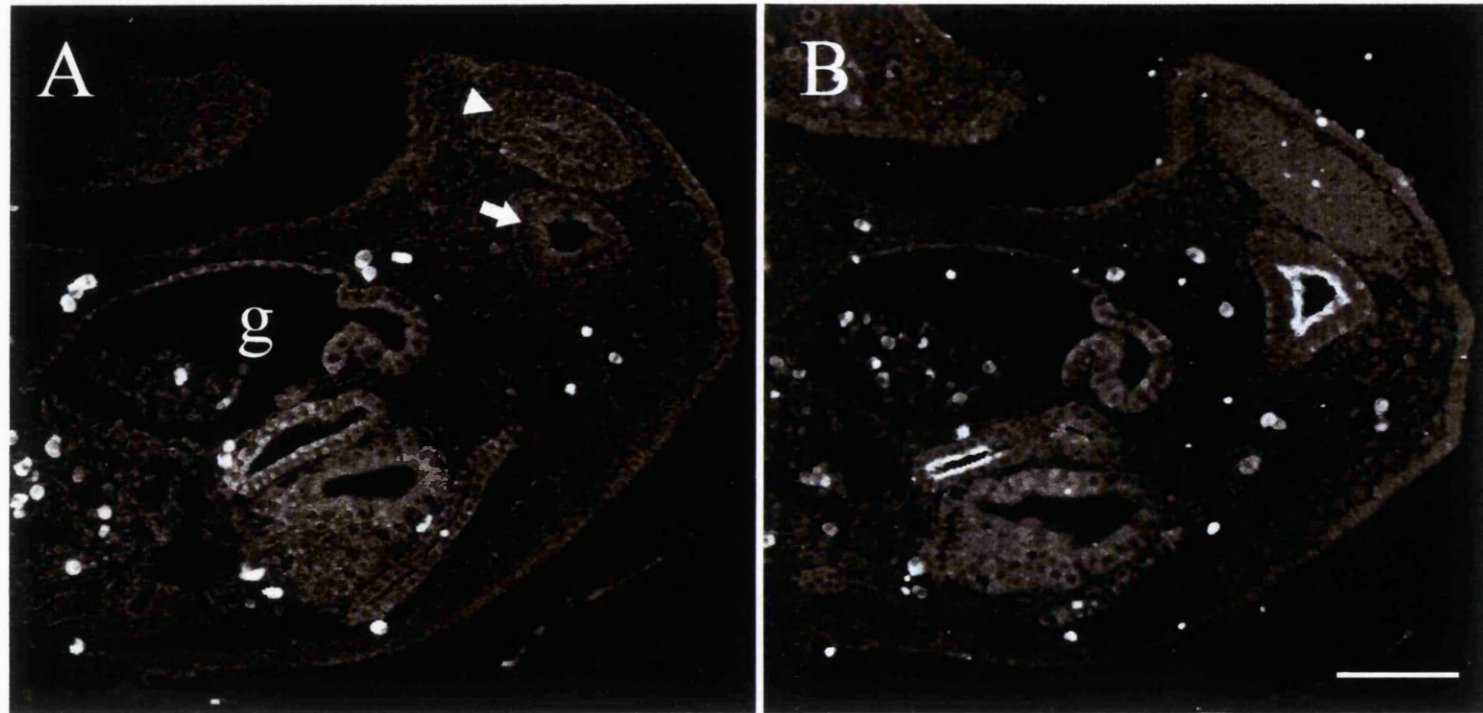
Figure 40. Galectin-3 in the mesonephros. Confocal laser scanning photomicrographs of galectin-3 immunohistochemistry on sections of the mesonephros of a 42 day gestation embryo. A) is the control in which the galectin-3 antibody was omitted and this section shows a mesonephric glomerulus (g) and tubules, the mesonephric duct (arrow) and the paramesonephric duct (arrowhead). Note the autofluorescence in the mesonephric tubules. B) shows apical galectin-3 staining in the mesonephric duct and some of the mesonephric tubules. The paramesonephric duct is negative. Bar corresponds to 40 μm in both sections.
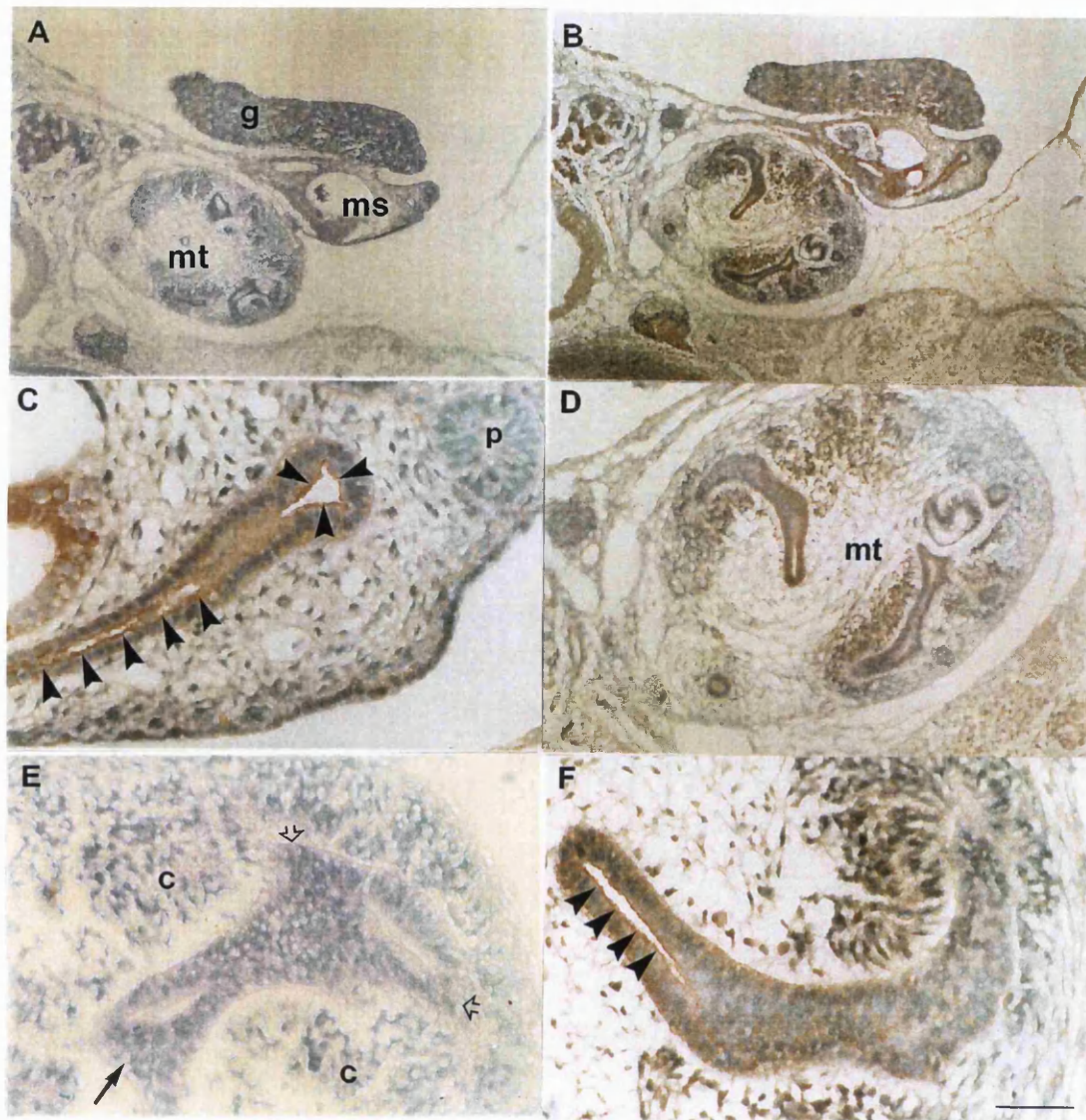
Figure 41. Galectin-3 in early kidney development. Light photomicrographs of galectin-3 immunohistochemistry on a 42 day gestation embryo, counterstained with methyl green. A) and E) are control sections without the primary antibody. A) and B) show the mesonephros (ms), metanephros (mt) and gonad (g). C) Galectin-3 is detected in a predominantly apical distribution in the mesonephric duct (converging arrowheads) and distal tubules of the mesonephros (line of arrowheads) which drain into it. The paramesonephric duct (p) is negative. Patchy galectin-3 immunoreactivity is also noted in the proximal type tubules. D) shows the whole of the metanephros whilst E) and F) show higher power views of the ureteric bud branch tips (open arrows), ureteric bud stalk (closed arrow) and condensates (c). Galectin-3 is again detected in a predominantly apical distribution, at this early stage of metanephric development, in the central ureteric bud (arrowheads). Condensing mesenchyme also appears weakly positive. Bar corresponds to 200 μm in A) and B), 30 μm in C), E) and F), and 80 μm in D).
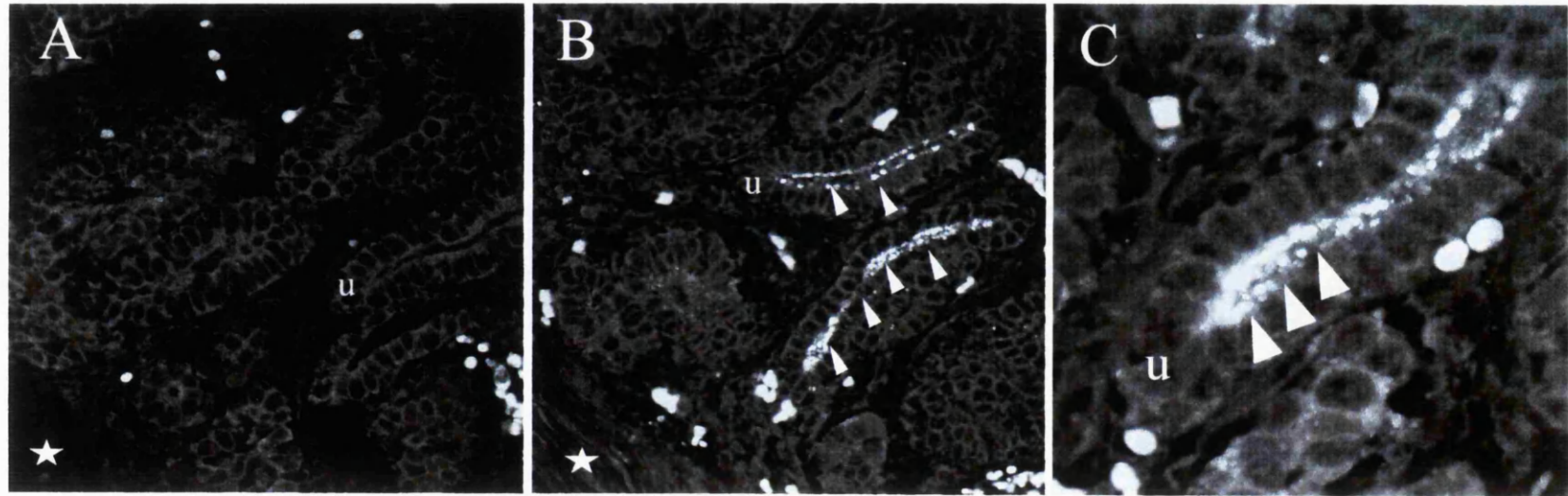
Figure 42. Galectin-3 in the nephrogenic cortex during development. Confocal laser scanning photomicrographs of galectin-3 immunohistochemistry on kidney sections from a 20 week gestation fetus. A) is the control section in which the galectin-3 antibody was omitted. The outer edge of the cortex is seen in the bottom left of the picture (*). Note intense autofluorescence of nucleated red cells and weak autofluorescence of the epithelia, including ureteric bud branches (u). B) and C) show a predominantly apical galectin-3 distribution (arrowheads) in the tips of ureteric bud branches. Bar corresponds to 30 μm in A) and B), and 10 μm in C).
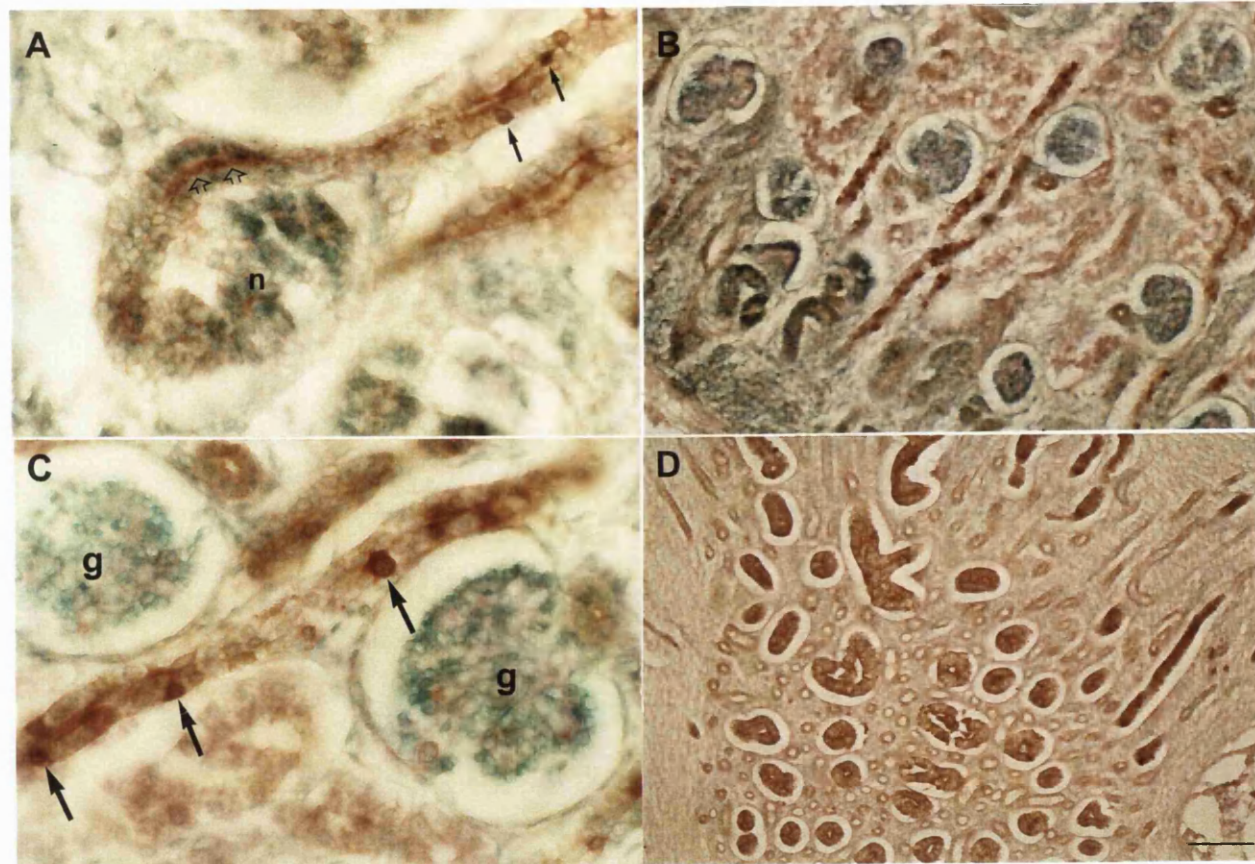
Figure 43. Galectin-3 in the cortex and medulla during development. Light photomicrographs of galectin-3 immunohistochemistry in a mid gestation kidney, counterstained with methyl green. A) to D) Progressively deeper areas, from the outer cortex to the medulla. A) Apical galectin-3 staining is detected (open arrows) in the ureteric bud where it fuses with the nephron (n) with coexistent cytoplasmic / nuclear protein distribution (black arrows) in specific cells deeper in the cortex. Some nearby proximal tubules show background peroxidase staining. B) and C) show further cells with diffuse galectin-3 staining, often in close proximity to the glomeruli (g). D) shows strongly positive collecting ducts in the medulla (see also Fig 44). Bar corresponds to 40 μm in A), 100 μm in B) and D), and 20 μm in C).
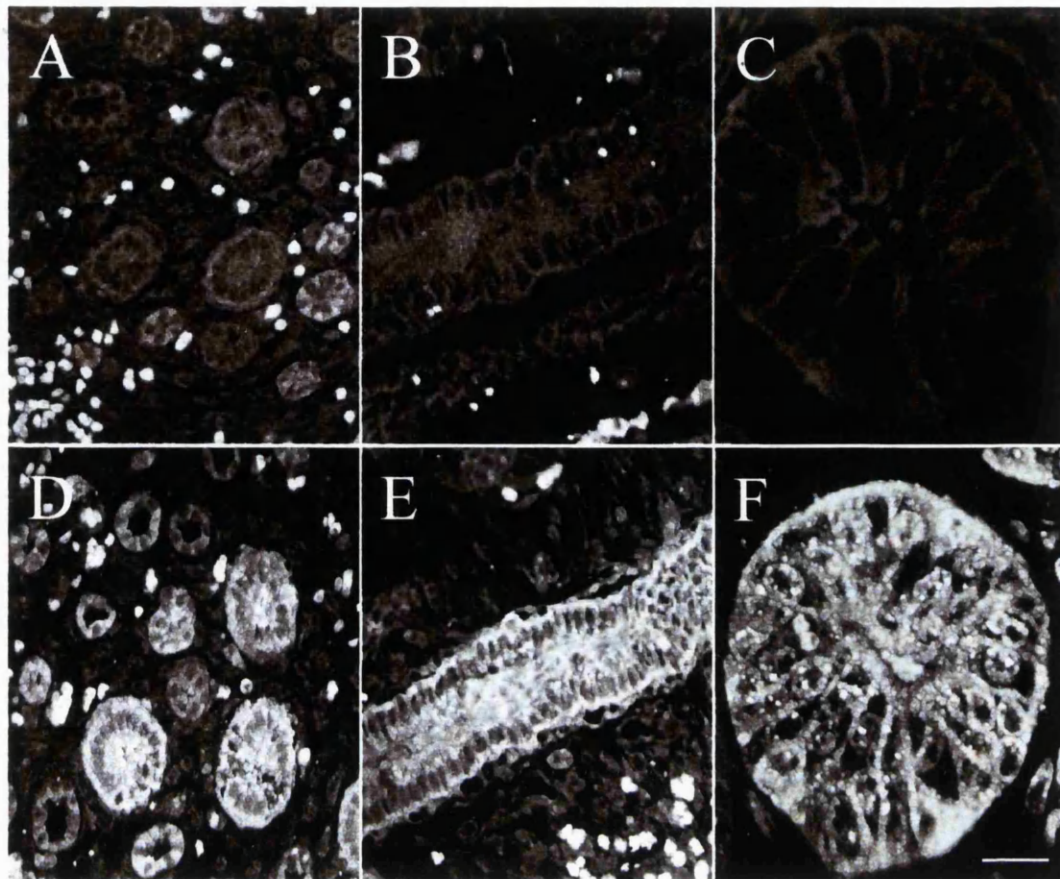
Figure 44. Galectin-3 in the medulla during development. Confocal laser scanning photomicrographs of galectin-3 immunohistochemistry on kidney sections from a 20 week gestation fetus. A) to C) are control sections in which the galectin-3 antibody was preincubated with excess galectin-3 protein. Weak background autofluorescence is seen in many of the tubules with intense autofluorescence in nucleated red cells. In D) to F) intense galectin-3 immunoreactivity is detected in the large collecting ducts. The protein is located in the cytoplasm as well as in apical, lateral and basal plasma membranes. Bar corresponds to 15 μm in C) and F), and 80 μm in all other sections.
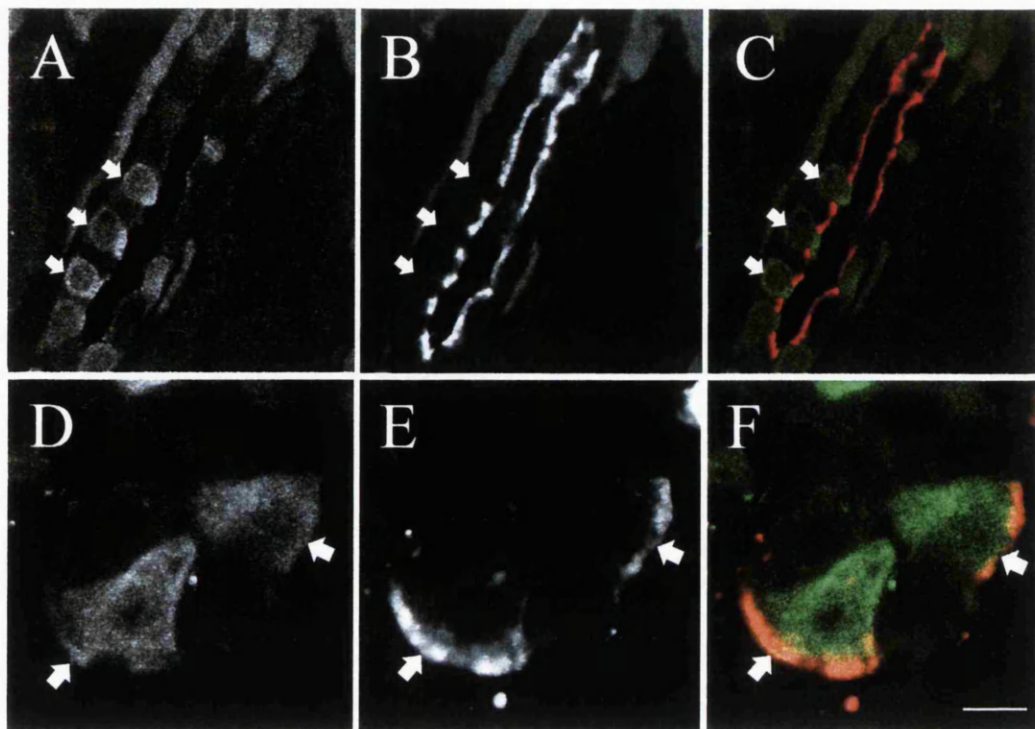
Figure 45. Galectin-3 in the mature cortex. Confocal laser scanning photomicrographs of double labeled kidney sections from mature cortex. A) to C) are the same section stained for galectin-3 (A), *Arachis hypogaea* (B) and a combined image (C) with galectin-3 in green and *Arachis hypogaea* in red. The positive labeling with *Arachis hypogaea* identifies the main tubule seen in this section as a collecting duct. A sub-population of cells in this collecting duct are positive for galectin-3 (arrowed in all) and do not bind *Arachis hypogaea*. D) to F) are the same section through a postnatal cortical collecting duct co-stained with galectin-3 (D), band 3 (E) or both of these images combined (F) with galectin-3 in green and band 3 in red.

D) Cytoplasmic / nuclear galectin-3 is seen in two of the cells (arrowed) in a transverse section of a collecting duct. E) The same cells are positive for band 3 on the basolateral surface which identifies them as α-intercalated cells. Bar corresponds to 40 μm in A) to C), and 15 μm in D) to F).
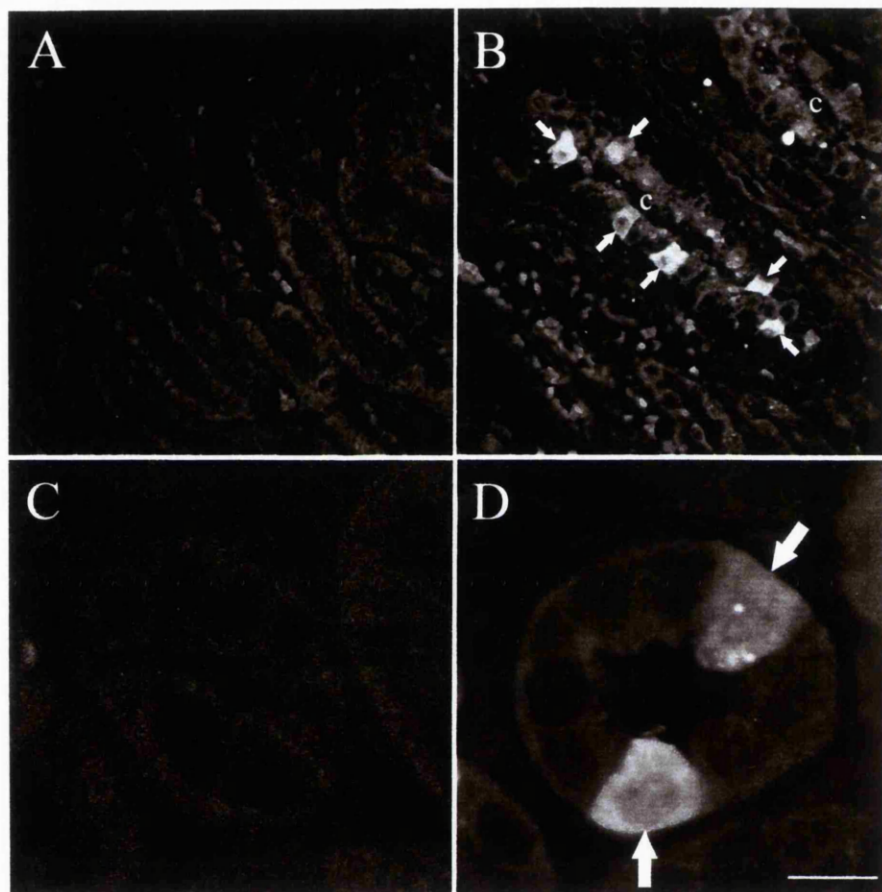
Figure 46. Galectin-3 in the mature medulla. Confocal laser scanning photomicrographs of galectin-3 immunohistochemistry on sections of mature renal medulla. The primary antibody was omitted in A) which is the control section for B) and the primary antibody was pre-absorbed with excess galectin-3 protein in C), the control section for D). Both of these controls are completely negative. B) and D) show collecting ducts (c) containing a subset of cells which are galectin-3 positive (arrowed). The protein is mainly seen in the cytoplasm with additional weak nuclear staining. Bar corresponds to 80 μm in A) and B); and 15μm in C) and D).
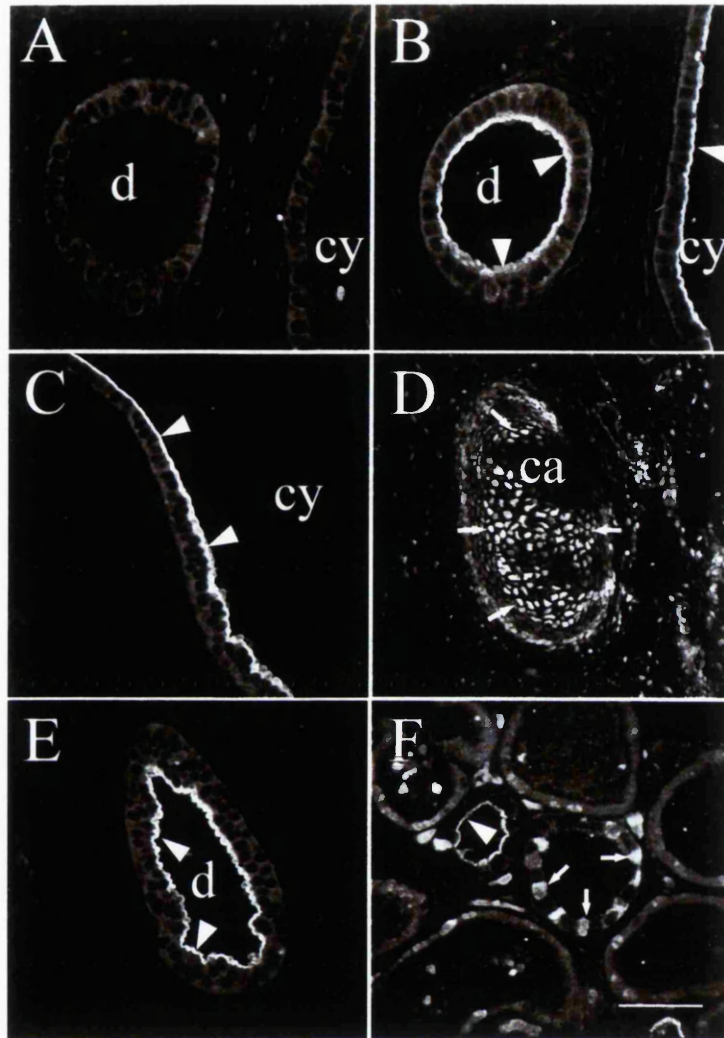
Figure 47. Galectin-3 in dysplastic kidneys. Confocal laser scanning photomicrographs of galectin-3 immunohistochemistry on sections of postnatal dysplastic kidneys. A) is a control section with galectin-3 antibody omitted. B), C) and E) show dysplastic tubules (d) and cysts (cy) with apical galectin-3 protein (arrowheads). D) metaplastic cartilage (ca) contains cells which are positive for galectin-3 (arrowed). F) shows an area of more differentiated tubules: note that one tubule has a mature cytoplasmic and nuclear galectin-3 pattern restricted to a subset of cells (arrowed), whereas the adjacent undilated tubule has an apical phenotype (arrowhead). Bars correspond to 20 μm in D) and 40 μm in all other sections.
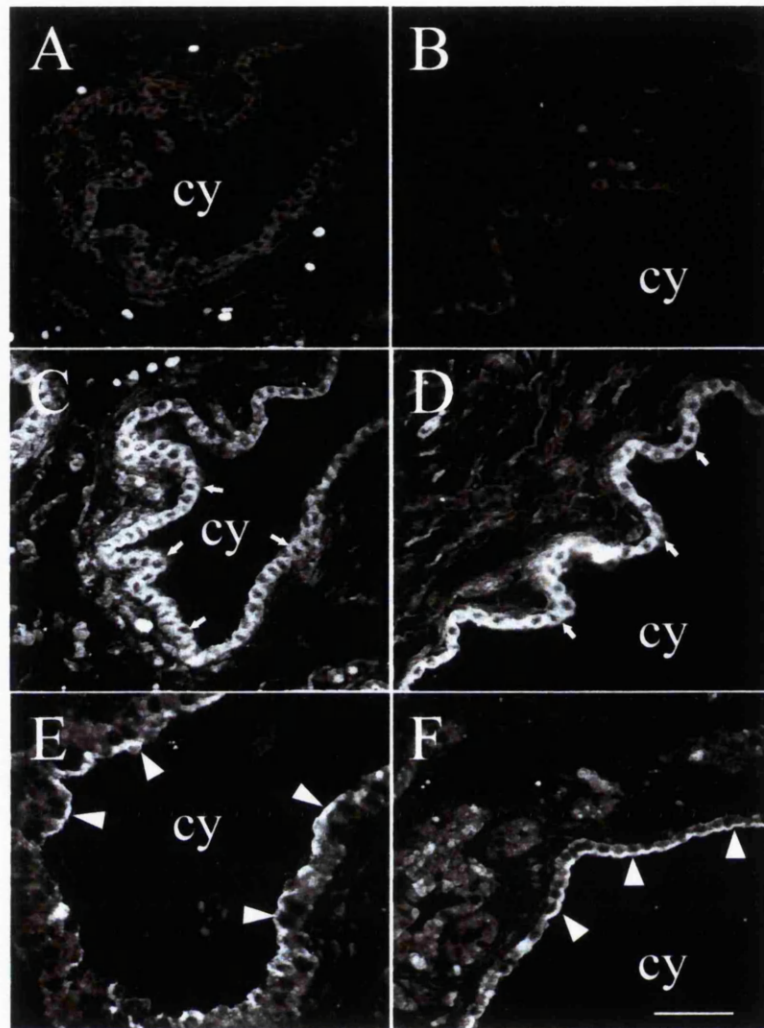
Figure 48. Galectin-3 in autosomal recessive polycystic kidneys.
Confocal laser scanning photomicrographs of galectin-3 immuno-
histochemistry on autosomal recessive polycystic kidney sections from
a mid gestation fetus in A) to D) and a child in E) and F). A) and B)
are control sections corresponding to C) and D) respectively.
Significant immunostaining is not seen in these controls. C) and D)
demonstrate strong cytoplasmic galectin-3 staining within cyst (cy)
epithelia (arrows). E) and F) show that postnatal epithelia also express
galectin-3 with a rare, predominantly apical galectin-3 phenotype
(arrowheads) in some cells. Nuclear staining is not detected in cystic
epithelia. Bars correspond to 80 μm.

Summary of PAX-2, WT-1, BCL-2 and galectin-3 distribution

In normal kidneys PAX-2 and BCL-2 were expressed in early nephron precursors and PAX-2 was also detected in ampullae of the ureteric bud. Both of these molecules were downregulated as the kidney matured. WT-1 protein was detected at low levels in mesenchymal condensates and expression levels increased to their peak in glomerular podocytes, which were the only site of expression in adult kidneys. Galectin-3 expression was almost exclusively confined to the ureteric bud and its derivatives but its subcellular distribution changed as this lineage matured. The expression pattern was apical in ampullae of the ureteric bud and cytoplasmic in α-intercalated cells in adult collecting ducts, with an intermediate phase of cytoplasmic / membranous distribution in maturing subcortical and medullary collecting ducts.

In dysplastic kidneys, PAX-2, BCL-2 and galectin-3 were all strongly expressed in dysplastic tubules and cyst epithelia. The galectin-3 protein was detected in the apical plasma membrane which is similar to its distribution pattern in the ureteric bud. This protein was also strongly expressed in a cytoplasmic / membranous location in polycystic epithelia. WT-1 protein was not detected in dysplastic epithelia, but was found in adjacent fibromuscular collarettes and more distant loosely packed cells. These results are summarised in Table 9 below.

	PAX-2	BCL-2	WT-1	Galectin-3
Normal kidneys				
Undifferentiated mesenchyme	-	-	-	-
Mesenchymal condensates and vesicles	++	++	+	rare +
S-shaped bodies	++	+	+	-
Glomerular podocytes	-	-	++	-
Tips of ureteric bud (ampullae)	++	-	-	+
Immature collecting ducts	+	-	-	++
Mature collecting ducts	rare +	-	-	+
Dysplastic kidneys (pre and postnatal)				
Dysplastic tubules	++	++	-	++
Cyst epithelium	++	++	-	++
'Fibromuscular collarettes'	-	-	+	-
Loose cells	-	-	+	-
Polycystic kidneys (pre and postnatal)				
Cyst epithelium	na	na	na	++
Cells adjacent to cysts	na	na	na	-
Undilated tubules	na	na	na	+
Cells around tubules	na	na	na	-

Table 9. PAX-2, WT-1, BCL-2 and galectin-3 distribution.

This table describes the patterns of protein distribution in normal, dysplastic and polycystic kidneys. '−' Indicates no staining, 'rare +' indicates that less than 10% of cells showed positive immunostaining and '+' to '++' indicates increasing levels and / or intensity of staining. PAX-2, BCL-2 and WT-1 distribution were not assessed in polycystic samples (na).

Chapter 10. Results

Culture of cells from dysplastic kidneys

Culture of animal cells is a well established technique (Freshney, 1987) but there have not been any previous reports describing culture of cells from dysplastic kidneys.

Primary culture

The first experiment aimed to grow cells from one dysplastic kidney in order to determine whether it was technically possible to establish them in primary culture. A sample of the dysplastic kidney was divided into small blocks, seeded onto 4 well chamber slides and cultured, as described in the *Methods* section of this thesis. Initially, the cells grew slowly and were confined to the areas close to tissue fragments. Next, the cells appeared to grow away from the tissue in streams and spread throughout the well. This stage lasted for a few days, and in the third stage the number of cells increased quickly in all areas of the slide. The cells were not allowed to become confluent, and in this initial experiment the cells were fixed in 4% PFA and stained for cytokeratin and vimentin (Fig. 49).

The dysplastic cells in this primary culture had an irregular multipolar outline similar to fibroblastic cells (Fig. 49C to F). Occasional long processes were also seen (Fig. 49F). Cells with an epithelial phenotype were not detected. The cells were universally positive for both vimentin and cytokeratin (Fig. 49C to F). Interestingly, WT-1 was also detected in the majority of the cells and it appeared to be confined to specific sites in the nucleus, which may be spliceosomes (Larsson *et al.*, 1995).

Extended culture and transduction

Tissue samples from two further dysplastic kidneys were cultured and used for transduction experiments. They were prepared as described above and initially grown in 9 cm petri dishes. The same phases of growth were seen in these larger plates, although cells from the first sample (designated PW1) grew more slowly than cells from the second sample (designated PW2).

The samples were passaged once, just before they reached confluence, and different phenotypes were observed. The PW1 cells had a 'fibroblastic' or 'mesenchymal' appearance (Fig. 50C to F), similar to the cells in the primary culture described above, whereas the PW2 cells were more cuboidal and formed a cobblestone appearance as they approached confluence. These latter cells, therefore, had more of an epithelial appearance (Fig. 51C to F) and interestingly they formed elongated branching tubule like structures as the cultures approached confluence (Fig. 51D).

After one passage, the cells were transferred to the level 3 biosafety laboratory at the Ludwig Institute, UCLMS, where transduction of the cells with the retroviral construct was carried out by Dr Mike O'Hare. The cells were then transferred back after positive selection using G-418 (0.5 g / l) and testing of the supernatant to ensure that they did not contain replication competent retroviruses. They were then cultured and passaged once at the permissive temperature of 33^0C without any signs of either senescence or ' blast crisis'. The phenotypes of the cell types were unchanged with 'fibroblastic' PW1 cells and 'epithelioid' PW2 cells (Figs. 50F and 51F).

Expression of the SV40 large T antigen was assessed by Western blotting of protein extracted from the cultured cells (Fig. 51). Both cell lines produced this protein at the permissive culture temperature of 33^0C (Fig. 52 lane 1 and 2) and non permissive temperature of 39^0C (Fig. 52 lane 3 and 4). The large T protein is said to undergo a conformational change at 39^0C which prevents its effects, but the antibody used in this experiment does not distinguish between the different forms (personal communication – Dr Parmjit Jat, UCLMS). Interestingly, both cell types also produced the galectin-3 protein (Fig. 51). Levels of galectin-3 protein appeared higher in the 'epithelioid' PW2 cells (Fig. 52 lanes 2 and 4) which is consistent with my finding that galectin-3 was expressed predominantly by epithelial cells in the kidney.

Summary of cell culture experiments

These preliminary experiments demonstrated that it is feasible to culture cells from dysplastic kidneys and that they continued to grow after one passage. Cells with a fibroblastic (2) and epithelial phenotype (1) were generated in these experiments. These phenotypes were maintained after transduction of the cells with a retrovirus which may lead to conditional immortalisation of the cells via a temperature sensitive SV40 large T antigen system. This protein was definitely expressed, along with galectin-3, by the cells after transduction but it is too early to say whether it will be possible to establish long term cultures of these cells. Culture and assessment of these cells is, however, an important part of the planned experiments in *Further work* which is described later in this thesis.
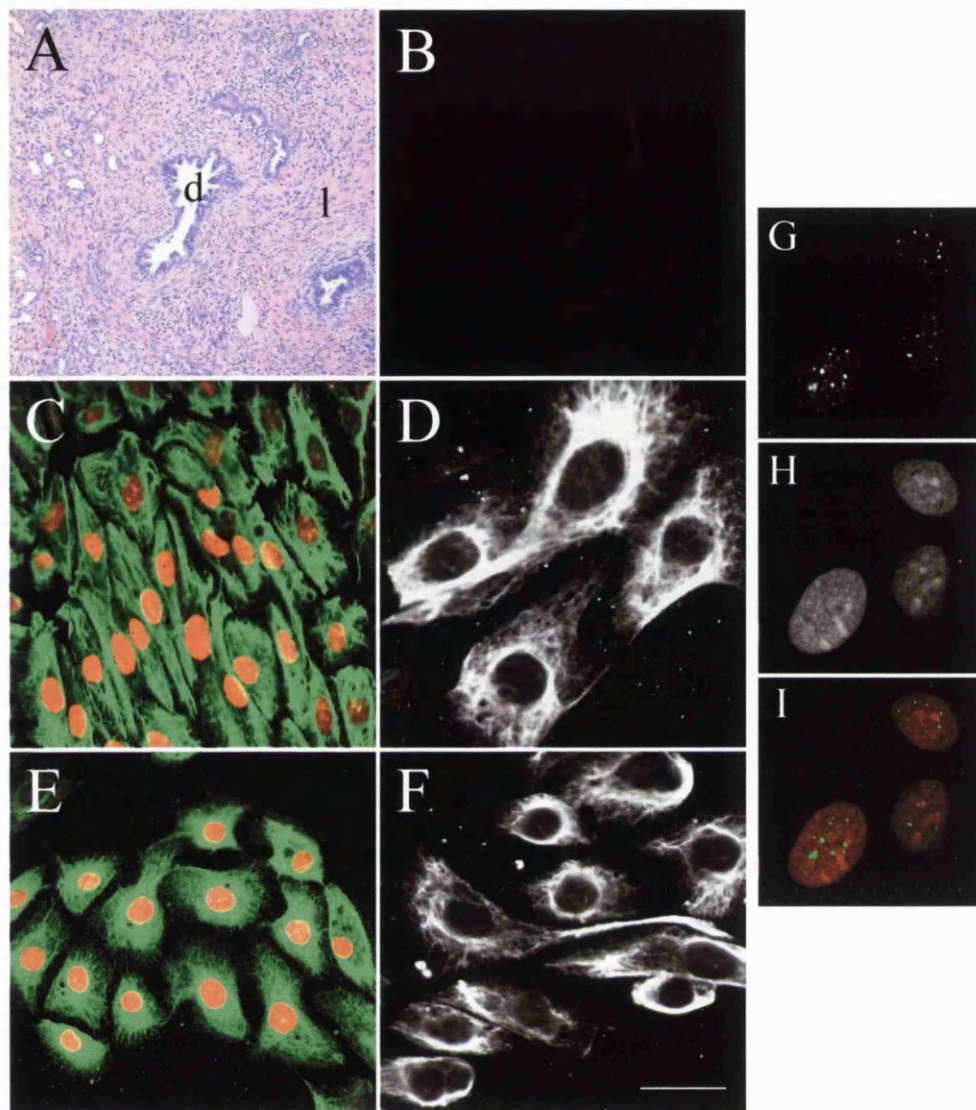
Figure 49. Primary culture of cells from a dysplastic kidney. Light photomicrograph of dysplastic upper pole (A) and confocal laser scanning photomicrographs of cells cultured from it (B to I). A) Shows the histology of the kidney with a dysplastic tubule (d) and loose mesenchyme (l). Note the inflammatory infiltrate. B) Control section, without the primary antibody, shows little background autofluorescence. C) and D) are stained for pan-cytokeratin and E) and F) for vimentin. C) and E) are counterstained with propidium iodide in red. The cells have elongated processes and a mesenchymal appearance. G) to I) are the same cells stained for WT-1 (G), with propidium iodide (H) and a combined image (I). The nuclei have punctate WT-1 staining, which may be in the spliceosomes. Bar corresponds to 500 μm in A), 40 μm in B), C) and E), 20 μm in D) and F), and 6 μm in G) to I).

214
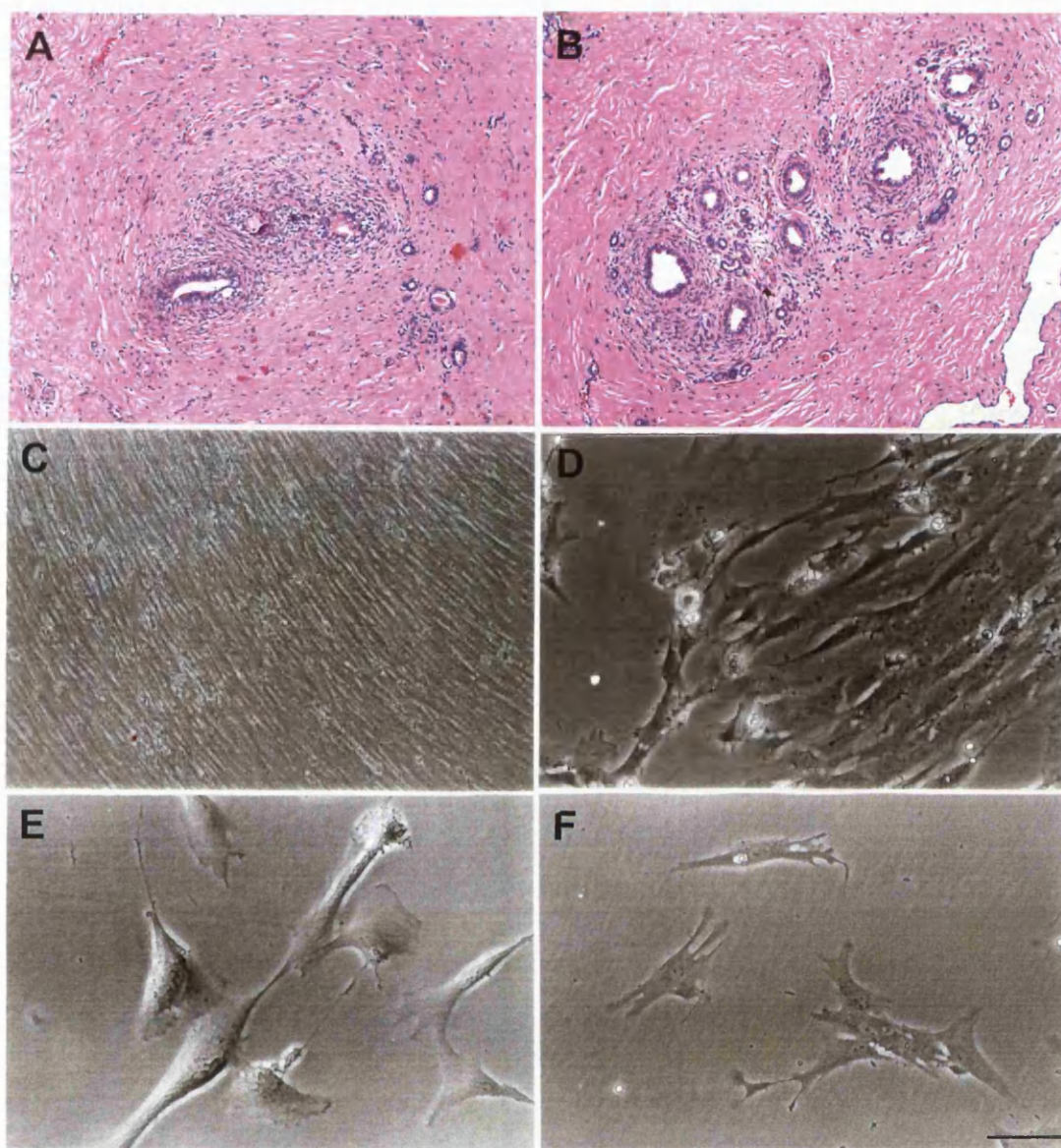
Figure 50. Primary culture and transduction of cells from a dysplastic kidney (PW1). Light photomicrograph of dysplastic kidney and dysplastic cells which were designated as sample PW1. A) and B) Haematoxylin and eosin stained section of a dysplastic kidney with multiple cysts removed at 6 months of age. Note the dysplastic tubules (d) and abundant surrounding loose mesenchyme (l) and fibrous tissue. All of the remaining sections show cells which were cultured from a fragment of this kidney: C) to E) are primary cultures and F) is after transduction with the retroviral construct. The cells have a mesenchymal appearance with elongated processes, which appears unchanged after transduction. Bar corresponds to 500 μm in A) and B), 100 μm in C), 50 μm in D) and 30 μm in E) and F).
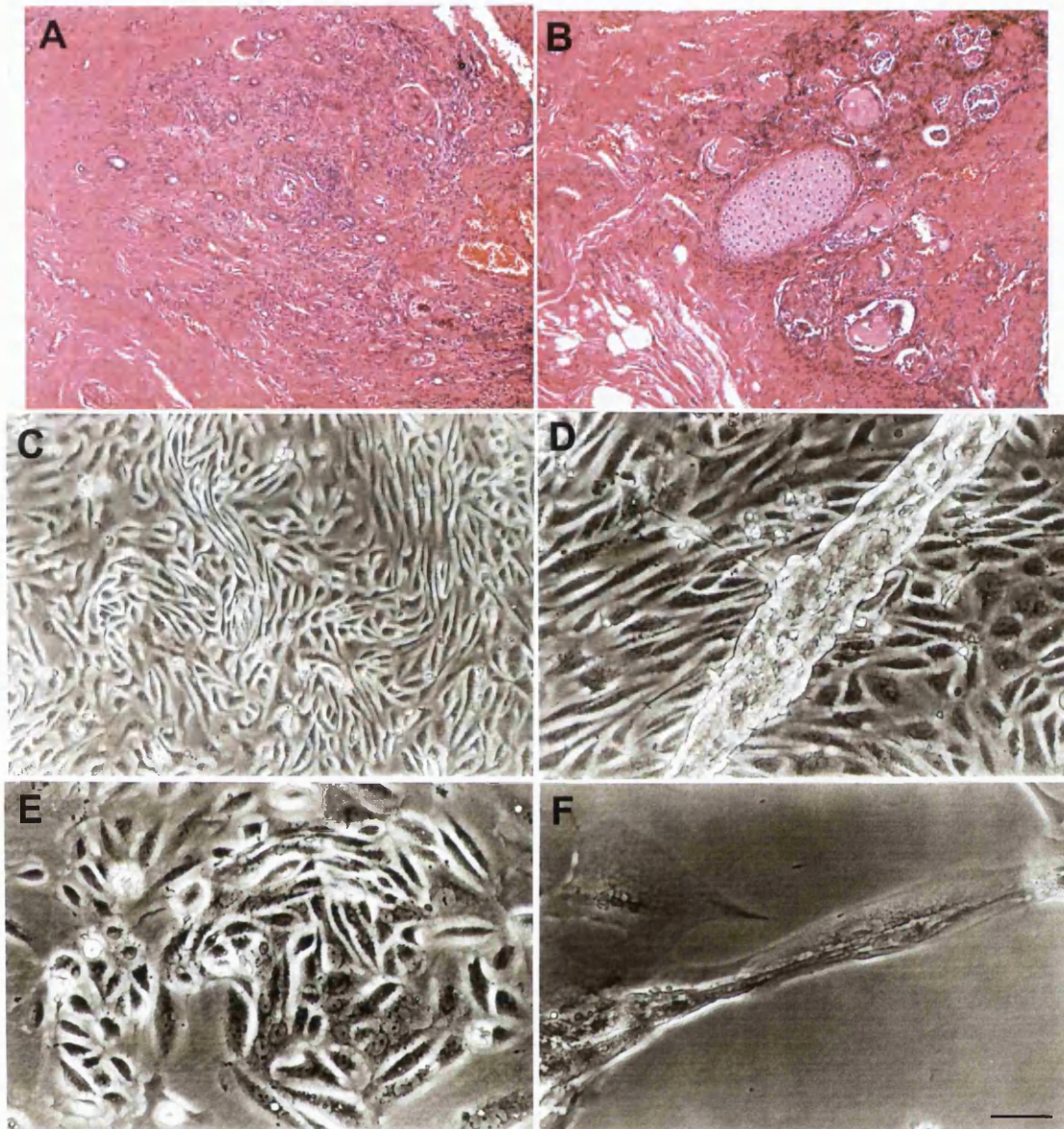
Figure 51. Primary culture and transduction of cells from a dysplastic kidney (PW2). Light photomicrograph of dysplastic kidney and dysplastic cells which were designated as sample PW2. A) and B) Haematoxylin and eosin stained section of a dysplastic kidney removed at 7 months of age. Note the dysplastic tubules, loose mesenchyme and cartilage. All of the remaining sections show cells which were cultured from a fragment of this kidney. C) to E) are primary cultures and F) is after transduction with the retroviral construct. The cells have an epithelial phenotype and form a cobblestone pattern when approaching confluence. Note the tubule like structures, shown in D), which formed in some areas of the culture. Bar corresponds to 500 μm in A) and B), 100 μm in C) and 50 μm in D) to F).
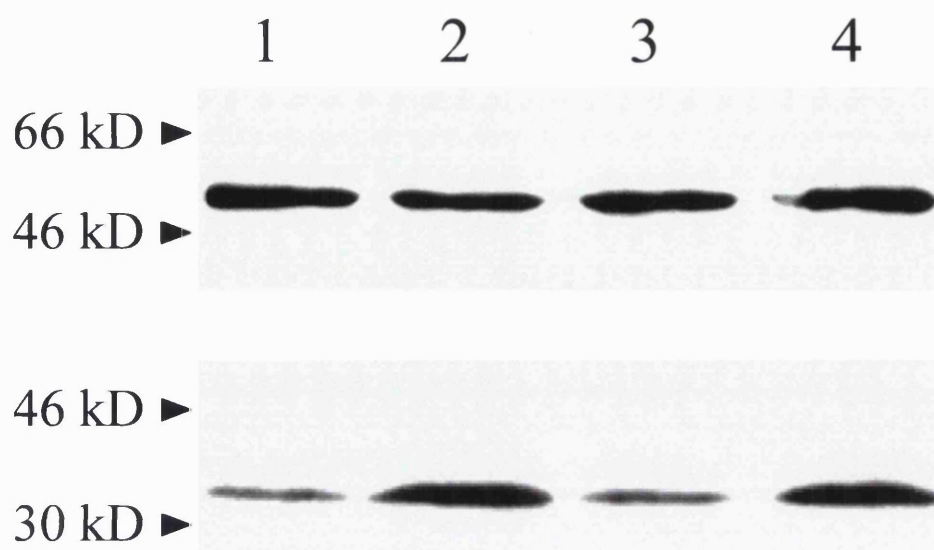
Figure 52. Western blot for large T antigen and galectin-3 in dysplastic cells. Composite Western blot of protein extracted from dysplastic cells (after transduction) probed with antibodies raised against the large T-antigen (upper panel) and galectin-3 (lower panel). Lanes 1) and 3) are from sample PW1 shown in Fig. 50 and lanes 2) and 4) are from sample PW2 shown in Fig. 51. Lanes 1) and 2) contain protein from cells cultured at the permissive temperature of 33^0C and lanes 3) and 4) contain protein from cells cultured at the non permissive temperature of 39^0C. Negative controls, in which the antibody was omitted, were completely clear. Sizes correspond to bands in rainbow marker lanes. The large T antigen is present in all of the lanes which confirms that the cells have been transduced. The antibody used here cannot, however, distinguish between active and inactive forms of this protein. Galectin-3 is also present in all of the samples, although there appears to be more protein in the epithelial sample (PW2) shown in lanes 2) and 4).

Chapter 11. Discussion

Renal dysplasia is the commonest single cause of chronic renal failure in children under five years of age (Warady *et al.*, 1997). The anatomy of dysplastic kidneys has been extensively reported (Bialestock, 1964; Bernstein, 1971; Risdon, 1971; Potter, 1972) and it has been hypothesised that renal dysplasia represents failure of normal development. This hypothesis is largely based on the histological resemblance between fetal and dysplastic structures, such as the ureteric bud and dysplastic tubules, and the microdissection studies of Osathanondh and Potter (Potter, 1972) which revealed that dysplastic epithelia were malformed branches of the ureteric bud. There is, however, little molecular evidence to support this view since very few studies have examined the cell biology of these malformations. The experiments described in this thesis were therefore designed to test this hypothesis by comparing the molecular biology of human dysplastic with normal developing and mature kidneys. Most of the data reported in this thesis has been published in a series of articles (Winyard *et al.*, 1996a and b, and 1997) which are bound into the back of this thesis.

The spectrum of dysplastic kidneys

In the pathology textbooks, multicystic dysplastic kidneys are said to be completely non functional, have large cysts and be connected to an atretic, or completely obstructed, ureter. Cystic dysplastic kidneys, on the other hand, may have some function and are reported to have smaller cysts usually connect to a patent urinary tract. These correlations were not observed, however, in either the prenatal or postnatal dysplastic kidneys which were examined during this thesis: some function was found on radioisotope imaging in nearly all of the postnatal samples, cysts were found in most specimens ranging from a few small cysts to numerous massive cysts and there was not a

218

consistent relationship between ureteric or lower urinary tract obstruction and either cyst size or number. Moreover, as discussed above, the patterns of proliferation, apoptosis and gene expression were similar in all of the cystic kidneys, irrespective of cyst size. It is therefore likely that multicystic dysplastic and cystic dysplastic kidneys are not distinct entities, but form part of a spectrum of dysplasia.

Intermediate filament staining and lectin binding in dysplastic kidneys

The majority of cells in the normal adult kidney are derived from two cell lineages during nephrogenesis: the ureteric bud gives rise to the collecting ducts and uroepithelium whilst the metanephric mesenchyme gives rise to the nephrons and stromal tissue. Specific intermediate filament proteins and lectin binding characteristics have been described in the normal development of these two lineages (Holthofer *et al.*, 1984; Oosterwijk *et al.*, 1990) and these were examined in dysplastic kidneys during this thesis.

Epithelial cells in dysplastic tubules were positive for both cytokeratin and vimentin intermediate filament proteins whereas cyst epithelia were positive for cytokeratin alone. The latter observation is consistent with epithelial differentiation in the normal developing kidney since Holthofer and colleagues (1984) and Oosterwijk and colleagues (1990) described cytokeratin expression in epithelia of the ureteric bud lineage, and developing nephrons from the renal vesicle. The additional vimentin expression in dysplastic tubules is harder to explain since vimentin was mainly detected in cytokeratin negative uninduced metanephric mesenchyme and developing podocytes in these studies. Qiao and colleagues (1995) demonstrated that cells derived from the vimentin positive metanephric blastema may contribute to the collecting system but the percentage of mesenchymally derived cells

was small. Transient expression of both vimentin and cytokeratin has, however, been reported in the collecting ducts and double positivity has also been described in renal tumours (Droz *et al.*, 1990). In addition, tubules regenerating after acute tubular necrosis have been reported to express vimentin (Witzgal *et al.*, 1994).

Most dysplastic tubules were positive for *Arachis hypogaea* agglutinin staining but a minority either bound *Tetragonolobus purpureas*, or were negative for both markers. The majority of dysplastic cysts were also positive for *Arachis hypogaea* binding, and *Tetragonolobus purpureas* staining was not seen. None of the tubules or cysts were positive for both agglutinins. These results are broadly similar to a limited study of lectin staining in three fetal multicystic dysplastic kidneys by Matsell and colleagues (1996). It may therefore appear that most dysplastic tubules and cysts have a ureteric bud origin while a few have a proximal tubule origin. It must be borne in mind, however, that these agglutinins bind to specific glycoproteins which have been well characterised in the adult kidney but not the developing kidney. For example, *Arachis hypogaea* binds to β-gal(1-3) GalNac which has been described in mature distal tubules and collecting ducts (Holthofer *et al.*, 1981), but this glycoprotein has also been reported in proximal tubules at 10 and 13 weeks of gestation (Hanioka *et al.*, 1990). It is therefore difficult to draw any conclusions about cell lineage from the lectin binding data since the aberrant differentiation postulated to underlie dysplastic development may perturb the expression of 'mature' segment markers.

The cells surrounding dysplastic tubules and cysts expressed vimentin and α-smooth muscle actin, but were negative for cytokeratin in both antenatal and post natal dysplastic kidneys. Similar findings were reported recently in antenatal specimens of multicystic dysplastic kidneys (Matsell *et al.*, 1996) and in antenatal samples associated with

220

obstructive uropathy (Daikha-Dahmane *et al.*, 1997). Alpha-smooth muscle actin was also detected in vessel walls, along with endothelial staining for von Willebrand factor and binding of *Ulex europaeus* agglutinin. Interestingly, the main renal arteries and veins connected to dysplastic kidneys were often abnormally small and tortuous but no difference was found between the labeling pattern of small vessels in normal and dysplastic kidneys (data not shown).

The evidence supporting the origin of dysplastic cells from either ureteric bud or mesenchymal lineages is therefore unclear since atypical intermediate filament protein and lectin biding patterns are seen in both tubules and cysts and the surrounding cells. One possible explanation for these findings would be de-differentiation of dysplastic cells leading to expression of misleading lineage markers. Alternatively, both lineages may both contribute to the development of dysplastic structures in a similar fashion to the mesenchymal contribution to developing collecting ducts and ureteric bud contribution to nephrons described by Qiao and colleagues using 'tagged' cells in murine organ culture (1995).

Further characterisation of dysplastic kidneys is therefore required before more definitive statements can be made about cell lineages. For example, specific cytokeratins such as cytokeratin 8 and 18 or cytokeratin 19 have been described in normal epithelial development (Oosterwijk *et al.*, 1990), whilst other intermediate filaments such as desmin could be used as mesenchymal markers. Further studies are also required to determine glycoprotein expression in normal early nephrogenesis in order to interpret the agglutinin binding results in dysplastic kidneys.

Apoptosis

Apoptosis had been described in a number of developmental and pathological contexts but it had not been assessed in the developing human kidney, or in dysplastic kidneys, until this study (Winyard *et al.*, 1996a).

Normal kidneys

In normal human fetal kidneys apoptosis was detected in two main areas, the nephrogenic cortex and the medulla. It was rare in the intermediate zone consisting of relatively mature nephrons. This distribution pattern is similar to that described by Coles and colleagues (1993) in perfusion-fixed kidneys from the rat where the commonest sites for apoptosis were the nephrogenic region and medullary papillae. It has been postulated that apoptotic cell death during development provides a mechanism by which the number, position or proportion of different cell types can be balanced (Jacobson *et al.*, 1997). For example, neurons which fail to develop synaptic connections die by apoptosis in the developing nervous system (Raff *et al.*, 1993). It is therefore possible that apoptosis in the comma and S-shaped bodies controls the number of cells which will constitute the nephron and facilitates its morphogenesis. Similarly, apoptosis may allow regression of the first generations of nephrons and remodeling of the collecting system in the medulla, a process which was reported by both Kampmeier and Potter (See Figs. 5 and 6) many years before apoptosis was defined by Kerr and colleagues (1972).

Isolated metanephric mesenchyme can be rescued from apoptosis in organ culture by both EGF (Koseki *et al.*, 1992) and FGF-2 (Perantoni *et al.*, 1995), whilst HGF increases survival of renal mesenchymal cells in serum-free organ culture (Woolf *et al.*, 1995). The significance of these observations is unclear, however, since I detected minimal

apoptosis in uninduced mesenchyme but a high level of apoptosis in early nephron precursors in normal human kidneys. Interestingly, Coles found that the level of apoptosis could be reduced in the neonatal rat kidney by administration of EGF and it may be that a localised lack of growth factors causes the apoptosis seen in normal development. Aberrations of various growth factors including EGF, HGF and IGFs have also been implicated in dysplastic and polycystic kidneys, as described below.

A low level of apoptosis was found in the tubular epithelia of normal sections of postnatal kidney tissue adjacent to Wilms' tumours. Apoptosis was never observed in glomeruli or interstitial cells in these sections. It could be argued, quite correctly, that these are not 'normal' samples but it is very difficult to obtain completely normal postnatal kidneys and several steps were taken to ensure that confounding issues which may have affected the levels of apoptosis were minimised. Firstly, all of the samples came from newly diagnosed patients in which the majority of WT-1 mutations had been excluded. Secondly, in other studies I performed which are not reported in this thesis, the effects of anaesthetic drugs and surgery were simulated in mice (Winyard et al., 1996a) and no differences were seen between kidneys which were removed either immediately after cervical dislocation, or after anaesthesia with clamping of the renal artery for 10 minutes. And, thirdly, the effects of a delay in fixing the specimens were assessed by comparing kidneys from mice which were processed immediately after death or following storage for 24 hours at 4°C; a statistically significant difference in the level of apoptosis was not detected (Winyard et al., 1996a). Moreover, review of the literature shows that apoptosis does not occur during acute renal ischaemia, although it can be generated by reperfusion (Schumer et al., 1992; Fuerstenberg et al., 1993) which was not a factor in any of these

223

human samples. It is therefore likely that the low levels of apoptosis which were detected in the 'normal' postnatal kidneys examined in this study are not artefactual.

Apoptosis has also been described in pathological conditions, such as glomerulonephritis, in the adult kidney (Savill *et al.*, 1992). In this context, apoptosis is postulated to be beneficial since there is swift phagocytic clearance of intact cells which may protect the tissues from further damage. In other conditions, such as polycystic kidney disease, however, apoptosis has been implicated in the destruction of normal tissues and progression of renal failure (Woo, 1995). The site and extent of apoptosis are, however, different in these pathological conditions and the normal kidneys reported above.

Dysplastic kidneys

I found that apoptotic cell death was increased in both pre- and postnatal dysplastic kidneys when compared to normal kidneys of similar age. The highest levels of apoptosis were detected in loosely-arranged cells distant from cysts and tubules. Apoptosis was rare in fibromuscular collarettes and even rarer in tubule or cyst epithelia. These results have been corroborated by a recent study which examined apoptosis in the dysplastic upper poles of duplex kidneys removed during childhood (Granata *et al.*, 1997): apoptosis was reported at low levels of 1 - 2 cells per 25 high power fields in the tubules and at a higher level of 5 - 8 cells per 25 high power fields in the mesenchyme. In the absence of compensatory high levels of proliferation (see below), the high levels of apoptosis detected in poorly differentiated areas between dysplastic tubules and cysts is likely to lead to a reduction in the number of cells in these areas. This may be one of the molecular mechanisms underlying the well documented spontaneous involution of dysplastic kidneys (Dungan *et al.*, 1990; Mesrobian *et al.*, 1993; Al-Khaldi *et al.*, 1994) and Fig. 8 of this thesis.

224

DNA laddering was only found in two of the three dysplastic kidneys examined, a somewhat surprising result since apoptosis was detected histologically in all of these samples. One possible explanation for this finding is that it has been reported that DNA is sometimes broken down into large fragments during apoptosis which cannot be visualised by the laddering technique (Bortner *et al.*, 1995). Alternatively, the fragment used for DNA extraction may have contained levels of apoptosis which were too low to detect by this technique since apoptosis was sometimes patchy within the samples. In future experiments, the sensitivity of detection could be increased by end-labeling the DNA fragments with a radio-labeled nucleotide and detecting the bands by autoradiography (Rosl, 1992).

Several of the dysplastic kidneys examined in this thesis drained into an obstructed urinary system and experimental obstruction during development has been implicated in causing renal dysplasia by some, but not all, investigators (Beck, 1971; Berman and Maizels, 1982; Steinhardt *et al.*, 1988). The occurrence of cell death was not, however, reported in these studies and I did not find any difference in the levels, or sites, of apoptosis between obstructed and non obstructed systems in the prenatal samples. Experimental ureteral obstruction has been reported to cause increased apoptosis in the perinatal and postnatal period (Kennedy *et al.*, 1994; Truong *et al.*, 1996; Chevalier *et al.*, 1996), however, but once again there was no correlation between obstruction and apoptosis in my human samples. In order to investigate the potential link between obstruction and dysplasia, our group has recently performed unilateral ureteric obstruction in the mid gestation fetal sheep (Attar *et al.*, 1998). We found that there was gross disruption of nephrogenesis with cyst formation, particularly glomerular cysts, but metaplastic cartilage was not detected. Increased levels of apoptosis were found between the

225

cysts with upregulation of pax-2 and increased proliferation in cyst epithelia. Interestingly, these abnormalities were generated after only 10 days of obstruction whereas obstruction was much more prolonged in the human samples examined. This may provide the explanation for the lack of benefit observed with many urinary diversion procedures *in utero* (Freedman *et al.*, 1996) since the normal pattern of nephrogenesis would already have been disrupted by the time of the procedure. It is also possible to speculate that there may have been transient, undetected obstruction in some of the cases which caused irreversible perturbation of development but then recovered.

Polycystic kidneys

High levels of apoptosis were also found in samples of polycystic kidney disease, both during and after completion of nephrogenesis. Seven of the eight samples examined were ARPKD although increased apoptosis has also been reported in patients predominantly with ADPKD (Woo, 1995). Apoptosis was not simply a non specific epiphenomenon of aberrant renal biology, however, since the sites of apoptosis were quite distinct in polycystic and dysplastic kidneys.

Apoptotic nuclei were commonly noted in cystic epithelia, a rare site for apoptosis in dysplastic kidneys. Apoptosis may have an important role in cystogenesis in this context since mice with null mutations of bcl-2 have fulminant metanephric apoptosis and develop cystic kidneys (Veis *et al.*, 1993; Sorenson *et al.*, 1995).

Increased apoptosis has also been described in conjunction with aberrant cell-matrix adhesion *in vitro* (Frisch and Ruoslahti, 1997) and abnormal matrix production has been described in polycystic kidneys *in vivo* (Wilson *et al.*, 1992). Moreover, polycystin 1, the product of the PKD1 gene is believed to be involved in cell-matrix interactions, although this may not be directly relevant to most of our samples since

226

the gene responsible for ARPKD has not been cloned and its exact function is therefore unknown (Zerres *et al.*, 1994).

Epithelial hyperproliferation has been described in polycystic kidneys (Grantham, 1992; Nadasdy *et al.*, 1995) and, although it was not formally examined in polycystic samples during this thesis, it is of note that apoptotic cells were often observed directly adjacent to heaped up layers of proliferating epithelial cells. The underlying cause of increased proliferation is unknown although, intriguingly, expression of factors such as the proto-oncogene c-myc can cause both proliferation and apoptosis in cell culture depending on the concentrations of growth factors (Harrington *et al.*, 1994). In addition, transgenic mice which overexpress c-myc develop renal cysts (Trudel *et al.*, 1991) and enhanced expression of c-myc occurs in *cpk/cpk* mice (Cowley *et al.*, 1987; Harding *et al.*, 1992). Taken together with the reported imbalance of egf in the *cpk/cpk* mice (Gattone *et al.*, 1990; Horikoshi *et al.*, 1991; Richards *et al.*, 1998) and HGF in human polycystic kidney diseases (Horie *et al.*, 1994), expression of factors such as C-MYC may provide a mechanism for both increased proliferation and apoptosis in cyst epithelia.

Pyknotic nuclei were also detected in the interstitial tissue around undilated tubules of ARPKD, an area where apoptosis was rarely found in normal postnatal kidneys, and in undilated tubules between large distal cysts. Destruction of these relatively normal tissues by apoptosis may therefore contribute to the destruction of functional renal tissue, whilst the cell proliferation described above and reported fluid secretion into cysts (Grantham, 1992) may lead to growth in size of the whole polycystic kidney.

Proliferation

Normal kidneys

The mature adult kidney develops from the metanephros which consists of less than a thousand cells at its inception in the fifth week of gestation (personal observation). It is not surprising, therefore, that there is extensive proliferation in the developing kidney but, interestingly, in this study proliferation was confined almost exclusively to the outer nephrogenic cortex. This rim of tissue is the site for new nephron formation throughout nephrogenesis. PCNA positive cells were detected in the branching tips of the ureteric bud, condensing mesenchyme and early nephron precursors such as the vesicles, comma and S-shaped bodies. PCNA expression was rapidly downregulated as the nephrons matured. This expression pattern correlated exactly with the distribution of PAX-2 protein and this relationship will be discussed later. A low level of proliferation was also detected in mature kidneys and this may be balanced by the low level of apoptosis.

These results are consistent with reports of PCNA staining in mice kidneys (Hanai *et al.*,1993) and proliferative activity in normal mature human kidneys (Laurent *et al.*, 1988; Nadasdy *et al.*, 1995).

Dysplastic kidneys

PCNA positive cells were found at high levels in both the tubules and cysts in dysplastic kidneys, again correlating with PAX-2 expression (see below). This high point prevalence suggests that epithelial cell proliferation may be an important part of the biology of dysplastic cyst formation, as it is in polycystic cystogenesis (Grantham, 1992; Nadasdy *et al.*, 1995). It is interesting, however, that apoptosis was much rarer in dysplastic than polycystic cyst epithelia since the same size cyst, in terms of cell numbers, could therefore be theoretically

228

generated with less proliferation in a dysplastic kidney. Further work is required to define whether dysplastic epithelia have an intrinsically higher proliferative activity than normal epithelia, or whether the higher levels of proliferation are caused by extrinsic factors such as the excess or imbalance of growth factors. These questions could be addressed by culturing isolated epithelial cells from dysplastic kidneys or by dissecting out and culturing intact cyst epithelia.

PAX-2, WT-1, BCL-2 and galectin-3 distribution in normal and dysplastic kidneys

PAX-2

In the metanephros, PAX-2 was detected in the tips of the ureteric bud and early nephron precursors, cell populations which are undergoing critical morphogenetic events such as mesenchymal / epithelial transition and branching morphogenesis. It was then down regulated in more mature structures. These expression domains are consistent with those reported for mouse pax-2 mRNA (Dressler et al., 1990) and protein (Dressler et al., 1992) and human mRNA (Eccles et al., 1992).

It was rare to identify nuclei which were positive for PAX-2 in the normal kidney in the postnatal period. In contrast, virtually all of the tubules and cysts expressed PAX-2 in dysplastic kidneys, both before and after birth. The intensity of staining for PAX-2 in these tubules and cysts was the highest detected in any of the samples. This finding, in conjunction with the report that primary overexpression of PAX-2 causes cysts in mice kidneys (Dressler et al., 1993), strongly implicates PAX-2 in cyst formation in dysplastic kidneys.

WT-1

The WT-1 protein was first detected in renal condensates and vesicles in this study, where staining was faint (Winyard *et al.*, 1996b). This result contrasts with another human study where low levels of WT-1 protein were detected in the renal mesenchyme but not in vesicles (Mundlos *et al.*, 1993) and a murine study where little protein expression was found in condensing renal mesenchyme (Ryan *et al.*, 1995). Different antibodies were used in each of these studies: I used an antibody raised against the carboxyterminus of WT-1, whereas Mundlos and colleagues used an antibody raised against the first alternative spice site of WT-1 and Ryan and colleagues used an antibody raised against amino acids 1 - 179 of mouse wt-1. These differences in expression pattern could possibly be attributed to recognition of different isoforms of WT-1 by the different antibodies. An alternative explanation is that the staining technique which I used is more sensitive since I used heat pre-treatment of the sections which reportedly allows 'antigen unmasking' (Shi *et al.*, 1991). This explanation seems more likely because homozygous wt-1 null mutant mice have absent kidneys due to lack of induction and subsequent apoptosis of renal mesenchyme (Kreidberg *et al.*, 1993) which appears to suggest that the low levels of WT-1 protein, which I detected in humans at the condensate or vesicle stages, are biologically important.

In accord with previous studies (Mundlos *et al.*, 1993; Ryan *et al.*, 1995), I observed that the level of WT-1 increased as the S-shaped bodies developed, and became restricted to the podocytes in maturing and adult glomeruli. This contrasts with dysplastic kidneys, where the WT-1 protein was detected in a large proportion of the cells around dysplastic tubules and cysts. It was never convincingly demonstrated in dysplastic epithelia.

BCL-2

The BCL-2 protein was detected in condensing renal mesenchyme and early nephron precursors in this study (Winyard *et al.*, 1996b). It was then downregulated in the maturing nephrons, aside from faint immunoreactivity in the loops of Henle. This result concurs with the general descriptions of BCL-2 in human (LeBrun *et al.*, 1993) and murine development (Novack and Korsmeyer, 1994). It is also consistent with a role for this gene in preventing apoptosis in early nephron precursors since bcl-2 null mutant mice are born with hypoplastic kidneys and metanephric growth in organ culture is restricted due to apoptosis (Sorenson *et al.*, 1995).

BCL-2 expression was not detected in normal mature kidneys. In dysplastic kidneys, however, BCL-2 was expressed in the majority of tubular epithelial cells and nearly 100% of cells in cystic epithelia. This report is consistent with BCL-2 expression described in abstract form by a Japanese group (Nagata *et al.*, 1998). This is further evidence that dysplastic epithelia express markers / proteins which are not normally expressed by the ureteric bud lineage (see *Cell lineages in dysplastic kidneys* above).

Galectin-3

I detected galectin-3 protein in both the mesonephros and metanephros in the human (Winyard *et al.*, 1997). Its expression domain was confined almost exclusively to the epithelia of the mesonephric duct, the ureteric bud and its derivatives. These findings are in general accord with, but much more detailed than, a recent report of galectin-1 and galectin-3 in the developing human kidney published during preparation of this thesis (Van den Brule *et al.*, 1997) and a study in rodents which described galectin-3 expression in tubules in the late nephrogenic period (Foddy *et al.*, 1990). Our group has also shown, in preliminary work, that galectin-3 mRNA is

detectable from embryonic day 11 and levels of galectin-3 protein peak at embryonic day 15 - 16 in the developing mouse kidney (Woolf *et al.*, 1996).

In the mesonephros and branching tips of the ureteric bud, galectin-3 was detected in the apical plasma membrane. Later in development the protein was detected in the cytoplasm and also lateral and basal plasma membranes of medullary and papillary collecting duct cells. Finally, in mature collecting ducts, galectin-3 was detected in the cytoplasm of α-intercalated cells. Theoretically, this distribution pattern may not reflect the cells which produce galectin-3 since the protein may be secreted (Sato *et al.*, 1993). If the protein was synthesised elsewhere, however, one would have to postulate that it was secreted, transported and then relocated to the specific domains described above. There is no evidence in favour of this hypothesis and it therefore appears more likely that the positive cells produce galectin-3. Definitive proof would, however, require *in situ* hybridisation studies.

In dysplastic kidneys, galectin-3 was markedly upregulated in cyst epithelia with virtually every cell expressing galectin-3 in the apical plasma membrane. A similar degree of upregulation was seen in ARPKD epithelia, although the distribution pattern was not polarised.

Roles of PAX-2, WT-1, BCL-2 and galectin-3 in human renal development

I have described both the temporal and spatial distribution of apoptosis and proliferation, and the expression domains of PAX-2, WT-1, BCL-2 and galectin-3 in normal and dysplastic human renal development in the experiments reported in this thesis, which are summarised in Figure 53. This data, in conjunction with functional studies in animals, is shown in Table 10 and discussed below and in an attempt to better understand the aberrations of biology involved in the pathogenesis of dysplastic renal malformations.
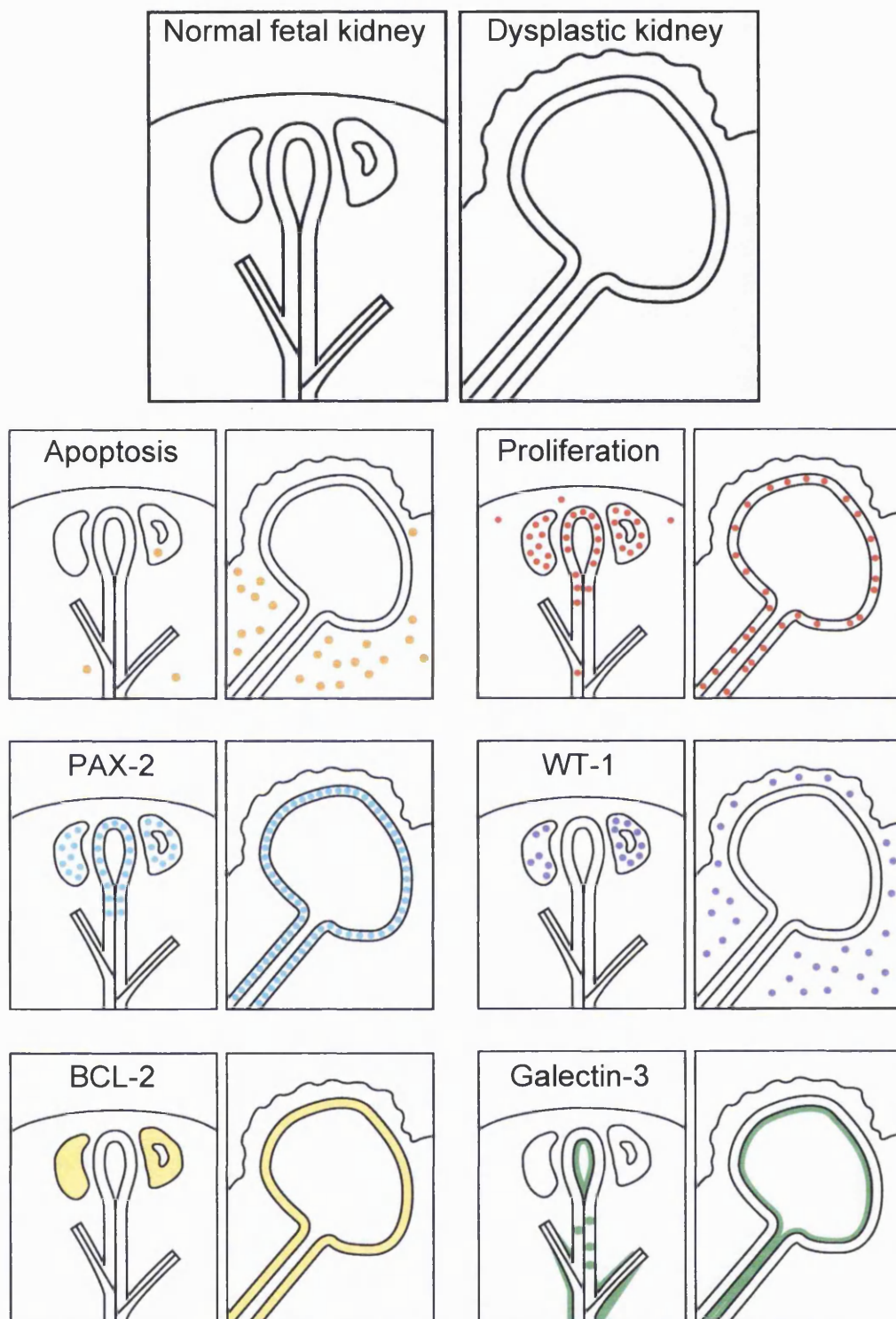
Figure 53. Apoptosis, proliferation and protein expression in normal fetal and dysplastic kidneys. Schematic representation showing cell turnover and protein expression in human normal fetal and dysplastic kidneys. Apoptosis was assessed by propidium iodide staining and end-labeling, proliferation by PCNA staining and protein distribution by immunohistochemistry.

234

Gene	Product	Location
Intermediate filaments		
Vimentin	protein	dysplastic tubules, collars and undifferentiated cells around tubules
Cytokeratin	protein	dysplastic tubules and cyst epithelia
Alpha-smooth muscle actin	protein	collars around dysplastic tubules
Transcription factors		
WT-1	protein	collars and undifferentiated cells around dysplastic tubules
PAX-2	protein	dysplastic tubules and cyst epithelia
Survival factors		
BCL-2	protein	dysplastic tubules and cyst epithelia
Growth factors / growth factor receptors		
HGF	protein	dysplastic tubules, surrounding cells and cyst fluid (Kolatsi-Joannou et al., 1997)
MET (HGF receptor)	protein	dysplastic tubules and cyst epithelia (Kolatsi-Joannou et al., 1997)
IGF-2	mRNA	collars and cells around dysplastic tubules (Matsell et al., 1997)
	protein	cyst epithelia (Matsell et al., 1997)
IGF binding protein-2	mRNA, protein	cyst epithelia (Matsell et al., 1997)
Cell adhesion molecules		
α1 integrin subunit	protein	cyst epithelia (Daikha-Dahmane et al., 1997)
α2 and α6 integrin subunits	protein	dysplastic tubules and cyst epithelia (Daikha-Dahmane et al., 1997)
Galectin-3	protein	apical location in dysplastic tubule and cyst epithelia
Miscellaneous		
PCNA	protein	nuclei of 10 – 50% of dysplastic tubule and cyst epithelial cells

Table 10. Gene expression in human dysplastic renal malformations. A summary of the current literature on gene expression in human dysplastic kidneys. References are given for results which were not obtained in this thesis.

Ureteric bud lineage

Ampullae

Active proliferation, but very little apoptosis, was detected in ampullae of the human ureteric bud. PAX-2 was strongly expressed in this site and upregulation of PAX-2 was always seen in areas of proliferation in both normal and abnormal human kidneys. A similar expression pattern occurs in the mouse, where pax-2 appears to be essential for further development of this lineage (Torres *et al.*, 1995). The constant association between PAX-2 expression and proliferation is consistent with a role for pax-2 in cyst formation when it is overexpressed (Dressler *et al.*, 1993) and also with the potential role of PAX genes in oncogenesis (Maulbecker and Gruss, 1993).

Galectin-3 was also expressed in ureteric bud ampullae, where the protein was detected predominantly in the apical domain of the epithelium. It is difficult to envisage an active role for galectin-3 in cell-matrix interactions, or mRNA splicing in this location. Similarly, a role in cell survival seems unlikely but must be considered because these cells do not express BCL-2, yet apoptosis was virtually never detected in this site. It is possible, on the one hand, that the cells express other anti-death molecules (e.g. BCL-X$_L$) or have lower levels of apoptosis-inducing molecules (e.g. BAX) (Oltvai *et al.*, 1993) although this has yet to be reported. On the other hand, galectin-3 may be implicated in cell survival at this site since transgenic overexpression in T-cells makes them resistant to apoptosis (Yang *et al.*, 1996) and the galectin-3 protein contains an NWGR amino acid sequence which is highly conserved in the BH-1 domain of the BCL-2 family (Akahani *et al.*, 1997). Increased expression of galectin-3 protein has also been reported in proliferating cells (Moutsatsos *et al.*, 1987; Agrwal *et al.*, 1989) although the subcellular location of galectin-3 was unfortunately not reported in these experiments.

There are undoubtedly other molecules involved in controlling the proliferation of cells in ureteric bud ampullae. These include renal mesenchymal-derived paracrine factors such as GDNF and HGF which signal through specific receptor tyrosine kinases such as RET (Towers *et al.*, 1998) and MET (Woolf *et al.*, 1995) located on the basal surface of these cells. Therefore, although the present study reinforces the importance of PAX-2 in normal human development, it is difficult to be certain about the true role of galectin-3, especially since its expression later in development in the collecting duct lineage does not correspond to areas of proliferation.

Collecting ducts

Collecting ducts are derivatives of ureteric bud ampullae and their development was characterised by a low level of both proliferation and apoptosis. WT-1 and BCL-2 were not expressed in these structures. PAX-2 was rapidly downregulated in maturing collecting ducts which suggests that molecules other than WT-1 switch off PAX-2 in this lineage (Ryan *et al.*, 1995). Galectin-3 was, however, detected in both developing and mature collecting ducts. At mid gestation galectin-3 was expressed in the cytoplasm and also the lateral and basal plasma membranes of medullary and papillary collecting duct cells. In the latter location the protein would be well placed to interact with laminin-1, a molecule which coats embryonic kidney epithelia and which has been implicated in epithelial morphogenesis by organ culture experiments (Klein *et al.*, 1988b). Indirect evidence for such an interaction comes from culture of MDCK cells in collagen type 1 gels where galectin-3 co-localises with laminin on the basal surface of developing cysts (Bao and Hughes, 1995). In this setting, addition of recombinant galectin-3 to the medium slows cyst expansion, whilst blocking antibodies enhance cyst growth (Bao and Hughes, 1995).

It is therefore possible that interaction between galectin-3 and matrix might regulate collecting duct growth *in vivo*. Moreover, preliminary data using mouse organ culture from our laboratory suggests that addition of recombinant galectin-3 perturbs epithelial morphogenesis (Woolf *et al.*, 1996).

In the postnatal, mature kidney galectin-3 was detected in a subset of tubular cells in the cortex and medulla where staining was predominantly cytoplasmic, although it was difficult to rule out a membranous distribution. Staining with *Arachis hypogaea* identified the tubules as collecting ducts (Holthofer *et al.*, 1981) and with band 3 identified the positive cells as α-intercalated cells (Tanner, 1996). A membranous location could be important in maintaining collecting duct integrity, whereas it would again be difficult to ascribe a function to cytoplasmic galectin-3. In either case, however, it is uncertain why it is only the acid secreting α-intercalated cells which expressed galectin-3. There is some evidence from *in vitro* experiments using mice collecting duct cells that β-intercalated cells can give rise to both α-intercalated and principal cells (Fejes-Toth and Naray-Fejes-Toth, 1992) and it would be interesting to examine galectin-3 expression during this process. In future it will also be interesting to examine the phenotypes and function of collecting duct cells in mice which are null mutants for galectin-3, although preliminary reports suggest that gross renal development is normal in these animals (personal communication – Professor Poirier, Institut Cochin de Genetique Moleculaire, Paris, France).

Mesenchyme lineage

Uninduced mesenchyme

The uninduced mesenchyme was characterised by a low prevalence of proliferation and apoptosis, and none of the genes examined in this study were expressed in cells in this area. Interestingly, in the mouse, c-myc is expressed in the uninduced mesenchyme (Mugrauer and Ekblom, 1991) but it does not appear to be associated with either proliferation or apoptosis in this site. The lack of proliferation is consistent with the reported expression of the p57-kip2 gene in 'stromal' cells, along with glomerular podocytes, during nephrogenesis (Zhang *et al.*, 1997). This gene is a cyclin kinase inhibitors which blocks proliferation by binding to the kinases in G1 / S phase. The bf-2 gene is also expressed in uninduced mesenchyme and this transcription factor is essential for normal development since mice with null mutations have rudimentary, fused kidneys and die soon after birth (Hatini *et al.*, 1996). Bf-2 is thought to modulate expression of a factor or factors from the 'uninduced' cells which is essential for further development of the ureteric bud and maturation of pretubular aggregates. This factor(s) has not yet been identified.

Condensed mesenchyme

The condensed mesenchyme had a high prevalence of proliferation and a very low prevalence of apoptosis. These findings are consistent with the fact that the highest levels of PAX-2 and BCL-2 protein detected in normal renal development were found in these cells. Pax-2 is known to be essential for mesenchymal condensation in murine organ culture since antisense pax-2 DNA oligonucleotides block this process (Rothenpieler and Dressler, 1993) and metanephroi fail top develop in pax-2 homozygous null mutant mice. BCL-2 expression, on the other hand, cannot be absolutely required since some nephrons,

albeit in reduced numbers, are formed in bcl-2 knockout mice (Veis *et al.*, 1993; Sorenson *et al.*, 1995). It may be that other members of the BCL-2 family can partially compensate for its loss in this site, although this has not been reported in detail.

Low levels of WT-1 were also found in condensed mesenchyme. WT-1 expression at this site must be essential for normal development since the mesenchyme fails to condense around the ureteric bud and dies by apoptosis in wt-1 homozygous null mutant mice (Kreidberg *et al.*, 1993). Interestingly, wt-1 isoforms have been shown to bind to multiple sites in the murine syndecan-1 promoter and function as transcriptional activators of syndecan-1 expression in transient transfection assays (Cook *et al.*, 1996). This potential relationship is mirrored by the expression pattern of this proteoglycan which is detected at low levels in uninduced mesenchyme and then strongly upregulated in condensing mesenchyme in the mouse (Vainio *et al.*, 1989), although I did not look at its distribution in this study.

Nephron formation

An increased prevalence of apoptosis and lower levels of proliferation characterised comma and S-shaped bodies. These findings correlated with, and may be explained by, downregulation of BCL-2 and PAX-2. At the same stage, WT-1 was upregulated in developing glomerular podocytes. This inverse relationship between WT-1 and PAX-2 in humans is consistent with the suggestion by Ryan and colleagues (1995) that increased wt-1 expression leads to downregulation of pax-2 in mice.

Low levels of both apoptosis and proliferation were seen in later nephron development where PAX-2 was not detected, BCL-2 expression was confined to occasional loops of Henle and WT-1 was restricted to glomerular podocytes.

Dysplastic kidneys

Dysplastic kidneys are characterised by the presence of primitive ducts surrounded by fibromuscular collars, often with nests of metaplastic cartilage. Several authors have hypothesised that the primitive ducts are malformed branches of the ureteric bud whilst the surrounding tissues represent uninduced metanephric mesenchyme. This hypothesis is based almost exclusively on the histological resemblance between these tissues and little is known about the molecular biology of renal dysplasia. In this thesis, I have therefore examined several aspects of the cell biology of dysplastic kidneys and compared them with normal developing and mature kidneys.

Specific patterns of proliferation and apoptosis were detected in dysplastic kidneys, which broadly correlated with the differential expression of the important nephrogenic molecules PAX-2, WT-1, BCL-2 and galectin-3. The distribution of proliferation and apoptosis also provides a potential molecular explanation for both cyst formation and involution of dysplastic kidneys. These findings are discussed below and shown diagrammatically in Table 10.

Dysplastic epithelia

High levels of proliferation and low levels of apoptosis were detected in the epithelia of dysplastic tubules and cysts at all ages examined. A similar pattern was observed in the normal ureteric bud, but both proliferation and apoptosis were rare in the mature kidney.

Dysplastic tubules and cysts from both preterm and postnatal kidneys expressed high levels of PAX-2. Lower levels of PAX-2 protein were detected in the tips of the normal ureteric bud and it was then downregulated in the mature kidney. The sites and intensity of PAX-2

staining always appeared to correlate directly with the extent of proliferation in this study. Overexpression of PAX-2 has also been shown to cause renal cysts in mice (Dressler *et al.*, 1993). The persistent high levels of PAX-2 expression in dysplastic epithelia are therefore likely to be an important factor in cyst formation.

Galectin-3 immunoreactivity was detected in virtually all of the cells in dysplastic epithelia. The protein was located in the apical plasma membrane, which was similar to the normal ureteric bud. In dysplastic kidneys, however, this pattern was seen in both prenatal and postnatal specimens, whereas galectin-3 was restricted to collecting duct α-intercalated cells in normal mature kidneys. This distribution pattern, along with the increased proliferation described above, would be consistent with immature development of the dysplastic epithelia. It is, however, interesting to speculate on the potential role of apical galectin-3 in both dysplastic and normal developing kidneys. It may, for example, have no function in this location. Alternatively, it may be the lack of basal or basolateral distribution which is important, since galectin-3 would be unable to interact with matrix molecules. In this case, there is a parallel with polycystic kidney disease since abnormal cell-matrix interactions have been described in both ARPKD and ADPKD. Galectin-3 was also upregulated in the polycystic samples examined in this thesis and a recent report described aberrant expression of alpha-integrin subunits in dysplastic and polycystic kidneys (Daikha-Dahmane *et al.*, 1997). In addition to these potential roles for galectin-3, this protein may also have a primary role in proliferation and / or in preventing apoptosis.

BCL-2 was also expressed in the majority of dysplastic tubules and nearly 100% of cells in cystic epithelia, at all ages examined. This is an important finding because dysplastic epithelia represent an ectopic site of distribution, since BCL-2 was not expressed in the ureteric bud lineage

242

during normal nephrogenesis. Hence, aberrant gene expression in these epithelia cannot be solely attributed to immaturity. Expression was also prolonged, since this protein was not detected in normal mature kidneys. This report is consistent with reported BCL-2 expression in cystic kidneys described in abstract form by a Japanese group (Nagata *et al.*, 1998). Persistent BCl-2 expression is likely to protect the cells in the dysplastic epithelia from apoptosis, which may be crucial for cyst formation.

Fibromuscular collarettes and loose 'dysplastic mesenchyme'

Rare proliferation and occasional apoptosis were detected in the fibromuscular collarettes immediately adjacent to tubules / cysts. This was similar to the high levels of proliferation detected at the early condensate stage and lower levels of apoptosis in the later comma and S-shaped body stage of normal kidneys. The loosely arranged 'mesenchymal' cells in dysplastic kidneys had low levels of proliferation with high levels of apoptosis, whereas normal uninduced mesenchyme had low levels of both proliferation and apoptosis.

Cells in both the fibromuscular collarettes and loose 'mesenchyme' expressed WT-1 protein, but they did not express PAX-2, BCL-2 or galectin-3. In normal kidneys by contrast, WT-1 was expressed in condensed mesenchyme but not uninduced mesenchyme. Expression of WT-1 could therefore be considered to be a marker of induction in normal kidneys. A further signal must be required, however, for the WT-1 expressing cells to undergo mesenchyme to epithelial transformation and develop into nephrons. PAX-2 and BCL-2 may be important in this context since these molecules were coexpressed in normal induced mesenchyme but absent in 'dysplastic mesenchyme'. Animal experiments support the importance of these factors since pax-2 is essential for the mesenchyme to epithelial transformation in organ culture

243

(Rothenpieler and Dressler, 1993) and decreased nephron numbers are observed in bcl-2 knockout mice (Sorenson *et al.*, 1995).

In view of the correlation between PAX-2 levels and proliferation, the absence of PAX-2 protein in fibromuscular collarettes and more loosely arranged 'dysplastic mesenchyme' may explain their low levels of proliferation, when compared to condensed mesenchyme in normal kidneys. Similarly, lack of BCL-2 in these areas may explain the increased apoptosis, although other factors must be important since this molecule was not detected in either the collarettes or the loose mesenchyme, yet cell death was much commoner in the latter site. One explanation for this finding could be that the collarette cells, which express α-smooth muscle actin, have undergone myofibroblastic differentiation and that this may reduce the extent of apoptosis compared to the relatively undifferentiated 'mesenchymal' cells. Other members of the BCL-2 family which predispose to apoptosis may also be expressed in these sites, although the distribution of these molecules has not yet been reported in dysplastic kidneys.

Molecular biology and natural history of dysplastic kidneys

The aberrations of molecular biology which I have described in dysplastic kidneys provide a potential explanation for several aspects of their natural history.

For example, expression of PAX-2, galectin-3 and BCL-2 in 'immature' dysplastic epithelia may result in high levels of proliferation and low levels of apoptosis. Persistent expression of this combination of proliferative and survival signals would then be expected to promote cyst development. It may also predispose to the genesis of tumours, although there is no convincing evidence that these are significantly more common in dysplastic kidneys.

Similarly, WT-1 expression in fibromuscular collarettes and loose 'mesenchyme' implies that the cells have received an induction signal, but the lack of PAX-2 and BCL-2 may cause them to undergo apoptosis rather than mesenchyme to epithelial transformation. This is likely to be the molecular mechanism for the involution of dysplastic kidneys.

It is more difficult, however, to explain the failure of branching of the ureteric bud and ineffective nephron formation, which is the fundamental defect in dysplastic kidneys. Similar genes were expressed in dysplastic and normal tissues but there were a number of differences which are difficult to explain on the basis of this study. Why, for example, were PAX-2 and galectin-3 upregulated, and BCL-2 ectopically expressed in dysplastic epithelia or why were PAX-2 and BCL-2 not expressed in dysplastic 'mesenchyme' ?

There are several possible explanations for these findings. For example, perturbed expression of other molecules has been reported in dysplasia, including MET and its ligand HGF (Kolatsi-Joannou et al., 1997) and IGF-2 and IGF-2 binding protein (Matsell et al., 1997). Perturbed expression of additional, as yet unidentified factors, may also be involved. Moreover, obstruction of the ureteric tract mimics some of the features of dysplasia (Attar et al., 1998) and exposure to teratogens may be contributory.

The pathogenesis of dysplasia is therefore likely to be multifactorial with a variable contribution from genetic factors, physical obstruction, teratogens and stochastic events. It would be very difficult to determine the exact importance of each of these factors in vivo in humans and this provides the rationale for my preliminary work on the culture of cells from dysplastic kidneys which is discussed below. Further cell culture and functional experiments will be an integral part of my future work, which aims to develop therapies to correct dysplastic nephrogenesis.

Cell lines

In this study I showed that it is feasible to grow cells from dysplastic kidneys in primary culture, the first report describing culture of these cells. The morphology of the cultured cells was similar to their tissue of origin: two of the cultures from kidneys which consisted mostly of poorly differentiated cells had a predominantly mesenchymal / fibroblastic morphology and one sample derived from a kidney containing numerous dysplastic epithelial structures had a predominantly epithelial phenotype. This morphology was maintained after one passage and aliquots of these cells have been stored for repeat culture at a later date. Two of the samples were transduced with a potentially immortalising SV40 large T antigen and were subsequently shown to produce this protein. The morphology of the cells appeared unchanged after one further passage, but it is too early to say whether these cells will continue to divide and / or go through the so called 'blast crisis' to generate truly immortalised cell lines (Bryan and Reddel, 1994).

Our group has previously cultured conditionally immortal cells derived from the kidney of a mouse transgenic for temperature-sensitive SV40 T antigen (Woolf *et al.*, 1995; Kolatsi-Joannou *et al.*, 1995). In these experiments it was possible to establish clonal cell lines with defined epithelial or mesenchymal characteristics. At this stage, it is impossible to say whether clonal cell lines with different characteristics can be generated from human dysplastic cells, but further growth and characterisation of these cells is an important part of my planned *Further work* described in the next chapter of this thesis.

Summary of thesis

In this thesis I have made a number of novel observations on apoptosis and proliferation in normal and dysplastic developing human kidneys, and correlated these findings with a detailed description of the distribution of proteins including PAX-2, WT-1, BCL-2 and galectin-3.

In normal developing kidneys, proliferation was prominent in the nephrogenic cortex whilst apoptosis was mainly detected in early nephron precursors and in the medulla. PAX-2 was expressed in actively proliferating cells in both ureteric bud ampullae and condensing mesenchyme whereas WT-1 and BCL-2 were solely detected in the condensing mesenchyme and developing nephrons. Galectin-3 was restricted to the ureteric bud lineage, with an apical distribution in the branching tips of the ureteric bud and a non polarised cytoplasmic / membranous distribution in the developing collecting ducts.

In the normal mature kidney low levels of proliferation and apoptosis were detected and both PAX-2 and BCL-2 were downregulated. WT-1 expression, however, persisted in podocytes and galectin-3 became restricted to the α-intercalated cells, in the collecting ducts.

In contrast, in dysplastic kidneys, the location of apoptosis and proliferation and the distribution of PAX-2, WT-1, BCL-2 and galectin-3 did not change between prenatal and postnatal specimens.

Proliferation was prominent in dysplastic tubules and cysts, which are thought to be derived from the ureteric bud. PAX-2 and galectin-3 were expressed at high levels in these epithelia, the latter in an 'immature' apical distribution. BCL-2 was also detected in dysplastic epithelia and this represents an ectopic site of distribution, since BCL-2 protein is confined to mesenchymal derivatives during normal nephrogenesis.

247

Therefore, cyst formation in dysplastic kidneys may be potentially explained by the combination of continuous proliferation signals and ectopic survival factors in these epithelia. It is, however, difficult to envisage how these aberrant signals could cause failure of ureteric bud branching.

Apoptosis was prominent in the loosely arranged cells surrounding dysplastic epithelia. These cells are considered to be 'mesenchymal' in origin and they expressed WT-1, which is a marker of induced mesenchyme during normal development. They did not, however, express other markers of induced mesenchyme such as PAX-2 or BCL-2. This suggests that these factors are essential for precursor survival and proliferation during nephron formation.

Dysregulation of cell survival and proliferation in dysplastic kidneys may also provide a molecular explanation for both the spontaneous involution and malignant change which have been reported in dysplastic kidneys. It is, however, uncertain whether intrinsic abnormalities such as mutations in the genes examined in this thesis or other genes, or extrinsic factors such as teratogens or urinary tract obstruction cause the aberrant gene expression which I observed in dysplastic kidneys. Therefore, in preliminary experiments, I have cultured cells from dysplastic kidneys, transduced them with a potentially immortalising gene construct and plan to use these cells in the future for a detailed analysis of the molecular biology of human renal malformations.

Chapter 12. Further Work

The ultimate goal of this work is to define the molecular abnormalities which cause human renal dysplasia and develop therapies to correct them. This strategy demands a much greater knowledge of both normal and dysplastic human kidney development. In this way, it may be possible to identify a common final pathway by which heterogeneous underlying disorders cause dysplastic development, and hence therapies could be targeted to this pathway. A number of different, but complementary avenues of further work should be considered, as detailed below.

Human gene expression studies

A number of genes have been implicated in, and found to be essential for, murine kidney development. Aberrant expression of these genes may also occur in dysplastic kidneys, yet few have been studied in this context. One further study, should therefore be to define the expression pattern of these genes in human dysplastic kidneys, once again comparing them to normal human renal development. Important genes which have been identified to date include wnt-4 (Stark *et al.*, 1994), RARs (Mendelsohn *et al.*, 1994), ros (Kanwar *et al.*, 1995), ret (Schuchardt *et al.*, 1994), epidermal growth factor receptor (Threadgill *et al.*, 1995) and myc (Mugrauer and Ekblom, 1991). In addition, other molecules in the BCL-2 family such as BAX, $BCL-X_L$, $BCL-X_s$ (Knudson and Korsmeyer, 1997) should be investigated.

Functional experiments in animal nephrogenesis

Metanephric organ culture provides an ideal milieu in which to test whether perturbation of specific molecules causes aberrant development. In the context of this thesis, further experiments are required to define the precise role of galectin-3 such as assessing the effects of both specific

blocking antibodies and exogenous galectin-3 on nephrogenesis. In the wider context, similar organ culture experiments should be performed in order to assess whether it is possible to rescue normal nephrogenesis in abnormal kidneys by manipulating other important nephrogenic molecules. For example, one could culture cystic kidneys from *cpk/cpk* or bcl-2 knockout mice and assess the effects of blocking apoptosis, or kidneys from the galectin-3 knockout mice which reportedly have normal gross renal development (personal communication – Professor Poirier, Institut Cochin de Genetique Moleculaire, Paris, France).

Some elements of dysplasia can be mimicked in the sheep by obstruction of the ureters at mid gestation, and our group have already examined apoptosis, proliferation and pax-2 expression in this model (Attar *et al.*, 1998). Further experiments are needed, however, to define the expression of other genes in this system and to determine whether it is possible to modify the effects of obstruction in a similar fashion to the organ culture experiments described above.

Culture of cells from human dysplastic kidneys

Cells from dysplastic kidneys were cultured and transduced with a retroviral construct which expresses the large T antigen as the final part of this thesis. Many more cell passages are required in order to determine whether these cells can be immortalised and to establish clonal cell lines with specific phenotypes. Moreover, this process must be repeated with several more dysplastic kidneys in order to ensure that representative cell lines are derived. The next step would then be to determine the response of these cell lines to exogenous factors in order to determine whether the cells have the potential for normal epithelial or mesenchymal development, and to identify the most important factors in this process. In this way, molecules which stimulate normal growth *in vitro* may turn out to be strong candidates for future therapies *in vivo*.

References

References are given in standard 'Harvard' format and arranged in first author alphabetical order, followed by date and second author order.

Abdelhak, S., Kalatzis, V., Heilig, R., Compain, S., Samson, D., Vincent, C., Weil, D., Cruaud, C., Sahly, I., Leibovici, M., Bitner-Glindzicz, M., Francis, M., Lacombe, D., Vigneron, J., Charachon, R., Boven, K., Bedbeder, P., Van Regemorter, N., Weissenbach, J. and Petit, C. (1997) A human homologue of the Drosophila eyes absent gene underlies branchio-oto-renal (BOR) syndrome and identifies a novel gene family. *Nat Genet* **15**, 157-164.

Adams, B., Dorfler, P., Aguzzi, A., Kozmik, Z., Urbanek, P., Maurer-Fogy, I. and Busslinger, M. (1992) Pax-5 encodes the transcription factor BSAP and is expressed in B lymphocytes, the developing CNS, and adult testis. *Genes Dev* **6**, 1589-1607.

Agrwal, N., Wang, J.L. and Voss, P.G. (1989) Carbohydrate-binding protein 35. Levels of transcription and mRNA accumulation in quiescent and proliferating cells. *J Biol Chem* **264**, 17236-17242.

Akahani, S., Nangia-Makker, P., Inohara, H., Kim, H.R. and Raz, A. (1997) Galectin-3: a novel antiapoptotic molecule with a functional BH1 (NWGR) domain of Bcl-2 family. *Cancer Res* **57**, 5272-5276.

Al-Khaldi, N., Watson, A.R., Zucollo, J., Twining, P. and Rose, D.H. (1994) Outcome of antenatally detected cystic dysplastic kidney disease. *Arch Dis Child* **70**, 520-522.

Alnemri, E.S., Livingston, D.J., Nicholson, D.W., Salvesen, G., Thornberry, N.A., Wong, W.W. and Yuan, J. (1996) Human ICE / CED-3 protease nomenclature. *Cell* **87**, 171.

Armstrong, J.F., Pritchard-Jones, K., Bickmore, W.A., Hastie, N.D. and Bard, J.B. (1993) The expression of the Wilms' tumour gene, WT1, in the developing mammalian embryo. *Mech Dev* **40**, 85-97.

Atiyeh, B., Husmann, D. and Baum, M. (1993) Contralateral renal abnormalities in patients with renal agenesis and noncystic renal dysplasia. *Pediatrics* **91**, 812-815.

Attar, R., Quinn, F., Winyard, P.J.D., Mouriquand, P.D.E., Foxall, P.J.D., Hanson, M.A. and Woolf, A.S. (1998) Short-term urinary flow impairment deregulates pax-2 expression, proliferation and cell survival in fetal sheep kidneys. *Am J Pathol* **152**, 1225-1235.

Aufderheide, E., Chiquet-Ehrismann, R. and Ekblom, P. (1987) Epithelial-mesenchymal interactions in the developing kidney lead to expression of tenascin in the mesenchyme. *J Cell Biol* **105**, 599-608.

Avner, E.D., Sweeney, W.E. and Nelson, W.J. (1992) Abnormal sodium pump distribution during renal tubulogenesis in congenital murine polycystic kidney disease. *Proc Natl Acad Sci USA* **89**, 7447-7451.

Bao, Q. and Hughes, C. (1995) Galectin-3 expression and effects on cyst enlargement and tubulogenesis in kidney epithelial MDCK cells cultured in three-dimensional matrices *in vitro*. *J Cell Sci* **108**, 2791-2800.

Barbaux, S., Niaudet, P., Gubler, M.C., Grunfeld, J.P., Jaubert, F., Kuttenn, F., Fekete, C.N., Souleyreau-Therville, N., Thibaud, E., Fellous, M. and McElreavey, K. (1997) Donor splice-site mutations in WT1 are responsible for Frasier syndrome. *Nat Genet* **17**, 467-470.

Bard, J.B.H. and Woolf, A.S. (1992) Nephrogenesis and the development of renal disease. *Nephrol Dial Transplant* **7**, 563-572.

Barondes, S.H., Castronovo, V., Cooper, D.N.W., Cummings, R.D., Drickammr, K., Feizi, T., Gitt, M.A., Hirabayashi, J., Hughes, R.C., Kasai, K., Leffler, H., Liu, F.T., Lotan, R., Mercurio, A.M., Monsigny, M., Pillai, S., Poirier, F., Raz, A., Rigby, P.W.J. and Rini, J.M. (1993) Galectins. A family of animal β galactoside binding lectins. *Cell* **76**, 597-598.

Barr, F.G., Galili, N., Holick, J., Biegel, J.A., Rovera, G. and Emanuel, B.A. (1993) Rearrangement of the Pax3 paired-box gene in the paediatric alveolar rhabdomyosarcoma. *Nat Genet* **3**, 113-117.

Barr, M.J. and Cohen, M.M.J. (1991) ACE inhibitor fetopathy and hypocalvaria: the kidney-skull connection. *Teratology* **44**, 485-495.

Barrett, D.M. and Wineland, R.E. (1980) Renal cell carcinoma in multicystic dysplastic kidney. *Urology* **15**, 152-154.

Baserga, R. (1991) Growth regulation of the PCNA gene. *J Cell Sci* **98**, 433-436.

Battin, J., Lacombe, D. and Leng, J.J. (1993) Familial occurrence of hereditary renal adysplasia with mullerian anomalies. *Clin Genet* **43**, 23-24.

Beales, P.L., Warner, A.M., Hitman, G.A., Thakker, R. and Flinter, F.A. (1997) Bardet-Biedl syndrome: a molecular and phenotypic study of 18 families. *J Med Genet* **34**, 92-98.

Beck, A.D. (1971) The effect of intra-uterine urinary obstruction upon the development of the fetal kidney. *J Urol* **105**, 784-789.

Bell, D.M., Leung, K.K., Wheatley, S.C., Ng, L.J., Zhou, S., Ling, K.W., Sham, M.H., Koopman, P., Tam, P.P. and Cheah, K.S. (1997) SOX9 directly regulates the type-II collagen gene. *Nat Genet* **16**, 174-178.

Bellairs, R., Lear, P., Yamada, K.M., Rutushauser, U. and Lash, J.W. (1995) Posterior extension of the chick nephric (Wolffian) duct: the role of fibronectin and NCAM polysialic acid. *Dev Dyn* **202**, 333-342.

Berman, D. and Maizels, M. (1982) The role of urinary obstruction in the genesis of renal dysplasia. *J Urol* **128**, 1091-1100.

Bernstein, J. (1971) The morphogenesis of renal parenchymal maldevelopment (renal dysplasia). *Pediatr Clin North Am* **18**, 395-407.

Bernstein, J., Risdon, R.A. and Gilbert-Barness, E. (1997) Renal system. In: Gilbert-Barness, E., (Ed.) *Potter's pathlogy of the fetus and infant*, 4th edn. pp. 863-935. St Louis, Missouri, USA: Mosby.

Bialestock, D. (1964) Studies of renal malformations and pyelonephritis in chidren, with and without associated vesico-ureteral reflux and obstruction. *Aust N Z J Surg* **34**, 120-136.

Bland, J.M. and Altmann, D.G. (1986) Statistical methods for assessing agreement between two methods of clinical measurement. *Lancet* **8476**, 307-310.

Bortner, C.D., Oldenburg, N.B.E. and Cidlowski, J.A. (1995) The role of DNA fragmentation in apoptosis. *Trends Cell Biol* **5**, 22-27.

Bottaro, D.P., Rubin, J.S., Faletto, D.L., Chan, A.M.L., Kmiecik, T.E., Vande Woude, G.F. and Aaronson, S.A. (1991) Identification of the hepotacyte growth factor as the c-met proto-oncogene product. *Science* **251**, 802-804.

Braverman, N., Dodt, G., Gould, S.J. and Valle, D. (1995) Disorders of peroxisome biogenesis. *Hum Mol Genet* **4**, 1791-1798.

Bravo, R., Frank, R., Blundell, P.A. and MacDonald-Bravo, H. (1987) Cyclin / PCNA is the auxillary protein of DNA polymerase-delta. *Nature* **326**, 515-517.

Brown, N.A. (1997) Chemical teratogens; Hazards, tools and clues. In: Thorogood, P., (Ed.) *Embyos, genes and birth defects*, pp. 69-88. Chichester, West Sussex, UK: John Wiley and Sons Ltd.

Bryan, T.M. and Reddel, R.R. (1994) SV40-induced immortalization of human cells. *Crit Rev Oncog* **5**, 331-357.

Burrow, C. and Wilson, P.D. (1993) A putative Wilms tumor-secreted growth factor activity required for primary culture of human nephroblasts. *Proc Nat Acad Sci USA* **90**, 6066-70.

Cain, D.R., Griggs, D., Lackey, D.A. and Kagan B.M. (1974) Familial renal agenesis and total dysplasia. *Am J Dis Child* **128**, 377-380.

Cale, C.M., Klein, N., Morgan, G. and Woolf, A.S. (1998) Tumor necrosis factor-α inhibits epithelial differentiation and nephrogenesis in the mouse metanephric kidney *in vitro*. *Int J Dev Biol* **42**, 663-674.

Camp, V. and Martin, P. (1996) The role of macrophages in clearing programmed cell death in the developing kidney. *Anat Embryol* **194**, 341-348.

Celis, J.E. and Celis, A. (1985) Cell cycle-dependent variations in the distribution of the nuclear protein cyclin proliferating cell nuclear antigen in cultured cells: subdivision of S phase. *Proc Natl Acad Sci USA* **82**, 3262-3266.

Cepko, C.L., Roberts, B.E. and Mulligan, R.C. (1984) Construction and applications of a highly transmissible murine retrovirus shuttle vector. *Cell* **37**, 1053-1062.

Chan, D., Wynshaw-Boris, A. and Leder, P. (1995) Formin isoforms are differentially expressed in the mouse embryo and are required for normal expression of fgf-4 and shh in the limb bud. *Development* **121**, 3151, -3162

Chapman, C.J., Bailey, R.R., Janus, E.D., Abbott, G.D. and Lynn, K.L. (1985) Vesicoureteric reflux: segregation analysis. *Am J Med Genet* **20**, 577-584.

Charlieu, J.P., Larsson, S., Miyagawa, K., van Heyningen, V. and Hastie, N.D. (1995) Does the Wilms' tumour suppressor gene, WT1, play roles in both splicing and transcription? *J Cell Sci Suppl* **19**, 95-99.

Chevalier, R.L., Chung, K.H., Smith, C.D., Ficenec, M. and Gomez, R.A. (1996) Renal apoptosis and clusterin following ureteral obstruction: the role of maturation. *J Urol* **156**, 1474-1479.

Chiang, C., Litingtung, Y., Lee, E., Young, K.E., Corden, J.L., Westphal, H. and Beachy, P.A. (1996) Cyclopia and defective axial patterning in mice lacking Sonic hedgehog gene function. *Nature* **383**, 407-413.

Cohen, G.M. (1997) Caspases: the executioners of apoptosis. *Biochem J* **326**, 1-16.

Coles, H.S.R., Burne, J.F. and Raff, M.C. (1993) Large-scale normal death in the developing rat kidney and its reduction by epidermal growth factor. *Development* **118**, 777-784.

Collins, M.K.L., Perkins, G.R., Rodriguez-Tarduchy, G., Nieto, M.A. and Lopez-Rivas, A. (1994) Growth factors as survival factors: regulation of apoptosis. *Bioessays* **16**, 133-138.

Cook, D.M., Hinkes, M.T., Bernfield, M. and Rauscher, F.J. (1996) Transcriptional activation of the syndecan-1 promoter by the Wilms' tumor protein WT1. *Oncogene* **13**, 1789-1799.

Coons, A.H., Leduc, E.H. and Connolly, J.M. (1955) Studies on antibody production. I. A method for the histochemical demonstration of specific antibody and its application to the study of the hyperimmune rabbit. *J Exp Med* **102**, 49-60.

Cowley, B.D.Jr., Smardo, F.L.Jr., Grantham, J.J. and Calvet, J.P. (1987) Elevated c-myc proto-oncogene expression in autosomal recessive polycystic kidney disease. *Proc Natl Acad Sci USA* **84**, 8394-8398.

Cromie, W.J., Engelstein, M.S. and Duckett, J.W. (1980) Nodular renal blastema, renal blastema and duplicated collecting systems. *J Urol* **123**, 100-102.

Dagher, S.F., Wang, J.L. and Patterson, R.J. (1995) Identification of galectin-3 as a factor in pre mRNA splicing. *Proc Natl Acad Sci USA* **92**, 1213-1217.

Daikha-Dahmane, F., Narcy, F., Dommergues, M., Lacoste, M., Beziau, A. and Gubler, M.C. (1997) Distribution of alpha-integrin subunits in fetal polycystic kidney diseases. *Ped Nephrol* **11**, 267-273.

Davies, J., Lyon, M., Gallagher, J. and Garrod, D. (1995) Sulphated proteoglycan is required for collecting duct growth and branching but not nephron formation during kidney development. *Development* **121**, 1507-1517.

Davis, A.P., Witte, D.P., Hsieh-Li, H.M., Potter, S.S. and Capecchi, M.R. (1995) Absence of radius and ulna in mice lacking hoxa-11 and hoxd-11. *Nature* **375**, 791-795.

Dehbi, M. and Pelletier, J. (1996) PAX8-mediated activation of the wt1 tumor suppressor gene. *EMBO J* **15**, 4297-4306.

Donehower, L.A., Godley, L.A., Aldaz, C.M., Pyle, R., Shi, Y.P., Pinkel, D., Gray, J., Bradley, A., Medina, D. and Varmus, H.E. (1995) Deficiency of p53 accelerates mammary tumorigenesis in Wnt-1 transgenic mice and promotes chromosomal instability. *Genes Dev* **9**, 882-895.

Dressler, G.R., Deutsch, U., Chowdhury, K., Nornes, H.O. and Gruss, P. (1990) Pax2 a new murine paired-box-containing gene and its expression in the developing excretory system. *Development* **109**, 787-795.

Dressler, G.R. and Douglas, E.C. (1992) Pax-2 is a DNA-binding protein expressed in embryonic kidney and Wilms tumor. *Proc Natl Acad Sci USA* **89**, 1179-1183.

Dressler, G.R., Wilkinson, J.E., Rothenpieler, U.W., Patterson, L.T., Williams-Simons, L. and Westphal, H. (1993) Deregulation of Pax-2 expression in transgenic mice generates severe kidney abnormalities. *Nature.* **362**, 65-67.

Droz, D., Rousseau-Merck, M.F., Jaubert, F., Diebold, N., Nezelof, C., Adafer, E. and Mouly, H. (1990) Cell differentiation in Wilms' tumor (nephroblastoma): an immunohistochemical study. *Hum Pathol* **21**, 536-544.

Dudley, A.T., Lyons, K.M. and Robertson, E.J. (1995) A requirement for bone morphogenetic protein-7 during development of the mammalian eye and kidney. *Genes Dev* **9**, 2795-2807.

Duke, V.M., Winyard, P.J.D., Thorogood, P., Soothill, P., Bouloux, P.M.G. and Woolf, A.S. (1995) KAL, a gene mutated in Kallmann's syndrome, is expressed in the first trimester of human development. *Mol Cell Endocrin* **110**, 73-79.

Dungan, J.S., Fernandez, M.T., Abbitt, P.L., Thiagarajah, S., Howards, S.S. and Hogge, W.A. (1990) Multicystic dysplastic kidney: natural history of prenatally detected cases. *Prenatal Diag* **10**, 175-182.

Durbeej, M., Larsson, E., Ibraghimov-Beskrovnaya, O., Roberds, S.L., Campbell, K.P. and Ekblom, P. (1995) Non-muscle α-dystroglycan is involved in epithelial development. *J Cell Biol* **130**, 79-91.

Dvergsten, J., Manivel, J.C., Correa-Rotter, R. and Rosenberg, M.E. (1994) Expression of clusterin in human renal diseases. *Kidney Int* **45**, 828-835.

Eccles, M.R., Wallis, L.J., Fidler, A.E., Spurr, N.K., Goodfellow, P.J. and Reeve, A.E. (1992) Expression of the PAX2 gene in human fetal kidney and Wilms' tumor. *Cell Growth Diff* **3**, 279-289.

Ekblom, P. (1981a) Formation of basement membranes in the embryonic kidney: an immunohistological study. *J Cell Biol* **91**, 1-10.

Ekblom, P., Lehtonen, E., Saxen, L. and Timpl, R. (1981b) Shift in collagen type as an early response to induction of the metanephric mesenchyme. *J Cell Biol* **89**, 276-283.

Ekblom, P. (1994) Embryology and prenatal development. In: Holliday, M.A., Barrett, T.M. and Avner, E.D., (Eds.) *Pediatric Nephrology*, 3rd edn pp. 2-18. Baltimore, Maryland, USA: Williams and Wilkins.

Ekblom, P., Ekblom, M., Fecker, L., Klein, G., Zhang, H.-Y., Kadoya, Y., Chu, M.L., Mayer, U. and Timpl, R. (1994) Role of mesenchymal nidogen for epithelial morphogenesis *in vitro*. *Development* **120**, 2003-2014.

Elbedour, K., Zucker, N., Zalzstein, E., Barki, Y. and Carmi, R. (1994) Cardiac abnormalities in the Bardet-Biedl syndrome: echocardiographic studies of 22 patients. *Am J Med Genet* **52**, 164-169.

Elder, J.S., Duckett, J.W.J. and Snyder, H.M. (1987) Intervention for fetal obstructive uropathy: has it been effective? *Lancet* **2**, 1007-1010.

Elenius, K., Maatta, A., Salmivirta, M. and Jalkanen, M. (1992) Growth factors induce 3T3 cells to express bFGF-binding syndecan. *J Biol Chem* **267**, 6435-6441.

European polycystic kidney disease consortium (1994) The polycystic kidney disease 1 gene encodes a 14 kb transcript and lies within a duplicated region on chromosome 16. *Cell* **77**, 881-894.

Favor, J., Sandulache, R., Neuhauser-Klaus, A., Pretsch, W., Chatterjee, B., Senft, E., Wurst, W., Blanquet, V., Grimes, P., Sporle, R. and Schughart, K. (1996) The mouse Pax2(1Neu) mutation is identical to a human PAX2 mutation in a family with renal-coloboma syndrome and results in developmental defects of the brain, ear, eye, and kidney. *Proc Natl Acad Sci USA* **93**, 13870-13875.

Fejes-Toth, G. and Naray-Fejes-Toth, A. (1991) Fluorescence activated cell sorting of principal and intercalated cells of the renal collecting duct. *J Tiss Cult Meth* **13**, 173-178.

Fejes-Toth, G. and Naray-Fejes-Toth, A. (1992) Differentiation of renal β-intercalated cells to α-intercalated and principal cells in culture. *Proc Natl Acad Sci USA.* **89**, 5487-5491.

Foddy, L., Stamatoglou, S.C. and Hughes, R.C. (1990) An endogenous carbohydrate binding protein of baby hamster kidney cells (BHK21 C13) cells. Temporal changes in cellular expression in the developing kidney. *J Cell Sci* **97**, 139-148.

Foe, J.R., Rooimans, M.A., Bosnoyan-Collins, L., Alon, N., Wijker, M., Parker, L., Lightfoot, J., Carreau, M., Callen, D.F., Savoia, A., Cheng, N.C., van Berkel, C.G., Strunk, M.H., Gille, J.J., Pals, G., Kruyt, F.A., Pronk, J.C., Arwert, F., Buchwald, M. and Joenje, H. (1996) Expression cloning of a cDNA for the major Fanconi anaemia gene, FAA. *Nat Genet* **14**, 488

Fowlis, D., Colnot, C., Ripoche, M.A. and Poirier, F. (1995) Galectin 3 is expressed in the notocord, developing bones, and skin of the postimplantation mouse embryo. *Dev Dyn* **203**, 241-251.

Fraser, F.C. and Lytwyn, A. (1981) Spectrum of anomalies in the Meckel syndrome, or: "Maybe there is a malformation syndrome with at least one constant anomaly". *Am J Med Genet* **9**, 67-73.

Freedman, A.L., Bukowski, T.P., Smith, C.A., Evans, M.I., Johnson, M.P. and Gonzalez, R. (1996) Fetal therapy for obstructive uropathy: diagnosis specific outcomes. *J Urol* **156**, 720-723.

Freshney, R.I. (1987) *Culture of animal cells: a manual of basic technique*, 2nd edn. New York, New York, USA: Wiley-Liss Inc.

Frisch, S.M. and Ruoslahti, E. (1997) Integrins and anoikis. *Curr Opin Cell Biol* **9**, 701-706.

Fuerstenberg, S.M., Torok, E.P., Straub, B. and Zager, R.A. (1993) Evidence against apoptosis as a dominant mechanism for post-ischemic/post-hypoxic proximal tubular necrosis. *J Am Soc Nephrol* **4**, 735 (Abstract).

Gage, J.C. and Sulik, K.K. (1991) Pathogenesis of ethanol-induced hydronephrosis and hydroureter as demonstrated following in vivo exposure of mouse embryos. *Teratology* **44**, 299-312.

Gattone, V.H., II, Andrews, G.K., Fu-wen, N., Chadwick, L.J., Klein, R.M. and Calvet, J.P. (1990) Defective epidermal growth factor gene expression in mice with polycystic kidney disease. *Dev Biol* **138**, 225-230.

Gavrelli, Y., Sherman, Y. and Ben-Sasson, S.A. (1992) Identification of programmed cell death *in situ* via specific labeling of DNA fragmentation. *J Cell Biol* **119**, 493-501.

Gershoni-Baruch, R., Nachlieli, T., Leibo, R., Degani, S. and Weissman, I. (1992) Cystic kidney dysplasia and polydactyly in 3 sibs with Bardet-Biedl syndrome. *Am J Med Genet* **44**, 269-273.

Gessler, M., Poustka, A., Cavenee, W., Neve, R.L., Orkin, S.H. and Bruns, G.A. (1990) Homozygous deletion in Wilms tumours of a zinc-finger gene identified by chromosome jumping. *Nature* **343**, 774-778.

Gherardi, E., Gray, J., Stoker, M., Perryman, M. and Furlong, R. (1991) Purification of scatter factor, a fibroblast-derived basic protein that modulates epithelial interactions and movement. *Proc Natl Acad Sci USA.* **86**, 5844-5848.

Gilbert, S.F. (1993) *Developmental Biology*, 3rd edn. Sunderland, Massachusetts, USA: Sinauer Associates Inc.

Glover, T.W. (1995) CATCHing a break on 22. *Nat Genet* **10**, 257-258.

Gnarra, J.R. and Dressler, G.R. (1995) Expression of Pax-2 in human renal cell carcinoma and growth inhibition by antisense oligonucleotides. *Cancer Res* **55**, 4092-4098.

Godley, L.A., Kopp, J.B., Eckhaus, M., Paglino, J.J., Owens, J. and Vermus, H.E. (1996) Wild-type *p53* transgenic mice exhibit altered differentiation of the ureteric bud and possess small kidneys. *Genes Dev* **10**, 863-850.

Gohda, E., Tsubouchi, H., Nakayama, H., Hirono, S., Sakiyama, O., Takahashi, K., Miyazaki, H., Hashimoto, S. and Daikuhara, Y. (1988) Purification and partial characterization of hepatocyte growth factor from plasma of a patient with fulminant hepatic failure. *J Clin Invest* **81**, 414-419.

Goodship, J., Robson, S.C., Sturgiss, S., Cross, I.E. and Wright, C. (1997) Renal abnormalities on obstetric ultrasound as a presentation of Di George syndrome. *Prenat Diagn* **17**, 867-870.

Goulding, M.D., Chalapakis, G., Deutsch, U., Erselius, J.R. and Gruss, P. (1991) Pax-3, a novel murine DNA binding protein expressed during early neurogenesis. *EMBO J* **10**, 1135-1147.

Granata, C., Wang, Y., Puri, P., Tanaka, K. and O'Briain, D.S. (1997) Decreased bcl-2 expression in segmental renal dysplasia suggests a role in its morphogenesis. *Br J Urol* **80**, 140-144.

Grantham, J.J. (1992) 1992 Homer Smith Award. Fluid secretion, cellular proliferation, and the pathogenesis of renal epithelial cysts. *J Am Soc Nephrol* **3**, 1841-1857.

Greene, L.F., Feinzaig, W. and Dahlin, D.C. (1971) Multicystic dysplasia of the kidney: with special reference to the contralateral kidney. *J Urol* **105**, 482-488.

Grobstein, C. (1955) Inductive interaction in the development of the mouse metanephros. *J Exp Zool* **130**, 319-340.

Grubb, G.R., Yun, K., Williams, B.R., Eccles, M.R. and Reeve, A.E. (1994) Expression of WT1 protein in fetal kidneys and Wilms' tumors. *Lab Invest* **71**, 472-479.

Gruss, P. and Walther, C. (1992) Pax in development. *Cell* **69**, 719-722.

Haber, D.A., Sohn, R.L., Buckler, A.J., Pelletier, J., Call, K.M. and Housman, D.E. (1991) Alternative splicing and genomic structure of Wilms' tumor gene WT1. *Proc Natl Acad Sci USA* **88**, 9618-9622.

Halder, G., Callaerts, P. and Gehring, W.J. (1995) Induction of ectopic eyes by targeted expression of the *eyeless* gene in *Drosophila*. *Science* **267**, 1788-1792.

Hanai, T., Usuda, N., Morita, T., Shimizu, T. and Nagata, T. (1993) Proliferative activity in the kidneys of aging mice evaluated by PCNA / cyclin immunohistochemistry. *Cell Mol Biol* **39**, 181-191.

Hanioka, K., Imai, Y., Watanabe, M. and Ito, H. (1990) Lectin histochemical studies on renal tumors. *Kobe J Med Sci* **36**, 1-21.

Hanson, I.M., Seawright, A., Hardman, K., Hodgson, S., Zaletayev, D., Fekete, G. and van Heyningen, V. (1993) Pax 6 mutations in aniridia. *Hum Mol Genet* **2**, 915-920.

Harding, M.A., Gattone, V.H., II, Grantham, J.J. and Calvet, J.P. (1992) Localization of overexpressed c-myc mRNA in polycystic kidneys of the *cpk* mouse. *Kidney Int* **41**, 317-325.

Harlow, E., Crawford, L.V., Pim, D.C. and Williamson, N.M. (1981) Monoclonal antibodies specific for simian virus 40 tumor antigens. *J Virol* **39**, 861-869.

Harrington, E.A., Bennett, M.R., Fanidi, A. and Evan G.I. (1994) c-Myc-induced apoptosis in fibroblasts is inhibited by specific cytokines. *EMBO J* **13**, 3286-3295.

Hatini, V., Huh, S.O., Herzlinger, D., Soares, V.C. and Lai, E. (1996) Essential role of stromal mesenchyme in kidney morphogenesis revealed by targeted disruption of Winged Helix transcription factor BF-2. *Genes Dev* **10**, 1467-1478.

Hayflick, L. (1965) The limited in vitro lifetime of human diploid cell strains. *Exp Cell Res* **37**, 614-636.

Heimler, A. and Lieber, E. (1986) Branchio-oto-renal syndrome: Reduced penetrance and variable expressivity in four generations of a large kindred. *Am J Med Genet* **25**, 15-27.

Herrmann, J., Turck, C.W., Atchison, R.E., Huflejt, M.E., Poulter, L., Gitt, M.A., Burlingame, A.L., Barondes, S.H. and Leffler, H. (1993) Primary structure of the soluble lactose binding lectin L 29 from rat and dog and interaction of its proline, glycine, tyrosine rich sequence with bacterial and tissue collagenase. *J Biol Chem* **268**, 26704-26711.

Herzlinger, D., Koseki, C., Mikawa, T. and Al-Awqati, Q. (1992) Metanephric mesenchyme contains multipotent stem cells whose fate is restricted after induction. *Development* **114**, 565-572.

Herzlinger, D., Qiao, J., Cohen, D., Ramakrishna, N. and Brown, A.M. (1994) Induction of kidney epithelial morphogenesis by cells expressing Wnt-1. *Dev Biol* **166**, 815-818.

Hill, R.E., Favor, J., Hogan, B.L., Ton, C.C., Saunders, G.F., Hanson, I.M., Prosser, J., Jordan, T., Hastie, N.D. and van Heyningen, V. (1991) Mouse small eye results from mutations in a paired-like homeobox-containing gene. *Nature* **354**, 522-525.

Hockenbery, D.M., Oltvai, Z.N., Yin, X.M., Milliman, C.L. and Korsmeyer, S.J. (1993) Bcl-2 functions in an antioxidant pathway to prevent apoptosis. *Cell* **75**, 241-251.

Holst, B.D., Goomer, R.S., Wood, I.C., Edelman, G.M. and Jones, F.S. (1994) Binding and activation of the promoter for the neural cell adhesion molecule by Pax-8. *J Biol Chem* **269**, 22245-22252.

Holthoffer, H., Virtanen, I., Pettersson, E., Tornroth, T., Alfthan, O., Linder, E. and Miettinen, A. (1981) Lectins as fluorescence microscopic markers for saccharides in the human kidney. *Lab Invest* **45**, 391-399.

Holthoffer, H., Miettinen, A., Lehto, V.P., Lehtonen, E. and Virtanen, I. (1984) Expression of vimentin and cytokeratin types of intermediate filament proteins in developing and adult human kidneys. *Lab Invest* **50**, 552-559.

Horie, S., Higashihara, E., Nutahara, K., Mikami, Y., Okubo, A., Kano, M. and Kawabe, K. (1994) Mediation of renal cyst formation by hepatocyte growth factor. *Lancet* **344**, 789-791.

Horikoshi, S., Kubota, S., Martin, G.R., Yamada, Y. and Klotman, P.E. (1991) Epidermal growth factor (EGF) in the congenital polycystic mouse kidney. *Kidney Int* **39**, 57-62.

Houston, C.S., Opitz, J.M., Spranger, J.W., Macpherson, R.I., Reed, M.H., Gilbert, E.F., Herrmann, J. and Schinzel, A. (1983) The campomelic syndrome: review and report of 17 cases. *Am J Med Genet* **15**, 3-28.

Howie, A.J. and Johnson, G.D. (1992) Confocal microscopic and other observations on the distal end of the thick limb of the human loop of Henle. *Cell Tissue Res* **267**, 11-16.

Howie, A.J., Smithson, N. and Rollason, T.P. (1993) Reconsideration of the development of the distal tubule of the human kidney. *J Anat* **183**, 141-147.

Howie, A.J., Rowlands, D.C., Reynolds, G.M. and Barnes, A.D. (1995) Measurement of proliferation in renal biopsy specimens: evidence of subclinical tubular damage in the nephrotic syndrome. *Nephrol Dial Transplant* **10**, 2212-2218.

Hsieh-Li, H.M., Witte, D.P., Weinstein, M., Branford, W., Li, H., Small, K. and Potter, S.S. (1995) Hoxa-11 structure, extensive antisense transcription, and function in male and female fertility. *Development* **121**, 1373-1385.

Hsu, D.K., Hammes, S.R., Kuwabara, I., Greene, W.C. and Liu, F.T. (1996) Human T lymphotropic virus I infection of human T lymphocytes induces expression of the β galactoside binding lectin galectin-3. *Am J Pathol* **148**, 1661-1670.

Hughes, R.C. (1994) Mac 2. A versatile galactose binding protein of mammalian tissues. *Glycobiology* **4**, 5-12.

Hughes-Benzie, R.M., Hunter, A.G., Allanson, J. E. and Mackenzie, A.E. (1992) Simpson-Golabi-Behmel syndrome associated with renal dysplasia and embryonal tumor: localization of the gene to Xqcen-q21. *Am J Med Genet* **43**, 428-435.

Hyatt, G.A., Schmitt, E.A., Marsh-Armstrong, N., McCaffery, P., Drager, U.C. and Dowling, J. E. (1996) Retinoic acid establishes ventral retinal characteristics. *Development* **122**, 195-204.

Jacobsen, M.D., Weil, M. and Raff, M.C. (1996) Role of Ced-3 / ICE-family proteases in staurosporine-induced programmed cell death. *J Cell Biol* **133**, 1041-1051.

Jacobson, M.D., Weil, M. and Raff, M.C. (1997) Programmed cell death in animal development. *Cell* **88**, 347-354.

Jat, P.S., Cepko, C.L., Mulligan, R.C. and Sharp, P.A. (1986) Recombinant retroviruses encoding simian virus 40 large T antigen and polyomavirus large and middle T antigens. *Mol Cell Biol* **6**, 1204-1217.

Jat, P.S. and Sharp, P.A. (1989) Cell lines established by a temperature sensitive Simian Virus 40 large-T-antigen gene are growth restricted at the nonpermissive temperature. *Mol Cell Biol* **9**, 1672-1681.

Jat, P.S., Noble, M.D., Ataliotis, P., Tanaka, Y., Yannoutsos, N., Larsen, L. and Kioussis, D. (1991) Direct derivation of conditionally immortal cell lines from an H-2Kb-tsA58 transgenic mouse. *Proc Natl Acad Sci USA* **88**, 5096-5100.

Jonsson, Z.O. and Hubscher, U. (1997) Proliferating cell nuclear antigen: more than a clamp for DNA polymerases. *Bioessays* **19**, 967-975.

Jordan, T., Hanson, I., Zaletayev, D., Hodgson, S., Prosser, J., Seawright, A., Hastie, N. and van Heyningen, V. (1992) The human PAX6 gene is mutated in two patients with aniridia. *Nat Genet* **1**, 328-332.

Joseph, D.B., Uehling, D.T., Gilbert, E. and Laxova, R. (1987) Genitourinary abnormalities associated with the Smith-Lemli-Opitz syndrome. *J Urol* **137**, 719-721.

Junien, C. and Henry, I. (1994) Genetics of Wilms' tumour A blend of aberrant development and genomic imprinting. *Kidney Int* **46**, 1264-1279.

Kampmeier, O.F. (1926) The metanephros or so called permanent kidney is in part provisonal and vestigial. *Anat Rec* **33**, 115-120.

Kanwar, Y.S., Liu, Z.Z., Kumar, A., Wada, J., and Carone, F.A. (1995) Cloning of mouse c-ros cDNA, its role in development and relationship to extracellular matrix glycoproteins. *Kidney Int* **48**, 1646-1659.

Karp, S.L., Ortiz-Arduan, A., Li, S. and Neilson, E.G. (1994) Epithelial differentiaion of metanephric mesenchymal cells after stimulation with hepatocyte growth factor or embryonic spinal cord. *Proc Natl Acad Sci USA* **91**, 5286-5290.

Kawaida, K., Matsumoto, K., Shimazu, H. and Nakamura, T. (1994) Hepatocyte growth factor prevents acute renal failure and accelerates renal regeneration in mice. *Proc Natl Acad Sci USA* **91**, 4357-4361.

Keller, S.A., Jones, J. M., Boyle, A., Burrow, L.L., Killen, P.D., Green, D.G., Kapousta, N.V., Hitchcock, P.F., Swant, R.T. and Meisler, M.H. (1994) Kidney and retinal defects (*krd*), a transgene-induced mutation with a deletion of mouse chromosome 19 that induces the Pax 2 locus. *Genomics* **23**, 309-320.

Kelman, Z. (1997) PCNA: structure, functions and interactions. *Oncogene* **14**, 629-640.

Kennedy, W.A., Sternberg, A., Lackgren, G., Hernsle, T.W. and Sawczuk, I.S. (1994) Renal tubular apoptosis after partial ureteral obstruction. *J Urol* **152**, 658-664.

Kennedy, W.A., Buttyan, R., Garcia-Montes, E., D'Agati, V., Olsson, C.A. and Sawczuk, I.S. (1997) Epidermal growth factor suppresses renal tubular apoptosis following ureteral obstruction. *Urology* **49**, 973-980.

Kent, J. , Coriat, A.M., Sharpe, P.T., Hastie, N.D. and van Heyningen, V. (1995) The evolution of WT1 sequence and expression pattern in the vertebrates. *Oncogene* **11**, 1781-1792.

Kent, J. , Wheatley, S.C., Andrews, J. E., Sinclair, A.H. and Koopman, P. (1996) A male-specific role for SOX9 in vertebrate sex determination. *Development* **122**, 2813-2822.

Kerr, J. F.R., Wyllie, A.H. and Currie, A.R. (1972) Apoptosis - a basic biological phenomenon with wide ranging implications in tissue kinetics. *Br J Cancer* **26**, 239-257.

Kestila, M., Mannikko, M., Holmberg, C., Korpela, K., Savolainen, E.-R., Peltonen, L. and Tryggvason, K. (1994) Exclusion of eight genes as mutated loci in congenital nephrotic syndrome of the Finnish type. *Kidney Int* **45**, 986-990.

Kiefer, M.C., Stephans, J.C., Crawford, K., Okino, K. and Barr, P.J. (1990) Ligand-affinity cloning and structure of a cell surface heparan sulfate proteoglycan that binds basic fibroblast growth factor. *Proc Natl Acad Sci USA* **87**, 6985-6989.

Kirk, J.M.W., Grant, D.B., Besser, G.M., Shalet, S., Smith, C.S., White, M., Edwards, O. and Bouloux, P.M.G. (1994) Unilateral renal aplasia in X-linked Kallmann's Syndrome. *Clin Genet* **46**, 260-262.

Klamt, B., Koziell, A., Poulat, F., Wieacker, P., Scambler, P., Berta, P. and Gessler, M. (1998) Frasier syndrome is caused by defective alternative splicing of WT1 leading to an altered ratio of WT1 +/-KTS splice isoforms. *Hum Mol Genet* **7**, 709-714.

Klein, G., Langegger, M., Garidis, C. and Ekblom, P. (1988a) Neural cell adhesion molecules during embryonic induction and development of the kidney. *Development* **102**, 749-761.

Klein, G., Langegger, M., Timpl, R. and Ekblom, P. (1988b) Role of lamninin A chain in the development of epithelial cell polarity. *Cell* **55**, 331-341.

Knudson, C.M. and Korsmeyer, S.J. (1997) Bcl-2 and Bax function independently to regulate cell death. *Nat Genet* **16**, 358-363.

Kolatsi-Joannou, M., Woolf, A.S., Hardman, P., White, S.J., Gordge, M. and Henderson, R.M. (1995) The hepatocyte growth factor / scatter factor (HGF / SF) receptor, *met*, transduces a morphogenetic signal in renal glomerular fibromuscular mesangial cells. *J Cell Sci* **108**, 3703-3714.

Kolatsi-Joannou, M., Moore, R., Winyard, P.J.D. and Woolf, A.S. (1997) Expression of hepatocyte growth factor / scatter factor and its receptor, MET, suggests roles in human embryonic organogenesis. *Pediat.Res* **41**, 1-9.

Koseki, C., Herzlinger, D. and Al-Awqati, Q. (1992) Apoptosis in metanephric development. *J Cell Biol* **119**, 1327-1333.

Kreidberg, J.A., Sariola, H., Loring, J.M., Maeda, M., Pelletier, J., Housman, D. and Jaenisch, R. (1993) WT-1 is required for early kidney development. *Cell* **74**, 679-691.

Kreidberg, J.A., Donovan, M.J., Goldstein, S.L., Rennke, H., Shepherd, K., Jones, R.C. and Jaenisch, R. (1996) Alpha 3 beta-1 integrin has a crucial role in kidney and lung organogenesis. *Development* **122**, 3537-3547.

Kroemer, G. (1997) The proto-oncogene Bcl-2 and its role in regulating apoptosis. *Nat Med* **3**, 614-620.

Kurki, P., Vanderlaan, M., Dolbeare, F., Gray, J. and Tan, E.M. (1986) Expression of proliferating cell nuclear antigen (PCNA)/cyclin during the cell cycle. *Exp Cell Res* **166**, 209-219.

Lackie, P.M., Zuber, C. and Roth, J. (1990) Polysialic acid and N-CAM localisation in embryonic rat kidney: mesenchymal and epithelial elements show different patterns of expression. *Development* **110**, 933-947.

Laemmli, U.K. (1970) Cleavage of structural proteins during the assembly of the head of bacteriophage T4. *Nature* **277**, 680-685.

Lai, E., Clark, K.L., Burley, S.K. and Darnell, J.E.J. (1993) Hepatocyte nuclear factor 3/fork head or "winged helix" proteins: a family of transcription factors of diverse biologic function. *Proc Natl Acad Sci USA* **90**, 10421-10423.

Lanoix, J., D'Agati, V., Szabolcs, M. and Trudel, M. (1996) Dysregulation of cellular proliferation and apoptosis mediates human autosomal dominant polycystic kidney disease (ADPKD). *Oncogene* **13**, 1153-1160.

Larsen, W.J. (1993) *Human embryology*, 1st edn. New York, New York, USA: Churchill Livingstone Inc.

Larsson, P., Roos, G., Stenling, R., Wilson, G.D. and Ljungberg, B. (1996) Cell proliferation in renal cell carcinoma - a comparative study of cell kinetic methods. *Urol Res* **24**, 291-295.

Larsson, S.H., Charlieu, J.P., Miyagawa, K., Engelkamp, D., Rassoulzadegan, M., Ross, A., Cuzin, F., van Heynigen, V. and Hastie, N.D. (1995) Subnuclear localization of WT1 in splicing or transcription factor domains is regulated by alternative splicing. *Cell* **81**, 391-401.

Laurent, G., Toubeau, G., Heuson-Stiennon, J.A., Tulkens, P. and Maldague, P. (1988) Kidney tissue repair after nephrotoxic injury: biochemical and morphological characterization. *Crit Rev Toxicol* **19**, 147-183.

LeBrun, D.P., Warnke, R.A. and Cleary, M.L. (1993) Expression of BCL-2 in fetal tissues suggests a role in morphogenesis. *Am J Pathol* **142**, 743-753.

Lechner, M.S. and Dressler, G.R. (1997) The molecular basis of embryonic kidney development. *Mech Dev* **62**, 105-120.

Lelongt, B., Makino, H., Dalecki, T.M. and Kanwar, Y.S. (1988) Role of proteoglycans in renal development. *Dev Biol* **128**, 256-276.

Letterio, J.J., Geiser, A.G., Kulkarni, A.B., Roche, N.S., Sporn, M.B. and Roberts, A.B. (1994) Maternal rescue of transforming growth factor-beta 1 null mice. *Science* **264**, 1936-1938.

Leveen, P., Pekny, M., Gebre-Medhin, S., Swolin, B., Larsson, E. and Betsholtz, C. (1994) Mice deficient for PDGF-β show renal, cardiovascular, and hematological abnormalities. *Genes Dev* **8**, 1875-1887.

Little, M. and Wells, C. (1997) A clinical overview of WT1 gene mutations. *Hum Mutat* **9**, 209-225.

Liu, S., Cieslinski, D.A., Funke, A.J. and Humes, H.D. (1997) Transforming growth factor-beta 1 regulates the expression of Pax-2, a developmental control gene, in renal tubule cells. *Exp Nephrol* **5**, 295-300.

Lotz, M.M., Andrews, C.W.J., Korzelius, C.A., Lee, E.C., Steele, G.D.J., Clarke, A. and Mercurio, A.M. (1993) Decreased expression of Mac 2 (carbohyrate binding protein 35) and loss of its nuclear localisation are associated with neoplastic progression of colon carcinoma. *Proc Natl Acad Sci USA* **90**, 3466-3470.

Luo, G., Hofmann, C., Bronckers, A.L., Sohocki, M., Bradley, A. and Karsenty, G. (1995) BMP-7 is an inducer of nephrogenesis, and is also required for eye development and skeletal patterning. *Genes Dev* **9**, 2808-2820.

Maas, R., Elfering, S., Glaser, T. and Jepeal, L. (1994) Deficient outgrowth of the ureteric bud underlies the renal agenesis phenotype in mice manifesting the limb deformity (ld) mutation. *Dev Dyn* **199**, 214-228.

Madden, S.L., Cook, D.M., Morris, J.F., Gashler, A., Sukhatme, V.P. and Rauscher, F.J. (1991) Transcriptional repression mediated by the WT1 Wilms tumor gene product. *Science* **253**, 1550-1553.

Marigo, V., Roberts, D.J., Lee, S.M., Tsukurov, O., Levi, T., Gastier, J.M., Epstein, D.J., Gilbert, D.J., Copeland, N.G. and Seidman, C.E. (1995) Cloning, expression, and chromosomal location of SHH and IHH: two human homologues of the Drosophila segment polarity gene hedgehog. *Genomics* **28**, 44-51.

Matsell, D.G., Bennett, T., Goodyer, P., Goodyer, C. and Han, V.K. (1996) The pathogenesis of multicystic dysplastic kidney disease: insights from the study of fetal kidneys. *Lab Invest* **74**, 883-893.

Matsell, D.G., Bennett, T., Armstrong, R.A., Goodyer, P., Goodyer, C. and Han, V.K.M. (1997) Insulin-like Growth Factor (IGF) and IGF Binding Protein gene expression in multicystic renal dysplasia. *J Am Soc Nephrol* **8**, 85-94.

Matsuo, T., Osumi-Yamashita, N., Noji, S., Ohuchi, H., Koyama, E., Myokai, F., Matsuo, N., Taniguchi, S., Doi, H., Iseki, S., Ninomiya, Y., Fujiwara, M., Watanabe, T. and Eto, K. (1993) A mutation in the Pax-6 gene in rat small eye is associated with impaired migration of midbrain crest cells. *Nat Genet* **3**, 299-304.

Maulbecker, C.C. and Gruss, P. (1993) The oncogenic potential of Pax genes. *EMBO J* **12**, 2361-2367.

Max, E.E., Wakatsuki, Y., Neurath, M.F. and Strober, W. (1995) The role of BSAP in immunoglobulin isotype switching and B- cell proliferation. *Curr Top Microbiol Immunol* **194**, 449-458.

McConnell, M.J., Cunliffe, H.E., Chua, L.J., Ward, T.A. and Eccles, M.R. (1997) Differential regulation of the human Wilms tumour suppressor gene (WT1) promoter by two isoforms of PAX2. *Oncogene* **14**, 2689-2700.

McKusick, V.A. (1992) *Mendelian inheritance in man,* 10th edn. Baltimore, Maryland, USA: Johns Hopkins University Press.

McPherson, E., Carey, J., Kramer, A., Hall, J.G., Pauli, R.M., Schimke, R.N. and Tasin, M.H. (1987) Dominantly inherited renal adysplasia. *Am J Med Genet* **26**, 863-872.

Mendelsohn, C., Lohnes, D., Decimo, D., Lufkin, T., LeMeur, M., Chambon, P. and Mark, M. (1994) Function of the retinoic acid receptors (RAR) during development. *Development* **120**, 2749-2771.

Merino, R., Ding, L., Veis, D.J., Korsmeyer, S.J. and Nunez, G. (1994) Developmental regulation of the Bcl-2 protein and susceptibility to cell death in B lymphocytes. *EMBO J* **13**, 683-691.

Merlino, G.T., Stahle, C., Jhappan, C., Linton, R., Mahon, K.A. and Willingham, M.C. (1991) Inactivation of a sperm motility gene by insertion of an epidermal growth factor receptor transgene whose product is overexpressed and compartmentalized during spermatogenesis. *Genes Dev* **5**, 1395-1406.

Merritt, A.J., Potten, C.S., Watson, A.J., Loh, D.Y., Nakayama, K. and Hickman, J.A. (1995) Differential expression of bcl-2 in intestinal epithelia. Correlation with attenuation of apoptosis in colonic crypts and the incidence of colonic neoplasia. *J Cell Sci* **108**, 2261-2271.

Merry, D.E., Veis, D.J., Hickey, W.F. and Korsmeyer, S.J. (1994) Bcl-2 protein expression is widespread in the developing nervous system and retained in the adult PNS. *Development* **120**, 301-311.

Mesrobian, H.G.J., Rushton, H.G. and Bulas, D. (1993) Unilateral renal agenesis may result from in utero regression of multicystic dysplasia. *J Urol* **150**, 793-794.

Miller, A.D. and Buttimore, C. (1986) Redesign of retrovirus packaging cell lines to avoid recombination leading to helper virus production. *Mol Cell Biol* **6**, 2895-2902.

Miyamoto, N., Yoshida, M., Kuratani, S., Matsuo, I. and Aizawa, S. (1997) Defects of urogenital development in mice lacking Emx-2. *Development* **124**, 1653-1664.

Moll, R. and Franke, W.W. (1982) Intermediate filaments and their interaction with membranes. The desmosome-cytokeratin filament complex and epithelial differentiation. *Pathol Res Pract* **175**, 146-161.

Montesano, R., Schaller, G. and Orci, L. (1991) Induction of epithelial tubular morphogenesis in vitro by fibroblast-derived soluble factors. *Cell* **66**, 697-711.

Moore, K.L. (1988) *The developing human. Clinically oriented embryology.* Philadelphia, Pennsylvania, USA: WB Saunders.

Moore, M.W., Klein, R.D., Farinas, I., Sauer, H., Armanini, M., Phillips, H., Reichardt, L.F., Ryan, A.M., Carver-Moore, K. and Rosenthal, A. (1996) Renal and neuronal abnormalities in mice lacking GDNF. *Nature* **382**, 76-9-9.

Morham, S.G., Lanhenbach, R., Loftin, C.D., Tiano, H.F., Vouloumanos, N., Jennette, J.C., Mahler, J.F., Kluckman, K.D., Ledford, A., Lee, C.A. and Smithies, O. (1995) Prostaglandin synthase 2 gene disruption cuases severe renal pathology in the mouse. *Cell* **83**, 473-482.

Moutsatsos, I.K., Wade, M., Schindler, M. and Wang, J.L. (1987) Endogenous lectins from cultured cells. Nuclear localization of carbohydrate-binding protein 35 in proliferating 3T3 fibroblasts. *Proc Natl Acad Sci USA* **84**, 6452-6456.

Mugrauer, G. and Ekbolm, P. (1991) Contrasting expression patterns of three members of the myc family of proto-oncogenes in the developing and adult mouse kidney. *J Cell Biol* **112**, 13-25.

Muller, U., Wang, D., Denda, S., Meneses, J.J., Pedersen, R.A. and Reichardt, L.F. (1997) Integrin alpha 8 beta 1 is critically important for epithelial-mesenchymal interactions during kidney morphogenesis. *Cell* **88**, 603-613.

Mundlos, S., Pelletier, J., Darveau, A., Bachmann, M., Winterpacht, A. and Zabel, B. (1993) Nuclear localization of the protein encoded by the Wilms' tumor gene WT1 in embryonic and adult tissues. *Development* **119**, 1329-1341.

Nadasdy, T., Laszik, Z., Blick, K.E., Johnson, L.D. and Silva, F.G. (1994) Proliferative activity of intrinsic cell populations in the normal human kidney. *J Am Soc Nephrol* **4**, 2032-2039.

Nadasdy, T., Laszik, Z., Lajoie, G., Blick, K.E., Wheeler, D.E. and Silva, F.G. (1995) Proliferative activity of cyst epithelium in human renal cystic diseases. *J Am Soc Nephrol* **5**, 1462-1468.

Nagata, M., Nemoto, S. and Watanabe, T. (1998) Abnormal expression of BCL-2 in epithelial phenotypes involved in maldevelopment of dysplastic kidneys. *Ped Nephrol* **12**, C4 (Abstract).

Nakamura, T., Nawa, K. and Ichihara, A. (1984) Partial purification and characterization of hepatocyte growth factor from serum of hepatectomized rats. *Biochem Biophys Res Commun* **122**, 1450-1459.

Nguyen, H.Q., Danilenko, D.M., Bucay, N., DeRose, M.L., Van, G.Y., Thomason, A. and Simonet, W.S. (1996) Expression of keratinocyte growth factor in embryonic liver of transgenic mice causes changes in epithelial growth and differentiation resulting in polycystic kidneys and other organ malformations. *Oncogene* **12**, 2109-2119.

Novack, D.V. and Korsmeyer, S.J. (1994) Bcl-2 protein expression during murine development. *Am J Pathol* **145**, 61-73.

Novak, R.W. and Robinson, H.B. (1994) Coincident Di George anomaly and renal agenesis and its relation to maternal diabetes. *Am J Med Genet* **50**, 311-312.

O'Hare, M.J., Ormerod, M.G., Monaghan, P., Lane, E.B. and Gusterson, B.A. (1991) Characterization *in vitro* of luminal and myoepithelial cells isolated from the human mammary gland by cell sorting. *Differentiation* **46**, 209-221.

O'Neill, F.J., Frisque, R.J., Xu, X., Hu, Y.H. and Carney, H. (1995) Immortalization of human cells by mutant and chimaeric primate polyomavirus T-antigen genes. *Oncogene* **10**, 1131-1139.

Oberhammer, F., Wilson, J.W., Dive, C., Morris, I.D., Hickman, J.A., Wakeling, A.E., Walker, P.R. and Sikorska, M. (1993) Apoptotic death in epithelial cells: Cleavage of DNA to 300 and / or 50 kb fragments prior to or in absense of internucleosomal fragmentation. *EMBO J* **12**, 3679-3684.

Oltvai, Z.N., Milliman, C.L. and Korsmeyer, S.J.(1993) Bcl-2 heterodimerises in vivo with a conserved homologue, bax, that accelerates programmed cell death. *Cell* **74**, 609-619.

Oosterwijk, E., Van Muijen, G.N., Oosterwijk-Wakka, J.C. and Warnaar, S.O. (1990) Expression of intermediate-sized filaments in developing and adult human kidney and in renal cell carcinoma. *J Histochem Cytochem* **38**, 385-392.

Paavola, P., Salonen, R., Weissenbach, J. and Peltonen, L. (1995) The locus for Meckel syndrome with multiple congenital anomalies maps to chromosome 17q21-q24. *Nat Genet* **11**, 213-215.

Pelletier, J., Bruening, W., Kashtan, C.E., Mauer, S.M., Manivel, J.C., Striegel, J.E., Houghton, D.C., Junien, C., Habib, R. and Fouser, L. (1991) Germline mutations in the Wilms' tumor suppressor gene are associated with abnormal urogenital development in Denys-Drash syndrome. *Cell* **67**, 437-447.

Perantoni, A.O., Dove, L.F. and Karavanova, I. (1995) Basic fibroblast growth factor can mediate the early inductive events in renal development. *Proc Natl Acad Sci USA* **92**, 4696-4700.

Pezzella, F., Tse, A.G., Cordell, J.L., Pulford, K.A., Gatter, K.C. and Mason, D.Y. (1990) Expression of the bcl-2 oncogene protein is not specific for the 14;18 chromosomal translocation. *Am J Pathol* **137**, 225-232.

Phelps, D.E. and Dressler, G.R. (1996) Identification of novel Pax-2 binding sites by chromatin precipitation. *J Biol Chem* **271**, 7978-7985.

Pichel, J.G., Shen, L., Sheng, H.Z., Granholm, A.C., Drago, J., Grinberg, A., Lee, E.J., Huang, S.P., Saarma, M., Hoffer, B.J., Sariola, H. and Westphal, H. (1996) Defects in enteric innervation and kidney development in mice lacking GDNF. *Nature* **382**, 73-76.

Pilia, G., Hughes-Benzie, R.M., MacKenzie, A., Baybayan, P., Chen, E.Y., Huber, R., Neri, G., Cao, A., Forabosco, A. and Schlessinger, D. (1996) Mutations in GPC3, a glypican gene, cause the Simpson-Golabi-Behmel overgrowth syndrome. *Nat Genet* **12**, 241-247.

Plachov, D., Chowdhury, K., Walther, C., Simon, D., Guenet, J-P.L. and Gruss, P. (1990) Pax8, a murine paired box gene expressed in the developing excretory system and thyroid gland. *Development* **110**, 643-651.

Poleev, A., Fickenscher, H., Mundlos, S., Winterpacht, A., Zabel, B., Fidler, A., Gruss, P. and Plachov, D. (1992) PAX8, a human paired box gene: isolation and expression in developing thyroid, kidney and Wilms' tumors. *Development* **116**, 611-623.

Porter, J.A., Young, K.E. and Beachy, P.A. (1996) Cholesterol modification of hedgehog signaling proteins in animal development. *Science* **274**, 255-259.

Potter, E.L. (1972) *Normal and abnormal development of the kidney.* Chicago, Illinois, USA: Year Book Medical Publishers Inc.

Pritchard-Jones, K., Fleming, S., Davidson, D., Bickmore, W., Porteous, D., Gosden, C., Bard, J., Buckler, A., Pelletier, J. and Housman, D. (1990) The candidate Wilms' tumour gene is involved in genitourinary development. *Nature* **346**, 194-197.

Pritchard-Jones, K. and Hawkins, M.M. (1997) Biology of Wilms' tumour. *Lancet* **349**, 663-664.

Qiao, J., Cohen, D. and Herzlinger, D. (1995) The metanephric blastema differentiates into collecting system and nephron epithelia in vitro. *Development* **121**, 3207-3214.

Qiao, J., Cohen, J. and Herzlinger, D. (1996) FGF-7 uncouples the mitogenic and nephron inducing activities of the ureteric bud. *J Am Soc Nephrol* **7**, 1604A (Abstract).

Raff, M.C., Barres, B.A., Burne, J.F., Coles, H.S., Ishizaki, Y. and Jacobson, M.D. (1993) Programmed cell death and the control of cell survival: lessons from the nervous system. *Science* **262**, 695-700.

Rauscher, F.J., Morris, J.F., Tournay, O.E., Cook, D.M. and Curran, T. (1990) Binding of the Wilms' tumor locus zinc finger protein to the EGR-1 consensus sequence. *Science* **250**, 1259-1262.

Raz, A., Zhu, D.G., Hogan, V., Shah, N., Raz, T., Karkash, R., Pazerini, G. and Carmi, P. (1990) Evidence for the role of 34-kDa galactoside-binding lectin in transformation and metastasis. *Int J Cancer* **46**, 871-877.

Read, A.P. (1995) Pax genes - Paired feet in three camps. *Nat Genet* **5**, 333-334.

Richards, W.G., Sweeney, W.E., Yoder, B.K., Wilkinson, J.E., Woychik, R.P. and Avner, E.D. (1998) Epidermal growth factor receptor activity mediates renal cyst formation in polycystic kidney disease. *J Clin Invest* **101**, 935-939.

Rickwood, A.M., Anderson, P.A. and Williams, M.P. (1992) Multicystic renal dysplasia detected by prenatal ultrasonography. Natural history and results of conservative management. *Br.J Urol* **69**, 538-540.

Risdon, R.A. (1971) Renal dysplasia. Part I. A clinicopathological study of 76 cases. *J Clin Path* **24**, 57-65.

Robertson, K., Mason, I. and Hall, S. (1997) Hirschsprung's disease: genetic mutations in mice and men. *Gut* **41**, 436-441.

Rogers, S.A., Ryan, G. and Hammerman, M.R. (1992) Metanephric transforming growth factor-α is required for renal organogenesis in vitro. *Am J Physiol* **262**, F533-F539.

Rogers, S.A., Ryan, G., Purchio, A.F. and Hammerman, M.R. (1993) Metanephric transforming growth factor-β1 regulates nephrogenesis in vitro. *Am J Physiol* **264** , F996-F1002.

Roodhooft, A.M., Birnholz, J.C. and Holmes, L.B. (1984) Familial nature of congenital absence and severe dysgenesis of both kidneys. *N Engl J Med* **310**, 1341-1345.

Rosl, F. (1992) A simple and rapid method for detection of apoptosis in human cells. *Nucleic Acids Res* **20**, 5243.

Rothenpieler, U.W. and Dressler, G.R. (1993) *Pax-2* is required for mesenchymal-to-epithelium conversion during kidney development. *Development* **119**, 711-720.

Rothman, K.J., Moore, L.L., Singer, M.R., Nguyen, U.S., Mannino, S. and Milunsky, A. (1995) Teratogenicity of high vitamin A intake. *N Engl J Med* **333**, 1369-1373.

Ruoslahti, E. and Yamaguchi, Y. (1991) Proteoglycans as modulators of growth factor activities. *Cell* **64**, 867-869.

Rupprecht, H.D., Drummond, I.A., Madden, S.L., Rauscher, F.J. and Sukhatme, V.P. (1994) The Wilms' tumor suppressor gene WT1 is negatively autoregulated. *J Biol Chem* **269**, 6198-6206.

Ryan, G., Steele-Perkins, S.V., Morris, J.F., Rausher, F.J. and Dressler, G.R. (1995) Repression of Pax-2 by WT1 during normal kidney development. *Development* **121**, 867-875.

Sainio, K., Hellstedt, P., Kreidberg, J.A., Saxen, L. and Sariola, H. (1997) Differential regulation of two sets of mesonephric tubules by WT-1. *Development* **124**, 1293-1299.

Sambrook, J., Fritsch, E.F. and Maniatis, T. (1989) *Molecular cloning - a laboratory manual*, Plainview, New York, USA: Cold Spring Harbour Laboratory Press.

Sanchez, M.P., Silos Santiago, I., Frisen, J., He, B., Lira, S.A. and Barbacid, M. (1996) Renal agenesis and the absence of enteric neurons in mice lacking GDNF. *Nature* **382**, 70-73.

Santos, H., Mateus, J. and Leal, M.J. (1988) Hirschprung disease associated with polydactlyly, unilateral renal agenesis, hypertelorism, and congenital deafness: a new autosomal recessive syndrome. *J Med Genet* **25**, 204-208.

Santos, O.F.P., Barros, E.J.G., Yang, X.M., Matsumoto, K., Nakamura, T., Park, M. and Nigam, S.K. (1994) Involvement of hepatocyte growth factor in kidney development. *Dev Biol* **163**, 525-529.

Sanyanusin, P., Schimmentl, L.A., McNoe, L.A., Ward, T.A., Pierpoint, M.E.M., Sullivan, M.J., Dobyns, W.B. and Eccles, M.R. (1995) Mutations of the PAX2 gene in a family with optic nerve colobomas, renal anomalies and vesicoureteral reflux. *Nat Genet* **9**, 358-364.

Sato, S. and Hughes, R.C. (1992) Binding specificity of a baby hamster lectin for H type I and II chains of polylactosamine glycans and appropriately glycosylated forms of laminin and fibronectin. *J Biol Chem* **267**, 6983-6990.

Sato, S., Burdett, I. and Hughes, R.C. (1993) Secretion of the baby hamster kidney 30 kDa galactose binding lectin from polarised and non polarised cells a pathway independent of the endoplasmic reticulum Golgi complex. *Exp Cell Res* **207**, 8-18.

Sato, S. and Hughes, R.C. (1994) Control of Mac 2 surface expression on murine macrophage cell lines. *Eur J Immunol* **24**, 216-221.

Savill, J., Smith, J., Sarraf, C., Ren, Y., Abbott, F. and Rees, A. (1992) Glomerular mesangial cells and inflammatory macrophages ingest neutrophils undergoing apoptosis. *Kidney Int* **42**, 924-936.

Schedl, A., Ross, A., Lee, M., Engelkamp, D., Rashbass, P., van Heyningen, V. and Hastie, N.D. (1996) Influence of PAX6 gene dosage on development: overexpression causes severe eye abnormalities. *Cell* **86**, 71-82.

Schimmenti, L.A., Cunliffe, H.E., McNoe, L.A., Ward, T.A., French, M.C., Shim, H.H., Zhang, Y.H., Proesmans, W., Leys, A., Byerly, K.A., Braddock, S.R., Masuno, M., Imaizumi, K., Devriendt, K. and Eccles, M.R. (1997) Further delineation of renal-coloboma syndrome in patients with extreme variability of phenotype and identical PAX2 mutations. *Am J Hum Genet* **60**, 869-878.

Schmid, P., Schulz, W.A. and Hameister, H. (1989) Dynamic expression pattern of the myc protooncogene in midgestation mouse embryos. *Science* **243**, 226-229.

Schmid, P., Lorenz, A., Hameister, H. and Montenarh, M. (1991) Expression of p53 during mouse embryogenesis. *Development* **113**, 857-865.

Schmidt, C., Bladt, F., Goedecke, S., Brinkmann, V., Zschiesche, W., Sharpe, M., Gherardi, E. and Birchmeier, C. (1995) Scatter factor / hepatocyte growth factor is essential for liver development. *Nature* **373**, 699-702.

Schoeppner, H.L., Raz, A., Ho, S.B. and Bresalier, R.S. (1995) Expression of an endogenous galactose binding lectin correlates with neoplastic progression in the colon. *Cancer* **75**, 2818-2826.

Schuchardt, A., D'Agati, V., Larsson Blomberg, L., Costantini, F. and Pachnis, V. (1994) Defects in the kidney and enteric nervous system of mice lacking the tyrosine kinase receptor Ret. *Nature* **367**, 380-383.

Schumer, M., Colombel, M.C., Sawczuk, I.S., Gobe, G., Connor, J., O'Toole, K.M., Olsson, C.A., Wise, G.J. and Buttyan, R. (1992) Morphological,biochemical and molecular evidence of apoptosis during the reperfusion phase after brief periods of renal ischemia. *Am J Pathol* **140**, 831-838.

Schwartz, L.M. and Osborne, B.A. (1993) Programmed cell death, apoptosis and killer genes. *Immunol Today* **14**, 582-590.

Schwartz, L.M., Smith, S.W., Jones, M.E. and Osborne, B.A. (1993) Do all programmed cell deaths occur via apoptosis? *Proc Natl Acad Sci USA* **90**, 980-984.

Sharon, N. and Lis, H. (1989) Lectins as cell recognition molecules. *Science* **246**, 227-234.

Shawlot, W. and Behringer, R.R. (1995) Requirement for Lim1 in head-organizer function. *Nature* **374**, 425-430.

Shi, S.R., Key, M.E. and Kalra, K.L. (1991) Antigen retrieval in formalin-fixed, paraffin-embedded tissues: an enhancement method for immunohistochemical staining based on microwave oven heating of tissue sections. *J Histochem Cytochem* **39**, 741-748.

Sonnenberg, E., Meyer, D., Weidner, K.M. and Birchmeier, C. (1993) Scatter factor/hepatocyte growth factor and its receptor, the c- met tyrosine kinase, can mediate a signal exchange between mesenchyme and epithelia during mouse development. *J Cell Biol* **123**, 223-235.

Sorenson, C.M., Rogers, S.A., Korsmeyer, S.J. and Hammerman, M.R. (1995) Fulminant metanephric apoptosis and abnormal kidney development in bcl-2 deficient mice. *Am J Physiol* **268**, F73-F81.

Sorenson, C.M., Padanilam, B.J. and Hammerman, M.R. (1996) Abnormal postpartum renal development and cystogenesis in the bcl-2 (-/-) mouse. *Am J Physiol* **271**, F184-F193.

Soriano, P. (1994) Abnormal kidney development and hematological disorders in platelet derived growth factor β-receptor mutant mice. *Genes Dev* **8**, 1888-1896.

Sorokin, L., Sonnenberg, A., Aumailley, M., Timpl, R. and Ekblom, P. (1990) Recognition of the laminin E8 cell-binding site by an integrin possessing the alpha 6 subunit is essential for epithelial polarization in developing kidney tubules. *J Cell Biol* **111**, 1265-1273.

Soussi-Yanicostas, N., Hardelin, J.P., Arroyo-Jimenez, M.M., Ardouin, O., Legouis, R., Levilliers, J., Traincard, F., Betton, J.M., Cabanie, L. and Petit, C. (1996) Initial characterization of anosmin-1, a putative extracellular matrix protein synthesized by definite neuronal cell populations in the central nervous system. *J Cell Sci* **109**, 1749-1757.

Stamps, A.C., Davies, S.C., Burman, J. and O'Hare, M.J. (1994) Analysis of proviral integration in human mammary epithelial cell lines immortalized by retroviral infection with a temperature-sensitive SV40 T-Antigen construct. *Int J Cancer* **57**, 865-874.

Stanton, B.R. and Parada, L.F. (1992) The N-myc proto-oncogene: developmental expression and in vivo site-directed mutagenesis. *Brain Pathol* **2**, 71-83.

Stapleton, P., Weith, A., Urbanek, P., Kozmik, Z. and Busslinger, M. (1993) Chromosomal localisation of seven Pax genes and cloning of a novel family member: Pax9. *Nat Genet* **3**, 292-298.

Stark, K., Vanio, S., Vassileva, G. and McMahon, A.P. (1994) Wnt-4 regulates epithelial transformation of metanephric mesenchyme in the developing kidney. *Nature* **372**, 679-683.

Steinhardt, G.F., Vogler, G., Salinas-Madrigal, L. and et al. (1988) Induced renal dysplasia in the young pouch opossum. *J Pediatr Surg* **23**, 1127-1130.

Steinhardt, G.F., Liapis, H., Phillips, B., Vogler, G., Nag, M. and Yoon, K.W. (1995) Insulin-like growth factor improves renal architecture of fetal kidneys with complete ureteral obstruction. *J Urol* **154**, 690-693.

Stoker, M., Gherardi, E., Perryman, M. and Gray, J. (1987) Scatter factor is a fibroblast-derived modulator of epithelial cell mobility. *Nature* **327**, 239-242.

Stuart, E.T., Haffner, R., Oren, M. and Gruss, P. (1995) Loss of p53 function through PAX-mediated transcriptional repression. *EMBO J* **14**, 5638-5645.

Suzuka, I., Daidoji, H., Matsuoka, M., Kadowaki, K., Takasaki, Y., Nakane, P.K. and Moriuchi, T. (1989) Gene for proliferating-cell nuclear antigen (DNA polymerase delta auxiliary protein) is present in both mammalian and higher plant genomes. *Proc Natl Acad Sci USA* **86**, 3189-3193.

Tagge, E.P., Hanson, P., Re, G.G., Othersen, H.B.J., Smith, C.D. and Garvin, A.J. (1994) Paired box gene expression in Wilms' tumor. *J Pediatr Surg* **29**, 134-141.

Takayama, H., La Rochelle, W.J., Anver, M., Bockman, D.E. and Merlin, G. (1996) Scatter factor/hepatocyte growth factor as a regulator of skeletal muscle and neural crest development. *Proc Natl Acad Sci USA* **93**, 5866-5871.

Tanner, M.J. (1996) Physiology: The acid test for band 3. *Nature* **382**, 209-210.

Tassabehji, M., Read, A.P., Newton, V.E., Patton, M., Gruss, P., Harris, R. and Strachan, T. (1993) Mutations in the Pax 3 gene causing Waardenburg syndrome type 1 and 2. *Nat Genet* **3**, 26-30.

Threadgill, D.W., Dlugosz, A.A., Hansen, L.A., Tennenbaum, T., Lichti, U., Yee, D., LaMantia, C., Mourton, T., Herrup, K., Harris, R.C., Barnard, J.A., Yuspa, S.H., Coffey, R.J. and Magnuson, T. (1995) Targeted disruption of mouse EGF receptor. Effect of genetic background on mutant phenotype. *Science* **269**, 230-234.

Tornell, J., Farzad, S., Espander-Jansson, A., Matejka, G., Isaksson, O. and Rymo, L. (1996) Expression of Epstein-Barr nuclear antigen 2 in kidney tubule cells induce tumors in transgenic mice. *Oncogene* **12**, 1521-1528.

Torres, M., Gomex-Pardo, E., Dressler, G.R. and Gruss, P. (1995) Pax-2 controls multiple steps of urogenital development. *Development* **121**, 4057-4065.

Torrey, T.W. (1954) The early development of the human nephros. *Contib Embryol* **239**, 175-197.

Towers, P.R., Woolf, A.S. and Hardman, P. (1998) Glial cell line-derived neurotrophic factor stimulates ureteric bud outgrowth and enhances survival of ureteric bud cells *in vitro*. *Exp Nephrol* **6**, 337-351

Trudel, M., D'Agati, V. and Costantini, F. (1991) c-Myc as an inducer of polycystic disease in transgenic mice. *Kidney Int* **39**, 665-671.

Truong, L.D., Petrusevska, G., Yang, G., Gurpinar, T., Shappell, S., Lechago, J., Rouse, D. and Suki, W.N. (1996) Cell apoptosis and proliferation in experimental chronic obstructive uropathy. *Kidney Int* **50**, 200-207.

Tse, H.K.W., Woolf, A.S., Gosling, J.A. and Shum, A.S.W. (1997) Embryonic development of renal agenesis in a mouse model. *Br Soc Dev Biol, Warwick, Spring 1997* (Abstract).

Vainio, S., Lehtonen, E., Jalkanen, M., Bernfield, M. and Saxen, L. (1989) Epithelial-mesenchymal interactions regulate the stage-specific expression of a cell surface proteoglycan, syndecan, in the developing kidney. *Dev Biol* **134**, 382-391.

Van den Brule, F.A., Fernandez, P.L., Buicu, C., Liu, F.T., Jackers, P., Lambotte, R. and Castronovo, V. (1997) Differential expression of galectin-1 and galectin-3 during first trimester human embryogenesis. *Dev Dyn* **209**, 399-405.

Vaux, D.L. (1993) Towards an understanding of the molecular mechanisms of physiological cell death. *Proc Natl Acad Sci USA* **90**, 786-789.

Vaux, D.L. and Weissman, I.L. (1993) Neither macromolecular synthesis nor myc is required for cell death via the mechanism that can be controlled by Bcl-2. *Mol Cell Biol* **13**, 7000-7005.

Vega, Q.C., Worby, C.A., Lechner, M.S., Dixon, J.E. and Dressler, G.R. (1996) Glial cell line-derived neurotrophic factor activates the receptor tyrosine kinase RET and promotes kidney morphogenesis. *Proc Natl Acad Sci USA* **93**, 10657-10661.

Veis, D.J., Sorenson, C.M., Shutter, J.R. and Korsmeyer, S.J. (1993) Bcl-2 deficient mice demonstrate fulminant lymphoid apoptosis, polycystic kidneys and hypopigmented hair. *Cell* **75**, 229-240.

Verani, R., Walker, P. and Silva, F.G. (1989) Renal cystic disease of infancy: results of histochemical studies. *Ped Nephrol* **3**, 37-42.

Vestweber, D. and Kemler, R. (1985) Identification of a putative cell adhesion domain of uvomorulin. *EMBO J* **4**, 3393-3398.

Wagner, S., Vogel, R., Lietzke, R., Koob, R. and Drenckhahn, D. (1987) Immunochemical characterization of a band 3-like anion exchanger in collecting duct of human kidney. *Am J Physiol* **253**, F213-F221

Wainwright, S.D., Tanner, M.J., Martin, G.E., Yendle, J.E. and Holmes, C. (1989) Monoclonal antibodies to the membrane domain of the human erythrocyte anion transport protein. Localization of the C-terminus of the protein to the cytoplasmic side of the red cell membrane and distribution of the protein in some human tissues. *Biochem J* **258**, 211-220.

Wallin, J., Eibel, H., Neubuser, A., Wilting, J., Koseki, H. and Balling, R. (1996) Pax1 is expressed during the development of the thymus epithelium and is required for normal T-cell maturation. *Development* **122**, 23-30.

Wang, L., Inohara, H., Pienta, K.J. and Raz, A. (1995) Galectin-3 is a nuclear matrix protein which binds RNA. *Biochem Biophys Res Commun* **217**, 292-303.

Wang, Y., Selden, C., Farnaud, S., Calnan, D. and Hodgson, H.J. (1994) Hepatocyte growth factor (HGF / SF) is expressed in human epithelial cells during embryonic development; studies by in situ hybridisation and northern blot analysis. *J Anat* **185**, 543-551.

Warady, B.A., Hebert, D., Sullivan, E.K., Alexander, S.R. and Tejani, A. (1997) Renal transplantation, chronic dialysis, and chronic renal insufficiency in children and adolescents. The 1995 Annual Report of the North American Pediatric Renal Transplant Cooperative Study. *Ped Nephrol* **11**, 49-64.

Webb, N.J., Lewis, M.A., Bruce, J., Gough, D.C., Ladusans, E.J., Thomson, A.P. and Postlethwaite, R.J. (1997) Unilateral multicystic dysplastic kidney: the case for nephrectomy. *Arch Dis Child* **76**, 31-34.

Weitlauf, H.M. and Knisley, K.A. (1992) Changes on surface antigens on preimplantation mouse embryos. *Biol Reprod* **46**, 811-816.

Wilkie, A.O., Slaney, S.F., Oldridge, M., Poole, M.D., Ashworth, G.J., Hockley, A.D., Hayward, R.D., David, D.J., Pulleyn, L.J. and Rutland, P. (1995) Apert syndrome results from localized mutations of FGFR2 and is allelic with Crouzon syndrome. *Nat Genet* **9**, 165-172.

Wilson, P.D., Hreniuk, D. and Gabow, P.A. (1992) Abnormal extracellular matrix and excessive growth of human adult polycystic kidney disease epithelia. *J Cell Physiol* **150**, 360-369.

Winyard, P.J.D., Nauta, J., Lirenman, D.S., Hardman, P., Sams, V.R., Risdon, A.R. and Woolf, A.S. (1996a) Deregulation of cell survival in cystic and dysplastic renal development. *Kidney Int* **98**, 135-146.

Winyard, P.J.D., Risdon, R.A., Sams, V.R., Dressler, G. and Woolf, A.S. (1996b) The PAX2 transcription factor is expressed in cystic and hyperproliferative dysplastic epithelia in human kidney malformations. *J Clin Invest* **98**, 451-459.

Winyard, P.J.D., Bao, Q., Hughes, R.C. and Woolf, A.S. (1997) Epithelial galectin-3 during human nephrogenesis and childhood cystic diseases. *J Am Soc Nephrol* **8**, 1647-1657.

Witzgall, R., Brown, D., Schwarz, C. and Bonventre, J.V. (1994) Localization of proliferating cell nuclear antigen, vimentin, c-Fos, and clusterin in the postischemic kidney. Evidence for a heterogenous genetic response among nephron segments, and a large pool of mitotically active and dedifferentiated cells. *J Clin Invest* **93**, 2175-2188.

Woo, D. (1995) Apoptosis and loss of renal tissue in polycystic kidney diseases. *N Engl J Med* **333**, 18-25.

Woo, D.D.L., Miao, S., Pelayo, J. and Woolf, A.S. (1994) Taxol inhibits congenital polycystic kidney disease progression. *Nature* **368**, 750-753.

Woolf, A.S. (1995) Clinical impact and biological basis of kidney malformations. *Sem Nephrol* **15**, 361-372.

Woolf, A.S., Kolatsi-Joannou, M., Hardman, P., Andermarcher, E., Moorby, C., Fine, L.G., Jat, P.S., Noble, M.D. and Gherardi, E. (1995) Roles of hepatocyte growth factor/scatter factor (HGF / SF) and met in early development of the metanephros. *J Cell Biol* **128**, 171-184.

Woolf, A.S., Bao, Q., Hughes, R.C. and Winyard, P.J.D. (1996) Galectin-3 in normal, polycycstic and dysplastic nephrogenesis. *J Am Soc.Nephrol* **7**, 1626 (Abstract).

Woolf, A.S. (1997) The kidney. In: Thorogood, P., (Ed.) *Embryos, genes and birth defects*, Chichester, West Sussex, UK: John Wiley and Sons Ltd.

Woolf, A.S. and Cale, C.M. (1997) Roles of growth factors in renal development. *Curr Opin Nephrol Hypertens* **6**, 10-14.

Woolf, A.S. and Loughna, S. (1998) Origin of glomerular capillaries: is the verdict in? *Exp Nephrol* **6**, 17-21.

Woolf, A.S. and Winyard, P.J.D. (1998) Advances in the cell biology and genetics of human kidney malformations. *J Am Soc Nephrol* **9**, 1114-1125.

Wride, M.A., Lapchak, P.H. and Sanders, E.J. (1994) Distribution of TNFα-like proteins correlates with some regions of programmed cell death in the chick embryo. *Int J Dev Biol* **38** , 673-682.

Wyllie, A.H. (1980) Glucocorticoid-induced thymocyte apoptosis is associated with endogenous endonuclease activation. *Nature* **284**, 555-556.

Wyllie, A.H., Kerr, J.F.R. and Currie, A.R. (1980) Cell death: the significance of apoptosis. *Int Rev Cytol* **68**, 251-306.

Xu, X.C., El Naggar, A.K. and Lotan, R. (1995) Differential expression of galectin-1 and galectin-3 in thyroid tumors. Potential diagnostic implications. *Am J Pathol* **147**, 815-822.

Yang, R.Y., Hsu, D.K. and Liu, F.T. (1996) Expression of galectin-3 modulates T cell growth and apoptosis. *Proc Natl Acad Sci USA* **93**, 6737-6742.

Zamzami, N., Susin, S.A., Marchetti, P., Hirsch, T., Gomez-Monterrey, I., Castedo, M. and Kroemer, G. (1996) Mitochondrial control of nuclear apoptosis. *J Exp Med* **183**, 1533-1544.

Zerres, K., Mucher, G., Bachner, L., Deschennes, G., Eggermann, T., Kaariainen, H., Knapp, M., Lennert, T., Misselwitz, J., von Muhlendahl, K.E., Neumann, H.P.H., Pirson, Y., Rudnik Schoneborn, S., Steinbicker, V., Wirth, B. and Scharer, K. (1994) Mapping of the gene for autosomal recessive polycystic kidney disease (ARPKD) to chromosome 6p21 cen. *Nat Genet* **7**, 429-432.

Zhang, P., Liegeois, N.J., Wong, C., Finegold, M., Hou, H., Thompson, J.C., Silverman, A., Harper, J.W., DePinho, R.A. and Elledge, S.J. (1997) Altered cell differentiation and proliferation in mice lacking p57KIP2 indicates a role in Beckwith-Wiedemann syndrome. *Nature* **387**, 151-158.

Zhu, W., Cowie, A., Wasfy, G.W., Penn, L.Z., Leber, B. and Andrews, D.W. (1996) Bcl-2 mutants with restricted subcellular location reveal spatially distinct pathways for apoptosis in different cell types. *EMBO J* **15**, 4130-4141.

Deregulation of cell survival in cystic and dysplastic renal development

PAUL J.D. WINYARD, JEROEN NAUTA, DAVID S. LIRENMAN, PATRICIA HARDMAN, VIRGINIA R. SAMS,
R. ANTHONY RISDON, and ADRIAN S. WOOLF

Developmental Biology Unit, Institute of Child Health, London, England, United Kingdom; Department of Paediatric Nephrology, Sophia Childrens Hospital, Rottterdam, The Netherlands; Department of Histopathology, Hospital for Sick Children, and Department of Histopathology, University College Medical School, London, England, United Kingdom

Deregulation of cell survival in cystic and dysplastic renal development. Various aberrations of cell biology have been reported in polycystic kidney diseases and in cystic renal dysplasias. A common theme in these disorders is failure of maturation of renal cells which superficially resemble embryonic tissue. Apoptosis is a feature of normal murine nephrogenesis, where it has been implicated in morphogenesis, and fulminant apoptosis occurs in the small, cystic kidneys which develop in mice with null mutations of *bcl-2*. Therefore, we examined the location and extent of apoptosis in pre- and postnatal samples of human polycystic and dysplastic kidney diseases using propidium iodide staining, *in situ* end-labeling and electron microscopy. In dysplastic kidneys cell death was prominent in undifferentiated cells around dysplastic tubules and was occasionally found in cystic epithelia. The incidence of apoptosis was significantly greater than in normal controls of comparable age both pre- and postnatally. In the polycystic kidneys there was widespread apoptosis in the interstitium around undilated tubules distant from cysts, in undilated tubules between cysts and in cystic epithelia. The level of apoptosis compared to controls was significantly increased postnatally. A similar increase of cell death was also noted in the early and late stages of renal disease in the polycystic *cpk/cpk* mouse model. We speculate that deregulation of cell survival in these kidneys may reflect incomplete tissue maturation, and may contribute to the progressive destruction of functional kidney tissue in polycystic kidneys and the spontaneous involution reported in cystic dysplastic kidneys.

Organogenesis involves an increase in cell numbers, cell differentiation and morphogenesis. In normal development the increase in cell number is determined by the balance between proliferation and death, which in this context has been called 'programmed cell death.' This term is often used interchangably with 'apoptosis,' first used by Kerr, Wyllie and Currie [1] to describe death in a variety of normal and pathological contexts when accompanied by nuclear condensation and fragmentation with cell shrinkage. These changes are striking on electron microscopy but can also be detected by light microscopy as pyknotic nuclei [2]. A common biochemical correlate of apoptosis is DNA digestion by endonucleases into nucleosome sized fragments which can be visualized as a 'ladder' on electrophoresis [3] and detected *in situ* by end-labeling [4]. Exceptionally, some programmed cell death during development is not accompanied by these morphological events [5] and laddering is not always detected in cells dying by morphological criteria of apoptosis, since the DNA is sometimes cleaved into larger fragments (50 to 300 kbp) [6]. In the worm *Caenorhabditis elegans* apoptosis is developmentally regulated by the expression of specific genes, and some of their mammalian homologues have been defined [7]. 'Growth factors' not only control proliferation and differentiation but can also enhance apoptosis [8] or act as survival factors [9]. In contrast to apoptosis, cells dying by necrosis swell with destruction of organelles and loss of integrity of cell membranes [10]. DNA laddering does not occur in necrosis, although some models show single-strand DNA breaks [6].

In nephrogenesis cell proliferation, differentiation and morphogenesis occur during the branching of the ureteric bud and in nephron formation [11–13]. Apoptosis has been demonstrated during normal murine renal development in the nephrogenic zone and also in the papilla; cell death can be reduced by epidermal growth factor (EGF) [2]. Koseki, Herzlinger and Al-Awqati showed that uninduced renal mesenchyme died by apoptosis when isolated from the ureteric bud, and that this process was ameliorated by EGF [14]. Similarly, hepatocyte growth factor (HGF) has been implicated in survival of renal mesenchymal cells in serum-free organ culture [15].

The pathogenesis of some human kidney diseases can be understood in the context of aberrant development. In polycystic kidney diseases (PKD) there is evidence of enhanced epithelial proliferation [16] and altered polarity [17–18], leading some authors to suggest that the epithelial cells are "locked" in an immature, dedifferentiated state [19]. Similarly, in dysplastic kidneys there is a failure of differentiation of renal mesenchyme into nephrons and decreased branching of the ureteric bud [11, 20, 21]. We therefore considered it pertinent to examine the location and quantity of apoptosis in normal human nephrogenesis and in kidney diseases which can be viewed as aberrations of normal nephrogenesis. In this study we demonstrate that the distribution and incidence of renal programmed cell death is increased in children with polycystic and dysplastic kidneys.

Methods

Experimental strategy

The aim of the study was to define the tissue location and quantify the extent of apoptosis during normal kidney development and in fetal and childhood polycystic and dysplastic kidneys. The methodologies we used included both histological and molecular techniques together with quantitative statistical analysis.

Classification of specimens

This research was approved by the hospitals' research ethics committees. During human development the metanephros can first be identified in the sixth week after fertilization, and sequential layers of nephrons are formed until 36 weeks after fertilization [11]. We therefore divided our specimens into experimental prenatal groups before 40 weeks gestation and postnatal groups after 40 weeks as follows:

(i) Normal prenatal kidneys ($N = 6$).
(ii) Polycystic prenatal kidneys ($N = 4$).
(iii) Dysplastic prenatal kidneys ($N = 6$).
(iv) Normal postnatal kidneys ($N = 6$).
(v) Polycystic postnatal kidneys ($N = 4$).
(vi) Dysplastic postnatal kidneys ($N = 4$).

Details of these patients and specimens are listed in Tables 1 and 2, including their sex, the gestational or chronological age, associated abnormalities in other organ systems, indications for termination of pregnancy or for removal of a kidney, plus the side affected by renal disease and the plasma creatinine in the childhood samples. There was no significant difference in age and sex distribution within the prenatal and postnatal groups. Kidney pathology was classified by gross morphology, routine histopathology and, in the cases of polycystic kidneys, by liver histology and family history. All of the polycystic kidneys were classified as autosomal-recessive polycystic kidney disease (ARPKD) apart from one postnatal sample, which had histology consistent with dominant disease (ADPKD), although ultrasound scans of the parents (aged 21 and 23) were normal. Two children with ARPKD had elevated plasma creatinines. The dysplastic samples all had classical histological criteria of this disorder, namely dysplastic tubules, undifferentiated 'mesenchymal' tissue and metaplastic cartilage.

Collection of specimens

For the normal prenatal kidney group we studied both spontaneous miscarriages and phenotypically normal kidneys from abortions performed for severe abnormalities in other organ systems that would have compromised the survival of the fetus or infant. These samples were compared with the polycystic and dysplastic kidneys which were collected under similar conditions. In these three groups the parents were given time to mourn the loss of the child. Then the fetus was stored at 4°C until autopsy when organs were fixed in 10% formalin. All specimens were processed within 24 hours.

The postnatal polycystic and dysplastic samples were harvested surgically. Therefore, as a comparable normal surgical group we used kidney tissue adjacent to, but unaffected by, Wilms' tumors. These kidneys were chosen to control for any potential changes in tissue morphology which may have been induced by general anaesthesia or surgery. Since both WT1 mutations and chemotherapy may cause apoptosis [6, 22], we excluded children who

Table 1. Prenatal kidneys

Gestational age *weeks*	Sex	Renal and associated pathology
Normal prenatal kidneys		
17	M	Abortion for neural tube defect
19	M	Spontaneous miscarriage
20	F	Abortion for trisomy 21 with atrial septal defect
20	F	Spontaneous miscarriage
21	M	Abortion for cephalocoele
22	F	Abortion for major skeletal malformations
Polycystic prenatal kidneys		
20	M	Abortion for ARPKD
34	F	Spontaneous premature labor, ARPKD
35	F	Spontaneous premature labor, liver fibrosis, ARPKD
35	M	Spontaneous premature labor, liver fibrosis, ARPKD
Dysplastic prenatal kidneys		
17	M	Abortion for multicystic dysplastic kidney with contralateral renal agenesis
19	F	Abortion for multicystic dysplastic kidney with contralateral renal agenesis
20	M	Abortion for bilateral renal cystic dysplasia
22	M	Abortion for bilateral renal cystic dysplasia, bladder dilated without anatomical urethral obstruction, atrial septal defect
24	F	Abortion for bilateral renal cystic dysplasia
34	M	Spontaneous premature labor, kidneys dysplastic, bladder dilated with partial urethral obstruction

Children born at 34 to 35 weeks died within hours because of respiratory failure due to hypoplastic lungs. Chromosomes were normal in all fetuses assessed except for the case of trisomy 21. Parents were normal by history in all cases.

had received chemotherapy, and none of our patients had mutations in the WT1 gene (personal communication, Dr. Richard Grundy, Dept. of Haematology and Oncology, Hospital for Sick Children, Great Ormond Street, London, UK). Surgical specimens were placed on ice, examined by a pathologist and immediately fixed in 10% formalin for histology. A limited number of dysplastic samples ($N = 3$) were snap frozen in liquid nitrogen for DNA extraction and fixed in glutaraldehyde for electron microscopy.

Detection of apoptosis by propidium iodide staining

All chemicals were supplied by Sigma (Poole, Dorset, England, UK) unless otherwise stated. Propidium iodide is a fluorescent dye which intercalates with nucleic acids. Apoptotic cells can be identified in tissue sections by their small, fragmented (pyknotic) nuclei which stain brightly when they are visualised under fluorescence miscoscopy. We used the technique of Coles, Burne and

Table 2. Postnatal kidneys

Age months	Side	Sex	Plasma creatinine μmol/liter	Renal pathology
Normal postnatal kidneys				
5	R	F	60	Wilms' tumor before chemotherapy
8	R	M	65	Wilms' tumor before chemotherapy
28	L	M	35	Wilms' tumor before chemotherapy
30	R	M	48	Wilms' tumor before chemotherapy
38	R	M	34	Wilms' tumor before chemotherapy
72	L	F	38	Wilms' tumor before chemotherapy
Polycystic postnatal kidneys				
10	R	F	98[a]	Diagnostic open surgical biopsy, ARPKD
11	L	M	14	Diagnostic open surgical biopsy, histological appearance of ADPKD
48	R	M	322[a]	Nephrectomy at time of renal transplant, ARPKD
72	R	M	50	Surgical biopsy because of recurrent infections, ARPKD
Dysplastic postnatal kidneys				
8	R	F	50	Cystic dysplastic upper pole with obstruction at pelvi-ureteric junction
15	R	M	33	Non-functioning multicystic dysplastic kidney
16	R	M	32	Non-functioning multicystic dysplastic kidney
60	L	F	38	Uilateral duplex ureters with non-functioning dysplastic upper pole

Creatinine is the immediate preoperative level.

[a] Two children in the polycystic group had abnormal creatinines, but this did not appear to correlate with the pyknotic index in these specimens (data not shown). No kidney disease was reported in any of the parents including the histologically defined ADPKD.

Raff [2] with minor modifications. Five micrometer paraffin sections were dewaxed through Histo-Clear (National Diagnostics, Atlanta, GA, USA) twice for 10 minutes, followed by rehydration through 100% alcohol (Hayman Ltd., Witham, Essex, England, UK) twice for five minutes and then stepwise through 95%, 90%, 75%, 50% and 30% alcohol for three minutes each. After washing in phosphate buffered saline (PBS, pH 7.4) for five minutes, they were incubated in propidium iodide (4 mg/liter)

with RNase A (100 mg/liter; Unipath, Basingstoke, Hampshire, England, UK) in PBS at 37°C for 30 minutes. After one further wash in PBS they were mounted in Citifluor™ (Chemical Labs, University of Kent, Canterbury, Kent, England, UK). Specimens were examined under fluorescence (wavelength 568 nm) on a Zeiss Axiophot microscope (Carl Zeiss, Oberkochen, Germany) and on a Leica confocal laser scanning microscope (CLSM Aristoplan-Leica, Heidleberg, Germany). The precise tissue location of apoptosis was determined in ARPKD samples by counter-staining with FITC conjugated *Tetragonolobus lotus* or *Arachis hypogaea* lectins. These bind to proximal tubules and distal segments (distal tubule and collecting ducts), respectively [23, 24]. After the propidium iodide staining the lectins were applied to the sections at 1:50 dilution in PBS at room temperature for four hours, mounted in Citifluor™ and examined under fluorescence (wavelength 488 nm). Apoptotic nuclei detected by the propidium iodide method were quantified by generating a pyknotic index and by calculating the percentage of pyknotic nuclei as described below.

Detection of apoptosis by in situ end-labeling

During apoptosis the nuclear DNA is digested by endonucleases leaving free 3′ ends. These ends can be tagged using terminal deoxytransferase to add labeled nucleotides which can be visualized on a tissue section using secondary detection systems. We modified the technique of Gavrelli, Sherman and Ben-Sassoon [4] by using an Apoptag™ kit (Oncor, Gaithersburg, MD, USA). Paraffin sections were dewaxed and rehydrated, treated with proteinase K (20 mg/liter) for 15 minutes and washed in PBS. Slides were then covered with equilibration buffer for 30 seconds, followed by terminal deoxytransferase and digoxigenin conjugated UTP from the Apoptag™ kit as recommended by the manufacturer. The reaction was terminated using the Apoptag™ stop buffer. Labeled nuclei were detected either (i) by light microscopy after incubation with a peroxidase conjugated anti-digoxigenin antibody and diamino benzidine (these sections were quenched with 3% hydrogen peroxide for 15 minites at room temperature as an initial step) or (ii) by fluorescent microscopy (wavelength 568 nm) after applying an anti-digoxigenin antibody conjugated with rhodamine (Boehringer Mannheim, Lewes, East Sussex, UK).

Quantitation of apoptosis in human kidneys

Preliminary experiments with both propidium iodide and *in situ* end-labeled specimens showed that the number of apoptotic cells could vary between different areas of the same section, although there was good correlation between the two techniques. Therefore, in order to integrate the quantity of apoptosis in each specimen we photographed 10 random fields stained with propidium iodide from throughout each sample at 20 × magnification on a Zeiss Axiophot microscope. The number of pyknotic nuclei was then counted by three observers in a blinded fashion, and we derived the Pyknotic Index for each specimen by taking the mean number of pyknotic nuclei per 10 fields. Results from each observer were also compared to ensure that there was no observer bias [25]. In this study we have also expressed the quantity of apoptosis as a percentage of the total number of nuclei. Since the pyknotic indices and the percentage of apoptotic cells in each experimental group were not normally distributed we transformed the data by converting to $\log_{10}$ values, thus allowing analysis by
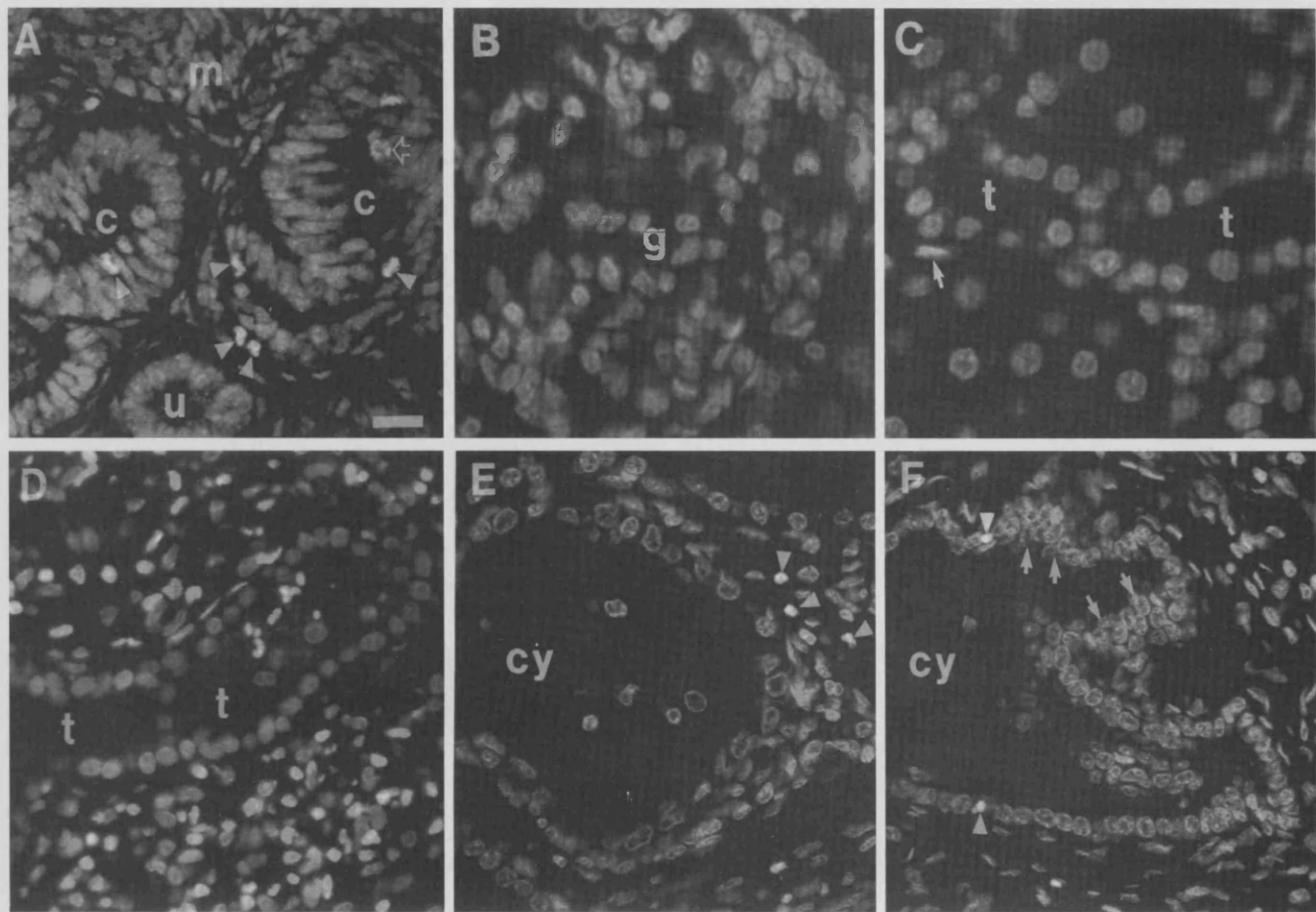
Fig. 1. *Location of apoptosis in propidium iodide stained sections of normal and polycystic kidneys.* (**A**) Nephrogenic zone from normal developing kidney, 20 weeks gestation. Note apoptotic nuclei in comma shaped bodies, which are primitive nephrons. (**B**) Glomerulus and (**C**) proximal tubule from normal postnatal kidney from patient aged 30 months. Note absence of apoptosis, although nuclei in the glomerulus appear generally brighter. A fibroblast is seen adjacent to the tubule epithelium in (C). It has a bright elongated nucleus but should not be confused with the smaller irregular pyknotic nuclei. (**D**) Undilated tubule from polycystic kidney harvested at 34 weeks of gestation surrounded by numerous apoptotic nuclei in interstitial tissue. (**E**) is from a child with ARPKD and shows a group of apoptotic nuclei in the interstitium between cysts. (**F**) is from an infant with dominant disease showing 2 apoptotic nuclei in the epithelium of a cyst close to a multilayered region of epithelium suggestive of hyperproliferation. Key: comma shaped body (c), cyst (cy), glomerulus (g), undifferentiated renal mesenchyme (m), tubule (t) and ureteric bud (u). Arrowheads indicate apoptotic nuclei, open arrow in (A) indicates a mitotic figure, closed arrow in (C) indicates a fibroblast and closed arrows in (F) point to multilayered epithelium. Bar is 20 μm.

Student's *t*-test. A probability value of $P < 0.05$ was considered to be statistically significant.

Detection of apoptosis by electron microscopy

Apoptotic cells have a characteristic appearance on electron microscopy with nuclear condensation around the periphery of the nucleus, cell shrinkage and budding off of both the nuclear and cell membranes. Samples of three dysplastic kidneys were fixed initially in 2% glutaraldehyde in 0.05 M cacodylate buffer,

then in 1% Osmium tetroxide and finally embedded in epoxy resin. Ultrathin sections contrasted with uranyl acetate and lead citrate were examined with a Jeol 100 CX transmission electron microscope.

Detection of apoptosis by DNA electrophoresis

During apoptosis endonuclease DNA digestion produces nucleotide fragments which are multiples of 180 to 200 bases [3] which can be visualized as a ladder on agarose gel electrophoresis.

Fig. 2. *Location of apoptotic nuclei assessed by in situ end-labeling in normal and polycystic kidneys.* (**A**), (**C**), (**E**) and (**G**) are control sections in which the terminal deoxytransferase enzyme was omitted. Note that labeled nuclei, which appear brown, are absent. (**B**), (**D**), (**F**) and (**H**) are adjoining sections which have been subjected to the complete end labeling proceedure. All sections counterstained with methyl green. (A) and (B). Normal mature kidney showing apoptotic nuclei in tubular epithelial cells. This section together with Figure 1C demonstrates the range of apoptosis in normal postnatal kidneys. (C to F) show sections from prenatal patients with ARPKD. There is a wide distribution of apoptotic nuclei in the cyst epithelium and interstitial cells in (D) and in the epithelial cells of relatively undilated tubules adjacent to a large cyst in (F). Note that in (F) the nuclei of the flattened epithelial cells lining the large cyst are not apoptotic, demonstrating the specificity of the technique. (G) and (H). Glomerulus from a child with ADPKD showing a cyst of Bowman's space with apoptotic nuclei in both the cyst wall and the glomerulus. Key: cyst (cy), glomerulus (G), and tubule (t). Arrowheads indicate apoptotic nuclei which appear brown. Bar is 40 μm.
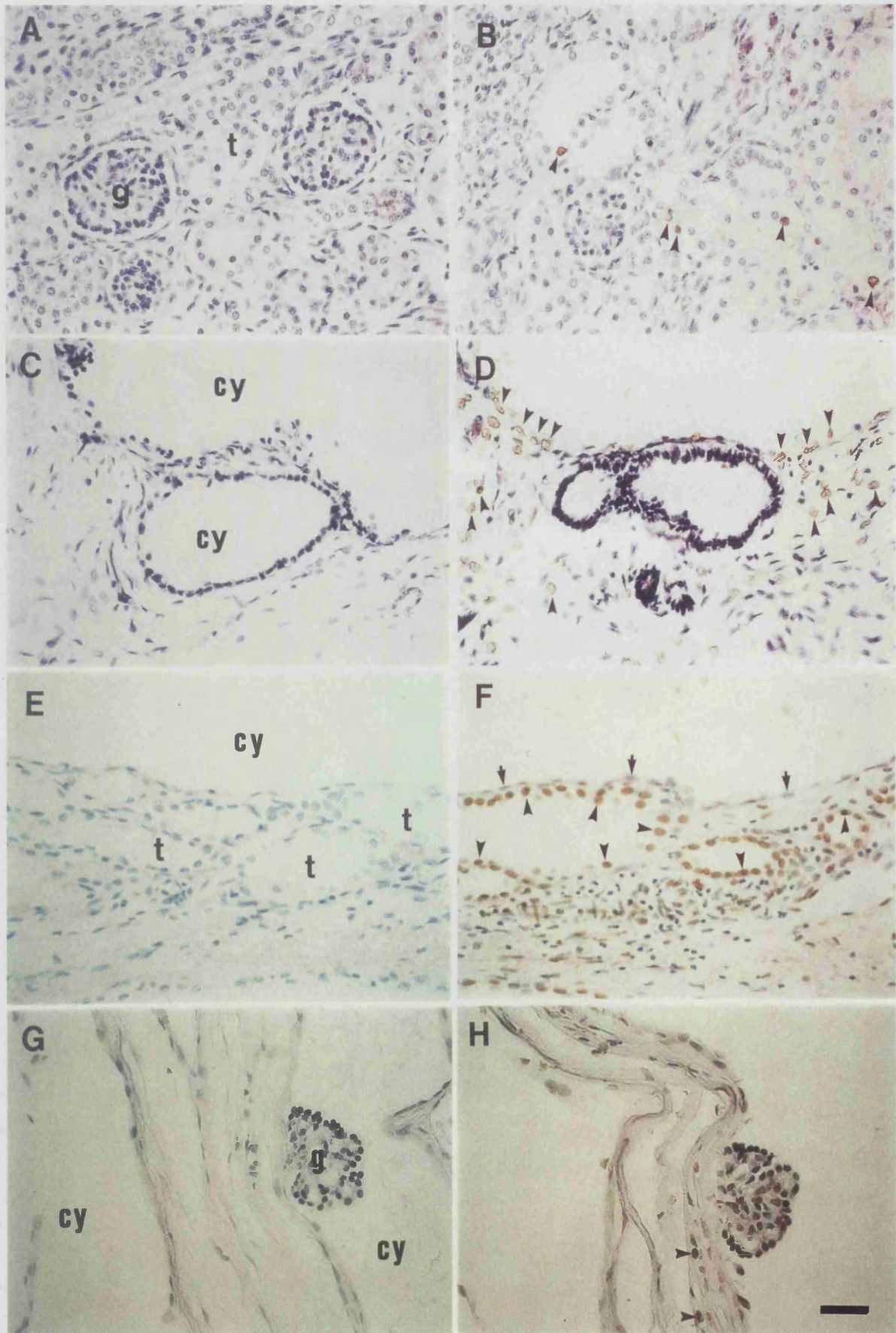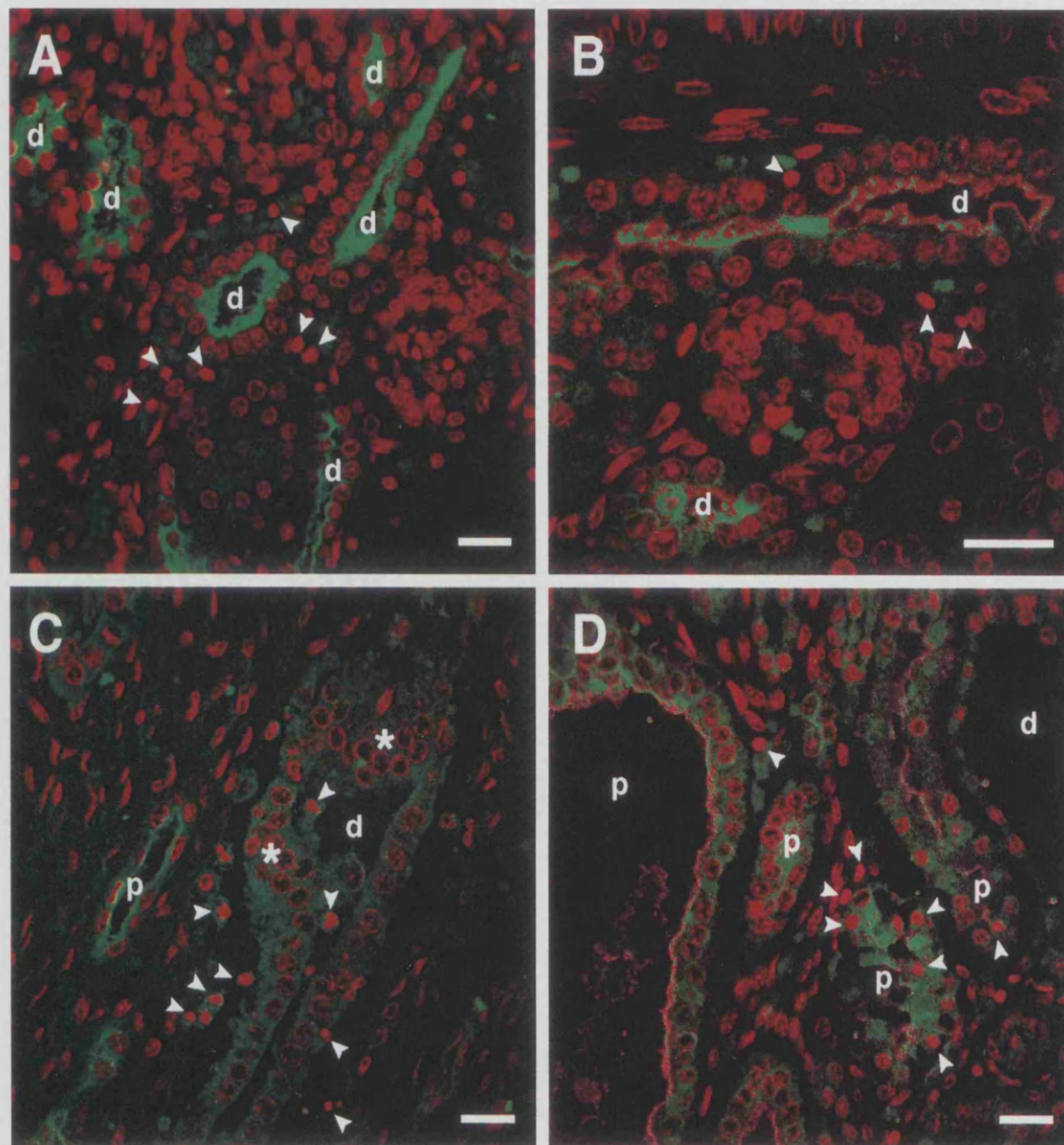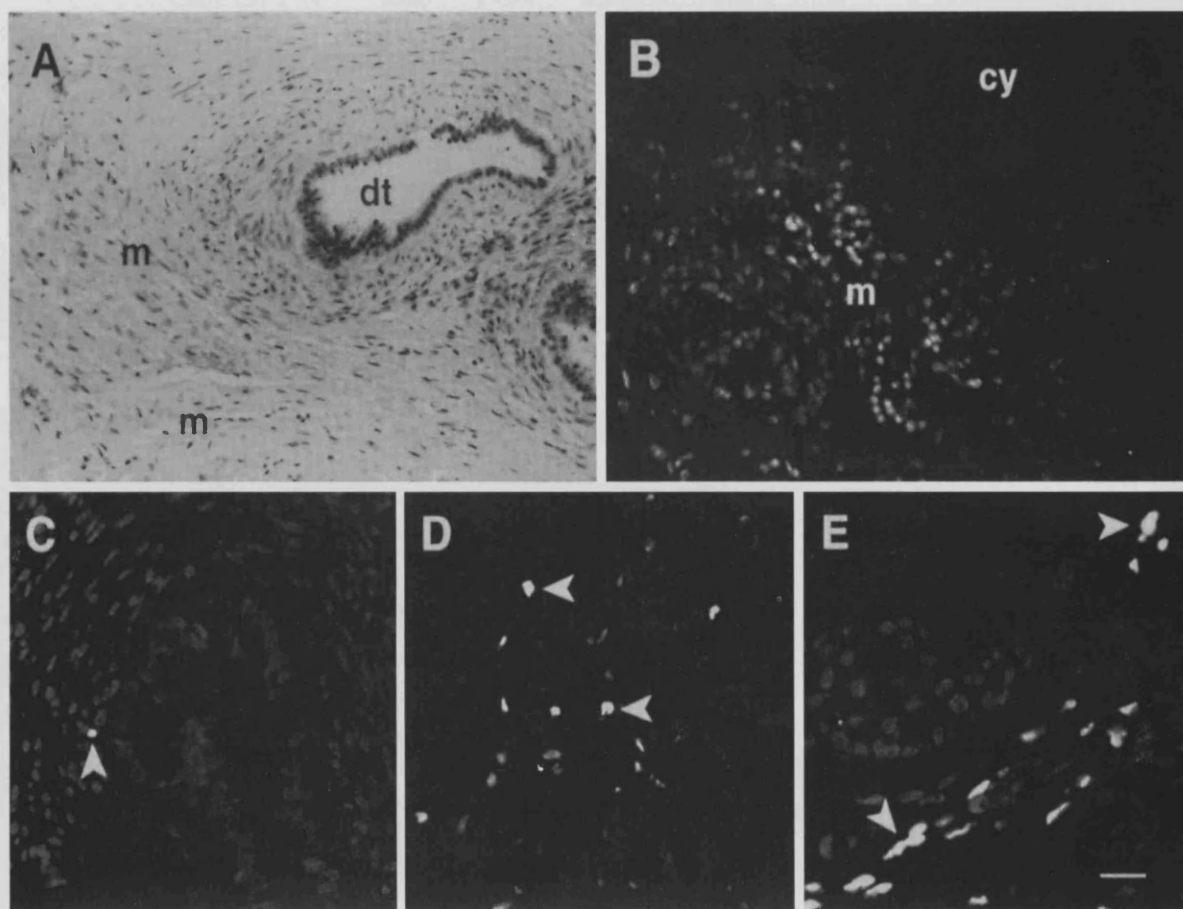
Fig. 3. *Location of apoptotic nuclei assessed by propidium iodide and lectin staining in polycystic kidneys.* All sections stained with propidiun iodide (red) and FITC-conjugated lectin (green) are from ARPKD. (**A** and **B**) (higher power) Area of undilated distal tubules stained with *Arachis hypogaea* lectin with several adjacent pyknotic nuclei. (**C** and **D**) *Tetragonolobus lotus* lectin staining shows proximal tubules. (**C**) Undilated proximal tubule next to distal tubule with adjacent pyknotic cells and hyperproliferative epithelium. Two apoptotic cells also seen in the lumen of the distal tubule. (**D**) Dilated proximal tubule on the left and dilated distal segment on the right. Three proximal tubules between cysts. One of these (right) contains a single apoptotic cell within its epithelium whereas the degenerating central tubule contains many apoptotic cells. Key: distal segment (d), hyperproliferative area (*), and proximal tubule (p). Arrowheads indicate apoptotic nuclei. Bar is 20 μm.

Fresh surgical specimens of three dysplastic kidneys were thawed to room temperature (after storage at −70°C), homogenized in a lysis buffer (10 mM Tris HCl (pH 8.0), 10 mM EDTA, 0.1% SDS, 100 μg/ml proteinase K) and incubated overnight at 52°C. DNA was then extracted using the phenol/chloroform technique [26]. Briefly, equal volumes of phenol (equilibrated pH 8.0) and chloroform were added to the specimen, which was then centrifuged at 5,000 × g. The aqueous layer was separated and the process repeated. DNA was then precipitated with an equal volume of ice cold 100% alcohol, washed in 70% ethanol and resuspended in TE buffer (0.1 M Tris-HCl, pH 8.0, 10 mM EDTA).

Two micrograms of DNA were subjected to electrophoresis through a 1.5% agarose gel containing ethidium bromide and visualised under UV illumination. This extraction technique should be specific for DNA, but any potential RNA contamination was eliminated by incubating the samples with 1 mg/liter of RNAse A for 30 minutes before electrophoresis.

Detection of apoptosis in mice with polycystic kidneys

Human ARPKD is a relatively heterogeneous condition. Therefore, we examined apoptosis in *cpk/cpk* mice which phenotypically ressemble human ARPKD, but in which the kidney histology is

Fig. 4. *Location of apoptotic nuclei in dysplastic kidneys.* (**A**) Low power view of dysplastic kidney from a 16 months old child counterstained with toluidine blue to show dysplastic tubules immediately surrounded by fibromuscular collarettes and adjacent areas of undifferentiated cells of mesenchymal appearance. (**B**) Propidium iodide labeling showing pyknotic nuclei in the interstitium between cysts. (**C** to **E**) are *in situ* end labeled sections using an anti-digoxigenin antibody conjugated to rhodamine. (**C**) Large dysplastic tubule with surrounding collarette containing one apoptotic nucleus. (**D**) Numerous apoptotic nuclei in area of undifferentiated cells, similar to the area in (**B**). (**E**) Small dysplastic tubule with many adjacent apoptotic nuclei. Key: collarette (ct), dysplastic tubule (dt) and undifferentiated mesenchyme-like cells (m). Arrowheads indicate apoptotic cells. Bar is 40 μm in A and B and 20 μm in all other sections.

more homogeneous and the progressive course of the disease is highly predictable [18, 27, 28]. Homozygous *cpk/cpk* mice (Jackson Laboratory, ME, USA) were sacrificed at birth when there was mild dilatation of the proximal tubules, and at day 14 when there were gross cystic changes in the collecting ducts. The extent of apoptosis was compared with phenotypically normal littermates (*cpk/+* and *+/+*) as discussed above.

Effects of storage on apoptosis in fetal mice kidneys

To assess the possible effects of storage on the quantity of renal apoptosis we performed the following experiment. Pregnant CD1 mice (Charles River UK Ltd, Margate, England, UK) were sacrificed by cervical dislocation at the 16th day of gestation, a stage when the fetal kidney contained a spectrum of nephrogenesis broadly equivalent to our human prenatal samples. Embryos were killed by cervical dislocation. In one group kidneys were immediately removed and fixed in 4% PFA, while in the other group the whole fetus was left at 4°C for 24 hours before removing and processing the kidneys. Subsequently, apoptosis was quantitated on histological sections.

Effects of anaesthesia and renal artery clamping on apoptosis in mice

We assessed the potential effects of anaesthesia and renal artery clamping on apoptosis by performing these procedures on mice. Adult CD1 mice (25 g) were anaesthatized with nitrous oxide/halothane and underwent laparotomy. The renal vessels were identified using a dissecting microscope and the renal arteries were clamped for 15 minutes. Mice were then sacrificed. Control mice underwent cervical dislocation with immediate dissection and processing of the kidneys. Apoptosis was quantitated as above.

Results

Location of apoptosis in normal human kidneys

In prenatal kidneys apoptosis was detected in nephron precursors in the nephrogenic cortex, typically in comma shaped bodies (Fig. 1A), and in interstitial cells in the medulla (not shown). Apoptosis was not found in either the undifferentiated mesenchyme (Fig. 1A) or in more mature nephrons towards the center
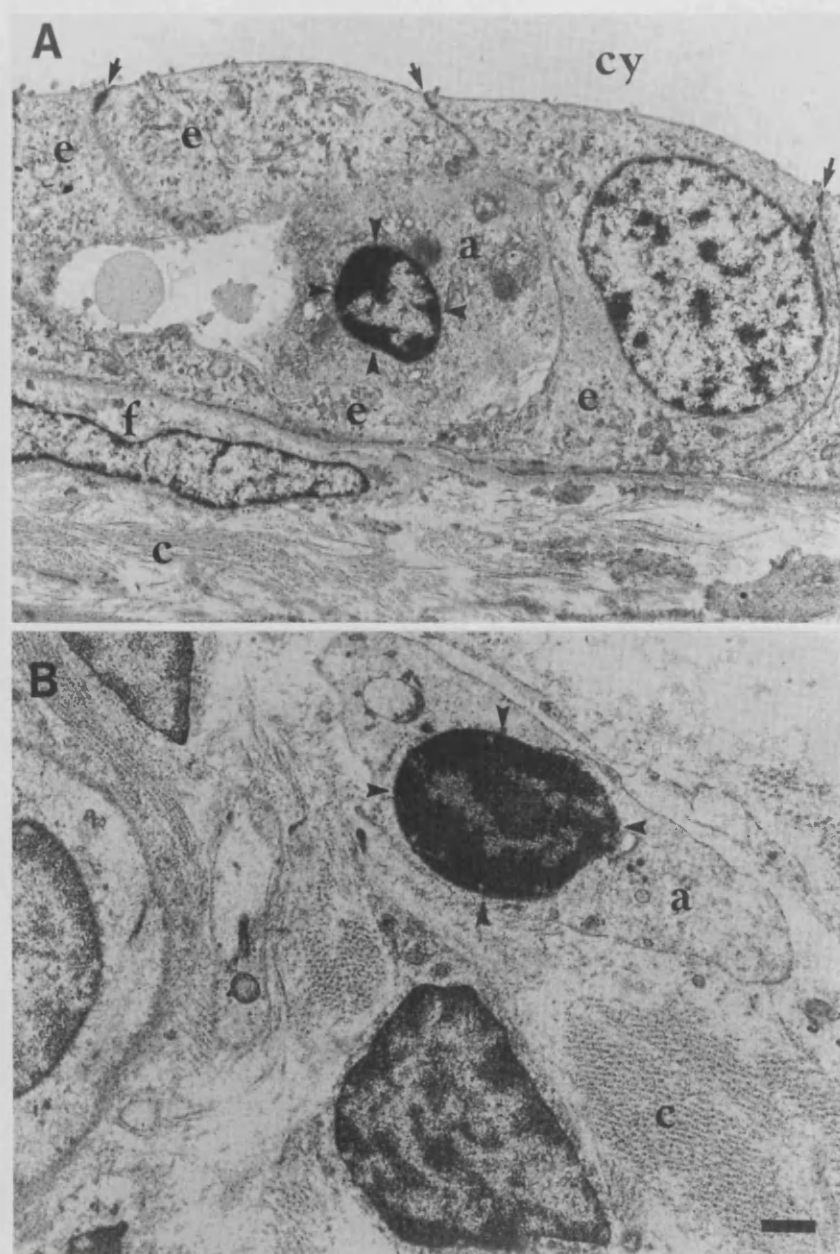
Fig. 5. *Electron microscopy of dysplastic kidneys.* (**A**) Cyst wall showing apoptotic cell with condensed pyknotic nucleus surrounded by normal epithelial cells. The apoptotic cell appears to be shrinking. (**B**) Poorly differentiated mesenchyme showing both normal cells and one cell undergoing apoptosis with nuclear condensation. Key: apoptotic cells (A), collagen (c), cyst (cy), epithelial cells (E), fibroblast (F). Arrows indicate the tight junctions between epithelial cells, arrowheads indicate pyknotic nuclei. Bar is 1 μm.

of the organ. In the postnatal samples rare apoptotic nuclei were detected in the epithelial cells of proximal tubules (Fig. 2B), but were never noted in glomeruli (Figs. 1B and 2B), interstitial cells (Figs. 1C and 2B) or loops of Henle.

Location of apoptosis in polycystic human kidneys

The distribution of apoptosis within the kidney was similar in both pre- and postnatal samples. In ARPKD apoptosis was detected (i) in the interstitium around undilated proximal and distal tubules (Figs. 1D, 3 A-C); (ii) within the epithelial lining of cysts, often adjacent to areas of epithelial hypercellularity (Figs. 1E, 1F, 2D, and 3C); (iii) and in the epithelium of undilated proximal tubules between large cysts (Fig. 3D). In the ADPKD sample apoptosis was additionally observed within glomeruli with cystic dilatation of Bowmans' capsule (Fig. 2H).

Location of apoptosis in dysplastic human kidneys

A similar histological pattern of cell death was seen in prenatal and postnatal specimens. Apoptosis was prominent in areas of undifferentiated cells (Figs. 4B, 4D and 5B) but was also, on occasion, observed in close proximity to dysplastic tubules (Fig. 4 C, E). In the multicystic dysplastic kidneys apoptosis was rarely detected in cystic epithelia, and areas of cartilage did not contain apoptotic cells (data not shown). These sites of apoptosis were confirmed on electron microscopy; Figure 5A shows an electron micrograph of an apoptotic cell adjacent to normal epithelial cells in the wall of a cyst. Figure 5B shows an apoptotic cell in an undifferentiated area which resembles uninduced mesenchyme. We found DNA laddering in two out of the three dysplastic samples (Fig. 6), although histology revealed apoptotic nuclei in
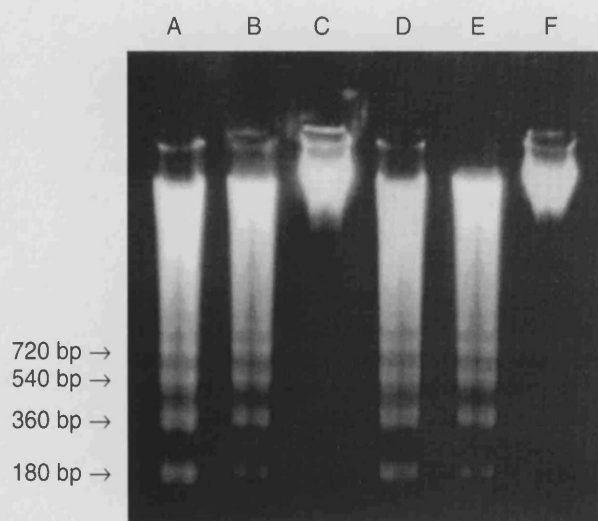
Fig. 6. *DNA laddering in dysplastic kidneys.* DNA was extracted from dysplastic kidneys from infants and children, then electrophoresed through a 1.5% agarose gel as described in the **Methods**. Lane A and Lane B. Dysplastic kidney showing laddering. Lane C Dysplastic kidney with no detectable ladder. Lanes D, E and F. Samples from the same kidney as A, B and C treated with RNAse A rule out RNA contamination.

all samples. This might be explained by the finding that DNA is sometimes broken down into large fragments during apoptosis, which cannot be visualized by the laddering technique [6].

Quantification of apoptosis in human kidneys

Apoptotic cells were rare in normal postnatal kidneys, but significantly more death was seen in normal prenatal organs (Fig. 7; $P < 0.01$). This difference provided the rationale for analyzing the quantity of apoptosis in dysplastic and polycystic patient samples in separate prenatal and postnatal groups. Dysplastic kidneys had more apoptosis than normal kidneys of a comparable age (Fig. 7; prenatally $P < 0.001$; postnatally $P < 0.002$), and the absolute levels of apoptosis fell significantly between the prenatal and postnatal period (Fig. 7; $P < 0.005$). In prenatal polycystic kidneys, apoptosis was not significantly greater than the normal group. In the postnatal period, however, a high level of cell death was maintained, and this value was significantly higher than normal controls (Fig. 7; $P < 0.001$). All postnatal polycystic kidneys contained high levels of apoptosis irrespective of the level of plasma creatinine (Table 2).

Apoptosis in animal experiments

Cpk/cpk mice had significantly more apoptosis than their phenotypically normal littermates both on the first day of life, when there was only mild dilation of the proximal tubules (Table 3; $P < 0.01$), and at postnatal day 14 when the kidneys were grossly distended by distal cysts (Table 3; $P < 0.01$). The location of apoptosis was similar to that seen in the human samples (data not shown). There was no significant difference in levels of apoptosis between mouse fetal kidneys which were either processed immediately or left *in situ* for 24 hours at 4°C before removal and fixation (Table 3). Similarly, no significant difference in the quantity of apoptosis was observed in mice kidneys which had been subjected to anaesthesia and renal artery clamping versus organs which were immediately removed and processed (Table 3).

Discussion

In the adult kidney apoptosis has been implicated in animal models of glomerulonephritis [29] and in experimental reperfusion injury [30]. The results from the current study suggest that apoptosis also occurs in dysplastic renal malformations and childhood polycystic kidney diseases.

Apoptosis in normal kidneys

In normal human fetal kidneys apoptosis was detected in the nephrogenic cortex and the medulla. In view of the high level of apoptosis in comma-shaped bodies (Fig. 1A) we speculate that it may be involved in both nephron morphogenesis and controlling the number of cells within a nephron. Apoptosis also occurs between branches of the collecting ducts [2], an area where Potter described regression of the first generations of nephrons [11]. It could be argued that a delay in processing human specimens may have altered the degree of apoptosis, but we did not find any difference in the level of cell death in embryonic mice kidneys after prolonged storage at 4°C (Table 3). In addition, the distribution of apoptosis was similar to that described in a study in rats where developing kidneys were perfusion fixed immediately before harvesting [2]. We found a low level of apoptosis in proximal tubules of normal postnatal specimens (Figs. 2 and 7), but apoptosis was never observed in glomeruli, Henle loops or interstitial cells (Figs. 1 and 2). Conflicting studies have suggested that hypoxia/ischemia causes apoptosis in renal epithelia in *ex vivo* experiments [31], but has no effect in cell culture [32]. In the current study, however, we found that anaesthesia and surgery did not increase renal apoptosis in an animal model (Table 3). Other workers have also shown that apoptosis *in vivo* is only enhanced in the reperfusion phase after renal artery clamping [30, 33]. We therefore suggest that there is balanced cell turnover in the mature human kidney with lost cells either dying by apoptosis or shed into the urine [34], and these are replaced by a low level of epithelial proliferation [35].

Deregulation of apoptosis in polycystic kidneys

We have made a number of original observations regarding apoptosis in polycystic kidneys obtained predominantly from patients with ARPKD. Firstly, in the postnatal period, pyknotic nuclei were observed in the interstitial tissue around undilated proximal and distal tubules (Figs. 1 to 3), but we never observed apoptosis in this location in normal postnatal kidneys. Secondly, apoptotis occurred in hyperproliferative epithelium of distal cysts (Figs. 1 and 3), and we also found undilated proximal tubules dying by apoptosis between cysts (Fig. 3). Lastly, the incidence of apoptosis was raised in postnatal polycystic kidneys (Table 3 and Fig. 7). Next we sought evidence of apoptosis in the *cpk/cpk* mouse; here the kidney phenotypically resembles human ARPKD, but the histology is more homogeneous and the disease progression is highly predictable [18, 27]. We found that apoptosis was increased, compared to phenotypically normal littermates, in both an early and a late stage of renal disease (Table 3). The animal data support our findings in human ARPKD and are also in accord with a study reporting apoptosis in human ADPKD [36]. Thus, enhanced apoptosis is found in different types of polycystic kidney disease. It is unknown how apoptosis relates to the genetic defects in human polycystic kidney diseases [37–40]. Evidence for a primary genetic deregulation of renal survival is, however,
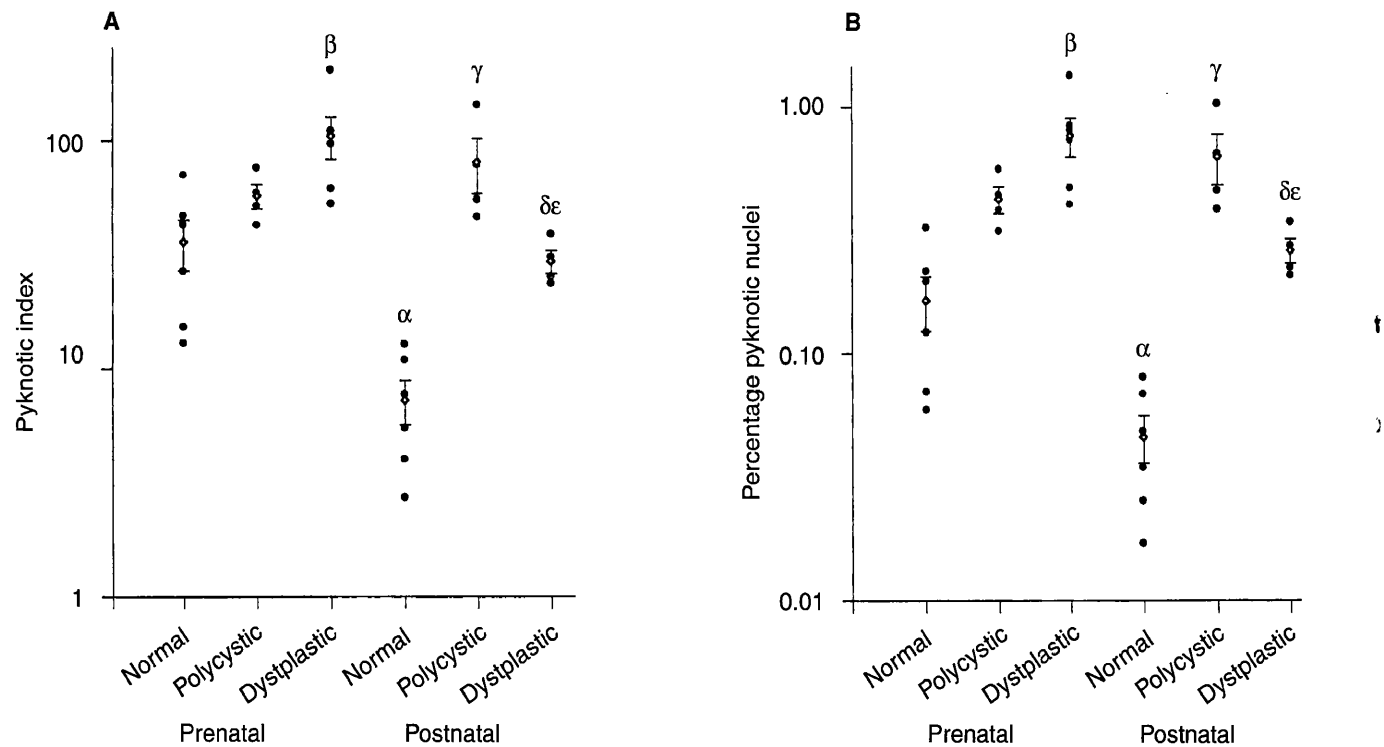
Fig. 7. *Quantitation of apoptosis.* Apoptosis was quantified in tissue sections using the propidium iodide method described in the text and expressed as (**A**) Pyknotic Index corresponding to the mean number of apoptotic cells per 10 random microscope fields from throughout the tissue and (**B**) Percentage of pyknotic nuclei. Groups were: normal prenatal kidneys, polycystic prenatal kidneys, dysplastic prenatal kidneys, normal postnatal kidneys, polycystic postnatal kidneys, dysplastic postnatal kidneys. Mean and SEM is shown. Significant differences were: α - normal prenatal versus normal postnatal ($P < 0.01$), β - dysplastic prenatal versus normal prenatal ($P < 0.001$), γ - postnatal polycystic versus normal postnatal ($P < 0.001$), δ - dysplastic postnatal versus normal postnatal ($P < 0.002$) and ϵ - dysplastic prenatal versus dysplastic postnatal ($P < 0.002$).

Table 3. Pyknotic index and percentage pyknotic nuclei in kidneys from animal experiments outlined in the text

Experimental group	Number	Pyknotic index/ mean (SD)	Percentage pyknotic nuclei/ mean (SD)
A			
Normal newborn	4	0.61 (0.10)	0.02 (0.004)
Polycystic newborn	4	1.58 (0.14)	0.07 (0.007)
Normal 14 day	4	0.41 (0.29)	0.02 (0.008)
Polycystic 14 day	4	1.37 (0.26)	0.08 (0.008)
B			
Control fetal mice	10	1.04 (0.76)	0.09 (0.06)
Storage for 24 hours	5	1.12 (0.84)	0.10 (0.07)
C			
Control adult mice	6	0.44 (0.25)	0.04 (0.02)
Operative group	8	1.08 (0.79)	0.09 (0.07)

(Group A) Significantly more apoptosis in both *cpk/cpk* polycystic groups compared to age matched controls ($P < 0.001$). (Group B) No significant difference between fetal kidneys processed immediately or stored in situ for 24 hours. (Group C) No significant difference in renal apoptosis between control adult mice and operative group which underwent anaesthesia and renal artery clamping.

provided by mice with *bcl-2* null mutations which develop cystic kidneys [41, 42]. Moreover, transgenic mice which overexpress c-*myc* develop renal cysts [43], and enhanced expression of this cellular protooncogene occurs in *cpk/cpk* mice [44, 45]. C-*myc* causes proliferation or apoptosis depending on the concentrations of ambient growth factors [46], and thus the imbalance of EGF

[47, 48] and HGF [49] reported in polycystic kidney diseases may affect cell survival. We speculate that proliferation and fluid secretion in polycystic kidney epithelia [16, 19, 50] outweigh the high levels of cell death reported in this study, hence causing increased size of the kidneys with concomitant destruction of functional renal tissue.

Deregulation of apoptosis in dysplastic kidneys

Most apoptosis in dysplastic kidneys occurred in cells located around dysplastic tubules. Cells in this area superficially resemble undifferentiated mesenchyme which, in the normal metanephros, will differentiate into nephrons [11–13]. We suggest that enhanced apoptosis in dysplastic organs may prevent the differentiation of these precursors. Moreover, we hypothesize that enhanced cell death may contribute to the well-recognized phenomenon of spontaneous involution of dysplastic kidneys [51–53]. During normal nephrogenesis, bcl-2 is highly expressed in nephron precursors [54, 55], and this protein may be required to prevent the death of cells during the mesenchymal to epithelial transition. Preliminary data from our own laboratory [54] suggest that bcl-2 is highly expressed in dysplastic tubules where apoptosis is rare, but is only weakly expressed in undifferentiated cells where prominent apoptosis is found. In humans, renal dysplasias may occur in conjunction with renal obstruction (such as posterior urethral valves) and some, but not all, animal studies suggest that prenatal obstruction causes dysplasia [56–58]. Increased apoptosis is seen in experimental urinary obstruction in the postnatal period [59, 60] and is associated with increased renal TGF-β [61],

a molecule implicated in epithelial apoptosis [8]. However, only a minority of our patients had obstructed kidneys (Tables 1 and 2). Renal malformations occur in mice with null mutations for *ret* [62], *wnt-4* [63] and *RARs* [64], but apoptosis has not been studied in these models, and none of them faithfully mimic human multicystic renal dysplasia.

Conclusions

In summary, we have found that apoptosis occurs during normal human kidney development in locations similar to those reported in animals, and continues at a very low level after birth. More importantly, apoptosis occurs at a high level in ARPKD and dysplastic kidneys, which are important causes of end-stage renal failure in infancy and childhood [21]. The fact that apoptosis can be reduced by various molecular means both *in vitro* and *in vivo* [2, 14, 65] suggest novel therapeutic strategies for these diseases.

Acknowledgments

Reprint requests to Dr. Paul J.D. Winyard, Developmental Biology Unit, Institute of Child Health, 30, Guilford Street, London WC1E 1EH, England, United Kingdom.

References

1. KERR JFR, WYLLIE AH, CURRIE AR: Apoptosis: A basic biological phenomenon with wide ranging implications in tissue kinetics. *Br J Cancer* 26:239–257, 1972
2. COLES HSR, BURNE JF, RAFF MC: Large-scale normal cell death in the developing rat kidney and its reduction by epidermal growth factor. *Development* 118:777–784, 1993
3. WYLLIE AH: Glucocorticoid-induced thymocye apoptosis is associated with endogenous endonuclease activation. *Nature* 284:555–556, 1980
4. GAVRELLI Y, SHERMAN Y, BEN-SASSOON SA: Identification of programmed cell death in situ via specific labeling of DNA fragmentation. *J Cell Biol* 119:493–501, 1992
5. SCHWARTZ LM, SMITH SW, JONES ME, OSBORNE BA: Do all programmed cell deaths occur via apoptosis? *Proc Natl Acad Sci USA* 90:980–984, 1993
6. BORTNER CD, OLDENBURG NBE, CIDLOWSKI JA: The role of DNA fragmentation in apoptosis. *Trend Cell Biol* 5:22–27, 1995
7. VAUX DL: Towards an understanding of the molecular mechanisms of physiological cell death. *Proc Natl Acad Sci USA* 90:786–789, 1993
8. OBERHAMMER F, WILSON JW, DIVE C, MORRIS ID, HICKMANN JA, WAKELING AE, WALKER PR, SIKORSKA M: Apoptotic death in epithelial cells: Cleavage of DNA to 300 and/or 50 kb fragments prior to or in the absence of internucleosomal fragmentation. *EMBO J* 12:3679–3684, 1993
9. COLLINS MKL, PERKINS GR, RODRIGUEZ-TARDUCHY G, NIETO MA, LOPÉZ-RIVAS A: Growth factors as survival factors: Regulation of apoptosis. *Bio Essays* 16:133–138, 1994
10. WYLLIE AH, KERR JFR, CURRIE AR: Cell death: The significance of apoptosis. *Int Rev Cytol* 68:251–306, 1980
11. POTTER EL: *Normal and Abnormal Development of the Kidney.* Chicago, Year Book Medical Publishers Inc., 1972
12. SAXEN L: *Organogenesis of the Kidney.* Cambridge, Cambridge University Press, 1987
13. HARDMAN P, KOLATSI M, WINYARD PJ, TOWERS PR, WOOLF AS: Branching out with the ureteric bud. *Exp Nephrol* 2:211–219, 1994
14. KOSEKI C, HERZLINGER D, AL-AWQATI Q: Apoptosis in metanephric development. *J Cell Biol* 119:1322–1333, 1992
15. WOOLF AS, KOLATSI-JOANNOU M, HARDMAN P, ANDERMARCHER E, MOORBY C, FINE LG, JAT PS, NOBLE MD, GHERARDI E: Roles of hepatocyte growth factor/scatter factor (HGF/SF) and met in early development of the metanephros. *J Cell Biol* 128:171–184, 1995
16. WILSON PD, HRENIUK D, GABOW PA: Abnormal extracellular matrix and excessive growth of human adult polycystic kidney disease epithelia. *J Cell Physiol* 150:360–369, 1992
17. AVNER ED, SWEENEY WE, NELSON WJ: Abnormal sodium pump distribution during renal tubulogenesis in congenital murine polycystic kidney disease. *Proc Natl Acad Sci USA* 89:7447–7451, 1992
18. WOO DDL, MIAO S, PELAYO J, WOOLF AS: Taxol inhibits congenital polycystic kidney disease progression. *Nature* 368:750–753, 1994
19. GRANTHAM JJ: 1992 Homer Smith Award. Fluid secretion, cellular proliferation, and the pathogenesis of renal epithelial cysts. *J Am Soc Nephrol* 3:1841–1857, 1992
20. RISDON RA: Renal dysplasia. Part 1: A clinico-pathological study of 76 cases. *J Clin Pathol* 24:57–71, 1971
21. WOOLF AS: Clinical impact and biological basis of renal malformations. *Semin Nephrol* 15:361–372, 1995
22. KREIDBERG JA, SARIOLA H, LORING JM, MAEDA M, PELLETIER J, HOUSMAN D, JAENISCH R: WT-1 is required for early kidney development. *Cell* 74:679–691, 1991
23. VERANI R, WALKER P, SILVA FG: Renal cystic disease of infancy: Results of histochemical studies. *Pediatr Nephrol* 3:37–42, 1989
24. HOLTHOFFER H, VIRTANEN I, PETTERSSON E, TORNROTH T, ALFTHAN O, LINDER E, MIETTINEN A: Lectins as fluorescence microscopic markers for saccharides in the human kidney. *Lab Invest* 45:391–399, 1981
25. BLAND JM, ALTMANN DG: Statistical methods for assessing agreement between two methods of clinical measurement. *Lancet* 8476:307–310, 1986
26. SAMBROOK J, FRITSCH EF, MANIATIS T: *Molecular Cloning: A Laboratory Manual.* Cold Spring Harbor, Cold Spring Harbor Laboratory Press, 1989
27. AVNER ED, STUDNICKI FE, YOUNG MC, SWEENEY WE JR, PIESCO NP, ELLIS D, FETTERMAN GH: Congenital murine polycystic kidney disease. *Pediatr Nephrol* 1:587–596, 1987
28. GATTONE VH II, CALVET JP, COWLEY BD JR, EVAN AP, SHAVER TS, HELMSTADTER K, GRANTHAM JJ: Autosomal recessive polycystic kidney disease in a murine model. A gross and microscopic description. *Lab Invest* 59:231–238, 1988
29. SAVILL J, SMITH J, SARRAF C, REN Y, ABBOTT F, REES A: Glomerular mesangial cells and inflammatory macrophages ingest neutrophils undergoing apoptosis. *Kidney Int* 42:924–936, 1992
30. SCHUMER M, COLOMBEL MC, SAWCZUK IS, GOBE G, CONNOR J, O'TOOLE KM, OLSSON CA, WISE GJ, BUTTYAN R: Morphological, biochemical and molecular evidence of apoptosis during the reperfusion phase after brief periods of renal ischemia. *Am J Pathol* 140:831–838, 1992
31. BEERI R, SYMON Z, BREZIS M, BEN-SASSON SA, BAEHR PH, ROSEN S, ZAGER RA: Rapid DNA fragmentation from hypoxia along the thick ascending limb of rat kidneys. *Kidney Int* 47:1806–1810, 1995
32. IWATA M, TOROK-STORB B, ZAGER RA: An evaluation of renal tubular DNA laddering in response to oxygen deprivation and oxidant injury. *J Am Soc Nephrol* 5:1307–1313, 1994
33. FUERSTENBERG SM, TOROK-STRAUB B, ZAGER RA: Evidence against apoptosis as a dominant mechanism for post-ischemic/post-hypoxic proximal tubular necrosis. (abstract) *J Am Soc Nephrol* 4:735, 1993
34. RACUSEN LC, FIVUSH BA, ANDERSSON H, GAHL WA: Culture of renal tubular cells from the urine of patients with nephropathic cystinosis. *J Am Soc Nephrol* 1:1028–1033, 1991
35. LAURENT G, TOUBEAU G, HEUSON-STIENNON JA, TULKENS P, MALDAGUE P: Kidney tissue repair after nephrotoxic injury: Biochemical and morphological characterisation. *CRC Crit Rev Toxicol* 19:147–183, 1988
36. WOO DDL: Apoptosis and loss of renal tissue in polycystic kidney diseases. *N Engl J Med* 333:18–25, 1995
37. ZERRES K, MUCHER G, BACHNER L, DESCHENNES G, EGGERMAN T, KAARIAINEN H, KNAPP M, LENNERT T, MISSELWITZ J, VON MUNLENDAHL KE, NEUMANN HPH, PIRSON Y, RUDNIK-SCHONEBORN S, STEINBICKER V, WIRTH B, SCHARER K: Mapping of the gene for autosomal

recessive polycystic kidney disease (ARPKD) to chromosome 6p21-cen. *Nature Genet* 7:429–432, 1994

38. EUROPEAN POLYCYSTIC KIDNEY DISEASE CONSORTIUM: The polycystic kidney disease 1 gene encodes a 14 kb transcript and lies within a duplicated region on chromosome 16. *Cell* 77:881–894, 1994

39. EUROPEAN CHROMOSOME 16 TUBEROUS SCLEROSIS CONSORTIUM: Identification and characterisation of the tuberous sclerosis gene on chromosome 16. *Cell* 75:1305–1315, 1993

40. LATIF F, TORY K, GNARRA J, YAO M, DUH F-M, ORCUTT ML, STACKHOUSE T, KUZMIN I, MODI W, GEIL L, SCHMIDT L, ZHOU F, LI H, WEI MH, CHEN F, GLENN G, CHOYKE P, WALTHER MM, WENG Y, DUAN D-SR, DEAN M, GLAVAC D, RICHARDS FM, CROSSEY PA, FERGUSON-SMITH MA, LE PASLIER D, CHUMAKOV I, COHEN D, CHINAULT AC, MAHER ER, LINEHAN WM, ZBAR B, LERMAN MI: Identification of the von Hippel-Lindau disease tumor suppressor gene. *Science* 260:1317–1320, 1993

41. VEIS DJ, SORENSON CM, SHUTTER JR, KORSMEYER SJ: bcl-2-deficient mice demonstrate fulminant lymphoid apoptosis, polycystic kidneys and hypopigmented hair. *Cell* 75:229–240, 1994

42. SORENSON CM, ROGERS SA, KORSEMEYER SJ, HAMMERMAN MR: Fulminant metanephric apoptosis in abnormal kidney development in bcl-2 deficient mice. *Am J Physiol* 268:73–81, 1995

43. TRUDEL M, D'AGATI V, COSTANTINI F: C-myc as an inducer of polycystic disease in transgenic mice. *Kidney Int* 39:665–671, 1991

44. COWLEY BD JR, SMARDO FL JR, GRANTHAM JJ, CALVET JP: Elevated c-myc proto-oncogene expression in autosomal recessive polycystic kidney disease. *Proc Soc Natl Acad Sci USA* 84:8394–8398, 1987

45. HARDING MA, GATTONE VH II, GRANTHAM JJ, CALVET JP: Localization of overexpressed c-myc mRNA in polycystic kidneys of the *cpk* mouse. *Kidney Int* 41:317–325, 1992

46. HARRINGTON EA, BENNETT MR, FANIDI A, EVAN GI: c-Myc induced apoptosis in fibroblasts is inhibited by specific cytokines. *EMBO J* 13:3286–3295, 1994

47. GATTONE VH II, ANDREWS GK, FU-WEN N, CHADWICK LJ, KLEIN RM, CALVET JP: Defective epidermal growth factor gene expression in mice with polycystic kidney disease. *Dev Biol* 138:225–230, 1990

48. HORIKOSHI S, KUBOTA S, MARTIN GR, YAMADA Y, KLOTMAN PE: Epidermal growth factor (EGF) in the congenital polycystic mouse kidney. *Kidney Int* 39:57–62, 1991

49. HORIE S, HIGASHIHARA E, NUTAHARA K, MIKAMI Y, OKUBO A, KANO M, KAWABE K: Mediation of renal cyst formation by hepatocyte growth factor. *Lancet* 344:789–791, 1994

50. YE M, GRANTHAM JJ: The secretion of fluid by renal cysts from patients with autosomal dominant polycystic kidney disease. *N Engl J Med* 329:310–313, 1993

51. DUNGAN JS, FERNANDEZ MT, ABBITT PL, THIAGARAJAH S, HOWARDS SS, HOGGE WA: Multicystic dysplastic kidney: Natural history of prenatally detected cases. *Prenat Diag* 10:175–182, 1990

52. MESROBIAN H-GJ, RUSHTON HG, BULAS D: Unilateral renal agenesis may result from in utero regression of multicystic dysplasia. *J Urol* 150:793–794, 1993

53. AL-KHALDI N, WATSON AR, ZUCOLLO J, TWINING P, ROSE DH: Outcome of antenatally detected cystic dysplastic kidney disease. *Arch Dis Child* 70:520–522, 1994

54. WINYARD PJD, RISDON RA, WOOLF AS: WT1 expression in the absence of BCL2 may explain excessive apoptosis which occurs in human kidney malformations. (abstract) *J Am Soc Nephrol* 6:729, 1995

55. LEBRUN DP, WARNKE RA, CLEARY ML: Expression of bcl-2 in fetal tissues suggests a role in morphogenesis. *Am J Pathol* 142:743–753, 1993

56. BERMAN D, MAIZELS M: The role of urinary obstruction in the genesis of renal dysplasia. *J Urol* 128:1091–1100, 1982

57. STEINHARDT GF, VOGLER G, SALINAS-MADRIGAL L, LEREGINA M: Induced renal dysplasia in the young pouch opossum. *J Ped Surg* 23:1127–1130, 1988

58. GONZALEZ R, REINBERG Y, BURKE B, WELLS T, VERNIER RL: Early bladder outlet obstruction in fetal lambs induces renal dysplasia and the prune-belly syndrome. *J Pediatr Surg* 25:342–334, 1990

59. CONNOR J, BUTTYAN R, OLSSON CA, D'AGATI V, O'TOOLE K, SAWCZUK IS: SGP-2 expression as a genetic marker of progressive cellular pathology in experimental hydronephrosis. *Kidney Int* 39:1098–1103, 1991

60. KENNEDY WA II, STERNBERG A, LACKGREN G, HERNSLE TW, SAWCZUK IS: Renal tubular apoptosis after partial ureteral obstruction. *J Urol* 152:658–664, 1994

61. PIMENTEL JL, KOPP JB, SUNDEN JL, MARTINEZ-MALDONADO M: TGF-β induction in unilateral ureteric obstruction. (abstract) *J Am Soc Nephrol* 4:474, 1993

62. SCHUCHARDT A, D'AGATI V, LARSSON-BLOMBERG L, COSTANTINI F, PACHNIS V: Defects in kidney and enteric nervous system of mice lacking the tyrosine kinase receptor Ret. *Nature* 367:380–383, 1994

63. STARK K, VAINIO S, VASSILEVA G, MCMAHON AP: Epithelial transformation of metanephric mesenchyme in the developing kidney regulated by Wnt-4. *Nature* 372:679–683, 1994

64. MENDELSOHN C, LOHNES D, DECIMO D, LUFKIN T, LEMEUR M, CHAMBON P, MARK M: Function of the retinoic acid receptors (RAR) during development. *Development* 120:2749–2771, 1994

65. KENNEDY WA II, BUTTYAN R, SAWCZUK IS: Epidermal growth factor (EGF) suppresses renal tubular apoptosis following ureteral obstruction. (abstract) *J Am Soc Nephrol* 4:738, 1993

ARTICLES

Epithelial Galectin-3 During Human Nephrogenesis and Childhood Cystic Diseases

PAUL J. D. WINYARD,* QI BAO,† R. COLIN HUGHES,† and ADRIAN S. WOOLF*

*Developmental Biology and Nephrourology Units, Institute of Child Health, London, United Kingdom, and †Laboratory of Protein Structure, National Institute for Medical Research, The Ridgeway, Mill Hill, London, United Kingdom.

Abstract. Galectin-3 is a β-galactoside-binding protein with putative roles in development, oncogenesis, and inflammation. Its expression in human nephrogenesis has not been previously reported. This study examines galectin-3 expression in early human embryos by Western blot and immunohistochemistry. This 33-kD protein was detected in the apical domain of distal tubules of the mesonephros and also in the mesonephric duct. In the metanephros, the adult kidney precursor, galectin-3 was detected in the apical domains of ureteric bud branches, and there was intense expression in fetal medullary and papillary collecting ducts in both the cytoplasm and plasma membranes. Low levels of galectin-3 were detected in the cytoplasm of a subset of cells in adult collecting ducts; these were α-intercalated cells because they expressed basal band 3 protein. In human multicystic dysplastic kidneys, all diseased epithelia had an embryonic apical expression pattern of galectin-3 and, in addition, all cystic epithelia in autosomal recessive polycystic kidneys expressed this molecule. It is concluded that galectin-3 is expressed by cells of the mesonephric duct/ureteric bud lineage, and it is speculated that the different subcellular locations may be implicated in both the regulation of normal growth and differentiation of this lineage, as well as in the pathogenesis of cystic epithelia. (J Am Soc Nephrol 8: 1647–1657, 1997)

Lectins are naturally occurring proteins that bind specific configurations of carbohydrate residues of glycoproteins (1). Galectins comprise a family of Ca^{2+}-independent water-soluble β-galactoside-binding lectins (2), and galectin-3 (formerly known as Mac-2) is a 30- to 42-kD molecule found in a variety of mammalian species (3). The galectin-3 protein consists of an amino-terminal half containing a repetitive domain sequence rich in proline, glycine, and tyrosine (4) that is sensitive to collagenases and elastases, in contrast to the carboxy-terminal half containing the carbohydrate recognition domain. The latter binds molecules with poly-N-acetyllactosamine side chains and ABH blood group determinants (5). Galectin-3 protein has been identified within cells and with nuclear and cytoplasmic distributions (3), and it also is a secreted molecule that can adhere to the cell surface (6) or appear in conditioned medium of galectin-3-expressing cell lines (7). The latter observations are interesting in view of the apparent absence of a secretory signal in the galectin-3 protein, suggesting the use of a novel secretory pathway that is independent of the endoplasmic reticulum and Golgi apparatus (7).

Galectin-3 is expressed by preimplantation embryos (8) and by notochord, skeleton, and skin later in development (9). In the adult mammal, galectin-3 expression has been described in a variety of epithelia in vivo, including the colon, and it can be detected on the surface of thioglycollate-elicited inflammatory macrophages (3). The distribution of galectin-3 in many different types of cells, together with varied subcellular localization of the protein, suggests many different roles for this molecule. In the nucleus, galectin-3 associates with ribonucleoproteins, and here it may play a role in pre-mRNA splicing (10,11). Interestingly, loss of nuclear galectin-3 staining has been reported in colonic neoplasia (12), and this correlates with neoplastic progression. Other reports linking this molecule to cell proliferation include the upregulation of galectin-3 in stimulated 3T3 cells before S phase (13,14), and in lymphocytes transformed with human T cell leukemia virus I (15). Similarly, in vivo, levels of galectin-3 are increased in a variety of tumors (16,17) and correlate with the metastatic potential of certain tumor cell lines (18). Furthermore, galectin-3 may also have a role in preventing programmed cell death, because overexpression of galectin-3 in T cells makes them resistant to apoptosis (19). Of note, galectin-3 has some homology with BCL-2, a survival factor associated with nuclear and mitochondrial membranes (19). Finally, secreted galectin-3 may mediate cell-matrix interactions because it is able to bind embryonic glycoforms of laminin and fibronectin, which have polylactosamine side chains (5), and galectin-3 has been shown to modulate laminin/integrin interactions, hence mediating cell attachment and spreading in vitro (5).

The galectin-3 protein has been reported to be expressed

during the late nephrogenic period in rodents (20), but detailed renal expression patterns were not defined. In this study, we have documented the ontogeny of galectin-3 protein distribution in humans from early nephrogenesis through postnatal maturity. We found that galectin-3 was expressed by the mesonephric duct and its ureteric bud/collecting duct derivatives. In view of this pattern, we further examined the expression of this molecule in multicystic dysplastic kidneys and autosomal recessive polycystic kidneys, disorders that involve aberrant development of ureteric bud branches and collecting ducts (21–24).

Materials and Methods

All chemicals were supplied by Sigma (Poole, Dorset, United Kingdom) unless stated otherwise.

Kidney Samples

This project was approved by the Hospital Research Ethics Committee. All samples were collected as described by Winyard *et al.* (21,22) and Kolatsi-Joannou *et al.* (23). Five normal embryonic kidneys (mesonephroi and metanephroi) were obtained from chemically induced (RU486) terminations at 5 to 10 wk of gestation, and six normal fetal kidneys at 17 to 22 wk were obtained from surgical terminations. Five normal postnatal kidney samples at 5 to 72 mo were obtained from tissue adjacent to, but unaffected by, Wilms' tumor, and five kidneys at 3 to 14 mo were obtained from children who died of Sudden Infant Death Syndrome in which no renal or other pathology was detected at autopsy. The Wilms' tumor samples did not have mutations of the Wilms' tumor 1 (WT1) gene (21).

Four prenatal multicystic dysplastic kidneys at 17 to 34 wk gestation were collected from pregnancies terminated for fetal renal malformations and oligohydramnios detected by ultrasonography. Parents were given time to mourn their loss, and the fetus was then stored at 4°C until autopsy. This mode of collection ensures good tissue preservation of fetal renal tissue (21). Four postnatal dysplastic kidneys at 8 to 60 mo were obtained at nephrectomy for nonfunctioning organs. All of these samples had classical histological features of renal dysplasia, including dysplastic tubules and cysts, surrounded by undifferentiated mesenchymal and stromal tissues, together with the presence of metaplastic cartilage (21–24).

Autosomal recessive polycystic kidneys were also collected. These comprised four prenatal samples at 20 to 35 wk gestation and four postnatal samples at 10 to 72 mo of age. Histologically these kidneys contained cysts derived from collecting ducts, and the diagnosis was secured by the presence of characteristic liver pathology, together with the absence of renal cysts in parents examined with renal ultrasonography.

Western Analysis

A 10-wk gestation fetal kidney and lower limb and three postnatal dysplastic kidneys were homogenized in lysis buffer (50 mM Tris, pH 8.0, 150 mM NaCl, 1% Nonidet P-40, 0.5% sodium deoxycholate, and 0.1% sodium dodecyl sulfate) containing protease inhibitors (1 μm sodium orthovanadate, 100 μg/ml phenylmethylsulfonyl fluoride, and 30 μl/ml aprotinin). Protein was also extracted from cultured Madin-Darby canine kidney (MDCK) cells, which are known to synthesize galectin-3 (3) by repetitive syringing in this lysis solution.

Samples were electrophoresed through a 5% stacking and 12% resolving Tris-glycine sodium dodecyl sulfate-polyacrylamide gel (Protogel, National Diagnostics, Atlanta, GA), and proteins were then electrophoretically transferred to a membrane (Hybond-C extra, Amersham, Amersham, Buckinghamshire, United Kingdom) by semidry blotting. The filters were placed overnight in block (10% marvel, 0.05% Tween in phosphate-buffered saline) and then incubated for 1 h with anti-galectin-3 antibody (bleed 7) at a dilution of 1:500 in block solution. This is a rabbit polyclonal antibody raised against the amino terminus of hamster galectin-3 protein (20), and it was either omitted or preincubated with galectin-3 protein (20 μg/ml) for 1 h in control experiments. Next, the membranes were washed three times for 10 min in block. They were then incubated for 2 h with a goat anti-rabbit peroxidase-conjugated secondary antibody (DAKO, High Wycombe, United Kingdom). This was washed three times in a large quantity of phosphate-buffered saline, and positive signal was detected with enhanced chemiluminescence reagent (enhanced chemiluminescence, Amersham).

Histochemistry

Kidneys were fixed in 10% formalin, embedded in paraffin wax, and sectioned at 4 to 6 μm. For immunohistochemistry, sections were dewaxed through a graded alcohol series to water and were microwaved for 8 to 12 min in citric acid buffer (2.1 g/L, pH 6.0), as described (21–23). Sections for immunoperoxidase staining were then treated with 3% hydrogen peroxide for 15 min to block endogenous peroxidase, but this step was omitted in samples that were analyzed by fluorescence detection systems.

After blocking in 10% goat serum for 1 h at room temperature, sections were incubated for 1 h at 37°C with rabbit anti-galectin-3 antiserum (bleed 7: see Western Analysis) at 1:50 dilution. Negative controls consisted of preimmune rabbit serum, omission of the primary antibody, or preincubation of the antibody with excess galectin-3 protein. In these samples, very weak background peroxidase activity or autofluorescence was noted in some tubules. Primary antibodies in tissue sections were detected using either FITC-immunofluorescence or peroxidase-based systems (counterstained with methyl green), as described previously (21–23).

Because galectin-3 protein has been located in nonrenal tissues in nuclei, cytoplasm, or plasma membrane (see introductory remarks), we attempted to determine the subcellular location of galectin-3 immunoreactivity in kidney tissues, using confocal laser scanning microscopy (Leica, Heidelberg, Germany). Fluorescent secondary antibody was visualized by scanning through tissue sections at 0.50-μm intervals. Using this methodology, nuclear localization could be unambiguously established. Similarly, in some cells, galectin-3 protein appeared to be associated only with the plasma membrane. Finally, other cells had galectin-3 immunoreactivity in their cytoplasm, and in these cases coincident membranous localization was sometimes indicated by intense staining.

In some tissues, we compared the distribution of galectin-3 on serial sections with PAX-2, using a polyclonal antibody to the carboxy-terminal domain (22). This transcription factor is expressed in the mesonephric (Wolffian) and paramesonephric (Müllerian) ducts and the metanephros (22,25). In addition, postnatal samples were fluorescently co-stained with tetramethylrhodamine isothiocyanate-conjugated *Arachis hypogaea* agglutinin and anti-band 3 antibodies. *Arachis hypogaea*, or peanut agglutinin, is a marker of distal tubules in humans (26), although it binds specifically to β-intercalated cells in collecting ducts in the rabbit (27). Band 3 is a transmembrane protein that is found in red cells, and a truncated protein is located on the basal surface of the hydrogen-secreting α-intercalated cells in the distal nephron (28,29). We used two monoclonal mouse anti-human band 3 antibodies (BRIC 154 and BRIC 155) that have been well character-

ized in red cells and react with the transmembrane domain in the kidney (30).

Results

Western Blotting

The specificity of the anti-galectin-3 antiserum was confirmed by Western blotting. Human galectin-3 protein has a predicted size of 33 kD, and a single band of this size was detected in a 10-wk gestation normal human fetal kidney (Figure 1, lane 1) and in three postnatal dysplastic kidneys (Figure 1, lanes 3 through 5). Galectin-3 has been described previously in developing cartilage (9). We also detected it in the lower limb of the 10-wk-old fetus (Figure 1, lane 2). Canine galectin-3 is larger than the human protein, and we found a 42-kD band in protein extracted from MDCK cells. No signal was detected when the primary antibody was omitted or preincubated with excess galectin-3 (data available on request).

Ontogeny of Galectin-3 in the Urinary Tract

The human mesonephros develops in the fifth week after fertilization and regresses after the first trimester (24). This segmental organ contains vascularized glomeruli draining into nephrons, which comprise "proximal" and "distal" tubules connected to the mesonephric duct (Figure 2, A through F). In the sixth week of gestation, the ureteric bud branches from the caudal mesonephric duct and grows into intermediate mesoderm to form the metanephros (Figure 2, A through C and G through L). Mutually inductive events cause the ureteric bud to branch serially to form the collecting ducts and urothelium of the renal pelvis and ureter, and the renal mesenchyme undergoes epithelial conversion to form nephrons (glomeruli, proximal tubules, and loops of Henle). The first human metanephric
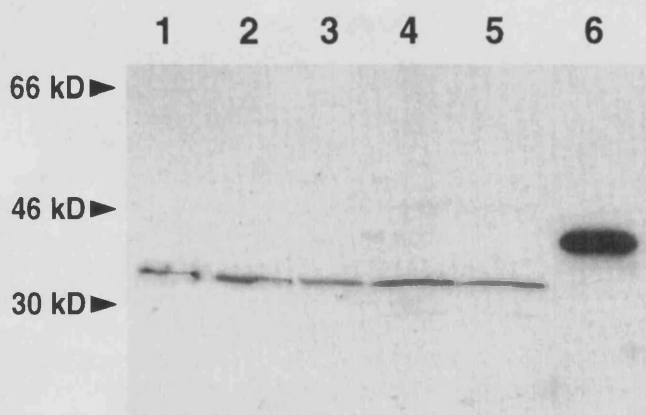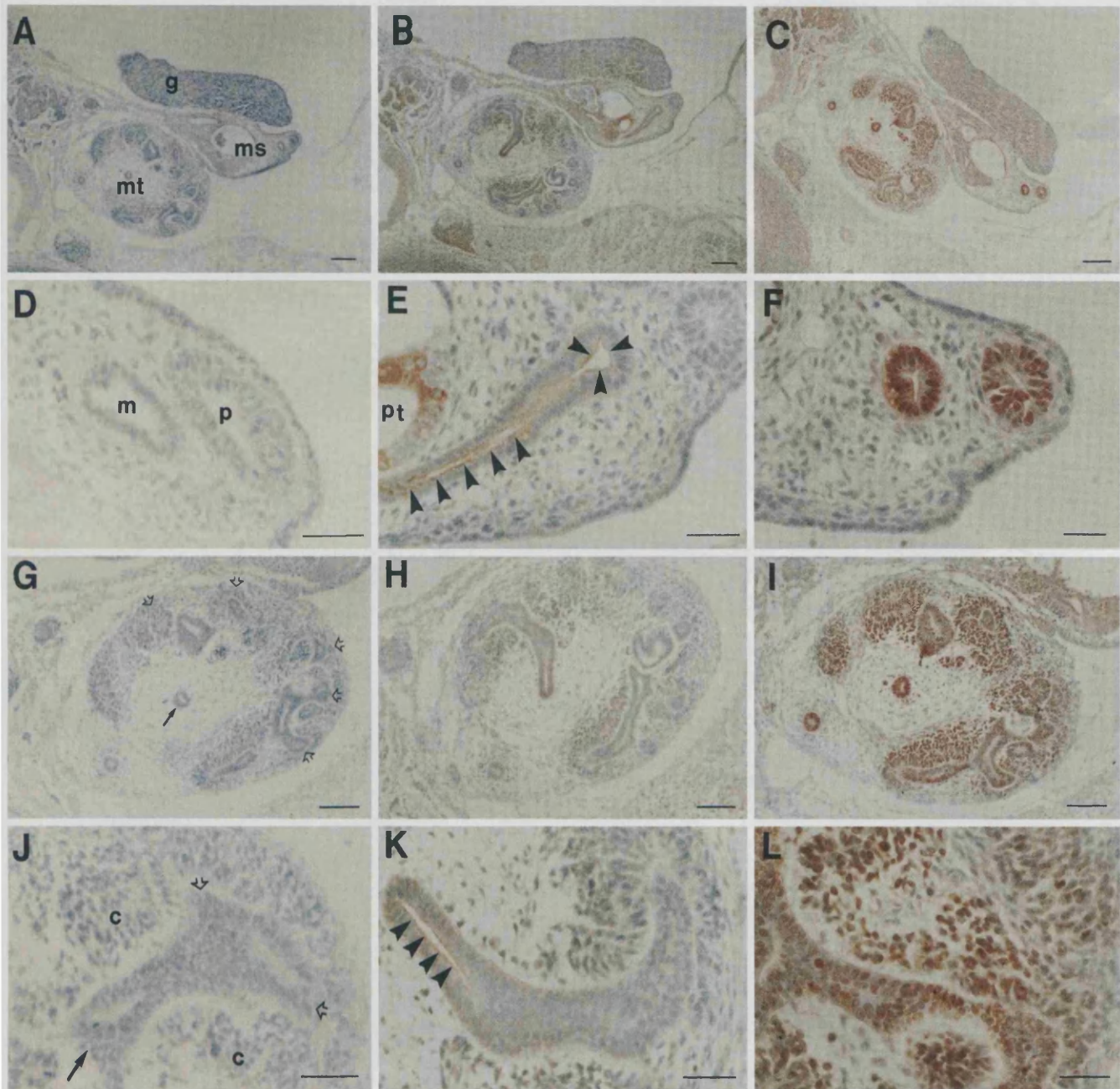

Figure 1. Western blot of galectin-3 in fetal tissues. All lanes were probed with rabbit polyclonal anti-galectin-3 antibody. Lane 1 shows a 10-wk gestation fetal metanephros. Lane 2 shows lower limb from the same fetus. Lanes 3 through 5 show three postnatal dysplastic kidneys. Lane 6 shows Madin-Darby canine kidney (MDCK) cells. A band of approximately 33 kD was detected in all of the human tissues, whereas a larger band was found in the MDCK cells. Preincubation of the antibody with galectin-3 specifically blocked these bands, and no signal was detected when the primary antibody was omitted (not shown).

glomeruli form at 9 wk, and the nephrogenic zone is maintained in the outer cortex until 34 to 36 wk of gestation (24).

Galectin-3 immunoreactivity was detected in the mesonephric duct and also in distal mesonephric tubules from 5 wk of gestation. In these cells, immunostaining appeared to be predominantly in the apical domain (Figure 2, B and E), probably in the plasma membrane. The paramesonephric duct was devoid of staining (Figure 2E). In contrast, PAX-2 was detected in both the mesonephric and paramesonephric ducts (Figure 2, C and F), where the staining was predominantly nuclear, as one would expect for this transcription factor. This difference in staining demonstrates the specificity of the galectin-3 pattern. Patchy cytoplasmic staining for galectin-3 was noted in the proximal tubules in the mesonephros (Figure 2E), whereas glomerular epithelia were negative. Within the 7-wk metanephric kidney, galectin-3 immunoreactivity was noted in the stalk of the ureteric bud, where staining was again detected in the apical plasma membrane (Figure 2, H and K). At this stage, the bud has branched 3 to 4 times, and mesenchymal condensates have appeared around the branch tips (Figure 2, G and J). We found a very low level of galectin-3 immunoreactivity in these condensates (Figure 2, H and K). PAX-2 was expressed at high levels in both the ureteric bud branches and condensing mesenchyme at this time point (Figure 2, I and L), as we have reported previously (22).

At later stages of normal nephrogenesis, three patterns of galectin-3 distribution were detected. These patterns coexisted in the same specimen, as shown in 20-wk gestation fetal kidney specimens depicted in Figures 3 and 4. First, in the nephrogenic cortex, a predominantly apical pattern of galectin-3 was seen in the branching tips of the ureteric bud (Figure 3, B and C). Second, in the subcortical region where tubules are maturing, galectin-3 continued to be expressed in the collecting duct lineage (Figure 3, D and E). Some cells in segments fused with primitive nephrons had a predominantly apical distribution (Figure 3, D and E, arrowheads), whereas in others, galectin-3 immunoreactivity was noted inside the epithelial cells (Figure 3, D and E, arrows). Third, the most intense signal for galectin-3 was found in medullary and papillary collecting ducts, where staining appeared to be cytoplasmic, and also in apical, lateral, and basal plasma membranes (Figure 4, D through F).

In adult kidneys, galectin-3 expression was detected in the cytoplasm, with lower levels in the nucleus as assessed by serial confocal laser scans at 0.50-μm intervals of a subset of cells in the cortex and medulla (Figure 3, F, G, and I; Figure 4, H and J). These cells were restricted to the collecting ducts because the tubules co-stained with *Arachis hypogaea* agglutinin, a marker of the distal nephron (26). Interestingly, cells that were positive for galectin-3 were negative for *Arachis hypogaea*. This agglutinin labels β-intercalated cells in rabbit collecting ducts (27) but has not been as well characterized in the human. Basal co-staining of galectin-3-positive cells was detected with both of the band 3 antibodies (Figure 3, G through I), and this suggests that these are α-intercalated cells. The renal pelvis and ureter, which are ureteric bud derivatives, also expressed galectin-3 protein (data not shown).
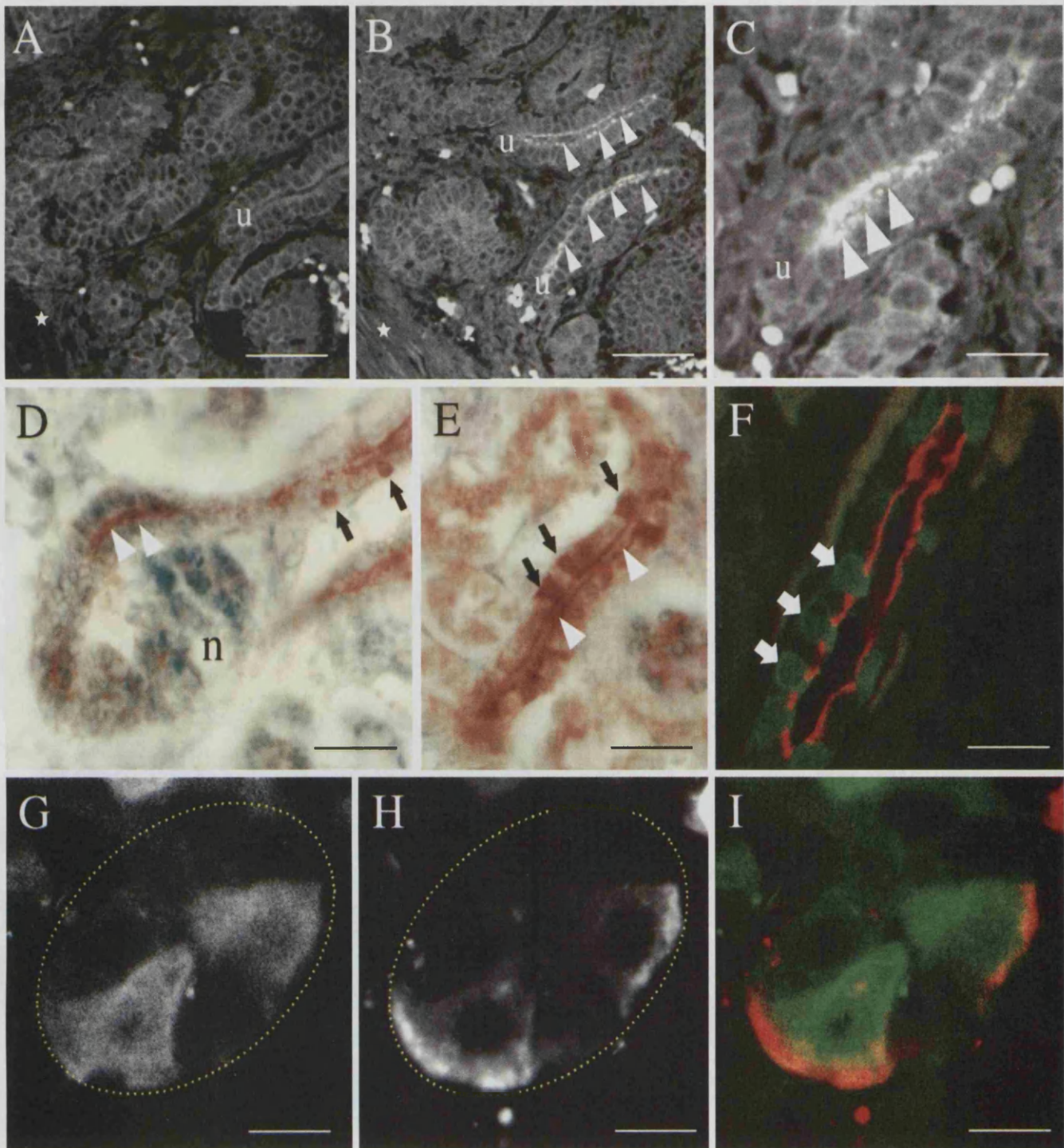
Figure 2. Galectin-3 immunohistochemistry in 7-wk gestation meso- and metanephros. All sections counterstained with methyl green. A, D, G, and J show control sections with primary antibody omitted. B, E, H, and K were immunostained for galectin-3, and C, F, I, and L were immunostained for PAX-2. A, B, and C show low-power views of the mesonephros (ms), metanephros (mt), and gonad (g), and D, E, and F show higher power of mesonephros, mesonephric duct (m), and paramesonephric duct (p). Galectin-3 was detected in a predominantly apical distribution in the mesonephric duct (converging arrowheads in E) and distal-type tubules of the mesonephros (line of arrowheads in E) that drain into it, whereas the paramesonephric duct was negative. Patchy galectin-3 immunoreactivity was also noted in the proximal-type tubules (pt in E). In contrast, PAX-2 protein was found in a predominantly nuclear distribution in both the mesonephric and paramesonephric ducts (C and F). G through L show the metanephros with the ureteric bud branch tips indicated by open arrows, ureteric bud stalk indicated by closed arrows, and condensates (c). H and K show predominantly apical galectin-3 in central ureteric bud with weakly staining condensing mesenchyme around branching tips of the ureteric bud. I and L show PAX-2-positive cells in both the ureteric bud and condensing mesenchyme. Bars: 150 μm in A through C; 30 μm in D through F and J through L; and 80 μm in G through I.

Galectin-3 in Dysplastic Kidney Epithelia

Multicystic dysplastic kidneys result from a failure of normal differentiation and development of both the ureteric bud and metanephric mesenchyme (24). Histologically they consist of dysplastic tubules (Figure 5A) that are thought to be mal-formations of ureteric bud branches. These tubules are connected to cysts and are surrounded immediately by fibromuscular-like cells and more distantly by looser-packed undifferentiated cells (Figure 5A). In these organs, galectin-3 immunostaining was found in 95% of the cysts examined

Figure 3. Galectin-3 immunohistochemistry in renal cortex. A through F are from 20-wk gestation fetus. In A and B, the edge of cortex is indicated by an asterisk. A is the control, with the primary antibody omitted. Note intense autofluorescence of nucleated red cells and weak autofluorescence of the epithelia. B and C show a predominantly apical galectin-3 distribution (arrowheads) in the tips of ureteric bud branches (u). D and E are light-field photomicrographs that show apical galectin-3 staining (white arrowheads) in the ureteric bud where it fuses with the nephron (n) and coexistent cytoplasmic/nuclear protein distribution (black arrows) in specific cells deeper in the cortex. Some nearby proximal tubules show background peroxidase staining. F shows a longitudinal view through a postnatal cortical tubule identified as a collecting duct because it stains with *Arachis hypogaea* agglutinin in red. This is co-stained with galectin-3 (green), and the subpopulation of galectin-3-positive cells (arrows) did not bind *Arachis hypogaea*. G through I are the same section through a postnatal cortical collecting duct co-stained with galectin-3 (G), band 3 (H), or both of these images combined (galectin-3 signal in green and band 3 in red). In G and H, the outline of the tubule is shown by the yellow dotted line, and two cells had cytoplasmic/nuclear galectin-3. The same cells were positive for band 3 on the basolateral surface, which identified them as α-intercalated cells. Bars: 80 μm in A and B; 40 μm in C and F; 60 μm in D and E; and 15 μm in G through I.
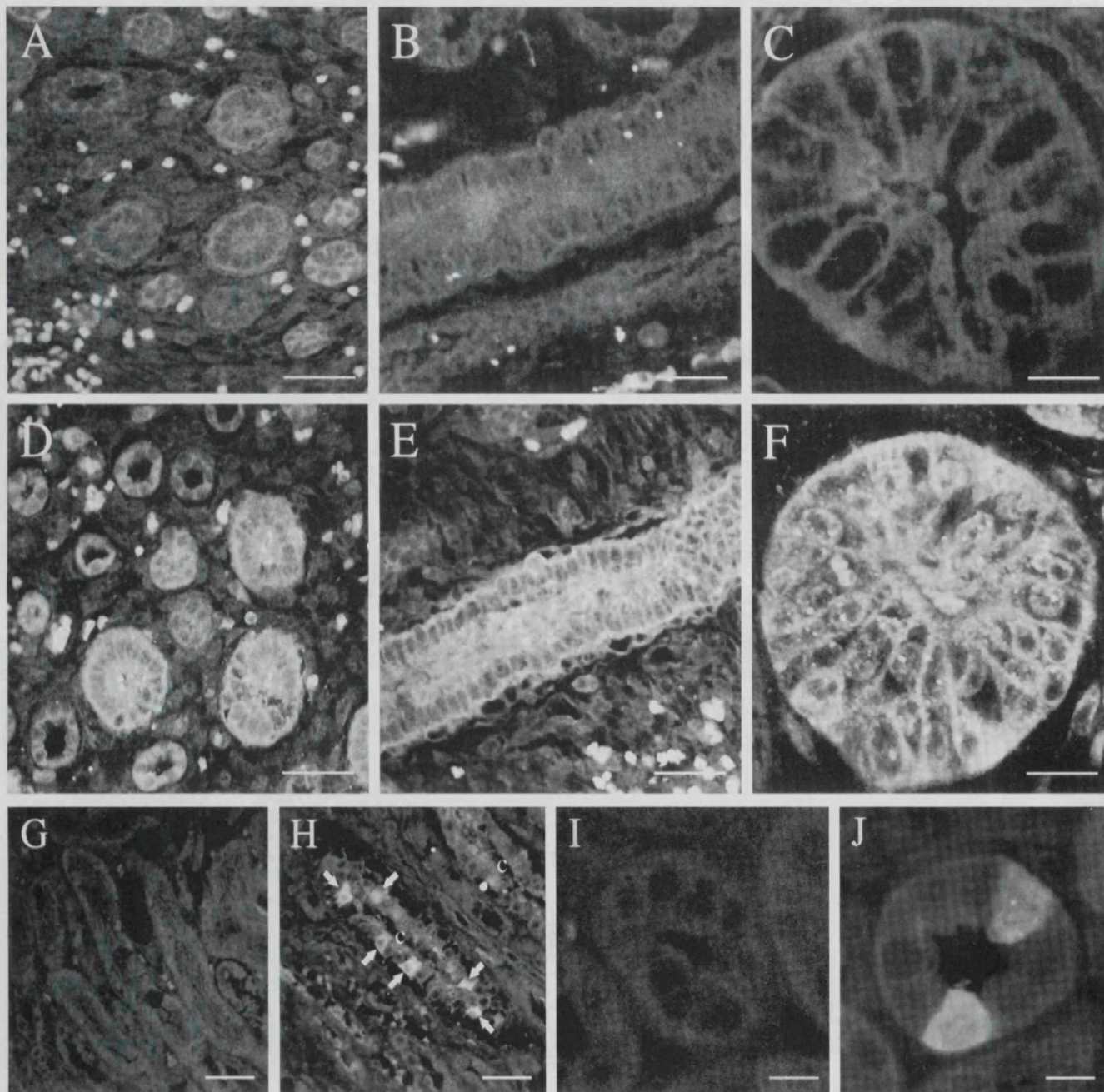
Figure 4. Galectin-3 immunohistochemistry in renal medulla. As controls in A through C and I, the primary antibody was preabsorbed with galectin-3 protein, and in G the primary antibody was omitted. Weak background autofluorescence was seen in many of the tubules with intense autofluorescence in nucleated red cells. A through F show the renal medulla from 20-wk gestation fetuses, and in D through F galectin-3 immunoreactivity was detected in the large collecting ducts. The protein was located in the cytoplasm as well as in apical, lateral, and basal plasma membranes. G through J show postnatal medulla. In H, the collecting ducts (c) contain a subset of cells that are positive for galectin-3 (arrowed) in the cytoplasm. This is shown at higher magnification in the two positive cells in J; weak nuclear staining is also present. Bars: 80 μm in A, B, D, E, G, H; and 15 μm in C, F, I, and J.

(Figure 5, B and C) in both preterm and postnatal specimens, with similar patterns in obstructed and nonobstructed systems. In the positive cysts, every epithelial cell expressed galectin-3 on the apical surface. In addition, dysplastic tubules showed a similar pattern (Figure 5, B and E). Galectin-3 immunoreactivity was also detected in the nuclei of chondrocytes in areas of metaplastic cartilage (Figure 5D). In one postnatal sample, part of the organ contained areas of tubules that looked rela-

tively normal (Figure 5F); an immature apical pattern was seen in some undilated tubules in these areas.

Galectin-3 in Polycystic Kidney Epithelia

In human autosomal recessive polycystic kidney disease, cysts derive from collecting ducts (Figure 6, A and B) (24). We therefore examined the expression of galectin-3 in these organs. Cystic epithelia were universally positive for galectin-3
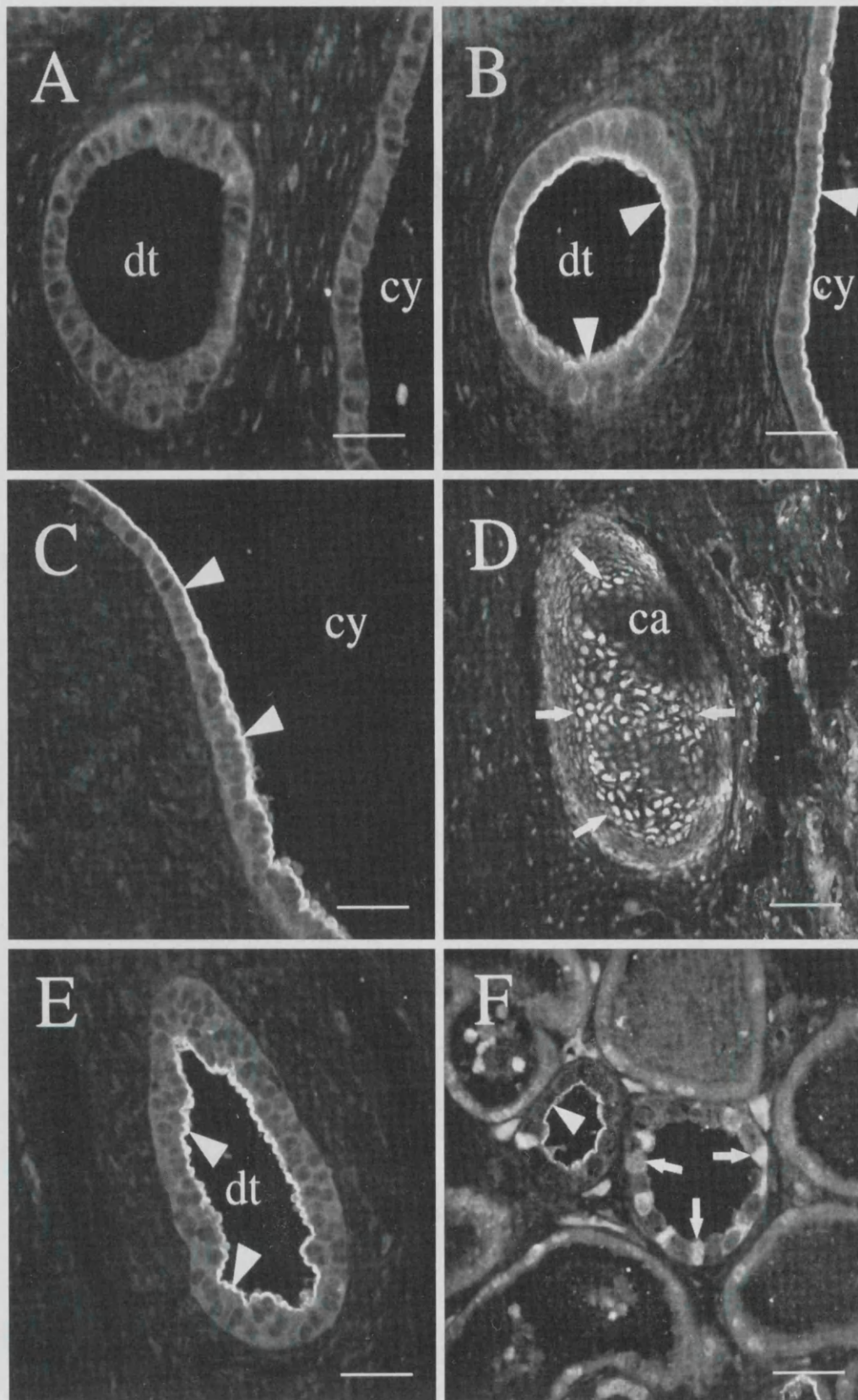
Figure 5. Galectin-3 in multicystic dysplastic kidneys. All sections show postnatal dysplastic kidneys, although prenatal samples showed the same staining pattern. Panel A shows a control section with galectin-3 antibody omitted. B, C, and E show dysplastic tubules (dt) and cysts (cy) with apical galectin-3 protein (arrowheads). In D, metaplastic cartilage (ca) was positive for galectin-3 (arrows). F shows an area of more differentiated tubules: Note that one tubule had a mature cytoplasmic and nuclear galectin-3 pattern restricted to a subset of cells (arrows), whereas the adjacent undilated tubule has an apical phenotype (arrowhead). Bars: 40 μm in A through C, E, and F; and 20 μm in D.
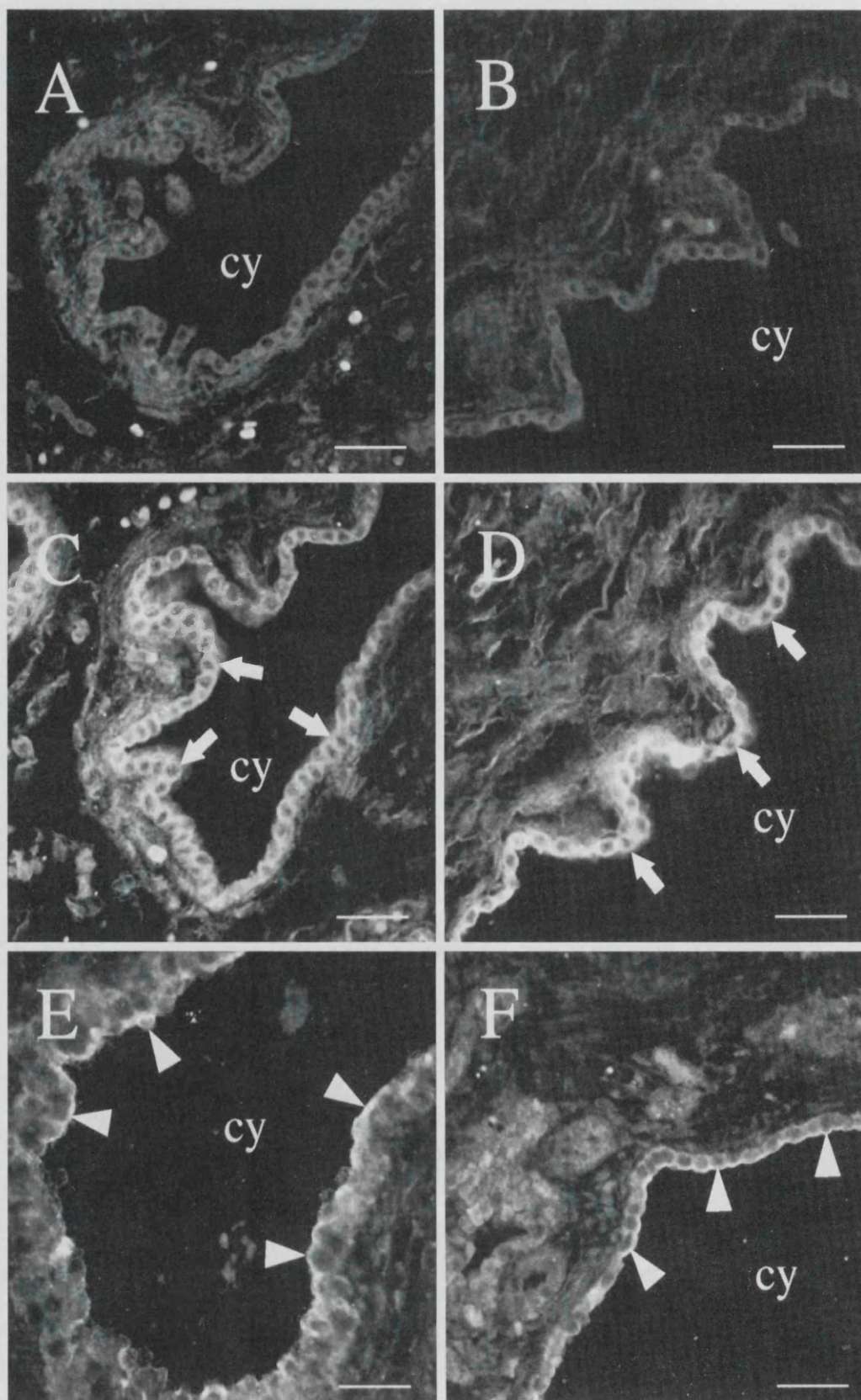
Figure 6. Galectin-3 in autosomal recessive polycystic kidneys. A and B are control sections of a 20-wk gestation fetus corresponding to C and D, respectively. C and D show a postnatal sample with cytoplasmic galectin-3 within cyst epithelium (arrows). E and F show examples of postnatal epithelia with a rare, predominantly apical galectin phenotype (arrowheads) in some cells. Nuclear staining was not detected in cystic epithelia. Bars, 80 μm.

both pre- and postnatally. In the majority of the cysts, galectin-3 was cytoplasmic (Figure 6, C and D), but in a subpopulation representing less than 10% of cysts, a predominantly apical location was detected (Figure 6, E and F). Using confocal laser scanning microscopy, we were unable to detect convincing nuclear staining in any of these samples.

Discussion

Galectins in the Kidney

Our study represents the first report of galectin-3 expression and distribution in the ontogeny of the human kidney. Both the mesonephric and metanephric kidneys develop by interaction between two types of tissue: the epithelia of the mesonephric duct/ureteric bud and the intermediate mesoderm. We found that galectin-3 was almost exclusively located in the former tissues and their derivatives, including the collecting ducts. Immunoreactivity often appeared within cells (*e.g.*, mature collecting ducts) or on the apical plasma membrane (*e.g.*, tips of ureteric bud branches), which suggests that these cells synthesize this molecule, although definitive proof would require *in situ* hybridization studies. These findings expand and confirm a previous study in rodents, which described galectin-3 expression in tubules in the late nephrogenic period (20). Our data also confirm that galectin-3 is produced *in vitro* by MDCK cells (7), an epithelial line with characteristics of collecting ducts. Other members of the galectin family are also expressed in the kidney. For example, Burger and colleagues (31) reported that galectin-1 was expressed by cultured human adult tubular epithelial cells and, in a preliminary report, Wada and coworkers cloned a novel galectin cDNA from murine metanephroi at 13 to 17 d of gestation (32).

Galectin-3 in the Collecting Duct Lineage

The metanephric kidney is the direct precursor of the adult kidney, and we found low levels of galectin-3 immunoreactivity in the branch tips of the ureteric bud. Galectin-3 protein appeared to be predominantly located in the apical domain of the epithelium. This population of cells has a high proliferative index and expresses PAX-2 (22), a transcription factor that is essential for the development of this lineage (25). Growth of these cells is known to be positively regulated by renal mesenchymal-derived paracrine factors (*e.g.*, glial cell line-derived neurotrophic factor and hepatocyte growth factor), which signal through specific receptor tyrosine kinases (*e.g.*, RET, MET, and also ROS) located on the basal surface of these cells (33,34).

It is difficult to envisage an active role for galectin-3 (*e.g.*, in mRNA splicing, in a BCL2-like role in survival, or in interactions with extracellular matrix) in this apical location in the immature ureteric bud. By midgestation, however, a new distribution was observed in cytoplasm and also in lateral and basal plasma membranes of medullary and papillary collecting duct cells (compare Figure 4E with Figure 3C). In the latter location, galectin-3 would be well placed to interact with laminin-1, a molecule that coats embryonic kidney epithelia and has been implicated in epithelial morphogenesis by organ culture experiments (35,36). Indirect evidence for such an

interaction comes from culture of MDCK cells in collagen type 1 gels, in which galectin-3 colocalizes with laminin on the basal surface of developing cysts (37). In this setting, addition of recombinant galectin-3 to the medium slows cyst expansion, whereas blocking antibodies enhance cyst growth (37). It is therefore possible that interaction between galectin-3 and matrix might regulate collecting duct growth *in vivo*. In mouse nephrogenesis, galectin-3 mRNA is detectable by reverse transcription-PCR from embryonic day 11 and, as assessed by Western blot, levels of galectin-3 protein peak at embryonic days 15 to 16 (38), a stage equivalent to midgestation in humans. Moreover, our preliminary data, using mouse organ culture, suggest that addition of recombinant galectin-3 perturbs epithelial morphogenesis (38).

Renal galectin-3 was detected postnatally in a subset of tubular cells in the cortex and medulla, where staining was predominantly cytoplasmic. Counterstaining with *Arachis hypogaea* identified these tubules as collecting ducts (26). Cells positive for galectin-3 were positive for band 3 in a basal distribution. These findings are consistent with galectin-3 being confined to α-intercalated cells. In the future, it will be interesting to examine the phenotypes and function of collecting duct cells in mice that are null mutants for galectin-3.

Galectin-3 in Aberrant Human Kidney Development

Dysplastic kidneys are a common cause of human renal malformations (39). Multicystic dysplastic kidneys have no excretory function, whereas some functioning nephrons may be present in milder cases of dysplasia. Unilateral multicystic cases often present as an abdominal mass in infancy, and these organs may regress and even involute completely (40). Bilateral cases of dysplasia make up a large portion of pediatric renal failure programs but, with advances in prenatal ultrasonography, many affected fetuses are now terminated. We have shown previously that dysplastic cyst epithelia have a high rate of proliferation and that this is correlated with the expression of PAX-2, a potentially oncogenic transcription factor, and BCL-2, a survival molecule (22). Conversely, tissue around dysplastic cysts fails to differentiate into functioning nephrons and has a high rate of apoptosis associated with a lack of BCL-2 and PAX-2 expression (21,22). There is also evidence that soluble signaling molecules, such as hepatocyte growth factor and insulin-like growth factor, are involved in the pathogenesis of these malformations (23,41).

In this study, we found galectin-3 protein in virtually all cells lining dysplastic tubules and their adjoining cysts. This observation is not surprising because the classical microdissection studies of Edith Potter (24) demonstrated that these structures are malformations of ureteric bud branches. The apical distribution of galectin-3 is further evidence for the failure of differentiation of these structures. It is interesting that this phenotype was maintained even in the postnatal samples. On the basis of the above reasoning, we suggest that apical galectin-3 is unable to interact with the extracellular matrix, and this may contribute to cyst expansion. Galectin-3 protein was also found in metaplastic cartilage, which is consistent with reports of galectin-3 in normal fetal cartilage (9). We are currently

attempting to address the possible role of galectin-3 in dysplastic kidneys by studying its action on the growth and morphogenesis of conditionally immortal cell lines from human dysplastic kidneys.

Galectin-3 and Polycystic Kidney Disease

Autosomal recessive polycystic kidney disease occurs in 1 in 10,000 live births and causes a spectrum of clinical problems, including renal failure in infancy through adulthood (42). All studied kindreds appear to be linked to a locus on chromosome 6, but the specific mutation has yet to be reported (43). The cysts arise exclusively from collecting ducts, unlike autosomal dominant polycystic kidney disease, in which all parts of the nephron can become cystic. The biology of renal cyst formation is currently under intensive investigation, with aberrations reported in epithelial cell survival, proliferation, polarity, physiology, and adhesion (44). However, relatively few studies have addressed aberrant biology of the recessive human disease. We recently reported that both apoptosis and proliferation are deregulated in these organs (21). In the current study, we found that galectin-3 protein was detected in all cystic epithelia, consistent with their derivation from collecting ducts. The subcellular localization of galectin-3 was heterogeneous, with most cysts showing a predominantly cytoplasmic pattern, but a minority had an apical distribution. Nuclear localization was not detected in any of the cystic epithelia, which is reminiscent of the loss of nuclear localization reported in neoplasia of the colon (12).

It is interesting to compare expression patterns of galectin-3 in renal ontogeny and cystogenesis with the polycystin protein, the product of the *PKD1* locus that is mutated in most patients with autosomal dominant polycystic kidney disease (45). Polycystin is predicted to have a long extracellular amino terminal with a carboxy terminal inserted into cell membranes, and the molecule may mediate cell/matrix interactions (45). A recent article described polycystin expression in ureteric bud branches and collecting ducts, the same sites we have found to express galectin-3 (46). In autosomal dominant polycystic kidney disease, the majority of cysts have been reported to overexpress polycystin (46) and, in the one sample of this condition that we have been able to examine, we found that galectin-3 is also expressed in most diseased epithelia, apart from in glomerular cysts (P. J. D. Winyard and A. S. Woolf, unpublished data). In the future, it would be intriguing to study potential interactions between these two molecules in normal and abnormal nephrogenesis.

Acknowledgments

References

1. Sharon N, Lis H: *Lectins,* London, Chapman & Hall, 1989
2. Barondes SH, Castronovo V, Cooper DNW, Cummings RD, Drickamer K, Feizi T, Gitt MA, Hirabayashi J, Hughes RC, Kasai K, Leffler H, Liu FT, Lotan R, Mercurio AM, Monsigny M, Pillai S, Poirier F, Raz A, Rigby PWJ, Rini JM: Galectins: A family of animal β galactoside binding lectins [Letter]. *Cell* 76: 597–598, 1993
3. Hughes RC: Mac 2: A versatile galactose binding protein of mammalian tissues. *Glycobiology* 4: 5–12, 1994
4. Herrmann J, Turck CW, Atchison RE, Huflejt ME, Poulter L, Gitt MA, Burlingame AL, Barondes SH, Leffler H: Primary structure of the soluble lactose binding lectin L-29 from rat and dog and interaction of its non-collagenous proline-, glycine-, tyrosine-rich sequence with bacterial and tissue collagenase. *J Biol Chem* 268: 26704–26711, 1993
5. Sato S, Hughes RC: Binding specificity of a baby hamster lectin for H type I and II chains, polylactosamine glycans, and appropriately glycosylated forms of laminin and fibronectin. *J Biol Chem* 267: 6983–6990, 1992
6. Sato S, Hughes RC: Control of Mac 2 surface expression on murine macrophage cell lines. *Eur J Immunol* 24: 216–221, 1994
7. Sato S, Burdett I, Hughes RC: Secretion of the baby hamster kidney 30 kDa galactose binding lectin from polarized and nonpolarized cells: A pathway independent of the endoplasmic reticulum Golgi complex. *Exp Cell Res* 207: 8–18, 1993
8. Weitlauf HM, Knisley KA: Changes in surface antigens on preimplantation mouse embryos. *Biol Reprod* 46: 811–816, 1992
9. Fowlis D, Colnot C, Ripoche MA, Poirier F: Galectin 3 is expressed in the notochord, developing bones, and skin of the postimplantation mouse embryo. *Dev Dyn* 203: 241–251, 1995
10. Dagher SF, Wang JL, Patterson RJ: Identification of galectin-3 as a factor in pre mRNA splicing. *Proc Natl Acad Sci USA* 92: 1213–1217, 1995
11. Wang L, Inohara H, Pienta KJ, Raz A: Galectin-3 is a nuclear matrix protein which binds RNA. *Biochem Biophys Res Commun* 217: 292–303, 1995
12. Lotz MM, Andrews CW Jr, Korzelius CA, Lee EC, Steele GD Jr, Clarke A, Mercurio AM: Decreased expression of Mac 2 (carbohydrate binding protein 35) and loss of its nuclear localization are associated with neoplastic progression of colon carcinoma. *Proc Natl Acad Sci USA* 90: 3466–3470, 1993
13. Agrwal N, Wang JL, Voss PG: Carbohydrate-binding protein 35: Levels of transcription and mRNA accumulation in quiescent and proliferating cells. *J Biol Chem* 264: 17236–17242, 1989
14. Moutsatsos IK, Wade M, Schindler M, Wang JL: Endogenous lectins from cultured cells: Nuclear localization of carbohydrate-binding protein 35 in proliferating 3T3 fibroblasts. *Proc Natl Acad Sci USA* 84: 6452–6456, 1987
15. Hsu DK, Hammes SR, Kuwabara I, Greene WC, Liu FT: Human T lymphotropic virus I infection of human T lymphocytes induces expression of the β galactoside binding lectin, galectin-3. *Am J Pathol* 148: 1661–1670, 1996
16. Schoeppner HL, Raz A, Ho SB, Bresalier RS: Expression of an endogenous galactose binding lectin correlates with neoplastic progression in the colon. *Cancer (Phila)* 75: 2818–2826, 1995
17. Xu XC, el Naggar AK, Lotan R: Differential expression of galectin-1 and galectin-3 in thyroid tumors: Potential diagnostic implications. *Am J Pathol* 147: 815–822, 1995

18. Raz A, Zhu DG, Hogan V, Shah N, Raz T, Karkash R, Pazerini G, Carmi P: Evidence for the role of 34-kDa galactoside-binding lectin in transformation and metastasis. *Int J Cancer* 46: 871–877, 1990

19. Yang RY, Hsu DK, Liu FT: Expression of galectin-3 modulates T cell growth and apoptosis. *Proc Natl Acad Sci USA* 93: 6737–6742, 1996

20. Foddy L, Stamatoglou SC, Hughes RC: An endogenous carbohydrate binding protein of baby hamster kidney (BHK21 C13) cells: Temporal changes in cellular expression in the developing kidney. *J Cell Sci* 97: 139–148, 1990

21. Winyard PJD, Nauta J, Lirenman DS, Hardman P, Sams VR, Risdon RA, Woolf AS: Deregulation of cell survival in cystic and dysplastic renal development. *Kidney Int* 49: 135–146, 1996

22. Winyard PJD, Risdon RA, Sams VR, Dressler G, Woolf AS: The PAX2 transcription factor is expressed in cystic and hyperproliferative dysplastic epithelia in human kidney malformations. *J Clin Invest* 98: 451–459, 1996

23. Kolatsi-Joannou M, Moore R, Winyard PJD, Woolf AS: Expression of hepatocyte growth factor/scatter factor and its receptor, MET, suggests roles in human embryonic organogenesis. *Pediatr Res* 41: 657–665, 1997

24. Potter EL: *Normal and Abnormal Development of the Kidney*, Chicago, Year Book Medical Publishers, Inc., 1972

25. Torres M, Gomex-Pardo E, Dressler GR, Gruss P: Pax-2 controls multiple steps of urogenital development. *Development* 121: 4057–4065, 1995

26. Holthoffer H, Virtanen I, Pettersen E, Tornroth T, Alfthan O, Linder E, Miettinen A: Lectins as fluorescence microscopic markers for saccharides in the human kidney. *Lab Invest* 45: 391–399, 1981

27. Fejes-Toth G, Naray Fejes-Toth A: Fluorescence activated cell sorting of principal and intercalated cells of the renal collecting duct. *J Tissue Cult Meth* 13: 173–178, 1991

28. Wagner S, Vogel R, Lietzke R, Koob R, Drenckhahn D: Immunochemical characterization of a band 3-like anion exchanger in collecting duct of human kidney. *Am J Physiol* 253: F213–F221, 1987

29. Tanner MJA: The acid test for band 3. *Nature (Lond)* 382: 209–210, 1996

30. Wainwright SD, Tanner MJ, Martin GE, Yendle JE, Holmes C: Monoclonal antibodies to the membrane-bound domain of the human erythrocyte anion transport protein: Localization of the C-terminus of the protein to the cytoplasmic side of the red cell membrane and distribution of the protein in some human tissues. *Biochem J* 258: 211–220, 1989

31. Burger A, Filsinger S, Cooper DNW, Hansch GM: Expression of the 14 kDa galactose binding protein, galectin-1, on human tubular epithelial cells. *Kidney Int* 50: 754–759, 1996

32. Wada J, Ota K, Kumar A, Kanwar YS: Identification of 36 kD novel β galactoside binding mammalian lectin in murine embryonic kidney [Abstract]. *J Am Soc Nephrol* 7: 1608, 1996

33. Woolf AS, Kolatsi-Joannou M, Hardman P, Andermarcher E, Moorby C, Fine LG, Jat PS, Noble MD, Gherardi E: Roles of hepatocyte growth factor/scatter factor and the met receptor in the early development of the metanephros. *J Cell Biol* 128: 171–184, 1995

34. Woolf AS, Cale CM: Roles of growth factors in renal development. *Curr Opin Nephrol Hypertens* 6: 10–14, 1997

35. Klein G, Langegger M, Timpl R, Ekblom P: Role of laminin A chain in the development of epithelial cell polarity. *Cell* 55: 331–341, 1988

36. Falk M, Salmivirta K, Durbeej M, Larsson E, Ekblom M, Vestweber D, Ekblom P: Integrin α6β1 is involved in kidney tubulogenesis in vitro. *J Cell Sci* 109: 2801–2810, 1996

37. Bao Q, Hughes RC: Galectin-3 expression and effects on cyst enlargement and tubulogenesis in kidney epithelial MDCK cells cultured in three dimensional matrices in vitro. *J Cell Sci* 108: 2791–2800, 1995

38. Woolf AS, Bao Q, Hughes RC, Winyard PJD: Galectin-3 in normal, polycystic and dysplastic nephrogenesis [Abstract]. *J Am Soc Nephrol* 7: 1626, 1996

39. Woolf AS: Clinical impact and biological basis of kidney malformations. *Semin Nephrol* 15: 361–372, 1995

40. Mesrobian H-GJ, Rushton HG, Bulas D: Unilateral renal agenesis may result from in utero regression of multicystic renal dysplasia. *J Urol* 150: 793–794, 1993

41. Matsell DG, Bennett T, Armstrong RA, Goodyer P, Goodyer C, Han VKM: Insulin-like growth factor (IGF) and IGF binding protein gene expression in multicystic renal dysplasia. *J Am Soc Nephrol* 8: 85–94, 1997

42. Kaplan BS, Fay J, Shah V, Dillon MJ, Barratt TM: Autosomal recessive polycystic kidney disease. *Pediatr Nephrol* 3: 43–49, 1989

43. Zerres K, Mucher G, Bachner L, Deschennes G, Eggermann T, Kaariainen H, Knapp M, Lennert T, Misselwitz J, von Muhlendahl KE, Neumann HPH, Pirson Y, Rudnik Schoneborn S, Steinbicker V, Wirth B, Scharer K: Mapping of the gene for autosomal recessive polycystic kidney disease (ARPKD) to chromosome 6p21 cen. *Nat Genet* 7: 429–432, 1994

44. Woolf AS, Winyard PJD: Unraveling the pathogenesis of cystic kidney diseases. *Arch Dis Child* 72: 103–105, 1995

45. Hughes J, Ward CJ, Peral B, Aspinwall R, Clark K, San Millan JL, Gamble V, Harris PC: The polycystic kidney disease gene 1 (PKD1) encodes a novel protein with multiple cell recognition domains. *Nat Genet* 10: 151–156, 1995

46. Geng L, Segal Y, Peissel B, Deng N, Pei Y, Carone F, Rennke HG, Glucksmann-Kuis AM, Schneider MC, Ericsson M, Reeders ST, Zhou J: Identification and localization of polycystin, the PKD1 gene product. *J Clin Invest* 98: 2674–2682, 1996

The PAX2 Transcription Factor Is Expressed in Cystic and Hyperproliferative Dysplastic Epithelia in Human Kidney Malformations

Paul J.D. Winyard,* R. Anthony Risdon,‡ Virginia R. Sams,§ Gregory R. Dressler,∥ and Adrian S. Woolf*

*Developmental Biology Unit, Institute of Child Health, University of London, London WC1E 1EH, United Kingdom; ‡Department of Histopathology, Hospital for Sick Children, London WC1N 1JH, United Kingdom; §Department of Histopathology, University College Medical School, London WC1E 6JJ, United Kingdom; and ∥Department of Pathology, Howard Hughes Medical Institute, University of Michigan Medical Center, Ann Arbor, Michigan 48109-0650

Abstract

Human dysplastic kidneys are developmental aberrations which are responsible for many of the very young children with chronic renal failure. They contain poorly differentiated metanephric cells in addition to metaplastic elements. We recently demonstrated that apoptosis was prominent in undifferentiated cells around dysplastic tubules (Winyard, P.J.D., J. Nauta, D.S. Lirenman, P. Hardman, V.R. Sams, R.A. Risdon, and A.S. Woolf. 1996. *Kidney Int.* 49:135–146), perhaps explaining the tendency of some of these organs to regress. In contrast, apoptosis was rare in dysplastic epithelia which are thought to be ureteric bud malformations. On occasion, these tubules form cysts which distend the abdominal cavity (the multicystic dysplastic kidney) and dysplastic kidneys may rarely become malignant. We now demonstrate that dysplastic tubules maintain a high rate of proliferation postnatally and that PAX2, a potentially oncogenic transcription factor, is expressed in these epithelia. In contrast, both cell proliferation and PAX2 are downregulated during normal maturation of human collecting ducts. We demonstrate that BCL2, a protein which prevents apoptosis in renal mesenchymal to epithelial conversion, is expressed ectopically in dysplastic kidney epithelia. We propose that dysplastic cyst formation may be understood in terms of aberrant temporal and spatial expression of master genes which are tightly regulated in the normal program of human nephrogenesis. (*J. Clin. Invest.* 1996. 98:451–459.) Key words: BCL2 • dysplastic kidney • nephrogenesis • PAX2 • WT1

Introduction

Development is orchestrated by regulatory genes expressed in a temporal and spatial cascade (1). Many such genes encode transcription factors that must first bind to, and then regulate the expression of, growth factor, cell adhesion, and also other

---

---

transcription factor genes (1–3). One transcription factor family contains the DNA-binding "paired" domain and is encoded by *PAX* genes (4), of which nine members have been identified in humans (5). *Drosophila* homologues control embryonic patterning (4) and cell specification (6), while a zebrafish *PAX* gene is implicated in retinal development (7). Expression patterns and functional ablation experiments show that mouse *PAX* genes regulate development of the brain, eye, lymphoid system, musculature, neural crest, thymus and vertebrae (8–12). Other studies reveal PAX overexpression causes cell transformation and tumor formation (13). In humans, familial and sporadic human mutations in *PAX3* and *PAX6* are associated with Waardenburg syndromes (14, 15) and aniridia (16) respectively, while rearrangement of *PAX3* causes soft tissue tumors (17).

Two *PAX* genes are relevant to nephrogenesis, *PAX2* and *PAX8* (18, 19). Mouse PAX2 is expressed in the mesonephric duct and its branch, the ureteric bud which gives rise to ureteric, renal pelvic and collecting duct epithelia. Both PAX2 and PAX8 are expressed in mesenchymal/epithelial conversion during nephron formation. These genes are downregulated as the kidney matures (18–20) but transgenic overexpression of PAX2 causes epithelial hyperproliferation and cyst formation (21). Conversely, genetic ablation of a single *PAX2* allele causes renal hypoplasia (9, 22) while antisense oligonucleotides, which reduce PAX2 protein in organ culture, inhibit the mesenchymal to epithelial transition (23). Homozygous *PAX2* null-mutant mice have no kidneys because the ureteric bud fails to branch from the mesonephric duct (22). Furthermore, the absence of mesonephric tubules suggests that PAX2 is required for mesenchymal/epithelial conversion in vivo, and Fallopian tubes are absent because PAX2 is expressed in Mullerian duct derivatives (24). *PAX2* mutations have also been found in humans, arising de novo or inherited in an autosomal dominant manner (25, 26). Heterozygous individuals with mutations of either the paired or octapeptide domains most likely have haploinsufficiency, a partial lack of functional protein. They suffer from optic nerve colobomas, vesicoureteric reflux, and "hypoplastic" kidneys, although histological analysis was not performed in the original report (25). Homozygous *PAX2* mutations have not been described in humans although known kindreds with kidney and Mullerian malformations superficially resemble the (female) mouse null-mutants (22, 27). PAX2 and PAX8 are overexpressed in Wilms tumor (20, 28–30), a malignant neoplasm containing tissues resembling the embryonic kidney, and also in renal cell carcinoma (31). Thus, in mice and humans, a deficiency of metanephric PAX2 protein is associated with growth failure while overexpression of the same protein is associated with cyst or tumor formation.

Human dysplastic kidneys are developmental aberrations which are responsible for many of the very young children who require dialysis and renal transplantation (32–35). They contain poorly differentiated metanephric cells in addition to meta-

plastic elements (32, 34, 35). We recently demonstrated that apoptosis was prominent in undifferentiated cells surrounding dysplastic tubules (36) perhaps explaining the tendency of some of these organs to involute (37). In contrast, apoptosis was less common in dysplastic epithelia (36) which are thought to be malformed branches of the ureteric bud (34). These tubules may form cysts large enough to distend the abdominal cavity (the multicystic dysplastic kidney) (34) and these kidneys may on occasion become malignant (38, 39). We now demonstrate that dysplastic tubules maintain a high rate of proliferation through the postnatal period, and that PAX2 protein, a potentially oncogenic transcription factor, is highly expressed in the nuclei of these epithelia. In contrast, both cell proliferation and PAX2 are downregulated during normal maturation.

Methods

Sources of normal and dysplastic organs. The modes of collection of specimens have been fully described (36). All abnormal kidneys met histological criteria for dysplasia based on the identification of immature tubules together with the presence of metaplastic cartilage (32, 34, 35). In addition, undifferentiated and fibromuscular-like cells are seen around dysplastic epithelia and multicystic dysplastic kidneys

Table IA. Prenatal Samples

Gestational age	Sex	Renal histology	Termination/ spontaneous abortion	Other abnormalities
wk				
17	M	Dysplasia	T	None
19	M	Dysplasia	T	Hydrocephalus
19	M	Dysplasia	T	Urethral obstruction
19	F	Dysplasia	T	None
20	M	Dysplasia	T	Hypoplastic lungs
22	M	Dysplasia	T	Urethral obstruction, atrial septal defect
22	M	Dysplasia	T	None
24	F	Dysplasia	T	Hypoplastic lungs
32	F	Dysplasia	S	Hypoplastic lungs
34	M	Dysplasia	S	Hypoplastic lungs
10	?	Normal	T	None
17	M	Normal	T	Neural tube defect
19	F	Normal	T	Trisomy 21
20	M	Normal	S	Thalassemia trait
20	F	Normal	S	None
22	M	Normal	T	Anorectal abnormality
25	M	Normal	S	Hyaline membrane disease
25	F	Normal	S	Hyaline membrane disease
27	M	Normal	S	Septicaemia
28	F	Normal	S	Growth retardation
32	F	Normal	S	Maternal pre-eclampsia
32	M	Normal	S	Pneumothorax, liver tear

Chromosomes were normal in all cases assessed apart from the single case of Trisomy 21. Two of the dysplastic samples were associated with urethral obstruction. All abnormal organs were multicystic dysplastic kidneys.

contain massive dilatated terminal segments of dysplastic tubules. In this study we have also included normal postnatal samples from children who died from Sudden Infant Death syndrome (SIDS). No renal or other pathology was detected in these samples at post mortem. The prenatal samples are documented in Table *IA* and postnatal samples in Table *IB*; obstructed kidneys are indicated. Kidneys were fixed in 10% formalin and embedded in paraffin wax. Sections were cut at 4–6 μm and were counterstained with methyl green.

Immunohistochemistry. For PAX2 immunohistochemistry we used a rabbit polyclonal antibody raised against amino acids 188–385 in the carboxy-terminal domain of PAX2 (20): this sequence does not include the highly conserved paired domain which is located in the amino-terminal region of the full length PAX2 protein (18). Using cells transfected with PAX2, 5, and 8 there is only appreciable reactivity to the former protein and, using deletion mutants of PAX2, this

Table IB. Postnatal Samples

Age	Sex	Renal histology	Additional pathology	Obstruction
mo				
4	F	Dysplasia	Obstructed ureterocoele	Yes
4	M	Dysplasia	Vesicoureteric junction obstruction	Yes
5	F	Dysplasia	None	No
6	M	Dysplasia	Nonobstructed megaureter	No
8	F	Dysplasia	Duplex with dysplastic obstructed upper pole	Yes
8	M	Dysplasia	Contralateral hydronephrosis	No
9	F	Dysplasia	Contralateral vesicoureteric reflux	No
9	F	Dysplasia	None	No
14	F	Dysplasia	None	No
15	M	Dysplasia	Ipsilateral reflux	No
19	M	Dysplasia	None	No
24	M	Dysplasia	None	No
3	F	Normal	SIDS	No
3	F	Normal	SIDS	No
3	F	Normal	SIDS	No
4	F	Normal	SIDS	No
4	F	Normal	SIDS	No
5	F	Normal	SIDS	No
5	M	Normal	SIDS	No
6	M	Normal	SIDS	No
7	M	Normal	SIDS	No
14	F	Normal	SIDS	No
5	F	Normal	Wilms tumor	No
8	M	Normal	Wilms tumor	No
28	M	Normal	Wilms tumor	No
30	M	Normal	Wilms tumor	No
38	M	Normal	Wilms tumor	No
72	F	Normal	Wilms tumor	No

All abnormal kidneys were cystic dysplastic and three were attached to obstructed urinary systems. Sudden infant death syndrome (SIDS) patients died without any pathological cause being found at post mortem examination. These kidneys were histologically normal. In the Wilms tumor samples we examined the normal surrounding renal tissue. None of these children had WT1 mutations (36).

	PAX2	PCNA	WT1	BCL2
Normal kidneys				
Undifferentiated mesenchyme	–	rare +	rare +	–
Mesenchymal condensate				
and vesicles	++	++	+	++
S-shaped bodies	++	++	+	+
Glomerular podocytes	–	rare +	++	–
Tips of ureteric bud (ampullae)	++	++	–	–
Immature collecting ducts	+	+	–	–
Mature collecting ducts	rare +	rare +	–	–
Dysplastic kidneys				
Dysplastic tubules	++	++	–	++
Cyst epithelia	++	++	–	+
Collarettes/undifferentiated cells	–	rare +	+	–

– Indicates no staining, + to ++ indicate increasing intensity of staining present in the majority of cells in the designated population. 'Rare +' indicates that < 10% of cells of these populations showed positive immunostaining.

antibody recognizes major epitopes between amino acids 270–338 (40). In homogenates of mouse metanephros the antibody recognizes a single major doublet (46–48 kD) on western blot (20). Our own unpublished observations show that this antibody recognizes similar bands on western blot of human fetal kidney (data available on request). For WT1 immunostaining we used a rabbit polyclonal IgG fraction raised against an epitope in the carboxy terminus of the human WT1 protein (C-19: Santa Cruz Biotechnology, Inc., CA). This antibody has been found by the manufacturer and also by other groups (41) to specifically recognize WT1 transcription factor/splicing factor protein on western blot. Our own unpublished observations also demonstrate that a protein doublet (45–50 kD) is recognized by this antibody in western blot of reduced homogenates of human fetal, mature and dysplastic kidney (data available on request). Mouse monoclonal antibody to proliferating cell nuclear antigen (PCNA)[1], a DNA-polymerase δ-associated protein expressed at high levels during S phase (42), was purchased from Oncogene Science, Inc., (Cambridge, MA) (PCNA Ab-1). Monoclonal mouse antibody to human BCL2 was purchased from DAKO (clone 124; DAKO A/S, Glostrup, Denmark). All other chemicals were supplied by Sigma (Poole, Dorset, UK) unless otherwise stated.

Immunohistochemistry was performed using conventional techniques as follows. Sections were dewaxed through Histo-Clear (National Diagnostics, Atlanta, GA) twice for 10 min, followed by rehydration through 100% alcohol (Hayman Ltd., Witham, Essex, UK) twice for 5 min and then stepwise through 95, 90, 75, 50, and 30% alcohol for 3 min each. After washing in phosphate buffered saline (PBS, pH 7.4) for 5 min and running tap water for ten minutes they were immersed in Citric acid buffer (2.1 g/l, pH 6.0) and boiled in a microwave for 8–15 min. They were then allowed to cool, rewashed in tap water and PBS, then incubated in 3% hydrogen peroxide for 15 min to quench endogenous peroxidase activity. After two further washes in PBS, non specific antibody binding was blocked with 10% fetal calf serum/PBS and the primary antibody was then applied for one hour at 37°C. WT1, PCNA, and BCL2 antibodies were used at a

1. *Abbreviation used in this paper:* PCNA, proliferating cell nuclear antigen.

1 in 50 dilution and the PAX2 antibody at a concentration of 10 mg/liter. Primary antibodies were detected using a streptavidin biotin peroxidase system (Dako, ABC Kit) followed by diamino benzidine (DAB). They were then counterstained with 0.5% methyl green for 10 min, washed three times with water and butanol, once in histoclear for 10 min, and mounted in DPX (BDH, Poole, UK). Specimens were examined and photographed on a Zeiss Axiophot microscope (Carl Zeiss, 7082 Oberkochen, Germany).

Results

Consistent patterns of gene expression were noted in each group. Results are summarized in Table II, are described below, and are illustrated in Figs. 1–4.

PAX2 in normal human nephrogenesis. The human metanephros can be identified at 5 wk gestation and consists of a ureteric bud and renal mesenchyme. The first glomeruli form at 9 wk and a nephrogenic zone is maintained to 34 wk (34). Renal mesenchymal cells do not express PAX2 protein (Fig. 1, *A, C–E* and Fig. 2, *A*). As this lineage differentiates PAX2 was expressed during mesenchymal to epithelial transition, first in mesenchymal condensates and then in vesicles and comma-shaped bodies (Fig. 1, *A, C* and *D*, and Fig. 2, *A*). As expected for a transcription factor, immunoreactivity was intense in nuclei, although some cytoplasmic staining was also noted (Fig. 1, *E* and *H*). In the next stage of nephron maturation, the S-shaped bodies, PAX2 was detected in all elements apart from precursors of glomerular visceral epithelia (Fig. 1, *E*). In the capillary loop stage of glomerulogenesis faint PAX2 immunoreactivity was present in parietal epithelia and in adjoining proximal tubules (Fig. 1 *G–H*). PAX2 protein was not detected in mature glomeruli (Fig. 1, *I*). In the ureteric bud lineage, intense PAX2 immunoreactivity was detected in branching ampullae, each of which is flanked by mesenchymal condensates (Fig. 1, *A, C* and *D* and Fig. 2, *A*). Nuclei in fetal cortical and medullary collecting ducts showed weaker but consistent immunostaining (Fig. 1, *F* and *G*). Mature collecting duct cells generally had no significant staining above control sections in which the anti-PAX2 antibody had been omitted, although occasional (< 10%) nuclei showed faint immunoreactivity (Fig. 1, *I* and Fig. 2, *C*).

PAX2 in human multicystic dysplastic kidneys. Multicystic dysplastic kidneys contain dysplastic tubules which are thought to be malformations of ureteric bud branches (34). Studies by Potter revealed that these tubules were connected to cysts (34). The tubules are immediately surrounded by fibromuscular-like cells and, further from the tubule, there are looser-packed undifferentiated cells (Fig. 2, *E* and *F*, Fig. 3, *C* and *D* and Fig. 4, *C* and *D*). All nuclei of epithelia lining the dysplastic tubules stained intensely with antiserum to PAX2 and the flattened epithelial cells lining cysts were also positive (Fig. 2, *E* and *G*). In contrast the poorly differentiated cells surrounding the tubules did not express PAX2 (Fig. 2, *E* and *G*). Strikingly, the same pattern of PAX2 expression was detected in both prenatal and postnatal multicystic dysplastic kidneys. Thus, PAX2 expression is not downregulated with time in these organs.

PCNA in normal and abnormal human nephrogenesis. PCNA is associated with DNA replication machinery and is strongly expressed in S phase (42). When identified in cell nuclei, it can be used as a surrogate marker of proliferation. In normal human nephrogenesis, nuclei with PCNA immunore-
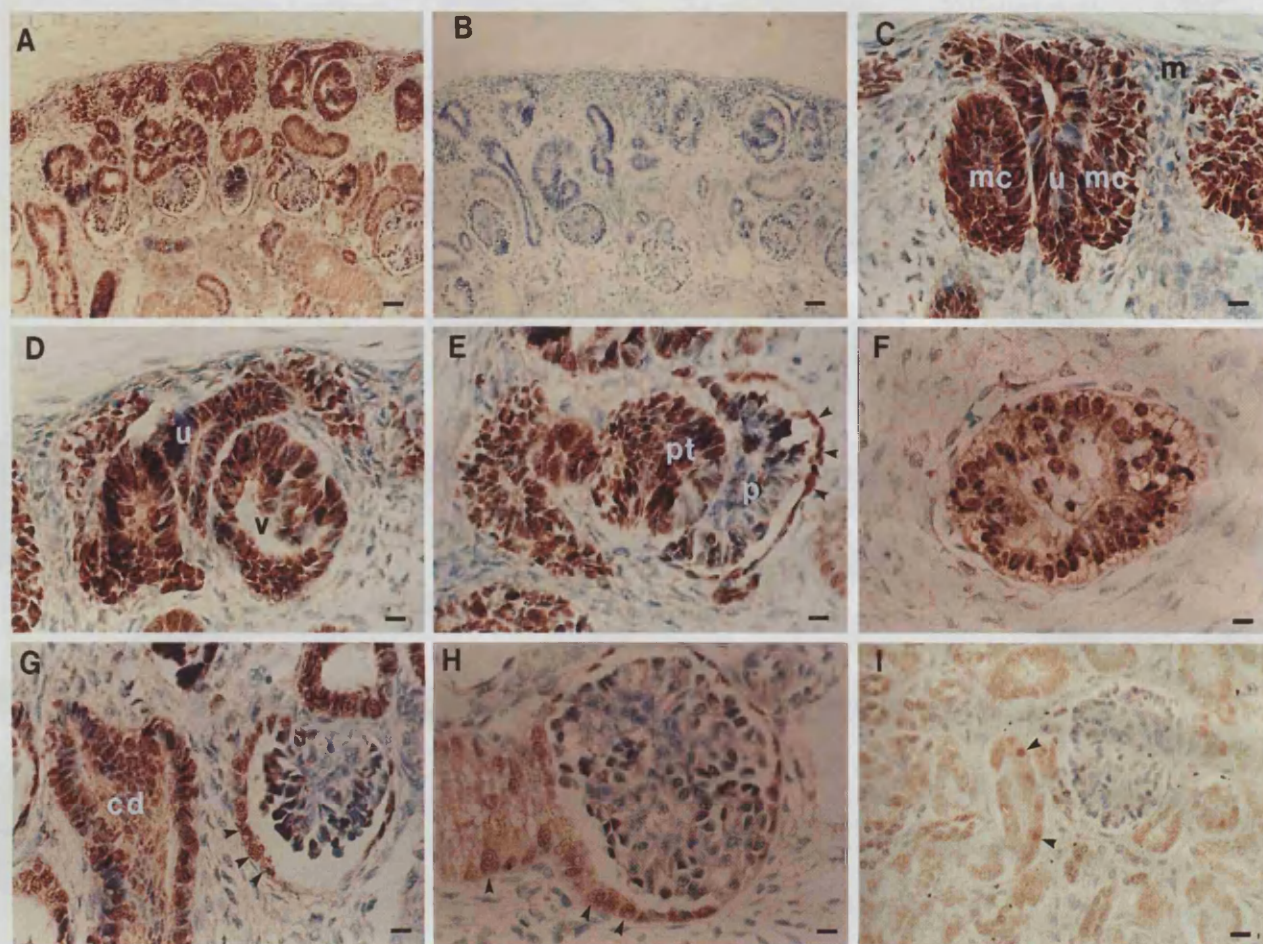
Figure 1. PAX2 immunostaining during normal human nephrogenesis. All sections are from a normal human 10-wk gestation kidney apart from (*I*) which is a 6-mo normal postnatal kidney. (*A*) Note PAX2 (brown color) in the nephrogenic zone with decreasing levels towards the maturing center. Bar, 12 μm. (*B*) Same field as *A* but no first antibody. Bar, 12 μm. (*C*) Intense PAX2 expression in a ureteric bud branch tip (u) and in mesenchymal condensates (*mc*). Note that the undifferentiated mesenchyme (*m*) has no PAX2 staining. Bar, 3 μm. (*D*) A little later in development, a vesicle (*v*) has formed. Bar, 3 μm. (*E*) PAX2 expression in a primitive proximal tubule (*pt*) and in parietal glomerular epithelia (*arrowheads*). Note PAX2 downregulation in maturing podocytes (*p*). Bar, 3 μm. (*F*) PAX2 in a fetal medullary collecting duct. Bar, 3 μm. (*G*) On the left a maturing cortical collecting duct has less intense staining: on the right, a fetal glomerulus shows only faint PAX2 staining in Bowman's capsule (*arrowheads*). Bar, 3 μm. (*H*) Capillary loops are noted in this fetal glomerulus with faint PAX2 staining in visceral epithelia and proximal tubule (*arrowheads*). Bar, 3 μm. (*I*) In the postnatal kidney PAX2 is downregulated but rare nuclei are faintly positive (*arrowheads*). Bar, 6 μm.

activity were scarce within the undifferentiated mesenchyme but the protein is highly expressed during the mesenchymal to epithelial transition and also in the ampullary tips of the branches of the ureteric bud (Fig. 2, *B*). In postnatal normal kidneys PCNA positive cells were still detected in all parts of the nephron (Fig. 2, *D*) but they were extremely scarce (< 1% of total nuclei). Within human kidney malformations, 20–100% of epithelial nuclei in dysplastic tubules were positive for PCNA (Fig. 2 *F*). Furthermore, staining was positive in a similar proportion of cells in cystic epithelia (Fig. 2, *H*). Multicystic kidneys harvested pre- and postnatally showed similar patterns. Thus, PAX2 expression is associated with proliferation in normal fetal kidneys and in dysplastic tubules and cysts. Additionally, some nuclei were positive for PCNA in undifferentiated tissue around dysplastic tubules (Fig. 2, *F*).

BCL2 in normal and abnormal human nephrogenesis. BCL2 protects developing cells from programmed cell death (43, 44). In normal fetal kidneys immunoreactivity was first detected in mesenchymal condensates (Fig. 3, *A* and *B*), a stage

at which both PCNA and PAX2 expression were present (Fig. 2, *A* and *B*). Thereafter, BCL2 was downregulated (Fig. 3, *A* and *B*) in the developing nephron apart from in descending loops of Henle (data not shown). We did not detect BCL2 immunoreactivity in ureteric bud derivatives such as ampullae and collecting ducts (Fig. 3, *A* and *B*). In dysplastic kidneys, BCL2 protein was consistently expressed within the cytoplasm of dysplastic tubule epithelia but was absent from surrounding collarettes and other poorly differentiated cells (Fig. 3, *C* and *D*). This is an ectopic pattern since dysplastic tubules are derived from the ureteric bud (34), but this lineage does not normally express BCL2. Moreover, we found that BCL2 expression was not downregulated postnatally in dysplastic tubules.

WT1 in normal and abnormal human nephrogenesis. WT1 is essential for early nephrogenesis (41, 45, 46). In normal fetal kidneys WT1 was faintly expressed in nuclei of condensates and vesicles (Fig. 4, *A*). The intensity of staining increased in the proximal limbs of S-shaped bodies, with the highest levels in immature glomerular podocytes (Fig. 4, *A*), a
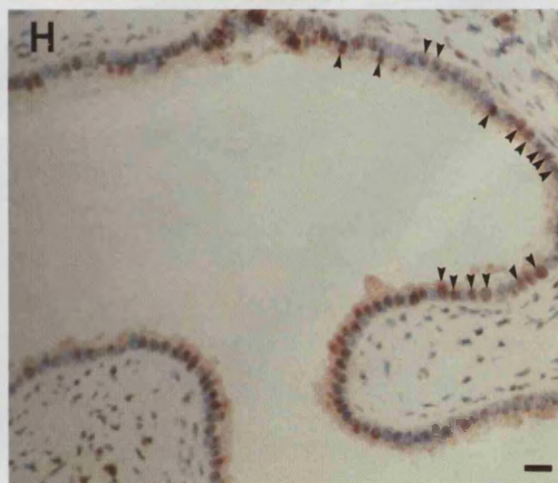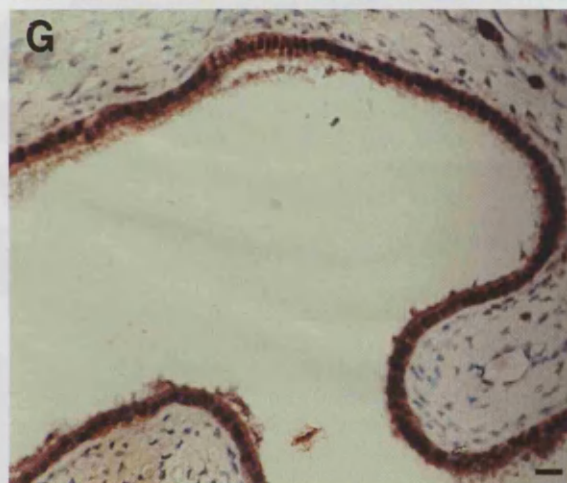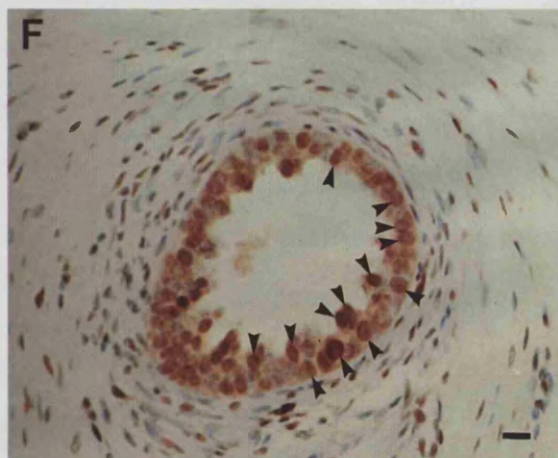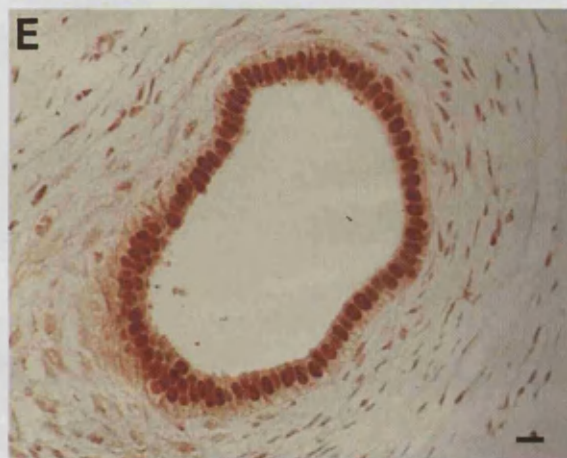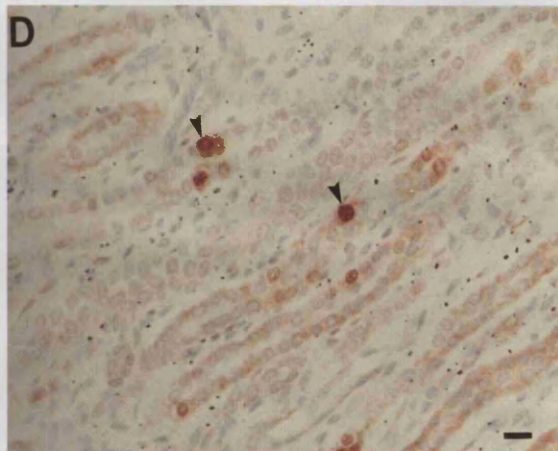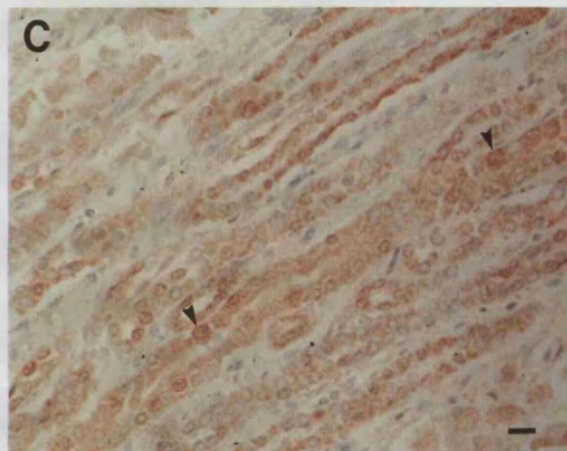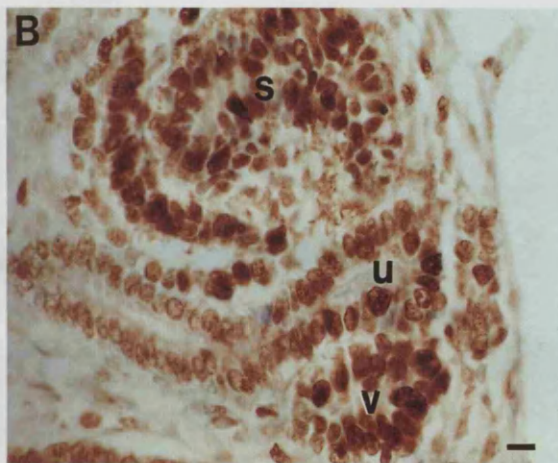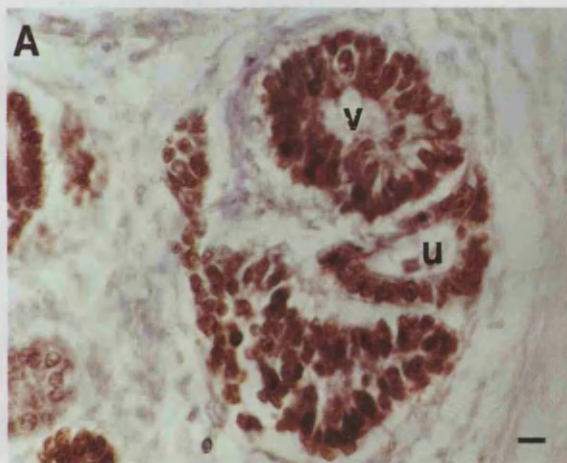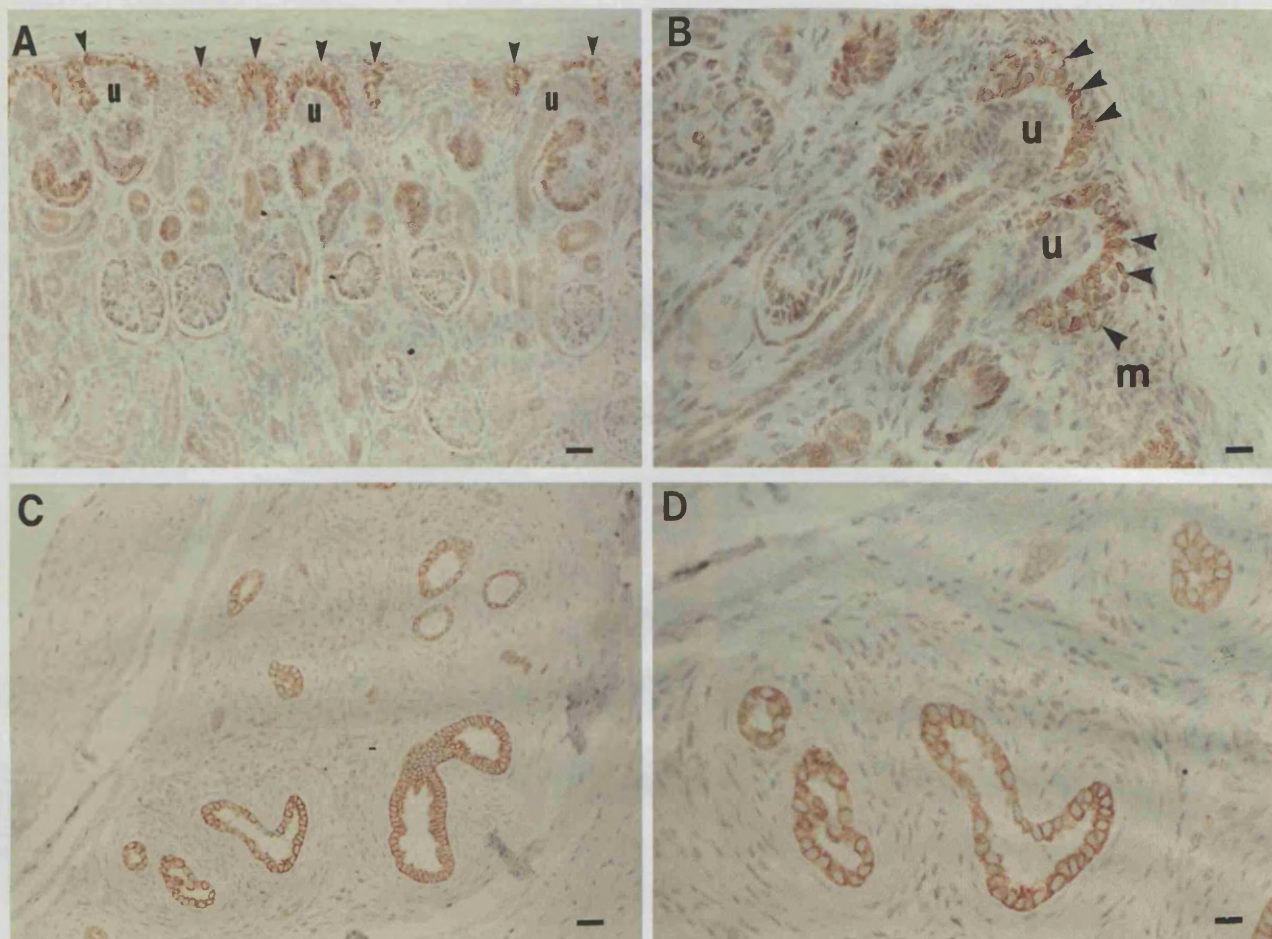
Figure 3. BCL2 immunostaining in dysplastic human kidneys. (*A*) 10-wk normal human fetal kidney. BCL2 is prominent in mesenchymal condensates (*arrowheads*). Bar, 12 μm. (*B*) High power of normal nephrogenic zone. Note intense BCL2 staining in mesenchymal condensates (*arrowheads*) but the ureteric bud branches (*u*) are negative. Bar, 4 μm. (*C*) Low power field of a dysplastic kidney. Numerous dysplastic tubules stain intensely for BCL2 protein while the surrounding collarettes and undifferentiated cells are negative. Bar, 12 μm. (*D*) Higher power of (*C*). Bar, 6 μm.

pattern which persisted postnatally (data not shown). WT1 protein was not detected in derivatives of the ureteric bud. In dysplastic kidneys, WT1 nuclear protein was absent in dysplastic epithelia but was detected in 10–80% of fibromuscular and undifferentiated cells around malformed tubules (Fig. 4, *C*). The intensity of staining in these cells was similar to that observed in the early stages of nephron formation but less than the nuclear staining in glomerular podocytes (Fig. 4, *A*).

Metaplastic cartilage was negative for PAX2, BCL2, and WT1. Gene expression patterns were similar in dysplastic kidneys with either patent or obstructed lower urinary tracts (see Table I, *A* and *B* for patient details).

Discussion

PAX2 and normal human nephrogenesis. This is the first study to document the detailed expression of PAX2 protein in hu-

man nephrogenesis. We found that PAX2 is regulated both in developmental space and time in cells undergoing critical morphogenetic events including both mesenchymal/epithelial transition and branching morphogenesis. Similar nephrogenic expression domains have been reported for mouse PAX2 mRNA (18) and protein (20) and human mRNA (28). In common with Hanai and co-workers (47), who used PCNA staining in mice kidneys, we found a high proliferation index in the nephrogenic cortex of fetal kidneys but that proliferation was markedly downregulated postnatally. Our data show that, in both mesenchymal and ureteric bud derivatives, the most intense expression of PAX2 protein occurred in populations of epithelial precursors with the highest proliferation index. In the postnatal period it was rare to identify nuclei which were positive for either PAX2 or PCNA.

Normal relationship of PAX2 expression to WT1. Mundlos and colleagues detected low levels of WT1 protein in human renal

Figure 2. PAX2 and PCNA immunostaining in dysplastic kidneys. *A, C, E,* and *G* are stained for PAX2. *B, D, F,* and *H* are stained for PCNA. *A* and *B* show a normal nephrogenic zone. PAX2 and proliferation are localized to bud branch tips (*u*) and flanking primitive nephrons; (*v*) is a vesicle stage and (*s*) is an S-shaped body. Bars, 2 μm. *C* and *D* show medulla of a normal postnatal kidney with rare PAX2 positive collecting ducts (*arrowheads* in *C*). Cell proliferation is also rare: arrowheads in (*D*). Bars, 6 μm. *E–H* are from a postnatal dysplastic kidney. Note PAX2 in dysplastic tubules (*E*) and cystic epithelia (*G*). Surrounding undifferentiated cells are negative. Many epithelial cell nuclei in these kidney malformations also stain for PCNA: (*arrowheads* in *F* and *H*). Bars, 6 μm.
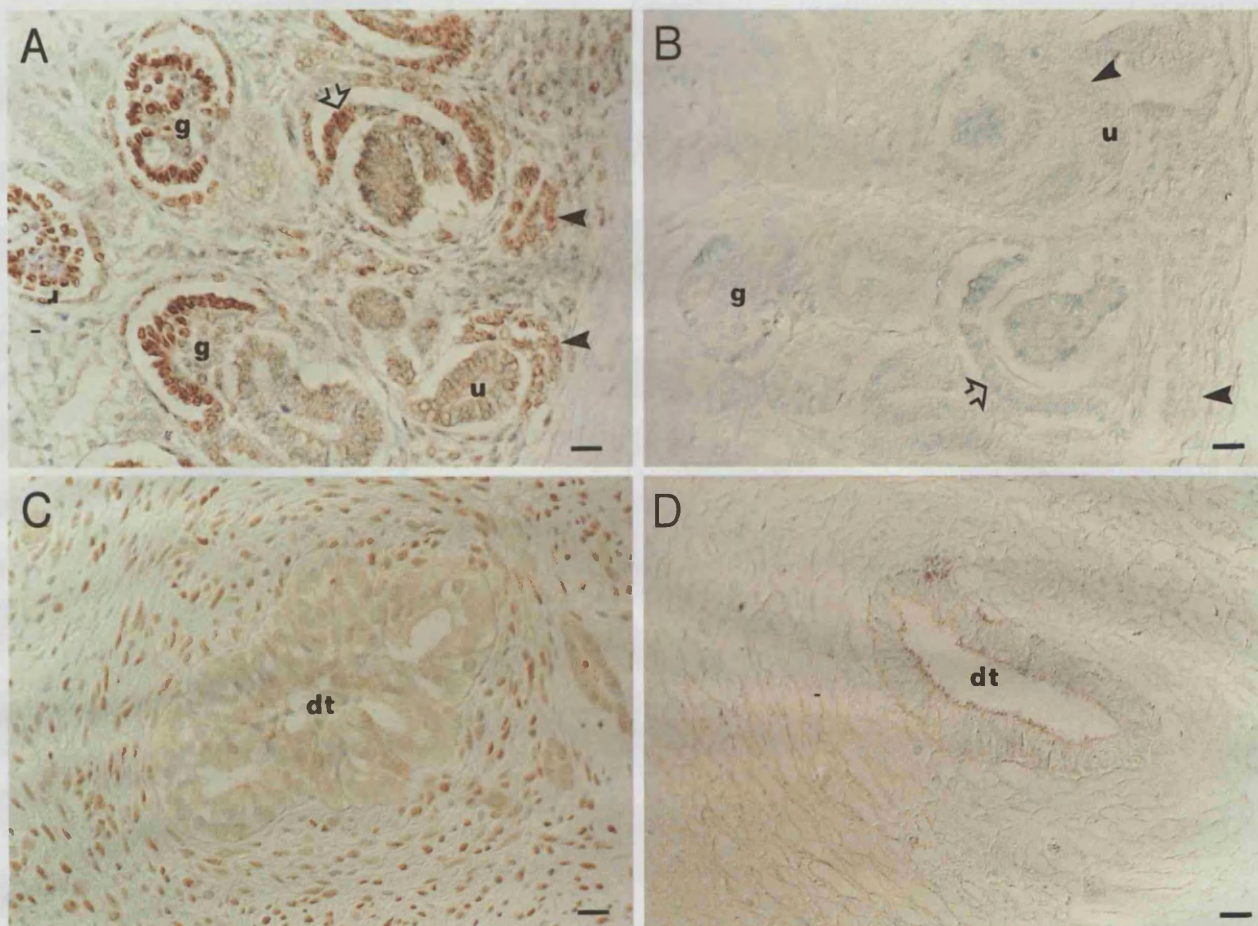
Figure 4. WT1 immunostaining in dysplastic human kidneys. (*A*) Normal human fetal kidney shows a gradient of WT1 immunoreactivity from nephrogenic cortex (*right*) to maturing nephrons (*left*). Note that cells in condensates and vesicles (*arrowheads*) are weakly positive for WT1 immunostaining. Expression increases in the mesenchymal to epithelial transition with high WT1 levels in the proximal limb of S-shaped bodies (*open arrowheads*) and the podocytes of fetal glomeruli (*g*). A ureteric bud branch tip (*u*) is negative. (*B*) Similar field to *A* but first antibody omitted shows no staining. (*C*) In human kidney malformations dysplastic tubules (*dt*) show no significant staining with the WT1 antibody. In contrast, nuclei of fibromuscular and undifferentiated cells located around the tubule are positive for WT1. (*D*) Similar field to *C* but first antibody omitted shows minimal background staining in the cytoplasm of the dysplastic tubule. Bars, 10 μm.

mesenchyme but not in vesicles with an antibody raised against the first alternative spice site in WT1 (48). Another group found little protein expression in condensing renal mesenchyme of mice with an antibody raised against aa 1-179 of WT1 (2). We found faint but positive WT1 staining in renal condensates and vesicles using an antibody raised against the carboxy terminus. In accord with previous studies (2, 48), we observed that the level of WT1 increased in S-shaped bodies and podocytes. Thus our study identified WT1 protein at a slightly earlier stage during the mesenchymal to epithelial transition as compared with previous reports. We suggest that this difference may be attributed to a more sensitive staining technique or to the fact that antibodies were raised to different regions of WT1 and may thus have the capacity to recognize different isoforms. Furthermore, the fact that homozygous *WT1* null mutant mice have absent kidneys due to lack of induction and subsequent apoptosis of renal mesenchyme (46) would appear to suggest that low, but biologically important, levels of WT1 protein are indeed expressed even before the condensate or vesicle stages. There is biochemical evidence that WT1 can repress transcription of PAX2 (2), consistent with the general inverse relationship between PAX2 and WT1 noted during glomerular podocyte maturation in our study. Of

note, the normal downregulation of PAX2 in maturing collecting ducts was not associated with WT1 expression, suggesting that other molecules switch-off PAX2 in this lineage.

Normal relationship of PAX2 expression to BCL2. Our observations of BCL2 expression in normal human nephrogenesis accord with a recent study (49). *Bcl2* null mutant mice are born with hypoplastic kidneys and metanephric growth in organ culture is restricted due to apoptosis (44, 50). Thus BCL2 is required to prevent death of proliferating nephron precursors. The fact that PAX2, BCL2, and PCNA proteins are highly expressed together in the mesenchymal condensate suggests that PAX2 and BCL2 are important molecules for cell proliferation and survival in this first morphogenetic step in nephron formation. Although we found that PAX2 expression correlated with proliferation in ureteric bud branches, BCL2 was not expressed in these normal ampullae, and our previous observations suggest that these structures are not sites of marked apoptosis (36). It is possible that these cells express other anti-death molecules (e.g., BCL_{XL}) or have lower levels of apoptosis-inducing molecules (e.g., BAX) (51).

Cell lineages and biology of multicystic dysplastic kidneys. Classical studies by Edith Potter described the anatomy of dys-

plastic kidneys (34). This and other work (52) suggests that dysplastic tubules are malformed branches of the ureteric bud while dysplastic cysts correspond to distended ampullae (34). The cells surrounding these epithelia are undifferentiated "mesenchymal" or "stromal" cells as well as metaplastic cells with characteristic fibromuscular morphology (the "collarettes" immediately surrounding dysplastic tubules) and cartilage (32, 34–36). These cells probably originate as renal mesenchymal or intermediate mesoderm cells which either fail to develop or differentiate along inappropriate pathways. Another possibility is that some of these cells derive from the ureteric bud since one recent study demonstrated a contribution of the bud to stroma in metanephric organ culture (53).

Very little is known about the cell biology of human multicystic dysplastic kidneys. We recently demonstrated that the incidence of apoptosis was increased in cells surrounding dysplastic epithelia but that programmed cell death was rare in the abnormal epithelia themselves (36). We suggested that the tendency for some of these organs to regress (37) and the failure to form mature nephrons might be explained by increased programmed cell death.

Aberrant PAX2 and BCL2 expression correspond with death and proliferation in renal dysplasia. We can now associate defined patterns of gene expression with hyperproliferation in dysplastic epithelia and with cell death in surrounding cells (36). Many of the cells around dysplastic tubules express WT1 protein with an intensity comparable to that found in the normal primitive nephron and thus appear to have been induced. If this is so, why do they fail to differentiate and why is apoptosis common? (36) We suggest that the answer lies firstly in the absence of PAX2 expression, causing failure to undergo mesenchymal/transition, and secondly in a lack of BCL2, resulting in a failure of precursor survival. Using similar reasoning we speculate that cyst formation in dysplastic kidneys is caused by persistent expression of PAX2, which would provide a continuous proliferation signal, and ectopic BCL2 expression which would prevent immature epithelia from dying. Moreover, the persistent postnatal expression of PAX2 could contribute to the genesis of the tumors which have been reported in dysplastic kidneys (38, 39).

Conclusions. We propose that cyst formation in human dysplastic kidney malformations can be understood in terms of aberrant temporal and spatial expression of master genes which are tightly developmentally-regulated during the normal program of human nephrogenesis. In the future it will be interesting to document the expression in these dysplastic organs of other molecules known to be associated with development of ureteric bud derivatives. These include met (54, 55), ros (56), ret (57), epidermal growth factor receptor (58), low affinity nerve growth factor receptor (59) and L-myc (60). Further studies are now necessary to determine whether the aberrant patterns of gene expression we have documented have their origin in either mutations of genes expressed in nephrogenesis or in nongenetic factors such as teratogens: both types of pathogenetic mechanism have been implicated in human and animal kidney malformations (61). Finally, although urinary tract obstruction has been implicated as causing renal dysplasia, we found no difference in gene expression between obstructed and nonobstructed organs.

Acknowledgments

References

1. Gilbert, S.F. 1991. *Developmental Biology*, Third Edition. Sinauer Associates, Inc. Sunderland, Massachusetts. 376–457.

2. Ryan, G., V. Steele-Perkins, J.F. Morris, F.J. Rauscher III, and G.R. Dressler. 1995. Repression of Pax-2 by WT1 during normal kidney development. *Development (Camb.).* 121:867–875.

3. Song, D.-L., G. Chalepakis, P. Gruss, and A.L. Joyner. 1996. Two Pax-binding sites are required for early embryonic brain expression of an *Engrailed-2* transgene. *Development (Camb.).* 122:627–635.

4. Gruss, P., and C. Walther. 1992. Pax in development. *Cell.* 69:719–722.

5. Stapleton, P., A. Weith, P. Urbanek, Z. Kozmik, and M. Busslinger. 1993. Chromosomal localisation of seven *Pax* genes and cloning of a novel family member, *Pax9. Nat. Genet.* 3:292–298.

6. Halder, G., P. Callaerts, W.J. Gehring. 1995. Induction of ectopic eyes by targeted expression of the *eyeless* gene in *Drosophila. Science (Wash. DC).* 267: 1788–1792.

7. Hyatt, G.A., E.A. Schmitt, N. Marsh-Armstrong, P. McCaffery, U.C. Drager, and J.E. Dowling. 1996. Retinoic acid establishes ventral retinal characteristics. *Development (Camb.).* 122:195–204.

8. Max, E.E., Y. Wakatsuki, M.F. Neurath, and W. Strober. 1995. The role of BSAP in immunoglobulin isotype switching and B-cell proliferation. *Curr. Topics Microbiol. Immunol.* 194:449–458.

9. Keller, S.A., J.M. Jones, A. Boyle, L.L. Barrow, P.D. Killen, D.G. Green, N.V. Kapousta, P.F. Hitchcock, R.T. Swank, and M.H. Meisler. 1994. Kidney and retinal defects (*Krd*), a transgene-induced mutation with a deletion of mouse chromosome 19 that includes the *Pax2* locus. *Genomics.* 23:309–320.

10. Matsuo, T., N. Osumi-Yamashita, S. Noji, H. Ohuchi, E. Koyama, F. Myokai, N. Matsuo, S. Taniguchi, H. Doi, S. Iseki, et al. 1993. A mutation in the Pax-6 gene in rat *small eye* is associated with impaired migration of midbrain crest cells. *Nat. Genet.* 3:299–304.

11. Goulding, M.D., G. Chalapakis, U. Deutsch, J.R. Erselius, and P. Gruss. 1991. Pax-3, a novel murine DNA binding protein expressed during early neurogenesis. *EMBO (Eur. Mol. Biol. Organ.) J.* 10:1135–1147.

12. Wallin, J., H. Eibel, A. Neubuser, J. Wilting, H. Koseki, and R. Balling. 1996. *Pax1* is expressed during the development of the thymus epithelium and is required for normal T-cell maturation. *Development (Camb.).* 122:23–30.

13. Maulbecker, C.C., and P. Gruss. 1993. The oncogenic potential of Pax genes. *EMBO (Eur. Mol. Biol. Organ.) J.* 12:2361–2367.

14. Read, A.P. 1995. Pax genes — *Paired* feet in three camps. *Nat. Genet.* 5: 333–334.

15. Tassabehji, M., A.P. Read, V. E. Newton, M. Patton, P. Gruss, R. Harris, and T. Strachan. 1993. Mutations in the *Pax 3* gene causing Waardenburg syndrome type 1 and 2. *Nat. Genet.* 3:26–30.

16. Hanson, I.M., A. Seawright, K. Hardman, S. Hodgson, D. Zaletayev, G. Fekete, and V. van Heyningen. 1993. *Pax 6* mutations in aniridia. *Hum. Mol. Genet.* 2:915–920.

17. Barr, F.G., N. Galili, J. Holick, J.A. Biegel, G. Rovera, and B.A. Emanuel. 1993. Rearrangement of the Pax3 paired-box gene in the paediatric solid tumour alveolar rhabdomyosarcoma. *Nat. Genet.* 3:113–117.

18. Dressler, G.R., U. Deutsch, K. Chowdhury, H.O. Nornes, P. Gruss. 1990. *Pax2,* a new murine paired-box-containing gene and its expression in the developing excretory system. *Development (Camb.).* 109:787–795.

19. Plachov, D., K. Chowdhury, C. Walther, D. Simon, J.-L. Guenet, and P. Gruss. 1990. *Pax8,* a murine paired box gene expressed in the developing excretory system and thyroid gland. *Development (Camb.).* 110:643–651.

20. Dressler, G.R., and E.C. Douglas. 1992. Pax-2 is a DNA-binding protein expressed in embryonic kidney and Wilms tumor. *Proc. Natl. Acad. Sci. USA.* 89:1179–1183.

21. Dressler, G.R., J.E. Wilkinson, U.W. Rothenpieler, L.T. Patterson, L. Williams-Simons, and H. Westphal. 1993. Deregulation of *Pax-2* expression in transgenic mice generates severe kidney abnormalities. *Nature (Lond.).* 362:65–67.

22. Torres, M., E. Gomex-Pardo, G.R. Dressler, and P. Gruss. 1995. *Pax-2* controls multiple steps of urogenital development. *Development (Camb.).* 121: 4057–4065.

23. Rothenpieler, U.W., and G.R. Dressler. 1993. *Pax-2* is required for mesenchyme-to-epithelium conversion during kidney development. *Development (Camb.).* 119:711–720.

24. Fickenscher, H.R., G. Chalepakis, and P. Gruss. 1993. Murine Pax-2 protein is a sequence-specific *trans*-activator with expression in the genital system. *DNA Cell Biol.* 12:381–391.

25. Sanyanusin, P., L.A. Schimmentl, L.A. McNoe, T.A. Ward, M.E.M. Pierpoint, M.J. Sullivan, W.B. Dobyns, and M.R. Eccles. 1995. Mutations of the PAX2 gene in a family with optic nerve colobomas, renal anomalies and vesi-

coureteral reflux. *Nat. Genet.* 9:358–364.

26. Sanyanusin, P., L.A. McNoe, M.J. Sullivan, R.G. Weaver, and M.R. Eccles. 1995. Mutation of *PAX2* in two siblings with renal-coloboma syndrome. *Hum. Mol. Genet.* 4:2183–2184.

27. Battin, J., D. Lacombe, and J.J. Leng. 1993. Familial occurrence of hereditary renal adysplasia with Mullerian anomalies. *Clin. Genet.* 43:23–24.

28. Eccles, M.R., L.J. Wallis, A.E. Fidler, N.K. Spurr, P.J. Goodfellow, and A.E. Reeve. 1992. Expression of the *PAX2* gene in human fetal kidney and Wilm's tumor. *Cell Growth & Differ.* 3:279–289.

29. Poleev, A., F. Wendler, H. Fickensher, M.S. Zannini, K. Yaginuma, C. Abbott, and D. Plachov. 1995. Distinct functional properties of three human paired-box-protein, PAX 8, isoforms generated by alternative splicing in thyroid, kidney and Wilm's tumors. *Eur. J. Biochem.* 228:899–911.

30. Sharma, P.M., M. Bowman, B.F. Yu, and S. Sukumar. 1994. A rodent model for Wilm's tumors: embryonal kidney neoplasms induced by N-notroso-N'-methylurea. *Proc. Natl. Acad. Sci. USA.* 91:9931–9935.

31. Gnarra, J.R., and G.R. Dressler. 1995. Expression of *Pax-2* in human renal cell carcinoma and growth inhibition by antisense oligonucleotides. *Cancer Res.* 55:4092–4098.

32. Bernstein, J. 1992. Renal hypoplasia and dysplasia. *In* Pediatric Kidney Disease. C.M. Edelman, Jr., editor. Little, Brown. Boston, MA. 1121–1138.

33. Ehrich, J.H.H., G. Rizzoni, F.P. Brunner, W. Fassbinder, W. Geerlings, N.P. Mallick, A.E.G. Raine, N.H. Selwood, and G. Tufveson. 1992. Renal replacement therapy for end-stage renal failure before 2 years of age. *Nephrol. Dial. Transplant.* 7:1171–1177.

34. Potter, E.L. 1972. Normal and Abnormal Development of the Kidney. Year Book Medical Publishers Inc., Chicago. 1–350.

35. Risdon, R.A. 1971. Renal dysplasia. Part 1. A clinico-pathological study of 76 cases. *J. Clin. Path.* 24:57–71.

36. Winyard, P.J.D., J. Nauta, D.S. Lirenman, P. Hardman, V.R. Sams, R.A. Risdon, and A.S. Woolf. 1996. Deregulation of cell survival in cystic and dysplastic renal development. *Kidney Int.* 49:135–146.

37. Dungan, J.S., M.T. Fernandez, P.L. Abbitt, S. Thiagarajah, S.S. Howards, and W.A. Hogge. 1990. Multicystic dysplastic kidney: natural history of prenatally detected cases. *Prenatal Diag.* 10:175–182.

38. Barrett, D.M., and R.E. Wineland. 1980. Renal cell carcinoma in multicystic dysplastic kidney. *Urology.* 15:152–154.

39. Cromie, W.J., M.S. Engelstein, and J.W. Dickett. 1980. Nodular renal blastema, renal blastema and duplicated collecting systems. *J. Urol.* 123:100–102.

40. Phelps, D.A., and G.R. Dressler. 1996. Indentification of novel Pax-2 binding sites by chromatin precipitation. *J. Biol. Chem.* 271: 7978–7985.

41. Larsson, S.H., J.-P. Charlieu, K. Miyagawa, D. Engelkamp, M. Rassoulzadegan, A. Ross, F. Cuzin, V. van Heyningen, and N. Hastie. 1995. Subnuclear localisation of WT1 in splicing of transcription factor domains is regulated by alternative splicing. *Cell.* 81:391–401.

42. Bravo, R., R. Frank, P.A. Blundell, and H. MacDonald-Bravo. 1987. Cyclin/PCNA is the auxillary protein of DNA polymerase-delta. *Nature (Lond.).* 326:515–517.

43. Hockenberry, D.G., C. Nunez, C. Milliman, R.D. Schreiber, and S.J. Korsmeyer. 1990. Bcl-2 is an inner mitochondrial membrane protein that blocks programmed cell death. *Nature (Lond.).* 348:334–336.

44. Veis, D.J., C.M. Sorenson, J.R. Shutter, and S.J. Korsmeyer. 1994. Bcl-2-deficient mice demonstrate fulminant lymphoid apoptosis, polycystic kidneys and hypopigmented hair. *Cell.* 75:229–240.

45. Pritchard-Jones, K., S. Flemming, D. Davidson, W.A. Bickmore, D. Porteus, C. Gosden, J. Bard, A. Buckler, J. Pelletier, D. Housman, V. van Heyningen, and N. Hastie. 1990. The candidate Wilm's tumor gene is involved in genitourinary development. *Nature (Lond.).* 346:194–197.

46. Kreidberg, J.A., H. Sariola, J.M. Loring, M. Maeda, J. Pelletier, D. Housman, and R. Jaenisch. 1993. WT-1 is required for early kidney development. *Cell.* 74:679–691.

47. Hanai, T., N. Usuda, T. Morita, T. Shimizu, and T. Nagata. 1993. Proliferative activity in the kidneys of aging mice evaluated by PCNA/cyclin immunohistochemistry. *Cell Mol. Biol.* 39:181–191.

48. Mundlos, S., J. Pelletier, A. Darveau, M. Bachmann, A. Winterpacht, and B. Zabel. 1993. Nuclear localisation of the protein encoded by the Wilm's tumor gene WT1 in embryonic and adult tissues. *Development (Camb.).* 119: 1329–1343.

49. Veis, D.J., and S.J. Korsmeyer. 1994. Bcl-2 protein expression during murine development. *Am J Pathol.* 145:61–73.

50. Sorenson, C.M., S.A. Rogers, S.J. Korsmeyer, and M.R. Hammerman. 1995. Fulminant metanephric apoptosis and abnormal kidney development in bcl-2 deficient mice. *Am. J. Physiol.* 268:F73–F81.

51. Oltvai, Z.N., C.L. Milliman, and S.J. Korsmeyer. 1993. Bcl-2 heterodimerises in vivo with a conserved homologue, bax, that accelerates programmed cell death. *Cell.* 74:609–619.

52. Maizel, M., and S.B. Simpson. 1983. Primitive ducts of renal dysplasia induced by culturing ureteral buds denuded of condensed renal mesenchyme. *Science (Wash. DC).* 219:509–510.

53. Qiao, J., D. Cohen, and D. Herzlinger. 1995. The metanephric blastema differentiates into collecting system and nephron epithelia in vitro. *Development (Camb.).* 121:3207–3214.

54. Santos, O.F.P., E.J.G. Barros, Y.-M. Yang, K. Matsumoto, M. Park, and S.K. Nigam. 1994. Involvement of hepatocyte growth factor in kidney development. *Dev. Biol.* 163:525–529.

55. Woolf, A.S., M. Kolatsi-Joannou, P. Hardman, E. Andermarcher, C. Moorby, L.G. Fine, P.S. Jat, M.D. Noble, and E. Gherardi. 1995. Roles of hepatocyte growth factor/scatter factor and met in early development of the metanephros. *J. Cell Biol.* 128:171–184.

56. Kanwar, Y.S., Z.Z. Liu, A. Kumar, J. Wada, and F.A. Carone. 1995. Cloning of mouse c-*ros* cDNA, its role in development and relationship to extracellular matrix glycoproteins. *Kidney Int.* 48:1646–1659.

57. Schuchardt, A., V. D'Agati, L. Larsson-Blomberg, F. Costantini, V. Pachnis. 1994. Defects in the kidney and enteric nervous system of mice lacking the tyrosine kinase receptor Ret. *Nature (Lond.).* 367:319–320.

58. Threadgill, D.W., A. Dlugosz, L.A. Hansen, T. Tennenbaum, U. Lichti, D. Yee, C. LaMantia, T. Mourton, K. Herrup, R.C. Harris, J.A. Barnard, S.H. Yuspa, R.J. Coffey, and T. Magnuson. 1995. Targeted disruption of mouse EGF receptor: effect of Genetic Background on mutant phenotype. *Science (Wash. DC).* 269:230–234.

59. Sariola, H., M. Saarma, K. Sainio, U. Arumae, J. Palgi, A. Vaatokari, I. Thesleff, and A. Karavanov. 1991. Dependence of kidney morphogenesis on the expression of nerve growth factor receptor. *Science (Wash. DC).* 254:571–573.

60. Mugrauer, G., and P. Ekblom. 1991. Contrasting expression patterns of three members of the *myc* family of protooncogenes in the developing and adult mouse kidney. *J. Cell Biol.* 112:13–25.

61. Woolf, A.S. 1995. Clinical impact and biological basis of kidney malformations. *Semin. Nephrol.* 15:361–372.